Université de Strasbourg

UNIVERSITÉ DE STRASBOURG

École Doctorale des Sciences de la Vie et de la Santé STRASBOURG

ÉCOLE DOCTORALE DES SCIENCES DE LA VIE ET DE LA SANTE

IGBMC, UMR 7104 / U1258

THÈSE présentée par :

Grégoire MATHONNET

Soutenue le 30 Janvier 2023

pour obtenir le grade de : **Docteur de l'université de Strasbourg**

Discipline/ Spécialité : Sciences de la vie et de la santé

Étude des relations entre architectures d'actine, contenu moléculaire et identité cellulaire au cours de l'embryogénèse précoce de *C. elegans*

THÈSE dirigée par :

Dr. Anne-Cécile REYMANN	CR, CNRS, IGBMC, Strasbourg, France

RAPPORTEURS :

Dr. Marie-Emilie TERRET	DR2 INSERM, CIRB, Collège de France, Paris, France
Dr. Ana Xavier de CARVALHO	Group leader, i3S, Université de Porto, Portugal

AUTRES MEMBRES DU JURY :

Dr. Sophie JARRIAULT	DR, CNRS, IGBMC, Strasbourg, France

INVITÉS :

Dr. Sophie QUINTIN	CR, CNRS, IGBMC, Strasbourg, France

TABLE OF CONTENTS

LIST OF FIGURES

Remerciements

Avant d'écrire cette section, j'avais pour ambition d'utiliser cette partie « remerciement » comme témoignage de mon parcours au sein du milieux académique et scientifique de la recherche fondamentale en France entre 2018 et 2023 en incluant des observations sur la société civile aussi bien que sur la communauté scientifique. Après un délai relativement (très et trop) long, beaucoup de réflexion de doute et de résignation j'ai décidé de ne pas vous imposer ce témoignage ici mais de le faire maturer pour le retranscrire ultérieurement au sein d'un livre qui sera publié sous pseudonyme et en partenariat avec d'autres camarades qui ont vécu durant cette période (sachez que les grandes lignes et plusieurs chapitres sont déjà écrits). Nous allons donc partir ici sur un déroulement classique selon le plan de l'indémodable remerciement en incluant les constructions de phrases avec des incises (= partie de phrase mal lue et très souvent, tout le temps, incomprise) et les fautes d'orthographes typique qui me donne cette unique part de modernité stylistique, par tout temps décriée mais secrètement jalousée!

Je voudrais commencer par remercier les personnes qui m'ont soutenues jusqu'au bout et celles qui ont partagé ma foi dans cette Aventure, cette Histoire et ce projet de Vie.

En commençant par remercier particulièrement le Dr Anne-Cécile Reymann qui, en 2018, en voyant arrivé le jeune homme que j'étais, m'a donné une chose que peu de personnes ont le courage de donner et qu'encore moins de personne ont l'humilité de saluer et de reconnaitre de l'avoir reçu : une chance. Une chance de pouvoir réaliser ce doux rêve d'étudiant et de jeune homme. Grandir et murir à travers les épreuves inhérentes au rôle de thésard. Cette chance de passer du statut d'étudiant avec un certain bagage théorique à celui d'aspirant chercheur pour espérer avoir une chance d'aller au bout d'une idée, une chance de découvrir et de trouver. Cette chance n'aurait pas eu lieu s'il n'y avait pas eu les qualités morale et managériale et surtout la patience d'Anne-Cécile. Elles m'ont permis d'évoluer en liberté dans le meilleur des cadres. J'aimerais également soulever que la mise en place de nos discussions hebdomadaire sur les résultats, projets, papiers, affaires personnelles a été un tournant significatif pour traverser ces épreuves, elles m'ont énormément aidées et fais progresser. Une fois de plus, je t'en remercie et j'avoue même qu'elle me manque!

Je voudrais également remercier mes anciens professeurs et encadrants qui m'ont mis la puce à l'oreille et le pied à l'étrier (sans pour autant mettre la cuillère à la bouche!) : Patrick Cormier de la station biologique de Roscoff à qui j'ai particulièrement pensé pendant la phase de recherche sur les filopodes de l'embryon d'oursin, Aude Dupré et Catherine Jessus du laboratoire de biologie de l'ovocyte à l'IBPS pour leurs sensibilisation sur la thématique de l'embryogénèse et pour mes premiers pas en tant que chercheur! Ainsi que Sandrine Etienne-Manneville, Cécile Leduc et Yamini Yogalaskshmi du laboratoire Polarité et Migration Cellulaire de l'institut Pasteur qui mon accompagné et conforter dans l'idée que je me fais de cette art.

Un remerciement chaleureux et fraternel maintenant! Pour les membres de mon jury Marie-Emilie Terret, Ana Xavier de Carvalho, Sophie Jarriault et Sophie Quintin qui ont su m'accompagner pendant toute la durée de cette épreuve et en étant un soutien tout particulier pendant les étapes clés de cette épreuve.

De plus, je souhaite adressé mes remerciement et mes félicitations pour ces personnes de l'ombres qui accompagnées de leur patience et de leur bienveillance qui ont permis une certaine fluidité organisationnelle et administrative. Leur importance est inversement proportionnelle à la reconnaissance qu'ils reçoivent, ils sont peu considérés, décriées et souvent même maltraitées de tous les côtés. Je pense ici à l'équipe de la plateforme de microscopie : Bertrand, Erwan, Elvire et Yves, Evelyne de l'accueil de l'institut, au secrétariat de l'école doctorale et à toute ces personnes que j'ai croisé, à qui leurs noms m'échappe mais qui m'ont partagé leur histoire.

Par la suite, je voudrais remercier mes camarades de lutte laborantine pour leur fraternité : Roxanne Benoit pour son soutien aussi bien sur des problématiques scientifiques, professionnelles et personnelles, les pauses clopes à palabrer me manques énormément. Théo Hecquet pour son appétit du savoir, sa curiosité naturelle, sa sensibilité graphique et sa passion légèrement teintée d'arrogance, ne perds pas ton panache!

Au risque d'en oublier (comme toujours) je voudrais citer et saluer ici les personnes qui m'ont directement, accompagnées, pendant cette épopée : Mes compagnons de route : Nadine, Sophie, le labo Jarriault et d'autres personnes de passage dans le labo Reymann : *Pierro* (Le Chauve), qui a changé de direction de vie et a choisi de sauter le pas de la recherche académique. *Anaïsseule*, qui a décidé de mettre à l'épreuve son endurance et de prolonger ses études, qui sait, peut-être même pour une thèse, courage pour la suite et prend soin de ton Grégoire! Caroline, notre émigrée belge, prend garde je risque de débarqué un jour! Rita, bonne chance pour la suite et n'hésite pas à aller vers les autres!

Je souhaite remercier une personne que j'ai rencontrée pendant la partie finale de cette histoire. Ce petit ours polaire qui a réussi à recréer des connections et une vision que je croyaient disparus au travers des épreuves. Elle m'a reconnecter à ce que je suis réellement, à cette énergie, cette positivité, cette joie de vivre, au gout des autres, au réel ,enfin ce qui doit l'être, à donner un sens et une vision à ma vie. Pour tous cela, je la remercie. J'espère arrivé à lui apporter le soutien adéquat pour qu'elle puisse terminer elle aussi cette épreuve et ce tourner ensemble vers un prochain défis fou! Pour sa protection et sa pudeur naturelle je ne la nommerais pas ici. Elle et les personnes qui me connaissent la reconnaitront <3.

Je voudrais également saluer bien bas mes camarades contemporains qui étaient également des voisins de labos : Dimitra, incarnant la fougue, la détermination et le courage de la déesse Déméter! Vasilisa, une camarade avec un parcourt exténuant, après des expériences mouvementées en master, elle est partie de sa mère patrie pour faire une escale en France afin de réaliser sa thèse, aujourd'hui elle effectue un post-doctorat au Québec. En parallèle de ses escapades, elle arrive à avoir le courage d'endosser le rôle le plus dure de notre condition humaine : la vie de parent avec son petit Vasil qui selon moi et mon existentialisme romantique, est la plus belle représentation de l'Espoir. Mon petit Basile,

pensée toute particulière à une amie que j'ai rencontré grâce au destin, lors d'une formation de microscopie : Maël, avec qui je partage le même goût et la même curiosité sur ce qui se passe à l'échelle de l'infiniment petit, la même appétence pour l'élucidation des mécanismes qui nous entoures et une approche très similaire de la Vie. Une amie avec qui nous avions envisagé faire beaucoup de choses. Entre autres, continuer ensemble notre carrière académique (notre complémentarité aurait été implacable). Il faut savoir qu'au départ elle ne se destinait pas à une carrière de scientifique et que par la force des choses, sa volonté et son talent d'écriture elle a réussi à se hisser en haut de l'échelle! Je voudrais également adresser une salutation distinguée pour mes camarades des promotions ultérieures et ceux à qui je n'ai malheureusement pas eu le temps de faire suffisamment connaissance : Yulia, Sabrina, Grégory, Marjolaine, Maxime et beaucoup d'autres!

Je voudrais aussi /cheer mes dudzes d'Azeroth que j'ai rencontré depuis l'été 2019 et avec qui nous avons affronté les dérives de la tyrannie sanitaire, les aléas de la vie personnelle de chacun, les arrivées flamboyantes, les départs grisonnants. Nous avons réussi un défi incroyable, penser vous qu'un groupe d'une cinquantaine de joueurs amateurs boomeurs des 4 coins du monde arriveraient à organiser leurs vies, personnelle et en ligne ; passer outre leurs différences et les frictions sociales ; pour accomplir des performances d'un niveaux compétitif sur une activité vidéo-ludique avec une longévité de 6 ans aujourd'hui ? Essayé d'organiser une réunion active de plusieurs heures en distancielle et de façon bi-hebdomadaire et on en reparle!

Je voudrais adresser un gros et légendaire /all TY, GG WP, jeu aisé à mes 2 camarades de la faille qui m'ont accompagné et soutenues depuis le master 1 : Emilien et Thomas. Grâce à eu j'ai trouvé et affiner une méthode de travail à la fois endurante, robuste et tout terrain!

Sans rentrer dans un étalement sentimental pour cette dernière partie Je voudrais également remercier ma famille pour leur soutien constant durant les différentes épreuves de cette période. Peut-importe les détours, les travers, les erreurs du passé, tout est entièrement pardonné et je n'en retire que du positif. Le flambeau est passé, et maintenant grande question, serais-je à la hauteur quand ces situations se présenteront à moi ?

Je souhaite également avoir une pensée particulière pour mes Grands-parents qui sont pour moi une source d'inspiration pour leur résilience, leurs expériences, leurs visions et leurs sagesses. Avec une attention toute singulière pour mes grands-parents paternels qui nous ont quittés pendant la réalisation de cette histoire et avec qui je partageais une soif mécanistique, une curiosité et un respect de l'Histoire, des connaissances et de ceux qui les établissent. Avec un salut là-haut pour ma grand-mère qui vivait au travers de mes yeux, la réalisation d'un rêve de jeunesse.

Avec ces dernière pensées et l'ombre fatale de la course du temps je profite de cette occasion pour faire un témoignage indélébile, intemporel et inconditionnel de l'amour que j'ai pour toute cette famille et je donne un défis à ma génération (frères, sœur, cousin.e.s), conserver et améliorer les liens que nos Parents ont construit, la tâche est déjà en très bonne voie et vous pouvez compter sur moi, c'est le défi de notre génération, maintenir ou construire.

Je veux ici saluer bien bas, cette fois, les personnes qui m'ont accompagné dans mes pensées, mes rêveries et mes projections et qui ont contribués à garder et à paufiner une identité psychique dans cette période troublée, une sorte de relais parental des songes. La liste est succincte mais les manquants ne manqueront pas de me le rappeler! Charles de Batz, Armand de Sillègue, Isaac de Portau et Henri d'Aramitz, Joseph Boniface, Louis de bussy, Jean-Antoine d'Anglerais, Savinien de Bergerac, Pierre Aronnax et le capitaine, ainsi que toute la famille de Sainte-Hermine, encore merci à eux et je terminerais cette partie par une des leçons qu'ils m'ont apprises : Tout homme et, à plus forte raison, tout chercheur, désire être reconnu. Je le désire aussi. Mais il ne m'a pas été possible d'apprendre votre décision sans comparer son retentissement à ce que je suis réellement. Comment un homme presque jeune, riche de ses seuls doutes et d'une œuvre encore en chantier, habitué à vivre dans la solitude du travail ou dans les retraites de l'amitié, n'aurait-il pas appris avec une sorte de panique un arrêt qui le portait d'un coup, seul et réduit à lui-même, en centre d'un ponzi académique ? De quel cœur aussi pouvait-il recevoir cet honneur à l'heure où, en Europe et partout dans le monde, d'autres chercheurs, parmi les plus grands, sont réduits au silence, et dans le temps même où sa terre natale connaît un malheur intérieur croissant ? J'ai connu ce désarroi et ce trouble intérieur. Pour retrouver la paix, il m'a fallu, en somme, me mettre en règle avec un sort trop généreux. Et, puisque je ne pouvais m'égaler à lui en m'appuyant sur mes seuls mérites, je n'ai rien trouvé d'autre pour m'aider que ce qui m'a soutenu, dans les circonstances les plus contraires, tout au long de ma vie : l'idée que je me fais de cet art que certains appel la science et du rôle de chercheur. Permettez seulement que, dans un sentiment de reconnaissance et d'amitié, je vous dise, aussi simplement que je le pourrai, quelle est cette idée. Je ne puis vivre personnellement sans mon art. Mais je n'ai jamais placé cet art au-dessus de tout. S'il m'est nécessaire au contraire, c'est qu'il ne se sépare de personne et me permet de vivre, tel que je suis, au niveau de tous. Cet art et plus particulièrement la Biologie, n'est pas à mes yeux une réjouissance solitaire et égoïstement vécu. Il est un moyen d'émouvoir le plus grand nombre d'Hommes en leur offrant une image privilégiée de la complexité, de la diversité et de la beauté du monde qui nous entoure et qui n'est pas capté par nos sens primitifs. Il oblige donc l'artiste (le chercheur) à ne pas s'isoler ; il le soumet à la vérité la plus humble et la plus universelle. Et celui qui, souvent, a choisi son destin d'artiste parce qu'il se sentait différent, apprend bien vite qu'il ne nourrira son art, et sa différence, qu'en avouant sa ressemblance avec tous. L'artiste se forge dans cet aller-retour perpétuel de lui aux autres, à mi-chemin de la beauté dont il ne peut se passer et de la réalité à laquelle il ne peut s'arracher. C'est pourquoi les vrais artistes ne méprisent rien ; ils s'obligent à comprendre au lieu de juger. Ces artistes sont contraints, de par leurs privilèges, d'être situé à l'avant-garde de l'évolution naturelle, intellectuelle et civilisationnelle de leur temps. Et, s'ils ont un parti à prendre en ce monde, ce ne peut être que celui d'une société où, selon le grand mot de Nietzsche, ne régnera plus le juge, mais le créateur, qu'il soit travailleur ou spirituel ou intellectuel. Le rôle du chercheur du même coup, ne se sépare pas de devoirs difficiles. Par définition, il ne peut se mettre aujourd'hui au service de ceux qui font l'histoire : il est au service de ceux qui la subissent. Ou, sinon, le voici seul et privé de son art. Toutes les armées de la tyrannie avec leurs millions d'individues ne l'enlèveront pas à la solitude, même et surtout s'il consent à prendre leur pas. Mais le silence d'un exilé, social volontaire, et inconnu, abandonné aux humiliations, suffit à retirer le chercheur de l'exil, chaque fois, du moins, qu'il parvient, au

milieu des privilèges de la liberté, à ne pas oublier ce silence et à le faire retentir par les moyens de l'art. Aucun de nous n'est assez grand pour une pareille vocation. Mais, dans toutes les circonstances de sa vie, obscur ou provisoirement célèbre, jeté dans les fers de la tyrannie ou libre pour un temps de s'exprimer, le chercheur peut retrouver le sentiment d'une communauté vivante qui le justifiera, à la seule condition qu'il accepte, autant qu'il peut, les deux charges qui font la grandeur de son métier : le service de la vérité et celui de la liberté. Puisque sa vocation est de réunir le plus grand nombre d'Hommes possible, elle ne peut s'accommoder du mensonge et de la servitude qui, là où ils règnent, font proliférer les solitudes. Quelles que soient nos infirmités personnelles, la noblesse de notre métier s'enracinera toujours dans trois engagements difficiles à maintenir, le refus de mentir sur ce que l'on sait, l'ancrage à la réalité et à la résistance à l'oppression. Pendant plus de vingt ans d'une histoire démentielle, perdu sans secours, comme tous les hommes de mon âge, dans les convulsions du temps, j'ai été soutenu ainsi par le sentiment obscur que découvrir était aujourd'hui un honneur, parce que cet acte obligeait, et obligeait à ne pas découvrir seulement. Il m'obligeait particulièrement à porter, tel que j'étais et selon mes forces, avec tous ceux qui vivaient la même histoire, le malheur et l'espérance que nous partagions. Ces Hommes, nés pendant les années 90, qui ont eu quinze ans au moment où disparaissaient la notion de famille, l'illusion de démocratie et la liberté d'expression, ont été confrontés ensuite, pour parfaire leur éducation, à la mondialisation des plaies, la religion de l'individualisme uniforme, la déconstruction de la Famille, le terrorisme, les crises économiques, les épidémies de grippes bovines, porcines, aviaire, les guerres sémites; ainsi qu'à la privation progressive de leurs liberté par le cloud des oligarques européens et aux dommages auxiliaires du Covid-19. Ces Hommes doivent aujourd'hui élever leurs fils et leurs œuvres dans un monde dirigé par des pilotes déconnectés, privés de leurs sens et manchot qui, à l'aube de la troisième guerre mondiale, réfléchie bénéfice/risque d'une destruction nucléaire. Personne, je suppose, ne peut leur demander d'être optimistes. Et je suis même d'avis que nous devons comprendre, sans cesser de lutter contre eux, l'erreur de ceux qui, par une surenchère de désespoir et par supériorité intellectuelle et morale fictives ont revendiqué le droit au déshonneur, et se sont rués dans les nihilismes de l'époque. Mais il reste que la plupart d'entre nous, dans mon pays et en Europe, ont refusé ce nihilisme et se sont mis à la recherche d'une légitimité de leurs pères et pairs. Il leur a fallu se forger un art de vivre par temps de catastrophe, pour naître une seconde fois, le moment venu, et lutter ensuite, à visage découvert, contre l'instinct de mort et de destruction à l'œuvre dans notre Histoire. Chaque génération, sans doute, se croit vouée à refaire le monde. La mienne sait pourtant qu'elle ne le refera pas. Mais sa tâche est peut-être plus grande. Elle consiste à empêcher que le monde ne se défasse. Héritière d'une histoire corrompue où se mêlent les révolutions déchues, les techniques devenues folles, les dieux morts et les idéologies exténuées, où de médiocres pouvoirs peuvent aujourd'hui tout détruire mais ne savent plus convaincre, où l'intelligence s'est abaissée jusqu'à se faire la servante de la haine et de l'oppression, cette génération a dû, en elle-même et autour d'elle, restaurer à partir de ses seules négations un peu de ce qui fait la dignité de vivre et de mourir. Devant un monde menacé de désintégration, où nos grands inquisiteurs risquent d'établir pour toujours les royaumes de la mort, elle sait qu'elle devrait, dans une sorte de course folle contre la montre, redéfinir le concept de nation et de restaurer entre ces nations une paix qui ne soit pas celle de la servitude, réconcilier à

nouveau travail et culture, et refaire avec tous les Hommes une arche d'alliance. Il n'est pas sûr qu'elle ne puisse jamais accomplir cette tâche immense, mais il est sûr que, partout dans le monde, elle tient déjà son double pari de vérité et de liberté, et, à l'occasion, sait mourir sans haine pour lui. C'est elle qui mérite d'être saluée et encouragée partout où elle se trouve, et surtout là où elle se sacrifie. C'est sur elle, en tout cas, que, certain de votre accord profond, je voudrais reporter l'honneur que vous venez de me faire. Du même coup, après avoir dit la noblesse du métier de chercheur, je l'aurais remis à sa vraie place, n'ayant d'autres titres que ceux qu'il partage avec ses compagnons de lutte, vulnérable mais entêté, injuste et passionné de justice, construisant son œuvre sans honte ni orgueil à la vue de tous, toujours partagé entre la douleur et la beauté, et voué enfin à tirer de son être double les créations qu'il essaie obstinément d'édifier dans le mouvement destructeur de l'histoire. Qui, après cela, pourrait attendre de lui des solutions toutes faites et de belles morales ? La vérité est mystérieuse, fuyante, toujours à conquérir. La liberté est dangereuse, dure à vivre autant qu'exaltante. Nous devons marcher vers ces deux buts, péniblement, mais résolument, certains d'avance de nos défaillances sur un si long chemin. Quel chercheur dès lors oserait, dans la bonne conscience, se faire prêcheur de vertu ? Quant à moi, il me faut dire une fois de plus que je ne suis rien de tout cela. Je n'ai jamais pu renoncer à la lumière, au bonheur d'être, à la vie libre où j'ai grandi. Mais bien que cette nostalgie explique beaucoup de mes erreurs et de mes fautes, elle m'a aidé sans doute à mieux comprendre mon métier et mon Rôle, elle m'aide encore à me tenir, aveuglément, auprès de tous ces Hommes silencieux qui ne supportent dans le monde la vie qui leur est faite que par le souvenir ou le retour de brefs et libres bonheurs. Ramené ainsi à ce que je suis réellement, à mes limites, à mes dettes, comme à ma foi grandissante, j'espère que vous aurez retrouvez ici, la source d'inspiration de ce texte qui n'est autre qu'un discours d'un écrivain lors d'une cérémonie particulière, qui résonne particulièrement bien avec la conjoncture actuelle, en plus du parcours de cette écrivain qui mériterait plus d'attention. En gardant son identité provisoirement mystérieuse pour des raisons pédagogie, vous êtes bien entendus invitez à une petite partie de recherche et d'écoute, auquel cas, ma tentative n'aura pas été vaine. Cela dit, je me sens plus libre de vous montrer, pour finir, l'étendue et la générosité de la distinction que vous venez de m'accorder, plus libre de vous dire aussi que je voudrais la recevoir comme un hommage rendu à tous ceux qui, partageant le même combat du doctorat et qui n'en ont reçu aucun privilège, mais ont connu au contraire malheur et désespoir. Il me restera alors à vous en remercier, du fond du cœur, et à vous faire publiquement, en témoignage personnel de gratitude, la même et ancienne promesse de fidélité que chaque artiste vrai, chaque jour, se fait à lui-même, dans le silence.

Preamble

Adaptation is the driving force of survivability, leading to evolution. Metazoan cells have the specific abilities to change their shape, move, divide, anchor, communicate and differentiate according to extracellular and environmental cues. All these processes are standard features needed at any living scale, from the lonely zygotic cell to a completely mature multicellular organism with its inner symbiosis between different tissue layers. My PhD project focuses on the steps between these two extreme parts of the development spectrum. Especially the phases that succeed the fertilisation up to the 6-cell stage. Specific molecular and cellular content segregation is needed during each early embryonic phase to achieve the proper differentiation processes. This vital phenomenon relies on precise and delicate spatio-temporal regulation of cell events such as polarisation, division and cell interaction. Together it will physically segregate molecular content according to the cellular neighbourhood position. All the previously quoted cell mechanism relies on a close interplay between the three types of the cytoskeleton. These three cellular “bones” comprise microtubules, intermediate filaments and actin. Microtubules are responsible for the global architecture of the cells, arranging organelles and playing an indispensable role in chromosome segregation and vesicular and organelle trafficking. Intermediate filaments are relatively stable structures, and their role is to reinforce cellular cohesion by anchoring mechanisms. Actin filaments provide mechanical forces to drive cell shape changes, motility and cytokinesis. They also directly influence cytoplasm viscosity and are connected with all the organelles, the nucleus, and the plasma membrane to coordinate every cellular partner during cellular events, cell shape changes and movement. The fundamental unit of this actin cytoskeleton is the single monomer of the globular actin protein, G-Actin. This building block is polymerising into filaments (F-Actin). A plethora of regulatory proteins is called Actin Bindings Proteins (ABPs) and taken together with G-Actin, and F-Actin, they compose the actin proteome. This actin proteome will cooperate in organising these filaments into structured networks of different natures, either parallel, anti-parallel, branched or crosslinked. Then, these structures assemble and lead to dedicated architectures that are the mechanical basis to drive motility, interactions, polarisation, division, differentiation and, in fine, adaptation. My PhD work is focused on studying this actin proteome and dedicated architecture during the early development of the *C. elegans* embryo.

Introduction

Chapter 1: Actin Proteome and their architectures

1- Actin assembly dynamics and Actin Bindings Proteins

The diversity of actin architectures and the fulfilment of their functions rely on a variety of auxiliary proteins called Actin Bindings Proteins. These ABPs must be finely spatio-temporally regulated to adapt the cellular response regarding the *in vivo* actin dynamics.

a. Globular actin and Filamentous actin

Actin is one of the most abundant proteins in eukaryotic cells. Its globular and monomeric form, called G-Actin, is a protein of 42kDa with a diameter of ≈ 5.4nm (Collins and Elzinga, 1975). This G-Actin assembles and polymerises into filaments composed of a double right-handed helix called filamentous actin or F-Actin with a diameter of 8nm. They have a persistent length of approximately 10µm and a helical pitch of 72 nm (Fujii et al., 2010; Holmes et al., 1990; Oda et al., 2009). Actin is a polarised protein, and its polarity is transferred at the scale of the filament (Figure 1), which has a fast-growing end, called the "barbed" end or the "+" end, which is highly dynamic and a slow-growing end, called the "pointed" end or the "-" end, which is less dynamic. The barbed end is the target-binding cleft where regulatory protein can tune the filament elongation, and the pointed end is the nucleotide-binding groove where ATP is located (Pollard, 2016) (Figure 1.A.B). To polymerise, G-actin has to nucleate. This nucleation step consists of forming an actin seed composed of dimers or trimers of G-actin (Kabsch et al., 1990). After reaching this step, the elongation continues more efficiently, and the elongation rate is a direct function of the available monomers (Pollard, 2016) (Figure 1.C). Nevertheless, *in vitro* data showed that the kinetics of this nucleation step is thermodynamically unfavourable (Pollard, 2016). *In vivo*, G-actin uses ABPs from the nucleator family to overcome this thermodynamic barrier (Pollard, 2016) (Figure 1.D).

The monomeric form of actin is encoded by six different sequences in the Human Genome: ACTA1, ACTA2, ACTB, ACTC1, ACTG1, and ACTG2. These sequences have 90% of identity despite a broad cellular or tissue localisation pattern. Indeed, ACTB and ACTG1 encode the "cytoplasmic" actin and the four others code for the "muscular" actin. Cytoplasmic

actin can be considered ubiquitous because it is present in any cell type at any given time (Chen et al., 2021, p. 202; Kyheröinen and Vartiainen, 2020; Parker et al., 2020). *C. elegans* has five coding sequences for actin: *act-1, act-2, act-3, act-4* and *act-5.* Their nucleotide sequences are heavily conserved as the human actin sequences, and their cellular and tissue expression can vary. *Act-1, act-2* and *act-3* form a cluster on the chromosome V of the *C. elegans* genome and encode for the cytoplasmic actin. Interestingly *act-2* share 98% of its identity with the human ACTB and 97% with the human ACTG1. These sequence similarities make the study of *C. elegans* cytoplasmic actin particularly relevant and portable to the *Homo Sapiens* actin.

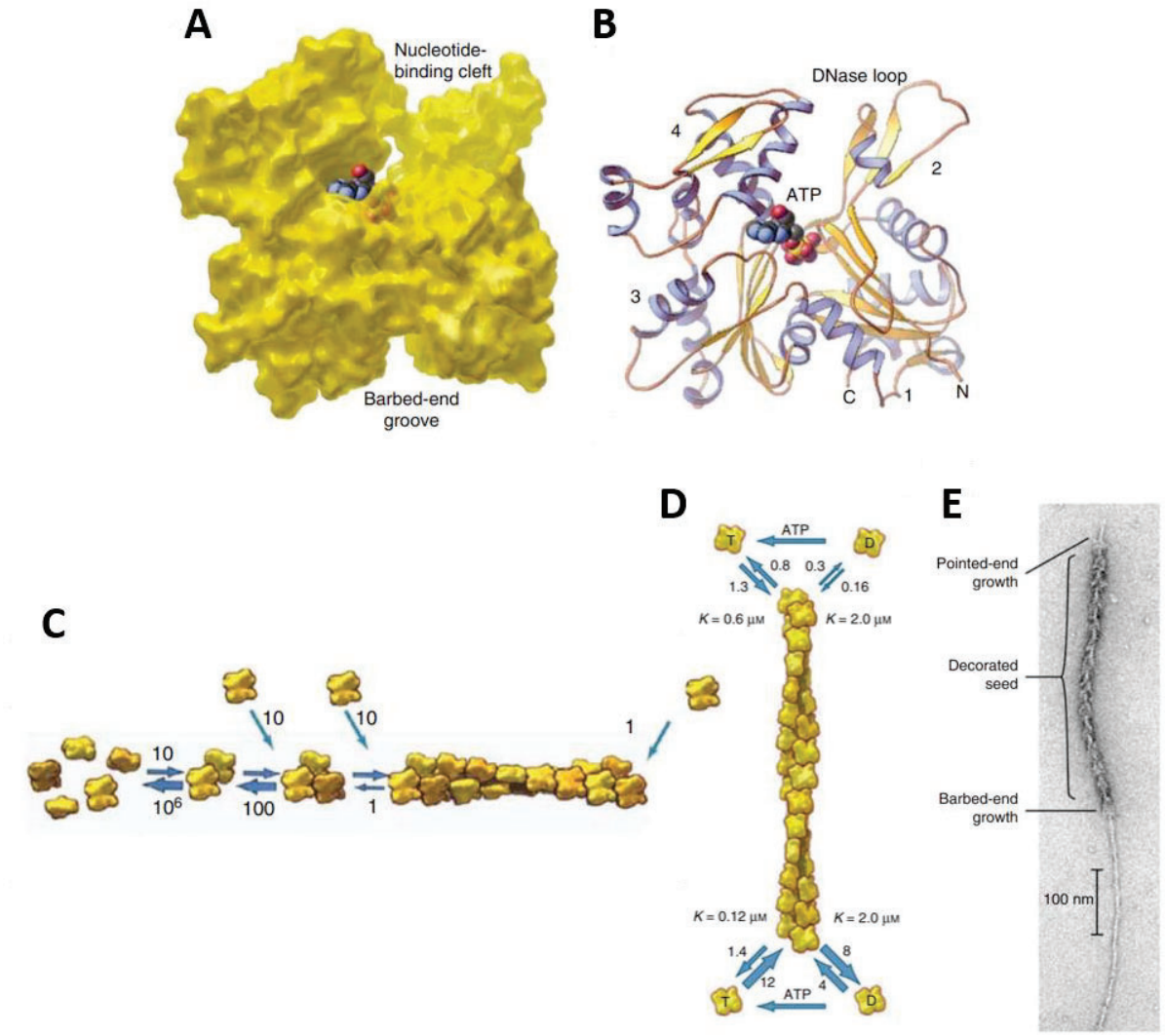

Figure 1: From Globular actin to Filamentous actin

(**A**) Space-filling model of actin showing the nucleotide-binding cleft with ATP in situ and barbed-end groove. (**B**) Ribbon diagram of the actin molecule with space-filling ATP . N, amino terminus; C, carboxyl terminus. Numbers 1, 2, 3, and 4 labels the four subdomains. (**C**) Mechanism of nucleation, showing monomers, a dimer, a trimer, and a filament, with estimates of the rate constants for each step. Unit of association rate constants, $\mu m^{-1}sec^{-1}$; unit of dissociation rate constants, sec^{-1}.(**D**) Diagram showing the rate constants for actin association and dissociation at the two ends of an actin filament. The pointed end is at the top, and the barbed end is at the bottom. Unit of association rate constants, $\mu m^{-1}sec^{-1}$; unit of dissociation rate constants, sec^{-1}. The K values are the ratios of dissociation rate constants to association rate constants, the critical concentrations for each of the four reactions. The horizontal arrows indicate the exchange of adenosine diphosphate (ADP) for ATP.(**E**) Electron micrograph of a negatively stained actin filament. A seed was first decorated with myosin heads and then allowed to grow bare extensions. Elongation was faster at the barbed end than at the pointed end.Figures and legends are extracted from (Pollard, 2016).

b. Profilin

In vivo, available monomers of G-Actin for spontaneous nucleation can be sequestered by Actin Binding Proteins called Profilin. Profilin is a small protein of about 14 KDa that binds to actin-G monomers' barbed ends (Schutt et al., 1993) (Figure 2). It has different isoforms with considerable variation in its primary structure. Despite these variations, the overall protein fold is well conserved (Eads et al., 1998; Thorn et al., 1997). In *C. elegans*, profilin is encoded by three different genes, which are *Pfn-1, Pfn-2* and *Pfn-3*. Notably, *Pfn-1* is reported to be essential for the early embryogenesis process (Polet et al., 2006). Profilin plays a prominent role in actin cellular homeostasis due to steric interference with G-Actin barbed end availability for polymerisation (Almo et al., 1994; Kang et al., 1999; Pollard et al., 2000). Profilin functions are triple. First, inhibiting the spontaneous formation of the actin seed (dimer and trimers of actin monomers), thus inhibiting spontaneous nucleation (Pollard et al., 2000); second, blocking polymerisation at the pointed end, which leads to a polarity of the actin assembly at the barbed end of the actin filament (Pring et al., 1992); third, Profilin complexed with G-actin can interact with others ABPs that catalyse the nucleation process, these proteins are called actin nucleators, which are the Arp2/3 (Chereau et al., 2005) complex and the formins (Paul et al., 2008).

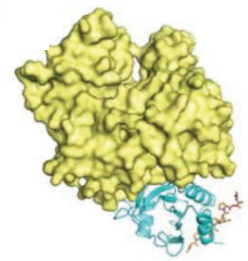

Figure 2: Profilin

Space-filling models of the actin monomer with ribbon diagrams of Profilin. The ATP-binding cleft is at the top and the barbed end groove is at the bottom. Figures and legends are extracted from (Pollard, 2016).

c. Formin

Formin protein was discovered initially from the transcriptional analysis of mouse limb deformity (Woychik et al., 1990). Formin is a large family of proteins. There are 15 different formins in humans (Schönichen and Geyer, 2010) and 7 in *C. elegans* (Mi-Mi et al., 2012) (Figure 3.A). These proteins have very conserved multi-domains and are dimeric, with about 1000 amino acids in total. These domains are Formin Homology 1 (FH1) and Formin Homology 2 (FH2). Outside of these highly conserved FH1 and FH2 domains, the Formin family have distinct features that regulate their localisation and activity state. First, an anchoring domain or Binding Domain (BD) interacts with specific membrane lipids (e.g., PIP2). Second, an activation domain, which is composed of a RhoGTPase-Binding-Domain (GBD) that can bind to small GTPase (e.g., CDC-42), a Diaphanous Inhibitory Domain (DID) and a Diaphanous Autoregulatory Domain (DAD). Mechanistically, FH1 and FH2 domains have a distinct role in fulfilling the two purposes of this large family of proteins: catalysing actin nucleation and actin filament elongation.

On the one hand, Formins and specially FH2 domains interact in a Homodimeric manner. Two FH2 domains form a ring-shaped structure surrounding the actin filament barbed ends (Xu et al., 2004). This association between barbed end and FH2 domains directly impacts the two formins' roles. First, during the nucleation step, the FH2 domain binds directly to the actin monomer's barbed end and stabilises the actin seed's formation (Otomo et al., 2005). Second, during the elongation step, the FH2 domains follow the actively polymerising barbed end in a processive manner (Kovar and Pollard, 2004).

On the other hand, the FH1 domain is an intrinsically disordered protein(Courtemanche and Pollard, 2012; Higgs, 2005) with a proline-rich region that binds to the profilin or the profilin-actin complexes, which increases the local concentration of available actin monomers for polymerisation at the barbed end of a growing filament (Paul et al., 2008). This protein family have its regulatory mechanism. At an inactivated state, the DID and DAD domains interact, wrapping in a "close" form the FH1 and FH2 domains together, which prevents actin polymerisation. At an activated state, GTPase, like RhoA, Rac1 or Cdc42, interacts with the GBD domain, which removes the interaction between the DID and DAD domains (Földi et al., 2017) (Figure 3.B). FH1 and FH2 domains are now in an "open" form. They allow FH2 to bind to the barbed end and processively follow FH1, which is here to gather

profilin-actin complexes, catalysing the addition of actin monomers to the nascent filament, which is built in a linear manner (Courtemanche, 2018) (Figure 3.C). *In vivo*, the nucleation step catalysed by formin needs to be spatio-temporally regulated. Spatial regulation came from the Bindings Domain (BD) of formin. It allows the protein to be embedded in the plasma membrane. Temporal regulation comes from the Rho signalling pathway, which begins at the plasma membrane. Downstream, the Rho signalling pathway releases the DAD domain from the DID domain inhibition and brings the formin to the "open" conformation allowing nucleation to be promoted and the actin polymerisation to start at the actin cortex at a specific timing point. These regulatory characteristics of formins tune the dynamics of the actin cytoskeleton and drive physiological processes such as cell division, cell polarisation, cell migration and morphogenesis (Rottner et al., 2017). Together, formins are recruited beneath the plasma membrane to overcome the actin seed nucleation process's thermodynamic barrier and increase the polymerisation rate of the growing actin filament toward its barbed end. These linear filaments will serve as building blocks for a complex meshwork with dedicated actin architectures necessary for crucial cellular processes, such as the actomyosin cortex, cytokinesis ring, stress fibres cell junctions, and filopodia.

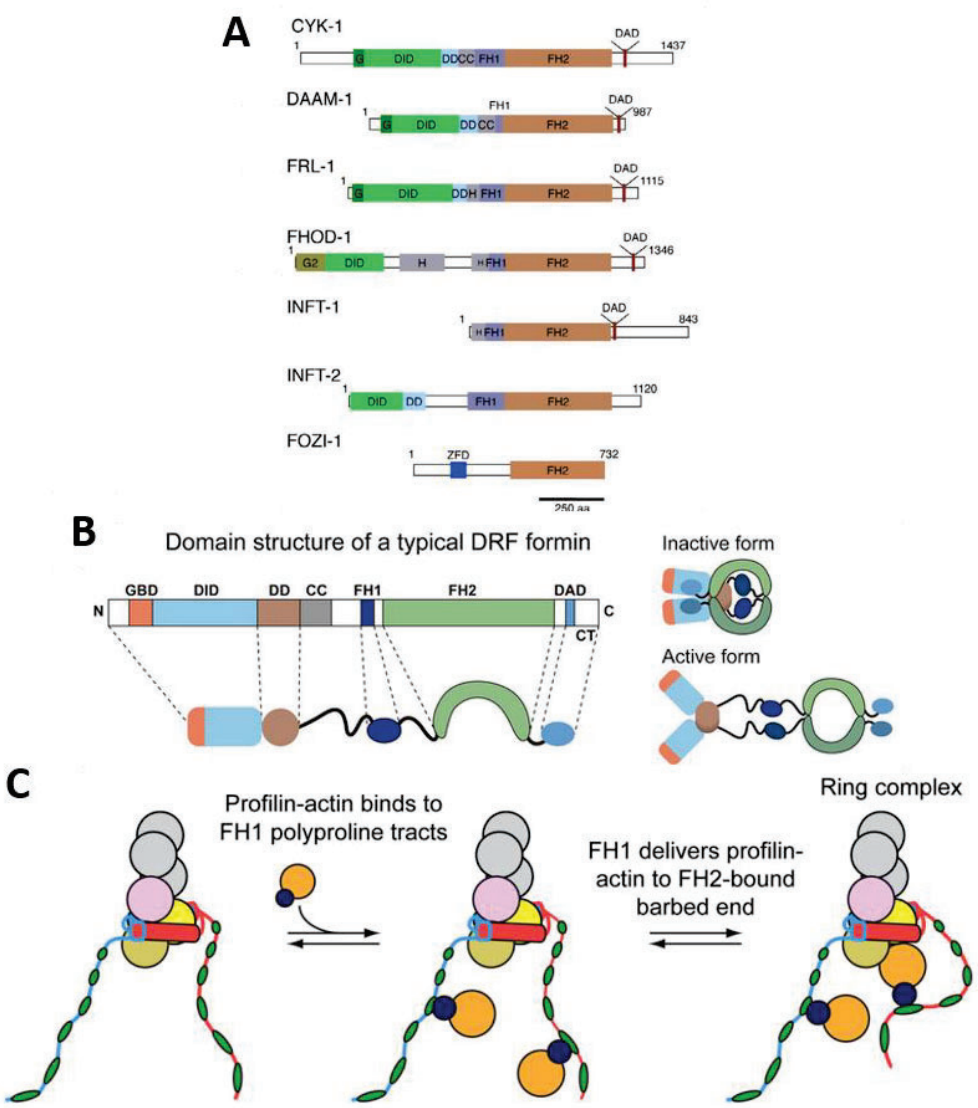

Figure 3: Formins and their mechanics of activation and filaments elongation

(**A**) Seven formin genes of C. elegans with protein-coding exons colour-coded to match predicted product structural domains, including DIA-related formin G domains (dark green), FHOD-specific G domain (G2; olive), DIDs, dimerisation domains (DD), helical (H) or coiled-coil (CC) regions, FH1 domains, FH2 domains, core DAD sequences, and zinc finger domain (ZFD). Extracted from (Mi-Mi et al., 2012) (**B**) Domain structure and regulation of a formin (DRF). The domains abbreviated are as follows: GTPase binding domain (GBD), diaphanous inhibitory domain (DID), dimerisation domain (DD), coiled-coil region (CC), formin homology 1 (FH1) and 2 (FH2) domains, followed by the diaphanous auto-regulatory domain (DAD) and the C-terminal tail (CT). formins are regulated by auto-inhibition, where binding of the DAD to the DID domain keeps the molecule closed and inactive. The binding of an activated Rho GTPase to the GBD releases the DAD from DID, subsequently opening and activating the protein. Extracted from (Földi et al., 2017). (**C**) Cartoon representation of the addition of a profilin-bound actin subunit (dark blue and orange circles) to the barbed end of an actin filament bound by a representative formin FH1FH2 construct. The unstructured FH1 domains extend outwards from the FH2 dimer and contain multiple polyproline tracts (in this case, six green ovals per FH1 domain). Profilin-actin complexes bind the polyproline tracts and are delivered directly to the barbed end in a Bloop closure. Extracted from (Courtemanche, 2018).

d. Arp2/3 complex

Arp2/3 complex is composed of the Actin-related proteins Arp2 and Arp3, as well as five other proteins named ARPC1(p41), ArpC2(p34), ARPC3(p21), ArpC4(p20), and ArpC5(p16), make up the seven tightly bound subunits that make up the Arp2/3 complex (Machesky et al., 1994; Rouiller et al., 2008) (Figure 4.A.B). Based on its affinity for the actin monomer-binding protein profilin, the complex was initially isolated from *Acanthamoeba castellanii* (Machesky et al., 1994). It was subsequently purified from several different species, including humans (Welch et al., 1997), the yeast Saccharomyces cerevisiae (Winter et al., 1997) and other organisms (Ma et al., 1998; Rohatgi et al., 1999). *C. elegans* homologues of the Arp2/3 complex are *arx-1* for Arp3, *arx-2* for Arp2, *arx-3* for p41, *arx-4* for p34, *arx-5* for p21, *arx-6* for p20, and *arx-7* for p16 (Sawa et al., 2003). These different purified protein complexes share the same component composition, indicating that the complex originated early in the development of eukaryotic cells. The nascent Arp2/3 complex is inactive (Blanchoin et al., 2000; Machesky and Gould, 1999; Robinson et al., 2001). To be activated, it requires the presence of a pre-existing actin filament (Machesky et al., 1999) and an activator of the Nucleation Promoting Factor (NPF) family (Machesky et al., 1999; Welch et al., 1998). The NPF family is characterised by a C-terminal homology domain called VCA divided into three motifs, each of which plays a major role in activating the Arp2/3 complex. First, the V motif (for "Verprolin homology" or also called WH2 for "WASp homology 2"). Second, the central C-connector motif. Third, the C-terminal A motif consists of an "Acid" sequence. Both the C and A motifs contribute to the association with the Arp2/3 complex (Marchand et al., 2001) and allow conformational change of the latter heterodimer (Goley et al., 2004; Rodal et al., 2005). The V motif interacts with a G-actin monomer (Chereau et al., 2005; Marchand et al., 2001). The VCA domain is sufficient for activating the Arp2/3 complex and initiating branching actin polymerisation (Machesky et al., 1999). In the inactive form, the two subunits, Arp2 and Arp3, are distant from each other (Pollard, 2007; Rouiller et al., 2008; Volkmann et al., 2001). Following activation of the complex by an NPF, Arp2 and Arp3 dimerised and mimicked the barbed end of an actin filament, which can then be elongated (Robinson et al., 2001; Rouiller et al., 2008; Volkmann et al., 2001). Taken together, it forms the actin seeds that initiate the daughter filament's elongation. This activation responds to upstream cues that trigger the formation of new actin filaments. From a cytoskeletal structure point of view, Arp2/3 complex

cross-links newly generated filaments into arrays of Y-branches with a characteristic branch angle of 70° (Blanchoin et al., 2000; Mullins et al., 1998) (Figure 4.C). This interaction between the NPF and the "mother filament" keep the Arp2/3 complex in its active and stable form (Goley et al., 2004; Rodal et al., 2005) and also stabilised by the Arp2/3 complex, which is located at the base of the Y-branch between the filaments, both *in vitro* and *in vivo* (Svitkina and Borisy, 1999; Volkmann et al., 2001). Based on investigations of the formation of cortical actin networks at the leading edge of motile cells, specifically in lamellipodia and the reconstitution of actin-based motility from pure proteins *in vitro*, Arp2/3 complex-mediated the assembly of a dense and contractile meshwork of short actin filament. These short filamentous networks require an interplay with another Actin Binding Protein, Capping proteins, to generate sufficient actin-driven forces that can deform a membrane or push objects forward (Loisel et al., 1999).

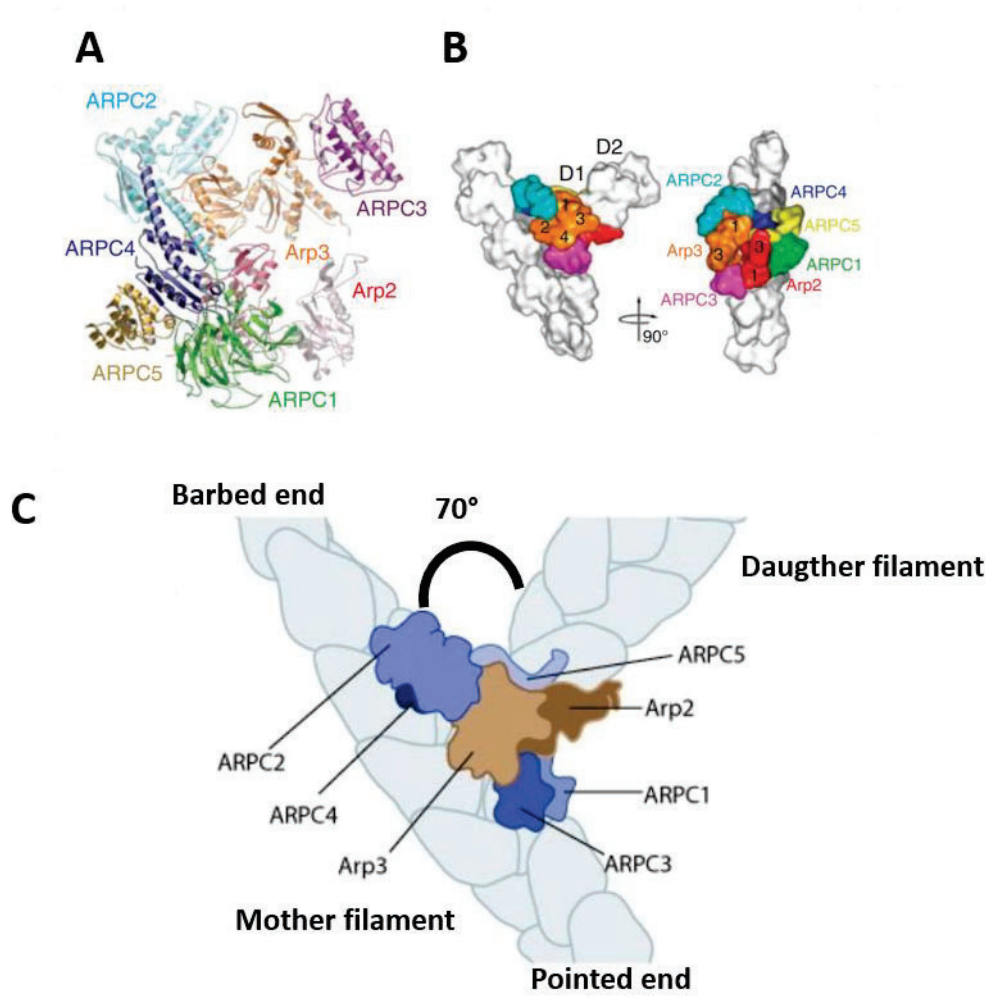

Figure 4:The Arp2/3 complex and its Y branching

(**A**)Ribbon diagram showing the seven subunits of the Arp2/3 complex. (**B**) Model of the branch junction from reconstructions of electron micrographs. (**C**) Arp2/3 complex binding on a mother filament and initiating a new branched and recruiting actin monomers. Figure adapted from (Rouiller et al., 2008).

e. Capping protein

Capping protein is a heterodimer of 64 kDa containing alpha- and beta-subunits (Eckert et al., 2012) which are comparable in structure and that firmly bind to actin filament barbed ends, preventing the polymerisation and depolymerisation of G-Actin at this barbed end (Edwards et al., 2014; Kim et al., 2010; Wear et al., 2003). This steric blocking machinery is realised by the "mushroom" conformation between the alpha and the beta subunit (Edwards et al., 2014) (Figure 5). Capping proteins are highly conserved in nearly all eukaryotic species, including humans, fungi, and plants, and it is present in all of their cells and tissues (Cooper and Sept, 2008). In *C. elegans*, capping protein is also found and is composed of two subunits encoded by two genes, cap-1 (Alpha-subunit) and cap-2 (Beta-subunit); the proteins produced are respectively CAP-1 and CAP-2. Capping protein interactions largely influence the behaviour of the actin filament barbed ends. For instance, in striated muscle cells, capping proteins are a crucial component of the Z-disk in the sarcomere, giving rise to its other name CapZ, where it blocks the actin filaments barbed ends (Schafer et al., 1995). Capping proteins is also mandatory for establishing cortical actin and membrane protrusion in migratory cells (Cooper and Sept, 2008; Mejillano et al., 2004) in a close interplay with the Arp2/3 complex inside dendritic actin filament networks (Wear et al., 2003). Capping proteins are here to maintain the contractility of a dense and branched network with short actin filaments. Another role of capping protein is to inhibit the filament's growth and limits the surplus of filament, and maintain the availability of the pool of G-actin subunits for other filament nucleation and elongation at different locations. During *C. elegans* early embryogenesis, it has been reported that capping proteins play a role in stabilising the position of the pseudocleavage furrow and the correct completion of the polarisation steps with the proper definition of the pole of polarity proteins (PAR) PAR-2 and the PAR-6 domains (Bhanshali, 2016).

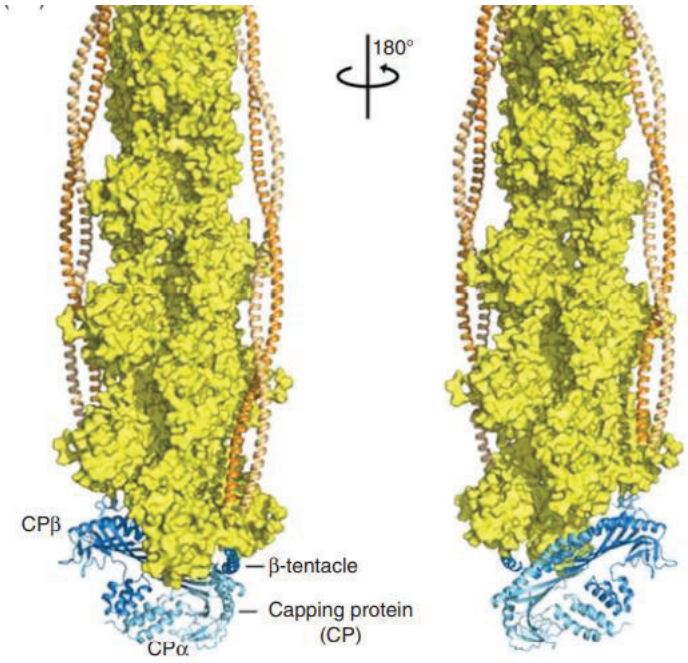

Figure 5: Capping protein in interaction with actin filaments

Space-filling model of a short filament with heterodimeric capping protein (CP) in cyan and blue at the filament barbed end. Figure adapted from (Pollard, 2016).

2- Actin *in vivo*, structures and roles

Actin is assembled in different architectures designed to fulfil various cellular roles. In this section, we uncover the main types of actin architectures found in a generic range of the cellular model. I will also focus on these structures encountered in our model system: the *C. elegans* embryo. Researchers have used the Caenorhabditis elegans model's transparency and reproducibility for decades to examine how actin networks are controlled and adapted during developmental processes (Agarwal 2019). The zygotic stage that happens right after fertilisation is particularly studied. During this phase, many remarkable cell events are entangled, such as cellular polarisation, specific segregation of molecular content (Rose and Gonczy 2014), symmetry breaking, microtubule assembly, and spindle displacement (Cowan 2004; Begasse 2011). The actin network is organised in various structures, such as the actomyosin cortex, the cytokinesis ring, and some motile architecture called lamellipodia and filopodia to achieve all these mechanisms (Blanchoin et al., 2014) (Figure 6).

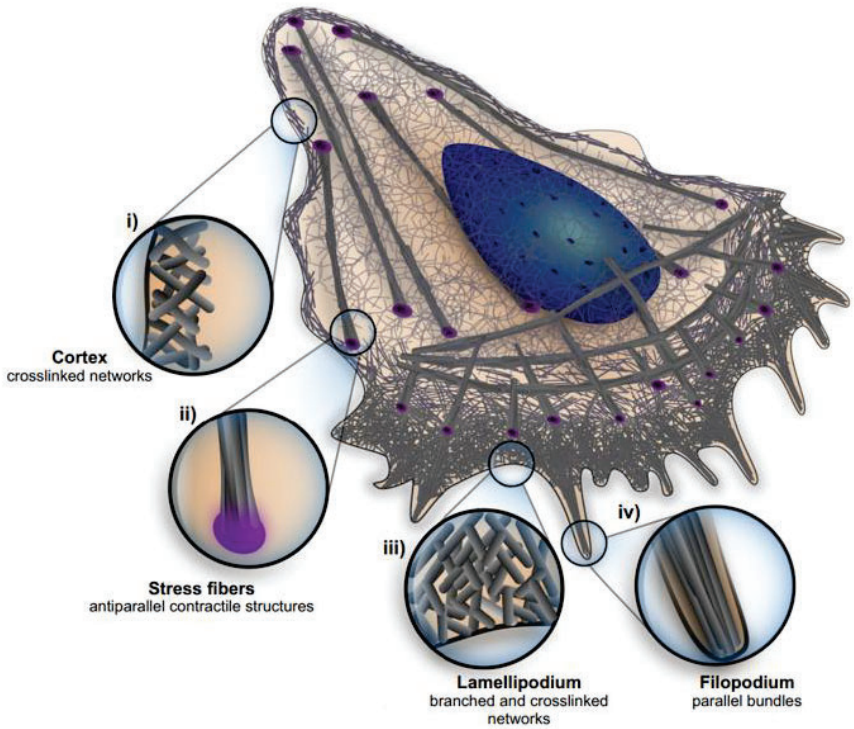

Figure 6: Overlay of actin architecture and mechanics in the moving cell.

schematic representation of the cell with the different architectures indicated: i) the cell cortex; ii) an example of a contractile fiber, the stress fiber; iii) the lamellpodium; and iv) filopodia. The zoom regions highlight architectural specificities of different regions of the cell. Figure and legend extracted from (Blanchoin et al 2014)

a. Actomyosin cortex

Most animal cells have a cellular cortex, a thin actin network located beneath the cellular plasma membrane that lines the inner side of the cell. This network is interconnected with actin-lipid bindings proteins such as the Ezrin family (Biro et al., 2013; Bretscher et al., 2002). Its thickness depends on the experimental model, ranging from 50nm to 200nm (Morone et al., 2006) and can increases up to 1.4 to 4 µm in meiotic mouse oocytes (Chaigne et al., 2013). It comprises a dense meshwork of actin filaments and about 150 regulatory proteins, the ABPs (Biro et al., 2013). This actin cortex is also named actomyosin cortex for the reason that, in addition to actin, its second crucial component is the molecular motor from the myosin family, especially the Non-Muscle Myosin-2 (NMY-2) (Henson et al., 2017). In cooperation with actin filament, this myosin gives the key features of this network its contractile properties (Salbreux et al., 2012; Sens and Plastino, 2015). Actin filaments are pulled by NMY-2, causing the network to constrict. These forces create cortical tension, a key element in determining cell surface tension. In addition, the cortical actin's turnover is a few tens of seconds (Fritzsche et al., 2013; Mukhina et al., 2007) and impacts the cortical viscoelasticity and its contractile properties (Hiraiwa and Salbreux, 2016; Salbreux et al., 2012; Turlier et al., 2014). Last but not least, the cortical tension is not only regulated by myosin activity and actin turnover; the activity of the actin regulatory proteins, ABPs, also regulates it. All these regulation partners, all along the cell surface, create a gradient of cortical tension that is implicated in cell shape changes such as those seen during cell migration, cell division, and tissue morphogenesis (Levayer and Lecuit, 2012; Maddox and Burridge, 2003; Maître et al., 2016; Matzke et al., 2001; Sedzinski et al., 2011; Stewart et al., 2011). These cell shape changes can be caused by a swift reaction of the actomyosin cortex to external stimuli. For instance, during cortical blebbing and cell migration (Charras and Paluch, 2008), cell division (Stewart et al., 2011), and tissue morphogenesis(Munjal and Lecuit, 2014). Importantly, improper control of cortical contractility has been connected to developmental abnormalities, such as problems in neural tube closure (Escuin et al., 2015) or even cancer and immunodeficiencies (Moulding et al., 2013; Remmerbach et al., 2009). Taken together, the actin cortex has a vital impact on cellular physical properties, and these control the behaviour of cells and can affect their commitment to a particular lineage (Engler et al., 2006; McBeath

et al., 2004; Paluch et al., 2016) and their gene expression and, thus, can modulate and feedback into cell fate (Ege et al., 2018; Knöll and Beck, 2011).

i. *C. elegans* zygotic actomyosin cortex

C. elegans is a unique system to study the actomyosin cortex, thanks to its large and completely transparent embryo, which allows detailed microscopic observation of a large and flat cortex (Reymann et al., 2016). We will examine the actomyosin cortex and its highly active and contractile properties during the zygotic stages, especially the polarisation phase. Like other systems, many ABPs cooperate to activate and regulate the mechanical properties of the actomyosin cortex and actin turnover (Najafabadi et al., 2022; Yan et al., 2022). A particular category of ABPs influences actin filament dynamics: actin nucleators, the formin family, the Arp2/3 complex, and the capping protein. These proteins are already described in section 1 of this chapter. Interestingly, the regulation between ABPs and cortical properties is particularly illustrated and studied during zygotic polarisation. Before this crucial phase, cortical actomyosin foci create cortical ruffles located around the oocyte cortex(Figure 7.A). When the sperm content approaches the future posterior pole, cell symmetry is lost. Sperm entry and its centrosome lead to a local downregulation of the cortical myosin (NMY-2) and, de facto, inhibits actomyosin contractility at the posterior pole of the newly fertilised zygote (P0) (Figure 7.B). It creates a density gradient of actomyosin between the anterior and the posterior pole, thus generating a contractility gradient. This generates an actomyosin flux toward the anterior side, increasing the density of the actomyosin cortex to the future anterior pole (Figure 7.C) (Pacquelet, 2017; Rose and Gönczy, 2014). Thus, initiating a shift of the cortical ruffles toward the anterior side of the freshly fertilised zygote (Figure 7.D). This cell shape changes correlate with a specific distribution of the PAR proteins embedded in the plasma membrane (Munro et al., 2004). Remarkably, NMY-2 cooperatively establishes the PAR protein's polarisation (Gross et al., 2019). Indeed, in parallel with the formation of these two cortical domains with different actomyosin activities, there is specific molecular segregation of the PAR proteins, which is also happening. The PAR proteins are separated into two categories, the anterior PAR proteins (aPAR), PAR-3 and PAR-6 and the posterior PAR proteins (pPAR), PAR-1 and PAR-2; both of these subgroups have a mutually antagonistic relationship between them (Rose and Gönczy, 2014). Importantly, pPAR has the ability to

inhibit NMY-2 activity. Together with the antagonistic effect between aPAR and pPAR and the NMY-2 inhibition by pPAR, it exacerbates the anterior accumulation of NMY-2 as well as aPAR, increasing the contrast between the anterior and the posterior pole in terms of actomyosin density and pole identity. This embryonic cortical polarisation reaches its paroxysm by forming a deeper ingression which can be morphologically comparable to the cytokinetic one, which is therefore named the pseudocleavage furrow (Figure 7.D), which creates the two cortical domains of polarity, the anterior pole and the posterior pole with an asymmetric spatial distribution between them prior to the anterior side (Munro et al., 2004). Polarisation continues until the maintenance phase (Lang and Munro, 2017). Moreover, this actomyosin polarisation does not only rely on NMY-2 and PAR proteins distribution. Indeed, cortical properties are also regulated by ABPs that are also polarised during this crucial step, with a mutualistic effect between the specific ABPs segregation that tunes the cortical mechanical parameters and the polarisation of PAR proteins (Munro et al., 2004). In addition, we can speak about the role of an actin bundler, such as PLST-1, in cortical stability. It plays an essential role in regulating the interconnectivity of the actin network and tuning the anterior cortical tension (Ding et al., 2017). Moreover, HMR-1, a cadherin reported to be involved in cell-cell adhesions, plays a role independently from its initial adhesion purpose because there is only one cell in the zygote. It was shown that HMR-1 is also involved in tethering the cortex to the cell membrane, spatially regulating the upstream Rho Signalling that affects the actomyosin cortex stability, flows, and attachment to the cell membrane (Padmanabhan et al., 2017). This relationship will be further discussed in detail in chapter 3. After this polarisation step, the asymmetric distribution of actomyosin, ABPs and PAR proteins define a specific position of the interface between the anterior and the posterior pole that is then fixed by the position of the future cytokinetic ring.

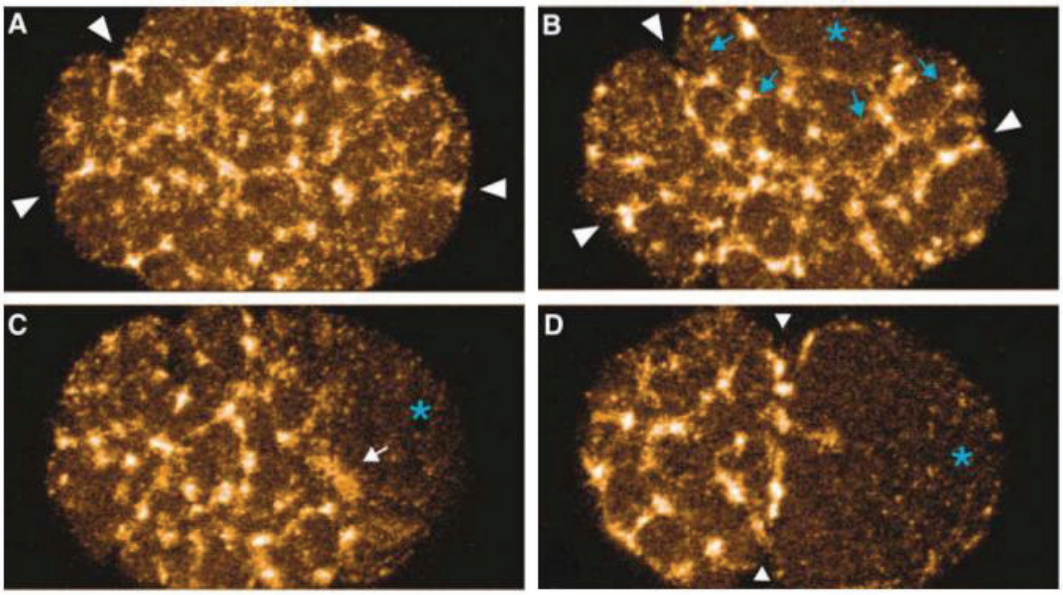

Figure 7: The dynamic reorganisation of *C. elegans* actomyosin cortex

Surface views of cortical NMY-2 during the polarisation phase. (**A**) at late meiosis II (**B-C**), during cortical flow, and (**D**) at pseudocleavage. Blue asterisks indicate positions of the sperm MTOC. Arrowheads in (**A**) and (**B**) indicate colocalization of foci and furrows on the egg's surface. Blue arrows in (**B**) indicate foci moving away from the sperm MTOC. White arrow in (**C**) indicates a new focus forming at the edge of posterior clear zone. Small white arrowheads in (**D**) indicate the pseudoclevage furrow. Figure extracted from (Munro et al., 2004).

b. The cytokinesis ring in *C. elegans* embryo

The anteroposterior polarity needs to be established entirely by realising the first embryonic division and giving rise to two different daughter cells, the AB and P1 cells. This division is realised by another cortical structure that emerges to seal this zygotic asymmetric division, the cytokinesis ring. The cytokinesis ring is a contractile actin structure that drives membrane ingression and segregates molecular and cellular components between two daughter cells (Figure 8.A.B) (Leite et al., 2018). Cytokinesis happens in two phases. The first is its assembly at a precise position in terms of centring or specific offset and orientation, and the second is its ingression with proper kinetics. The assembly step requires the cooperation of the Arp2/3 complex and CYK-1 to nucleate the actin filament network that belongs to the cortex during cytokinesis (Chan et al., 2018). It was also shown that actin filaments align at the cytokinetic ring location because of convergent cortical flows towards the cell equator. These flows were sufficient to drive the ring formation (Li and Munro, 2021; Reymann et al., 2016) (Figure 8.C.D). For the kinetics of cytokinesis, also called constriction, both nucleators, Arp2/3

and CYK-1, as well as NMY-2, are required for its completion. The Arp2/3 complex is mandatory to temporally regulate the assembly and constriction of the contractile ring (Chan et al., 2018). CYK-1 is necessary for cytokinetic ring constriction and equatorial membrane deformation (Chan et al., 2018). Interestingly, NMY-2 is required and not sufficient to drive the ring's contractile forces (Lecuit et al., 2011; Osório et al., 2019; Sellers, 2000). Interestingly, Arp2/3 is not enriched directly at the cleavage furrow position, unlike CYK-1, which is enriched at this position and also mandatory for filaments elongation. (Chan et al., 2018). Indeed, the Arp2/3 complex positively regulates the ring assembly and constriction, mitigating CYK-1 activity via a G-actin competition (Burke et al., 2014; Chan et al., 2018). ABPs controlling cortical parameters, like PLST-1 and HMR-1, influence the cytokinetic ring's position and assembly or ingression (Agarwal and Zaidel-Bar, 2019; Delattre and Goehring, 2021; Leite et al., 2018; Pacquelet, 2017; Rose and Gönczy, 2014; Samandar Eweis and Plastino, 2020).

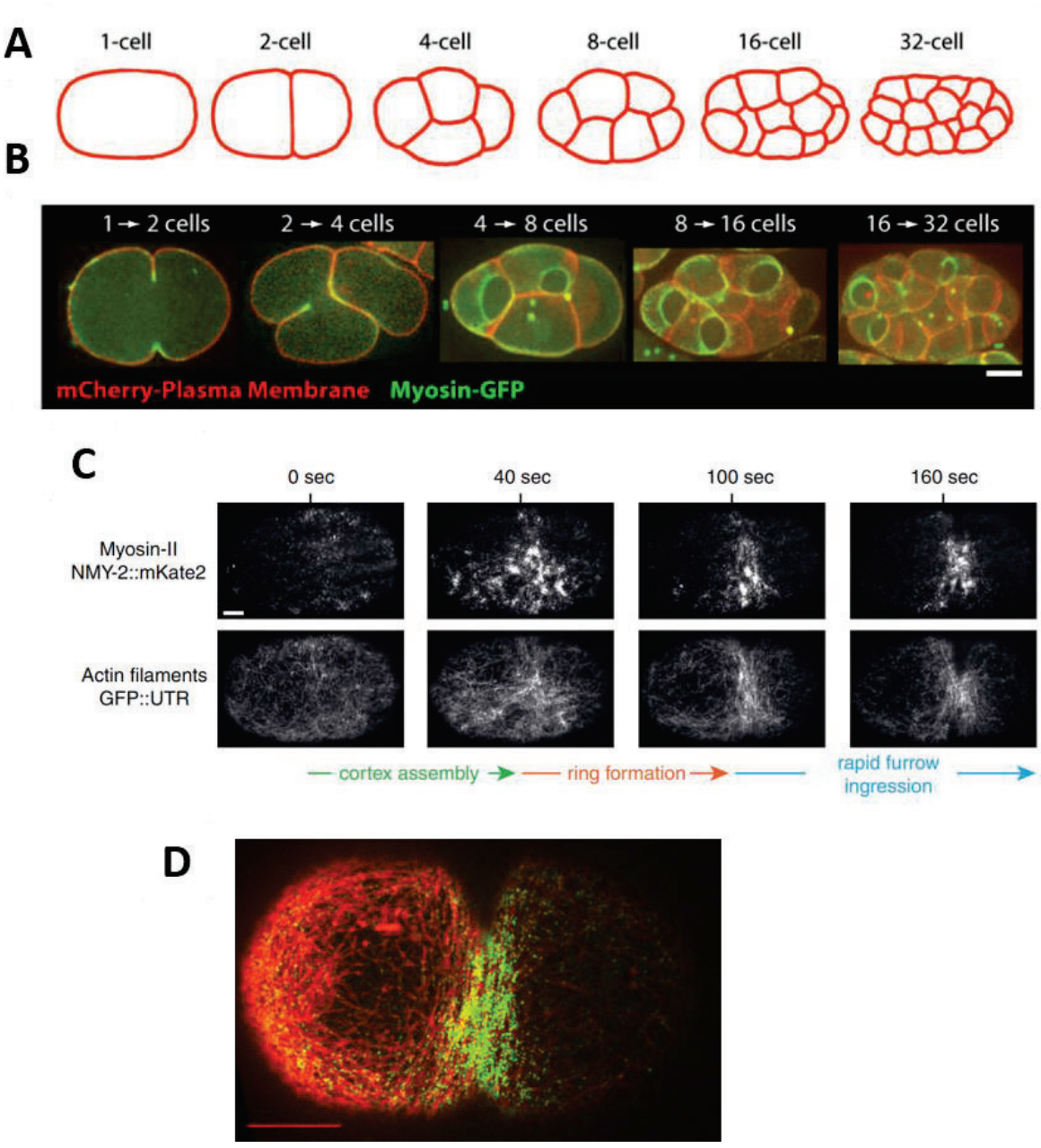

Figure 8: The cytokinesis in the early *C. elegans* embryo

(**A**) Schematic representation of cell membrane in C. elegans embryos from the 1 to the 32-cell stage. (**B**) Confocal images of embryos coexpressing NMY-2::GFP and a membrane probe tagged in mCherry (Red). Scale bar, 10 µm. Figure extracted from (Carvalho et al 2009). (**C**) Surface views of cortical myosin II (NMY-2::mKate2, top panels) and F-actin (UTR::GFP, bottom panels) obtained by near-TIRF imaging at the indicated starting by the anaphase onset Scale bars, 5 µm. Figure Extracted from (Li and Munro 2021). (**D**) Actomyosin cortical organization at the onset of cytokinesis in embryos expressing both Lifeact::mKate2 (Red) and NMY-2::GFP. Scale bar, 10 µm. Figure extracted from (Reyman et al 2016)

c. Lamelipodium and filopodium during embryogenesis

The lamellipodium is one of the main actin architectures in most motile systems. The lamellipodium comprises branched, crosslinked actin networks that assemble in a sheet-like structure protruding out at the migrating front of the cell (Figure 9.A.B). It is the fundamental element for cell movement. Localised actin polymerisation forces and pushes the cell membrane forward, thus translating the cellular centre of mass. The lamellipodium has a wide, persistent and thin optical section, allowing many studies to decipher its molecular composition. Its formation beneath the plasma membrane is triggered by the upstream signalling of the Rac subfamily of small GTPase (Ridley and Hall, 1992; Steffen et al., 2013) that will lead to the local activation of the Arp2/3 complex and the nucleation of branched actin networks (Steffen et al., 2014; Stradal and Scita, 2006). Capping proteins also accumulate at the leading edges of lamellipodia to prevent extensive actin filament elongation, keeping a dense distribution of shorter filaments and maintaining the availability of actin monomers for other nucleation events (Mejillano et al., 2004). Following nucleation, there is also a cooperative action of the other nucleator family, which is the formin. Some formins will generate actin filament subsets independent of the Arp2/3 complex, which is essential for creating lamellipodial forces and mechanical stability (Kage et al., 2017). The combined action of formins and Arp2/3 creates this important motility feature that needs to be directed to orientate cell expansion and migration (Figure 9.C).

All the types of cell migration need to be oriented (Yamada and Sixt, 2019), either if they travel along the Extra Cellular Matrix (ECM) or pass through the least resistant way. For this purpose, migrating cells used a dedicated actin structure called microspike, finger-like structure or filopodium. This filopodium is also located at the front of the cell. Filopodia are finger-like structures composed of an aligned bundle network that extends outward to the cellular body. It participates in different, sometimes independent, mechanisms such as anchoring, sensing, positioning and orientating cellular responses. They are composed of straight filaments nucleated by formins at their tip and parallelly aligned actin due to actin crosslinker proteins called fascin (Hoffmann et al., 2014; Jaiswal et al., 2013; Vignjevic et al., 2006). During embryogenesis, historically, filopodia first found in the sea urchin embryo during its first 4 and 8-cell stages (E.A Andrew, 1897). This actin finger-like structure is involved in embryonic coherence, completing cellular movement and morphogenetic events in a wide

variety of model organisms. For instance, the zippering of the epithelial sheet during the dorsal closure in the *Drosophila melanogaster* embryo (Millard and Martin, 2008); embryo compaction at the 8-cell stage in the *Mus musculus* embryo (Fierro-González et al., 2013). The questions about the molecular composition were addressed on the model organism *Dictyostelium discoideum*. It revealed that formin dDia2 were located at the tip of these filopodia, dDia2 interacted with the ABP profilin2 and Rac1, and filopodia bodies were composed of aligned parallel actin filaments (Schirenbeck et al., 2005). This specific architecture, assembly mechanism, and roles will be discussed in more detail in Chapter 2.

i. Motile structures in *C. elegans* embryo

Regarding our favourite model system, filopodia are implicated during the epibolic cellular movement of hypodermis during the ventral closure in the *Caenorhabditis elegans* lima bean stage (Williams-Masson et al., 1997). In addition, in the early stages of *C. elegans*, at the 8-cell stage, filopodia were reported to protrude toward the anterior side of the embryo (Pohl and Bao, 2010). At the same cell stage, a lamellipodium is also observed. It comes from ABpl and protrudes toward the dorsal side of the embryo (Pohl and Bao, 2010). Both of these structures are involved in chiral morphogenesis during the establishment of the bilateral body plan axis (Pohl and Bao, 2010). Recently, also during the 8-cell stage of *C. elegans* embryogenesis, another lamellipodium was described to protrude from ABpl, but this time, toward the EMS cytokinetic furrow during the EMS division, somehow participating in the EMS division itself (Caroti et al., 2021). These recent findings addressed a new set and scale of questions regarding the importance of these structures during embryogenesis and the putative dynamical diversity of their related implications.

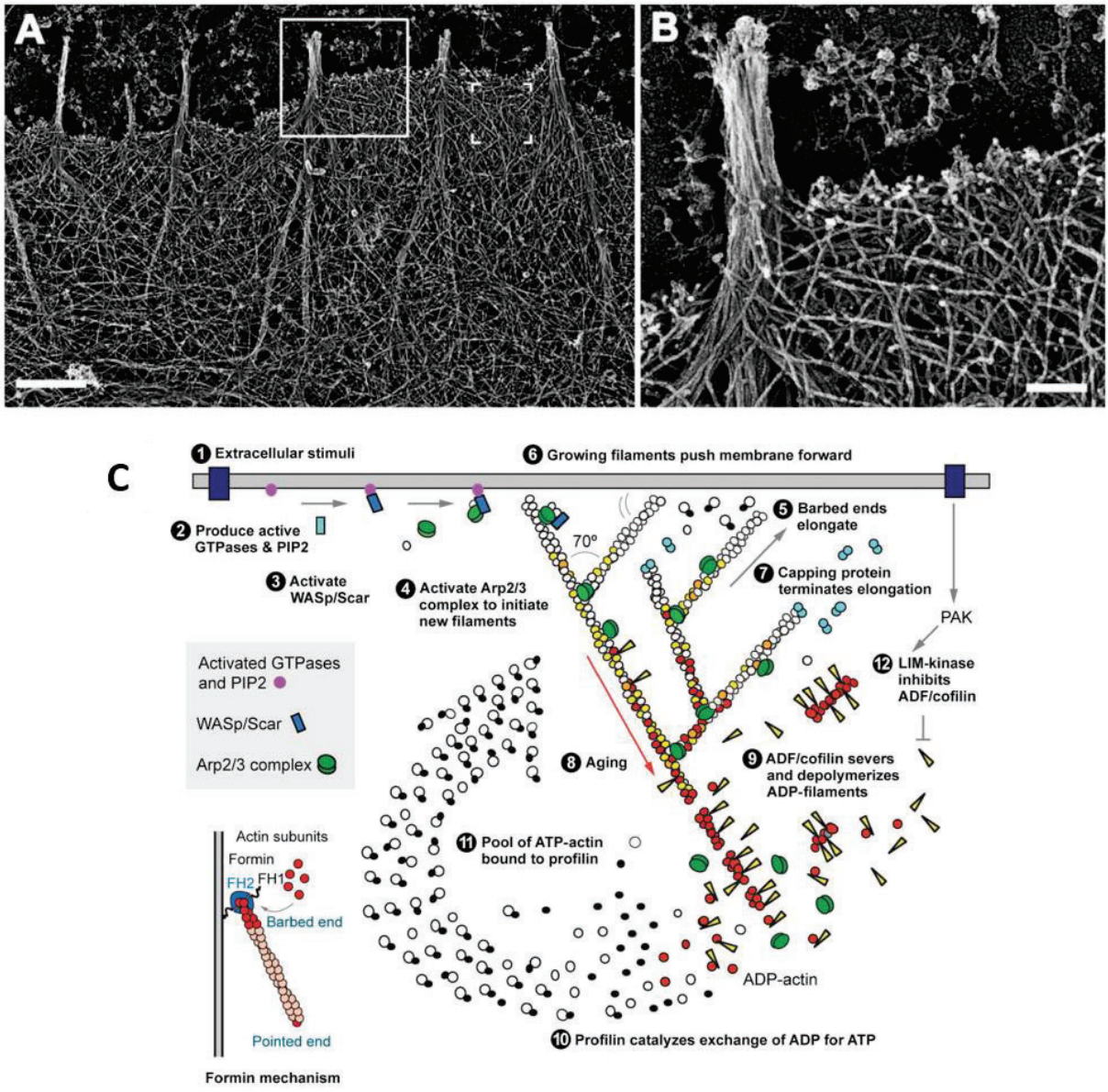

Figure 9: Details of motile structures

(**A**) EM Overview of the edge of protrusions in B16F1 Cells, scale bars indicate 1 µm. (**B**) Enlargement of the boxed region, scale bars indicate 0.2µm. Figures extracted from (Yang et al., 2007). (**C**) Overviews of the functions of actin nucleators at the leading edge of motile cells. Nucleation-promoting factors such as WASp and Scar/WAVE bring together Arp2/3 complex with an actin monomer on the side of a filament to nucleate a branch. The free barbed end of the branch grows until it is capped. Bottom left-hand corner: Formins nucleate unbranched filaments and remain attached to their barbed ends as they elongate. Processive actin polymerisation in association with a formin FH2 domain. Figure adapted from (Pollard, 2007).

Chapter 2: Filopodia, from bottom to the tip

1- Characteristic of these finger-like structures

Filopodia is a temporary protrusive structure at the leading edge of a motile cell that faces toward the extracellular environment. On an Evolutionary scale, filopodia are widely distributed in every Eukaryotes's phylogenetic group (Sebé-Pedrós et al., 2013). Filopodia are dedicated to a variety of roles, as discussed below. Nevertheless, if generalisation is still allowed in the 21st century, we can assume that filopodia, which are often associated with lamellipodia, are participating in cell migration or extension (Chhabra and Higgs, 2007; Pollard and Borisy, 2003). To fulfil these different roles, filopodia must adapt their morphology and molecular composition in coordination with precise spatio-temporal regulation of their initiation mechanisms.

a. Morphological characteristics and roles

This cellular protrusion has a morphology described as finger, antennae or tentacle, with a width ranging from 0.1 and 0.3µm and a length rarely exceeding 10µm. Their architecture can be separated into three different sections. The base that links filopodia to the underlying cell cortex, the core body and the tip often contain characterised functional features (Fig 10. A) (Fischer et al., 2019). Filopodia are used as a sensing mechanism to orientate cell migration. For instance, in cancer cells, fibroblasts or even macrophages. Cells produce an abnormally high number of filopodia that sense the surrounding extracellular environment (Vignjevic et al., 2007). Filopodia are also composed of receptors and act as signal transduction. They can also be composed of cell adhesion proteins that create adhesions sites, further used to pull and retract the cell and complete cellular migration or tissue reorganisation (Galbraith et al., 2007). This role can be observed in the dendritic filopodia of neuronal cells and leading-edge filopodia from migrating cells. These structures also have a role in intercellular interactions, wound healing, or embryogenesis with the fusion of epithelial sheets (Brockes et al., 2004; Raich et al., 1999; Wood and Martin, 2002). These mechanisms rely on calcium stimulation to form intertwined filopodia (Hakanpaa et al., 2018), which protrude from opposite cells and act as a zipper reinforcing intercellular contact area and total

tissue cohesion (Vasioukhin et al., 2000). As we have seen, filopodia have dedicated roles according to their implication during different cellular processes. Thus, various filopodia exist: molecular composition is adapted to each function or system, and their precise localisation within the cell is tightly regulated.

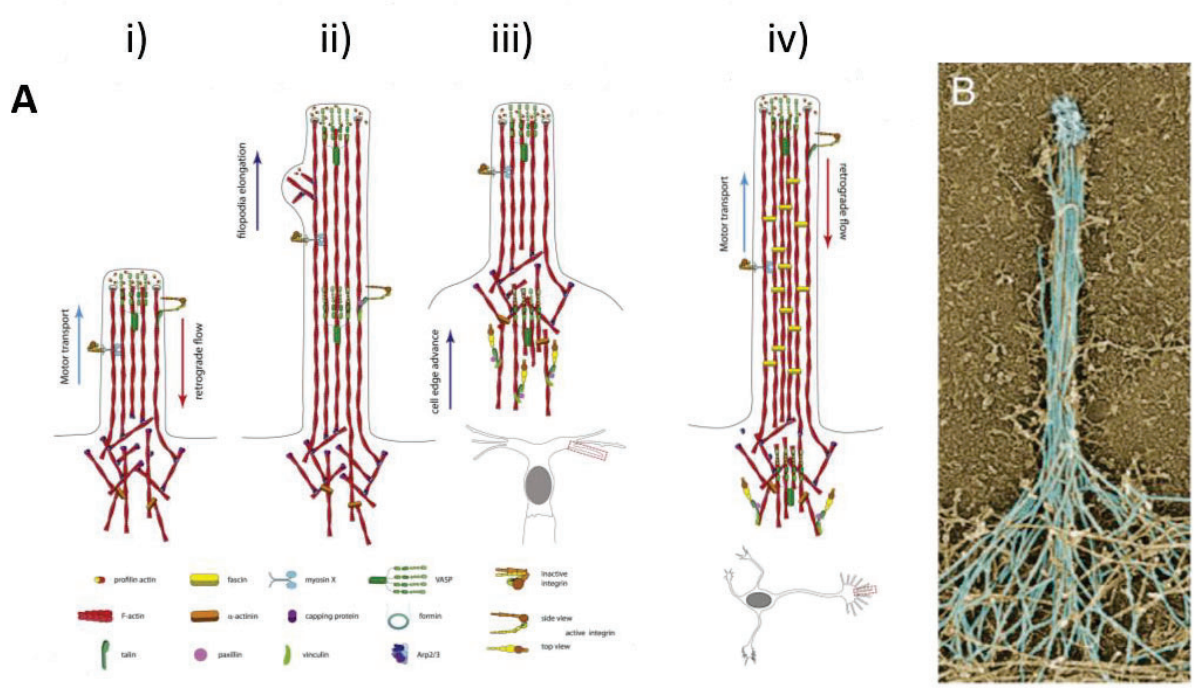

Figure 10 Morphologie and composition of a filopodium

(**A**) **i**) filopodia from endothelial tip cell, myosin X transports adhesion molecules, including integrins and VASP, to the filopodium tip**. ii**) Arp2/3 can also be activated and induces small side lamellipodia. VASP bundle filaments protect them from capping and collaborate with formins at the tip, allowing rapid F-actin polymerisation to advance the tip. **iii**) Tip advance is partially balanced by the retrograde flow of actin, which activates integrins in conjunction with talin binding. Retrograde flow and slippage of active integrins result in the accumulation of active focal adhesions at the base of filopodia. These adhesions grow and exert stronger traction allowing forward progress of the cell edge. **iv**) Key features of the neuronal filopodia architecture are similar to endothelial cells, except that fascin cross-linking generally results in tight parallel bundled actin filaments without branches. However, some examples of branched growth cone filopodia exist. Figure extracted from (Fischer et al., 2019). (**B**) electron micrograph showing the arrangement of actin filaments in a filopodium from a cell from (Vignjevic et al., 2006).and the Figure is extracted from. Figure extracted from (Mellor, 2010).

b. Molecular composition

Filopodia are composed of a diverse assortment of proteins. This diversity creates a wide range of different morphological characteristics and roles. These differences are even more pronounced when looking at other model organisms (Sebé-Pedrós et al., 2013). Despite this diversity, proteins family and their functions are conserved. Therefore, these paragraphs will focus on protein families rather than individual ones. Filopodia are composed mainly of the building blocks of all actin architectures, G-actin and F-actin, which are tightly organised in parallel bundles (Fig 10 A.B), surrounded by a double layer of the plasma membrane. Filopodia have common molecular components. These components can be regrouped into regulation-related categories: spatial regulators with membrane phospholipids, temporal regulators with signalling molecules, morphological regulators with actin nucleators, cross-linking proteins, functional regulators with molecular motors and anchoring proteins. All these molecular partners will cooperate to establish, elongate and functionalised the filopodia. Filopodia need to be dynamically regulated in a spatio-temporal manner. Spatial regulation comes from a specific type of lipids. One of these lipids is the phosphatidylinositol-4,5-bisphosphate (PtdIns(4,5)P_2), also called PIP2. This specific lipid is a molecular positioning hub where signalling molecules and their effectors are colocalising (Etienne-Manneville and Hall, 2002; Hirani et al., 2019; Jacquemet et al., 2019; Scholze et al., 2018). It goes in pair with the temporal regulation of filopodia. It is achieved through the activity of signalling molecules that belong to the GTPase family, such as RhoA, Rac1 and Cdc42 (Etienne-Manneville and Hall, 2002; Ridley, 2006). This GTPase family are responsible for regulating cell morphology and, by extent, actin cytoskeleton. GTPases are positively regulated by Guanine nucleotide Exchange Factors (GEF) located at the plasma membrane (Etienne-Manneville and Hall, 2002; Nobes and Hall, 1995; Ridley and Hall, 1992). Upon this step of functionalisation by GTPases, there is a downstream activation of the effectors, such as the formin proteins or the NPF WASP and N-WASP, which *in fine*, activate actin nucleation machinery and promote F-actin nucleation and elongation right beneath the plasma membrane. Filopodia initiation comes as long as there is a persistence of these activated signalling pathways. The precise localisation at the plasma membrane, of temporarily regulated partners, like GTPase, their GEF and NPF, promote a positive spatio-temporal regulation of actin nucleators. These nucleators must be activated by a GTPase such as RhoA, Rac1 or Cdc42 (Chen et al., 2010; Lebensohn and Kirschner, 2009;

Pellegrin and Mellor, 2005). Because of the close interaction between these GTPases with the lipids PIP2 and the presence of the BD of formin embedded into the plasma membrane, it ensures a targeted actin filament nucleation and a filament elongation at the cell cortex. Importantly, actin nucleators are crucial features for any actin cytoskeletal structure. As seen in chapter 1, there are two families of actin nucleators, the Arp2/3 complex and the formin. These two nucleators build two different actin filaments for filopodia formation (Mattila and Lappalainen, 2008). This combination of nucleators has two distinct roles at two different filopodia localisations. First, the Arp2/3 complex builds arrays of Y-branched filaments that converge at some branching points, establishing a filopodia base which connects the filopodia body and the actin cellular cortex and will, later on, promotes lamellipodia extension. Therefore, Arp2/3 is located at filopodia's base (Mellor, 2010; Yang and Svitkina, 2011). Second, the formin nucleates and elongates straight filaments that specifically push against the plasma membrane and extend the filopodia body toward the extracellular environment (Yang et al., 2007). Hence, formin is located at the tip of filopodia (Schirenbeck et al., 2005). These parallel actin filaments elongated by formins are further crosslinked by actin-binding proteins, such as the fascin, which is then mandatory (Vignjevic et al., 2006). To provide their extracellular anchoring, signal transduction and mechanical roles, filopodia are composed of adhesive proteins such as integrins and cadherins (Fierro-González et al., 2013; Lagarrigue et al., 2015), as well as molecular motors such as a member of the myosin family (Bornschlögl, 2013; Chan and Odde, 2008; He et al., 2017; Kim et al., 2018). Filopodia are straight, tightly aligned, parallel actin filaments embedded in the actin cortex. These can generate forces and trigger morphological changes at the cellular and tissue or embryonic scales. Despite an overall consensus on filopodia morphology and the elongation machinery, their initiation mechanism is not entirely elucidated and still needs to be characterised.

c. Initiation mechanism

The previous paragraphs mention the diversity of roles and molecular compounds associated with fulfilling the role attributed to filopodia. The only admitted paradigm is their finger-like, elongated shape and elongation mechanism. Their precise molecular composition and functions vary and are not causality linked. Filopodia are pioneers during cell positioning and movement and are often associated with lamellipodium formation. Nevertheless, a fundamental question remains about the mechanism implicated in filopodia initiation. The

wide diversity of processes and cellular models where filopodia are involved increases the difficulty for the scientific community to identify a common mechanism for this filopodia initiation. Therefore, Yang and associate focus their discussion on a standardised experimental system, the leading edge of a migrating cell (Yang and Svitkina, 2011) (Figure 11). After gathering all the knowledge in this field, two models of filopodia initiation emerge (Yang and Svitkina, 2011). First is the convergent model. Filopodia emerge from the actin network that is present actin cortex of a lamellipodium leading edge. Individual filaments that comprise the filopodial bundle arise at branching sites of other filaments, and filopodia far ascend from the lamellipodial actomyosin cortical meshwork. Typically, these branched points are dispersed throughout the filopodium's base through an interplay between the Arp2/3 complex and the capping protein. This cause the filaments to converge into bundles, and filopodia emerge from the edge of the lamellipodium and are elongated by a cluster of formins. This convergent model is supported by different experimental systems, such as disrupting the localisation of the Arp2/3 complex in macrophages (Machesky and Insall, 1998), the motility of neuronal cells (Korobova and Svitkina, 2008), the dorsal closure of the drosophila embryo where filopodia came out from a lamellipodium (Gates et al., 2007) and the thrombocytes lacking WASp (Falet et al., 2002). Secondly, the tip nucleation model or “de novo” initiation.

This second model came from experiments that perturb the system heavily and can be considered irrelevant (Block et al., 2008; Schirenbeck et al., 2005; Steffen et al., 2006). Nevertheless, this drastic approach reveals that Arp2/3 is not required for filopodia maintenance after initiation. The point of view shared in the community is that these two proposed models work simultaneously. Filopodia are characterised by the organisation of their inner actin filaments. They are straight, cross-linked and parallel. To do so, the elongation and maintenance of filopodia are done by the action of the actin nucleator, formin and the capping protein. Preceding the elongation, Arp2/3 play a central role in establishing a dense meshwork that sets the basement of filopodia, where formin is clustered and positioned with specific spatio-temporal dynamics with the engagement of the Rho Signaling pathway. The difficulties encountered in other experimental models and the remaining questions can be addressed by studying physiological, stereotyped and reproducible embryonic development.

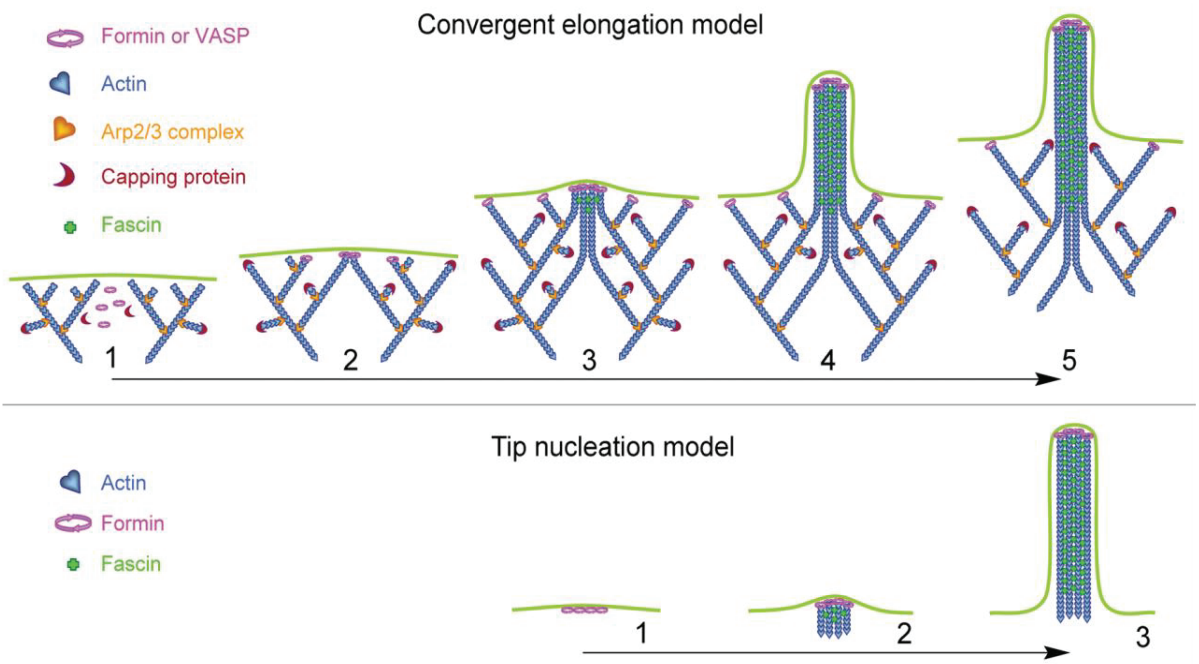

Figure 11Models of filopodia initiation

(**Top**) Convergent elongation model: (**1**) Branched actin network is formed in lamellipodial by Arp2/3-mediated nucleation. (**2**) Elongation factors (Ena/VASP or formin) maintain continuous elongation of some barbed ends. (**3**) Interaction between barbed ends, likely also mediated by Ena/VASP or formin, results in synchronised parallel elongation of several converged filaments. (**4**) Parallel filaments are cross-linked by fascin resulting in the formation of an actin bundle. (**5**) Over time, the Arp2/3 complex that nucleated filopodial filaments dissociate, leaving free pointed ends of the splayed actin filament. Tip nucleation model (bottom): (**1**) Activated formin is clustered on the plasma membrane. (**2**) Formin cluster nucleates a bunch of actin filaments and maintain their elongation. (**3**) Elongating filaments are cross-linked by fascin to form an actin bundle. Figure extracted from (Yang and Svitkina, 2011)

2- Embryonic presence in many other models

Embryogenesis and cellular differentiation rely on gene expression, which depends on molecular content segregation influenced by cell polarisation and position regarding their neighbourhood. The actin cytoskeleton governs these last features. It is particularly true at a tissue scale, where morphogenetics events drag entire cell tissues to reposition them and trigger cellular differentiation. During these particular morphogenetics events, filopodia are mandatory features that cooperate for sensing, anchoring and pulling on cells or tissues. Taken together, they are crucial parameters for cell positioning and cell motility. Here I will cover some significant discoveries about filopodia during embryogenesis across different model organisms, highlighting the structural and mechanical diversities and the crucial importance of filopodia during embryogenesis, shared among Metazoan, with a particular emphasis on *C. elegans* embryogenesis.

a. The Historical case of Sea urchin

In the late 19th century, embryogenic extracellular protrusions were first mentioned as "filose protoplastic" or "spinning activities " (E.A Andrew, 1897). These spinning filose were observed in echinoderms embryos, especially in the Sea urchin and Star-fish embryos from the first to the 8-cell stages (E.A Andrew, 1897). At this time, Andrews has a very inspiring and insightful hypothesis about the spatio-temporal dynamics of these spinning structures and their roles regarding cell cycle progression. These hypotheses remain poorly tested today (Sherlekar et al., 2020). As a pioneer observation, it leads to an opposition reflex from a sceptical embryology community, considering these structures abnormal (E.A Andrew, 1897). It was only in the middle of the 20th century, with technical improvement, Andrews's observation on spinning structures in the 8-cell stage Sea urchin embryo was proved to be accurate and received the named filopodia (Vacquier, 1968) (Figure 12). Interestingly, these Andrew's spinning structures, or filopodia, were first observed in different experimental conditions on other sea urchin strains, either at Woods Hole or at the Zoological Laboratory of the Sorbonne, Roscoff, Britany. In parallel, these structures were also observed in phylogenetically separated animals, from vertebrates to Echinoderms and passing by nematodes.

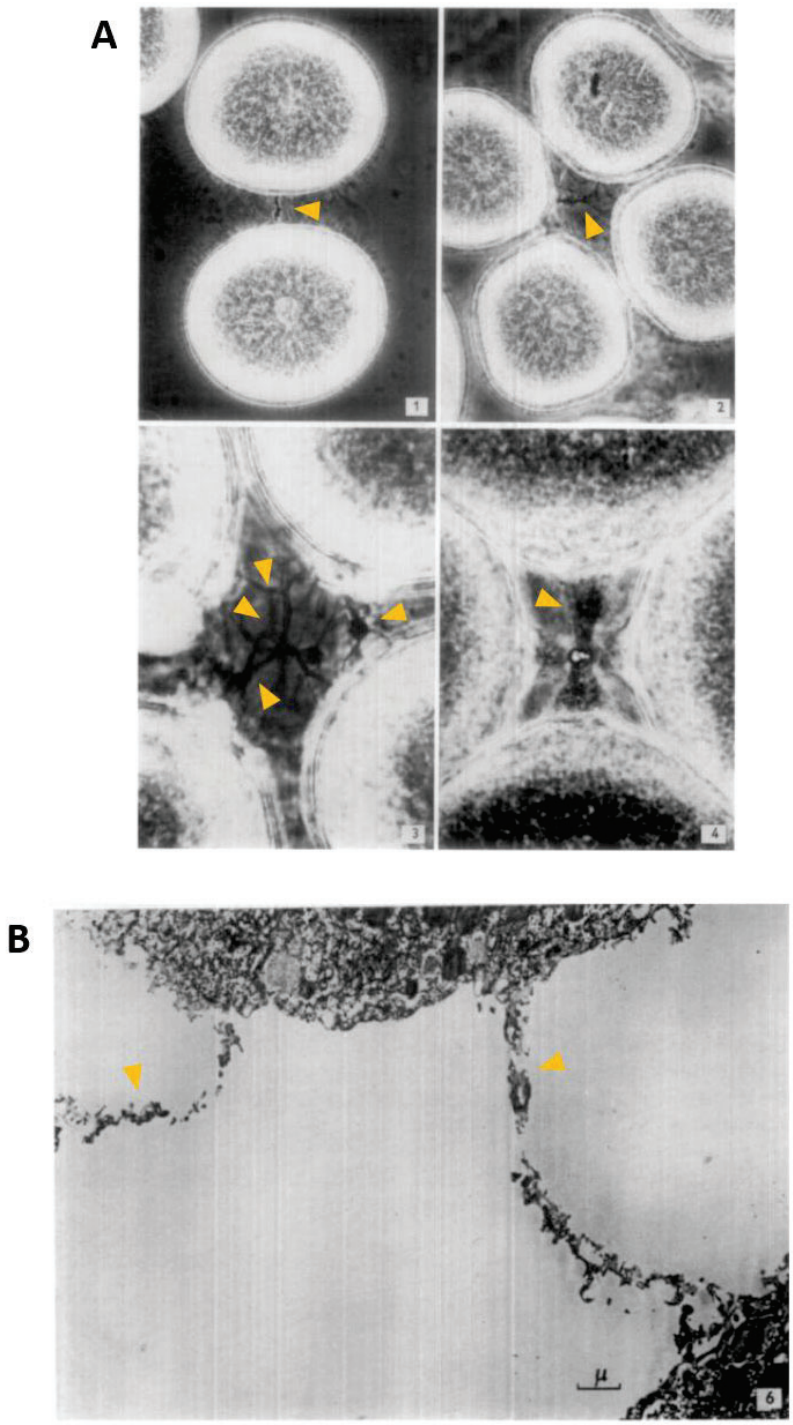

Figure 12: Filopodia in the Sea urchin early embryo

Orange arrows show the presence of filopodia during the early steps of Sea urchin embryogenesis. (A) Localisation of these structures during early embryogenesis. 1) the 2-cell stage. 2 and 3) at the 4 cell-stage ,4) in the central tube at the 8-cell stage. The lenght of the embryo is about 100µm. (B) Magnification of filopodia from the 4-cell stage. Scale bar, 1µm. Pictures extracted and adapted from (Vacquier, 1968).

b. Embryonic compaction in *Mus musculus* embryo

After fertilisation, early Mammalians embryos undergo a stereotypical series of cleavage and divisions, resulting in relatively rounded cells. With the example of the *Mus musculus* embryo at the 8-cell stage, cells flatten their membranes against one another, increasing cell-cell contact and forming the first epithelium-like structure. This morphogenetic process, called compaction, governs the mice embryo's early morphological establishment and lineage identities(Rossant and Tam, 2009). Compaction is crucial for preparing the embryo for implantation on the uterine wall (Johnson et al., 1986, 1981). The compaction of preimplantation embryos depends on cell-cell contacts mediated by adhesion molecules such as E-cadherin (E-cad) (Larue et al., 1994; Stephenson et al., 2010). E-cad links actin filaments and cell shape through dynamic interactions with intracellular catenins (Cavey and Lecuit, 2009). As an example of the consequence when E-cad is deleted: mouse embryo exhibit compaction abnormalities (Larue et al., 1994; Stephenson et al., 2010). These irregularities influence the success rate for embryonic implantation to the uterine wall, resulting in non-viable embryos (Landry et al., 2006). This makes compaction a primordial event for future embryo viability. This event needs proper Intercellular contacts. This requires dedicated cellular structures that regulate cell shape and mechanistically increase the contact area between cells by drawing them to each other. These structures are filopodia (Fierro-González et al., 2013) (Figure 13). In addition, these filopodia are dependent on E-cad and are composed of the molecular motor Myosin X which attracts cells to each other (Fierro-González et al., 2013). Interestingly, the first clue on the change in the intercellular contact area and these membrane protrusions was reported during the ’70s (Calarco and Epstein, 1973; Ducibella et al., 1977), and it took 40 years of dedicated perseverance in parallel with technical improvements to identify the reason for this phenomenon: Filopodia (Fierro-González et al., 2013).

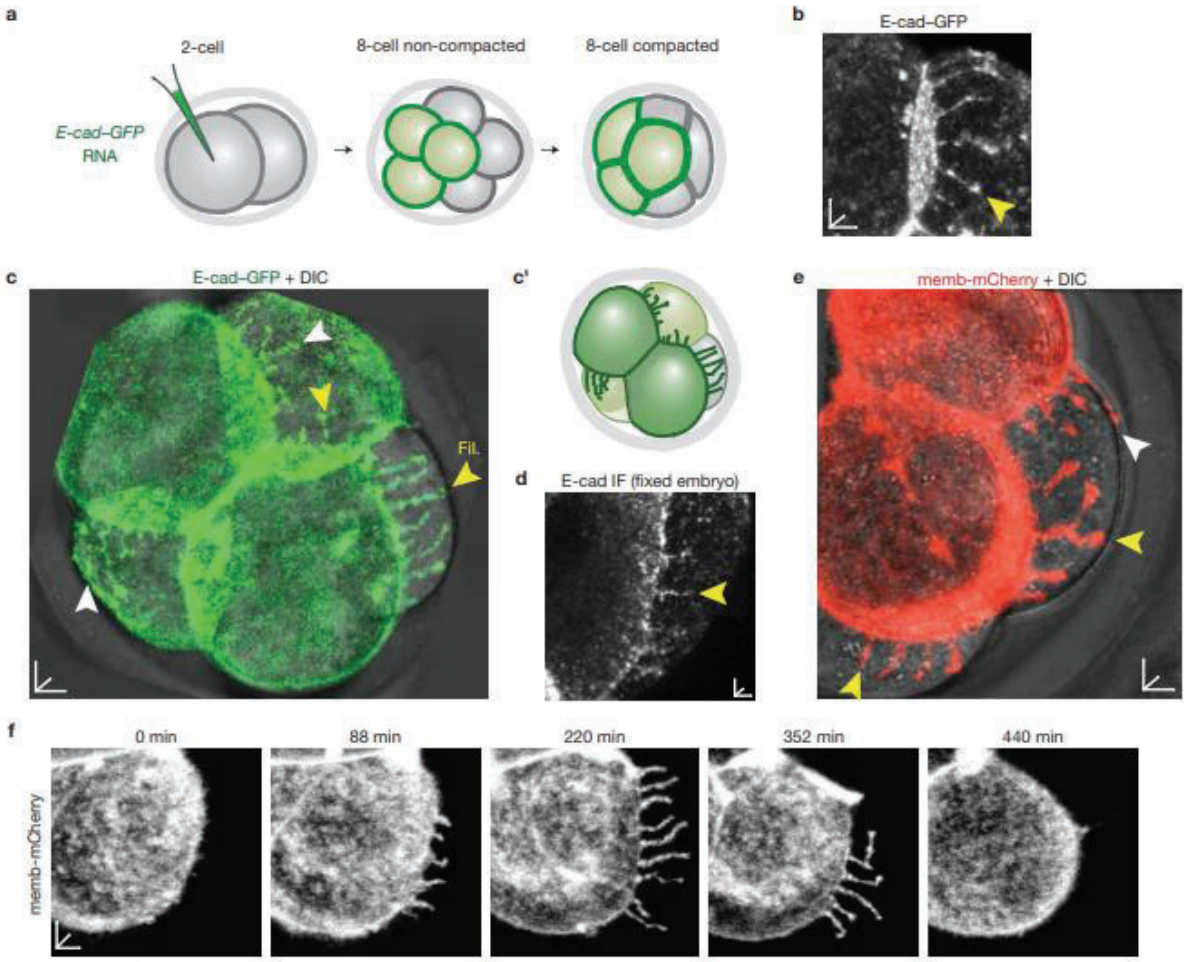

Figure 13: Filopodia form during *Mus musculus* embryo compaction

(a) Microinjection of RNA into one cell at the 2-cell stage allows visualization of E-cad–GFP in half of the cells of the embryo during compaction. (b,c) Microinjected live 8-cell stage embryos expressing E-cad–GFP. In b, E-cad–GFP-labelled filopodia (arrow) extend from the apical border membrane region of a filopodia-forming cell (left) on top of the neighbouring cell apical membrane (right). In c, two cells show E-cad–GFP-labelled filopodia (white and yellow arrowheads distinguish filopodia from each cell). (c') Schematic diagram of the embryo from c. (d) Detection of filopodia using E-cad antibodies. IF, immunofluorescence. (e) Membrane-targeted mCherry (memb-mCherry) labels bona fide E-cad filopodia extending from two cells (white and yellow arrowheads). (f) Selected time frames show extension and retraction of filopodia over time. Orthogonal scale bars, 5 µm. Figure and legends extracted from (Fierro-González et al., 2013).

c. Dorsal closure in the *Drosophila melanogaster* embryo

On another clade and another morphogenetic event, with *Drosophila melanogaster* at a later stage between stages 14 to 16. During this period, a specific morphogenetics event happened: the Dorsal Closure (DC) (Young et al., 1993). This process consists of the fusion of epithelial sheets, where a continuous epidermis is formed when two epithelial sheets approach each other on the surface of the embryo and meet at the dorsal midline. An analogy can be made with neural tube closure in vertebrates. This tissue migration and fusion process can also be observed during embryonic development and wound healing (Martin and Parkhurst, 2004). In case of an abnormal completion of this morphogenetic event, it leads to severe phenotypes such as spina bifida and cleft palate. These phenotypes can be observed in human embryonic development. Mechanistically, this mutual attraction between epithelial sheets is done by a zippering mechanism and realised by the action of filopodia. Filopodia protrude from one sheet to another, and when they match the corresponding sheet cell, they interdigitate and proceed to the fusion of the sheets (Millard and Martin, 2008) (Figure 14). This mechanism is dependent on the signalling of the GTPase Cdc42 and the localisation of Ena (Gates et al., 2007; Jacinto et al., 2002). To conclude, it reinforces the crucial role of filopodia in the completion of morphogenesis, using their sensing and zippering process.

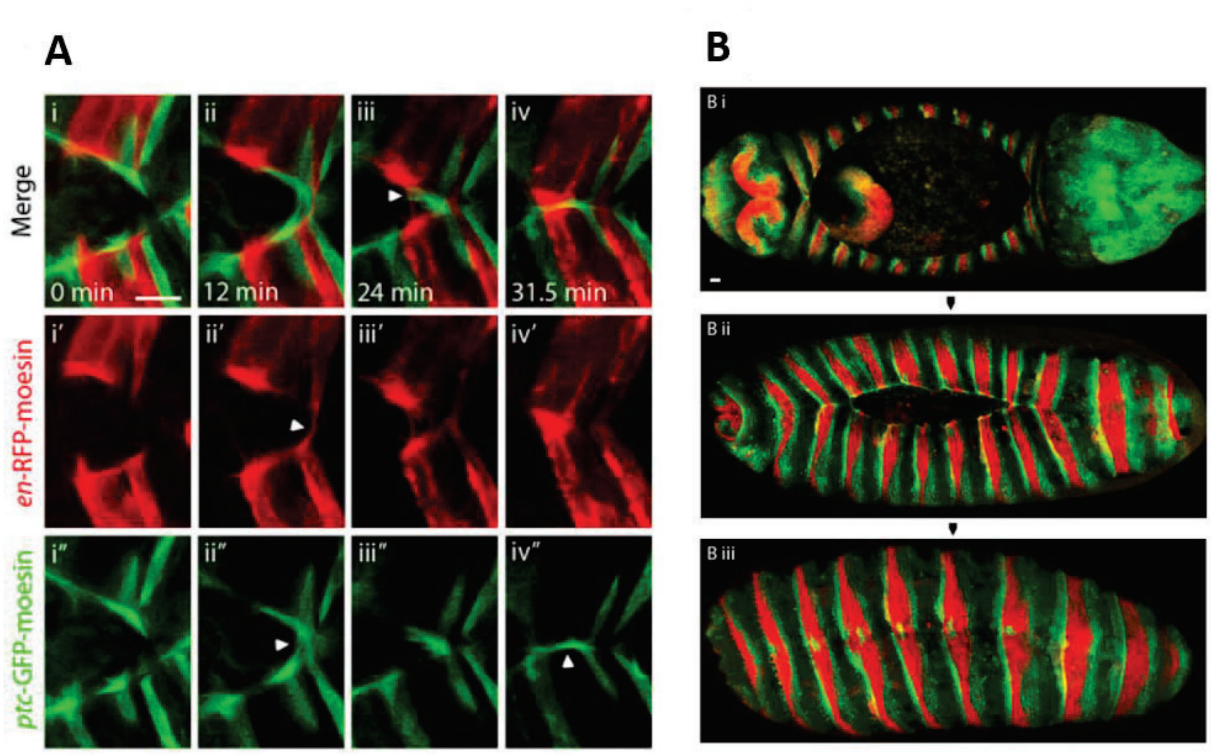

Figure 14: Close up to the Dorsal Closure in *Drosophila melanogaster* embryo

(A) Zippering in en-RFP-moesin (red), ptc-GFP-moesin (green) expressing embryos. Images showing filopodial matching. i) Red and green filopodia protrude from leading edge cells. ii) Contacts are made between red filopodia from opposing epithelia, while at the same time separate contacts are made between green filopodia. iii) Further contacts are made between red filopodia; however, green filopodia in close proximity to these red filopodial contacts do not interact. iii. Green filopodia transiently form contacts between ptc-GFP-moesin cells over the top of the fused red cells. Arrowheads indicate the described filopodial interactions. Scale bars 10 µm. (B) Dorsal view of embryos at the start i), midway through ii), and shortly after completion of DC iii). Figures and legends extracted from (Millard and Martin, 2008).

3- Special case of filopodia during *C. elegans* embryogenesis

After the previous observation of different model organisms ranging from echinoderms to mammals, we will now focus on the *C. elegans* embryogenesis and the presence of this structure that is starting to be familiar to our readers. *C. elegans* was intensively used to observe and characterise embryogenetic processes during the previous decades. Filopodia were observed at different stages of development. Here, we will highlight these structures in *C. elegans*, using the *C. elegans* homologous name of proteins and respecting the chronological order of discoveries.

a. Dorso-Ventral closure during the lima bean stage

Morphogenetic events that lead to embryonic tissue reorganisation are driven by cellular migration and intercellular interactions. These events need the protrusive and contractile characteristics of the actomyosin cortex and filopodia architecture. Epiboly is a morphogenetic event where the two opposite sides of a tissue layer (e.g., epithelial tissue) are moved and fused to encapsulate another tissue layer. Regarding the *C. elegans* embryo, In 1997, William-Masson described an epiboly event called the Dorso-Ventral closure, which happens during the lima bean stage (Williams-Masson et al., 1997) (Figure 15). Initially, epithelial cells are assembled in a sheet at the dorsal side. The two leading edges of this tissue move in an epiboly process. Indeed, they surround the inner tissue of the embryo and fuse together at the embryonic ventral midline (Williams-Masson et al., 1997). This Dorso-Ventral closure is a two-step mechanism. The first step is an initial migration, where the two posterior pair cells of each edge of the epithelial sheet migrate and pull the hypodermis. They circle the embryo and the two posterior cells anchor between their pair. Importantly, these cells used actin-rich protrusive structures called filopodia to fulfil these roles of migrating and anchoring. Once these four cells approach the ventral midline, the remaining cells of this tissue express a substantially increased density of F-actin located on the cellular side where they are contactless, which will lead to the formation of an actin ring. The second step is the closure itself; it depends on the contractility of this actin ring that will pull the double edge of the epithelial tissue toward the ventral midline in a “Tying” mechanism. Once the two edges are reunited, the newly localised ventral epithelial cells create junctions that seal and complete

this epiboly event (Williams-Masson et al., 1997). Morphologically, this process can be considered the equivalent of the dorsal closure in the Drosophila Melanogaster embryo.

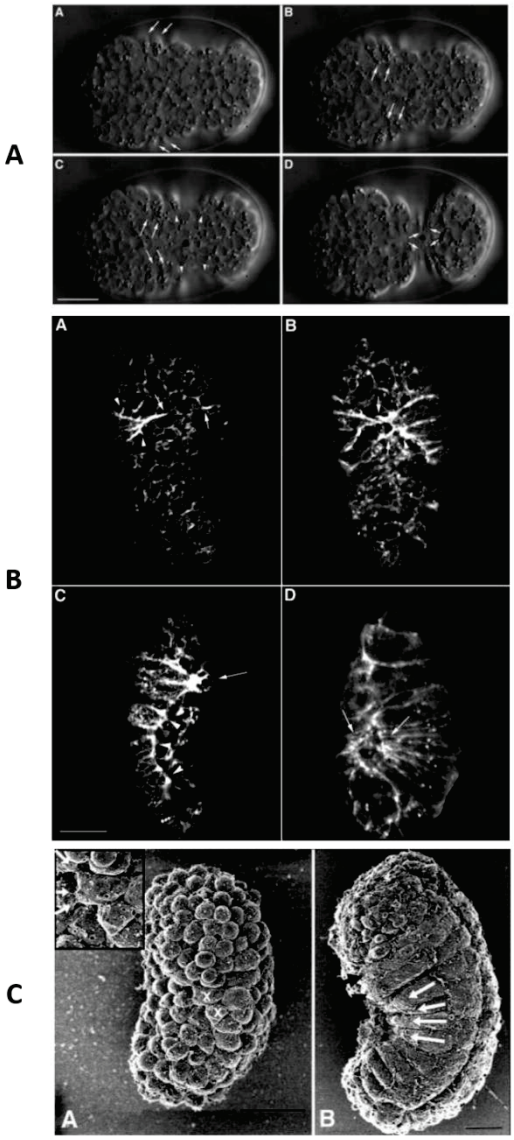

Figure 15: Dorso-Ventral closure during the lima bean stage of *C. elegans* embryo

(**A**) Nomarski micrographs of ventral enclosure and the different steps in chronological order from A to D. All views are ventral. Bar, 10 µm. (**B**) Wild-type embryos stained with phalloidin and viewed by laser scanning confocal microscopy during ventral enclosure and the different steps in chronological order from A to D. Scale bar, 10 µm. (**C**) Scanning electron micrographs of the early and late stages of ventral enclosure. A) Lateral view of a pre-enclosure embryo showing the left-hand leading cells; B) Lateral view of an enclosed embryo. The leading cells have met at the ventral midline, and have assumed a rectangular shape (black arrows). The ventral pocket cells have mostly enclosed, and have constricted ventral tips (white arrows). Anterior is toward the top, and dorsal is toward the right. Bar, 10 µm. Figures extracted from (Williams-Masson et al., 1997).

b. The 8-cell stage and the L-R body plan axis

Preceding the lima bean stage, during the 8-cell stage of the *C. elegans* embryo, filopodia and lamellipodia are reported to be present in the ABpl cell (Pohl and Bao, 2010). Indeed, ABpl forms three different actin structures: a lamellipodium on his dorsal side, another protrusion on his ventral side, and filopodia on this anterior side. Taken together, these will lead to a displacement of ABpl toward the anterior side (Pohl and Bao, 2010) (Figure 16.A). It has been reported that the formation of these dynamical protrusions needs a proper RhoGTPase signalling pathway (Pohl and Bao, 2010). Remarkably, these ABpl filopodia participate in the chiral morphogenesis that establishes the Left-Right Body plan axis in the 8-cell stage *C. elegans* embryo (Pohl and Bao, 2010). Simultaneously forming the ABpl ventral protrusion, the EMS cell starts its cytokinesis, creating the two daughter cells, the MS cell at the anterior side and the E cell at the posterior side. The ABpl ventral protrusion migrates toward the EMS cytokinesis groove (Pohl and Bao, 2010) (Figure 16.A). The question remains about the ABpl ventral protrusion migration, which can only be passive because of spatial opportunities created by the EMS cytokinesis groove or active with a defined purpose regarding the future MS and E cells and then this protrusion needs to be named lamellipodium instead of simply protrusion. Indeed, the molecular content of this protrusion is dynamically enriched in the adhesive proteins, the E-cadherin HMR-1 (Caroti et al., 2021). Before the EMS division, HMR-1 is localised all along the interface between ABpl and EMS. During cytokinesis, ABpl ventral protrusion dive into the groove of the EMS cytokinesis with an anteriorisation of HMR-1 toward the future MS cell. After cytokinesis completion, HMR-1 is explicitly located at the interface between ABpl ventral protrusion and MS. This polarised protein distribution depends on the Wnt signalling pathways making this ABpl ventral protrusion a clear lamellipodium (Caroti et al., 2021) (Figure 16.B).. Filopodia make the ABpl cell migrate toward the embryo's anterior side, positioning and anchoring its dorsal and ventral lamellipodia on other cells to establish the Left-Right body plan axis (Caroti et al., 2021; Pohl and Bao, 2010).

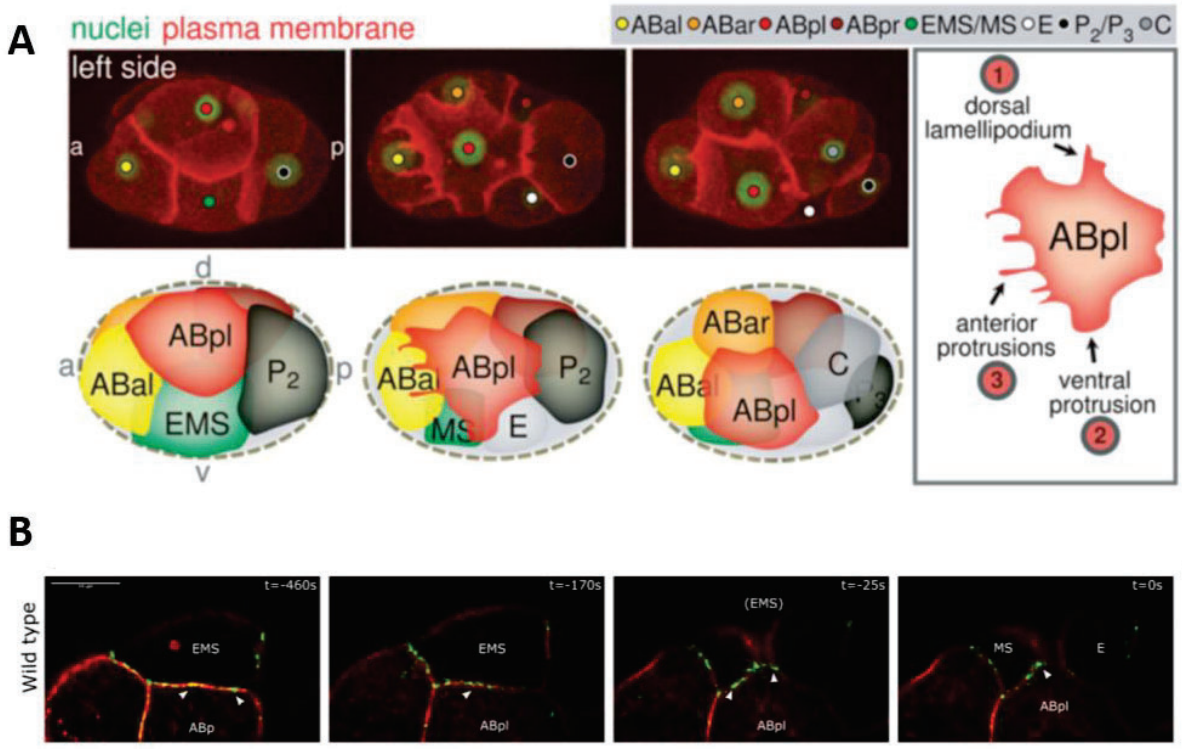

Figure 16: Motile structures in *C. elegans* 8-cell stages embryo

(**A**). Chiral morphogenesis and its underlying cellular behaviors. Left panels: 3D projection with matched schematics. The color code of this schematic matches that of the small circles. Plasma membrane is shown in red (PH-domain of PLC1δ1 fused to mCherry) and nuclei in green (HIS-72::GFP, HIS-72 is a H3 variant histone). Right panel: Features specific to ABpl and ABpr are indicated with circled numbers in the boxes outlined in gray.Figure extracted from (Pohl and Bao, 2010).(**B**) Distribution of the E-cadherin HMR-1 across the interface between EMS and ABp/ABpl. Note that ABpl forms a lamellipodium that precedes the ABpl movement following EMS division. Lifeact marking F-actin in red, the E-cadherin HMR-1 in green. Arrow heads indicate HMR-1 foci. Scale bar indicates 10 µm. Figure and legends extracted from (Caroti et al., 2021).

c. Very early stages

In this section, we will cover the most recent findings about filopodia presence discovered in the earliest step of embryogenesis. Before filopodia identification, Phosphatidylinositol 4,5-bisphosphate (PIP2) rich domains were reported to be asymmetrically enriched at the zygote's anterior (Nakayama et al., 2009; Scholze et al., 2018; Wang et al., 2017). A similar anterior enrichment was observed with the RhoGTPases family, CDC-42 and RHO-1, the RHO-1 regulator ECT-2, and a subpopulation of PAR-6 and PKC-3 associated with CDC-42. Additionally, these molecular partners are colocalising with the PIP2 domains (Motegi and Sugimoto, 2006; Panbianco et al., 2008; Scholze et al., 2018; Schonegg et al., 2007; Wang et al., 2017). It has been suggested that PIP2-enriched microdomains can operate as organising platforms for regulating cortical actin organisation, cell polarity, and asymmetric zygote division (Scholze et al., 2018) (Figure 17.A). Further investigations, in which I participated, revealed that these tubular microdomains were, in fact, a double membrane surrounding an entire structure to four layers of phospholipids that virtually correspond to a local enrichment of lipids with CYK-1 at their tips (Hirani et al., 2019) (Figure 17.B).. The core body of this structure is composed of actin filaments that are cross-linked and parallelly aligned by a cross-linking protein, PLST-1 (Hirani et al., 2019) (Figure 17.C). The tip of the filopodia contains the formin nucleator because of its processive activity (Hirani et al., 2019). All these characteristics allow us to qualify this structure, filopodia (Hirani et al., 2019). This publication also showed that these architectures were present at the 1, the 2 and the 4-cell stages of *C. elegans* embryogenesis (Hirani et al., 2019) (Figure 17.D). Nevertheless, a set of questions remains. What are their molecular composition and precise temporal dynamics during these three first embryonic steps? Are there any filopodia in the early cell stages? Are all these early filopodia the same? Is there another type of actin architecture? These preliminary questions will pave the way for answering the fundamental and ultimate question: what might be the role of these filopodia during early embryogenesis?

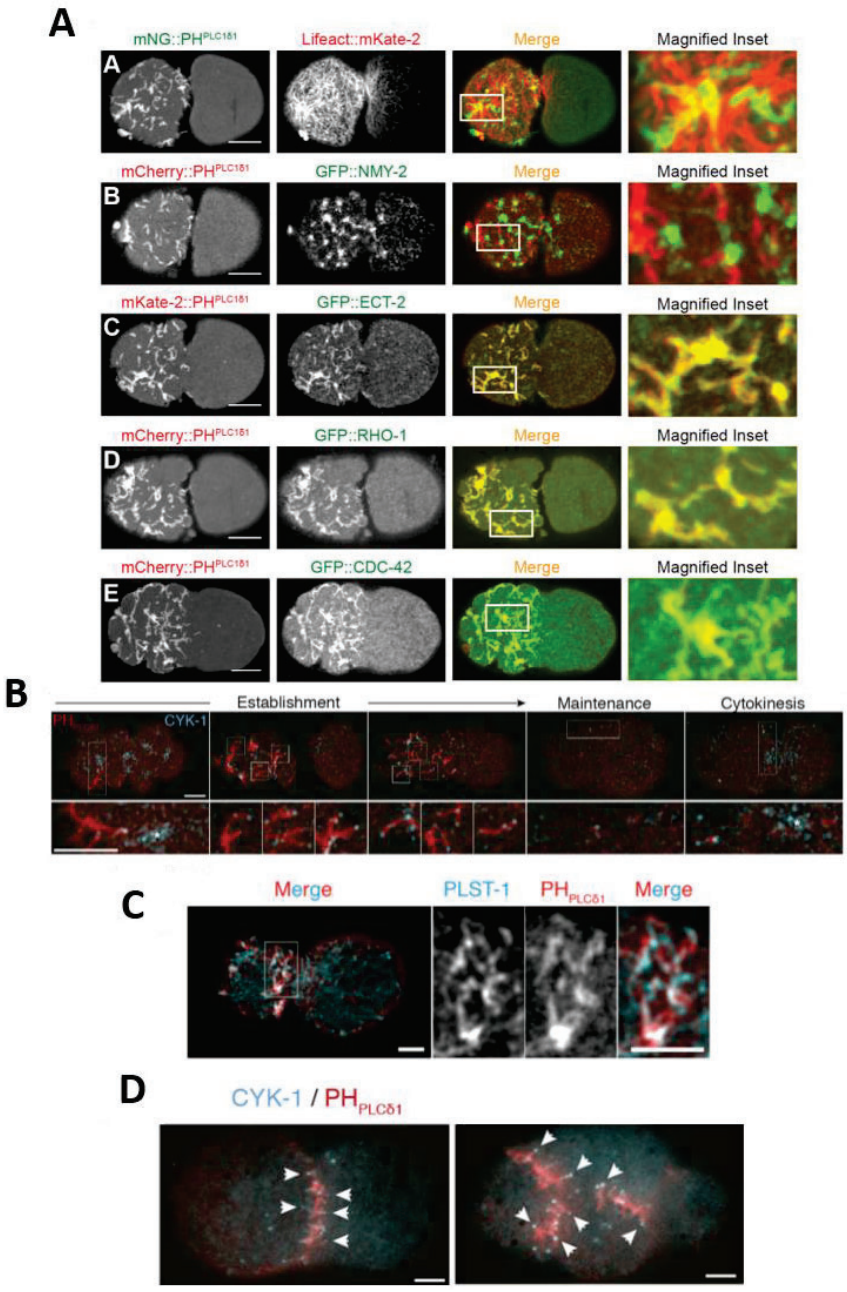

Figure 17: Filopodia in the early stages of *C. elegans* embryogenesis

(**A**) PIP2 cortical structures overlap with ECT-2, CDC-42 and RHO-1 and partially with actin. (A-E) Dual-color spinning disk confocal cortical imaging of pseudocleavage embryos harboring the indicated pairs of fusion proteins, with high magnification views of the boxed regions. Scale bars: 10 µm. Figure and legends extracted from (Scholze et al., 2018). (**B**) Confocal cortical images of embyro expressing CYK-1::GFP and mCherry::PHPLCδ1 at representative time points. Boxed areas are shown magnified 3× below. The asterisk indicates large pulsatile foci common at polarity establishment and cytokinesis. Scale bars: 5 µm. (**C**) Cortical images of two embryos expressing PLST-1::GFP and mCherry::PHPLCδ1 . Inset is marked and magnified on right showing merged and single channel images. (**D**) Surface images of 2 and 4-cell stage embryos expressing CYK-1::GFP and mCherry::PHPLCδ1. Arrowheads mark CYK-1-tipped membrane structures at cell contacts. Figures and legends fro B and C are extracted from (Hirani et al., 2019).

Chapter 3: *C. elegans* early embryogenesis

1- *C. elegans* early embryogenesis and body plan axis formation

C. elegans adult hermaphrodite has precisely 959 somatic cells. The entire lineage has been carefully and manually tracked thanks to the transparency of the cuticle and an enormous amount of patience and dedication (Kimble and Hirsh, 1979; Sulston et al., 1983; Sulston and Horvitz, 1977) and the finding that the cell lineage of *C. elegans* is almost entirely invariant between individuals. By retrospective analysis, we can predict embryonic development, which is essential when looking at single-cell levels during early embryogenesis (Sulston et al., 1983). The *C. elegans* embryogenesis combines an invariant lineage and early cell specification from the zygotic stage onwards. A combination of symmetry-breaking events of different natures enables the "tour de force" of assigning each cell its identity and setting the fate of the respective lineages in the first few divisions. Actomyosin cortex dynamics, cellular polarisation of membrane-associated proteins, spindle positioning, segregation of cell fate determinants, mechanical, chemical or diffusion gradients, and phase-separated granules (De Henau et al., 2020; Hamill et al., 2002). All the cited processes and molecular distributions are required to set the identity of the founder cells that will produce differentiated cell lineage (Gönczy and Rose, 2005). Before establishing differentiated cell lineage, the first step of the embryonic specification is the establishment of the body plan axis. These are, in chronological order, the Antero-Posterior axis (A-P), the Dorsal-Ventral axis(D-V) and the Left-Right axis (L-R) (Figure 18).

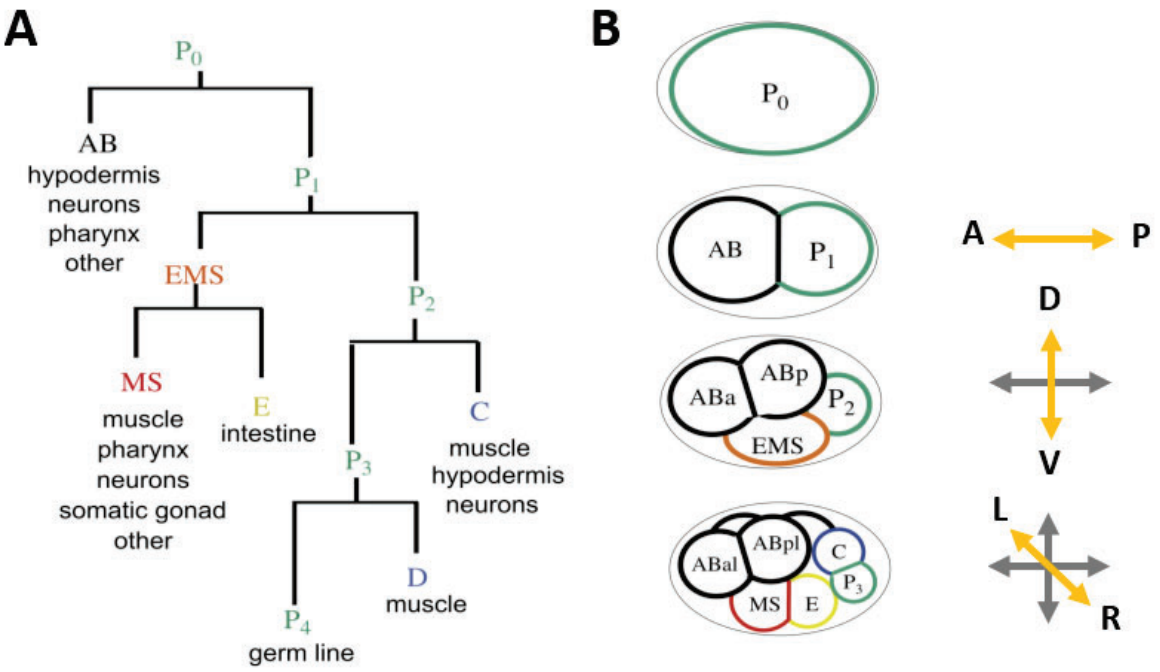

Figure 18: Early *C.elegans* embryonic lineage and body plan axis establishment

(**A**) Cell lineage of the early embryo. The horizontal lines connect sister cells; the length of the vertical lines indicates the relative cell cycle duration of each founder cell. The major cell types produced from each founder cell are shown. (**B**) Schematic diagram of cell positions at different stages. The germ-line precursors (P cells) are shown outlined with green, and each of the founder cells generated by asymmetric division are indicated with a different color. The daughters of founder cells are named by their position; e.g., ABa is the anterior daughter of AB, whereas ABal is the left daughter of ABa. The embryo proper is surrounded by an eggshell, schematized by a black line. On the Right panel, the correspond body plan axis acquired at this stages is represented in orange doube arrowhead. Figure Adapted from (Rose and Gönczy, 2014).

a. The Antero-Posterior axis (A-P)

In *C. elegans* hermaphrodites, a mature oocyte travels through the spermatheca, where it comes into contact with a sperm cell, fertilisation occurs, and the newly formed zygote (P0) is expulsed in the uterus. Sperm typically enters the egg on the opposite side of the oocyte nucleus and create the premise of the posterior side and, *de facto*, the anterior side. In addition to DNA, the sperm brings a pair of centrioles that establish the pericentriolar material (PCM) and form a centrosome that will build the zygotic microtubule cytoskeleton. This centrosome also contains the mitotic Kinase Aurora A (AIR-1) that influences many protein activities. Together, the newly arrived centrosome and its components interact and, per se, perturb the entire zygote cytoskeleton, especially the posterior actomyosin cortex. These cytoskeletal rearrangements will start a chain of events that causes the embryo to polarise and finalise the Antero-Posterior (AP) axis. In the beginning, NMY-2 foci are uniformly distributed in the actomyosin cortex of the oocyte (Munro et al., 2004). Once fertilisation happens, sperm brings the centrosome components, AIR-1, that will directly downregulate the cortical posterior NMY-2 activity (Zhao et al., 2019). This event will locally disrupt the contractile and the viscoelastic properties of the posterior actomyosin cortex and induce a cortical flow towards the anterior pole of the zygote that will polarise the cortical materials along the AP axis (Figure 19.A) (Munro et al., 2004). Importantly, to equilibrate the intracellular forces, this cortical flow orientated toward the anterior side induces a cytoplasmic stream directed toward the posterior side (Hird and White, 1993; Munro et al., 2004; Wallenfang and Seydoux, 2000). This cytoplasmic flow participates in the pronuclei fusion, the alignment and positioning of the mitotic spindle along the AP axis, and the polarisation of cytoplasmic materials such as mRNA and P-Granules (Albertson, 1984; Goldstein and Hird, 1996; Hird and White, 1993; Hyman and White, 1987; Strome and Wood, 1983). This polarisation induced by these double flows polarises the zygote in two approximately equal portions at 50% of the zygotic length. It already defines two cortical poles, one at the anterior side and the other at the posterior side (Hird and White, 1993). This results in an anterior enrichment of cortical components such as F-actin, NMY-2, other ABPs and, concomitantly, proteins physically linked to this cortex, the PAR proteins. The PAR proteins family are cortical proteins, the main proteins that dictate the polarisation in animal cells (Goldstein and Macara, 2007; Kemphues et al., 1988). This protein family comprises

supportive and antagonistic interaction rules by mutual phosphorylation inhibition mechanism (Kemphues, 2000; Ramanujam et al., 2018). During zygotic polarisation, PAR proteins are distributed on the two sides of the zygote and directly influence cortical dynamics (Lang and Munro, 2017). The PAR proteins family are segregated into two poles regarding their positioning along the embryo. This way, these two poles are defined as Anterior and Posterior, respectively, the Anterior PAR proteins (aPAR); with PAR-3, PAR-6, PKC-3; and the Posterior PAR proteins (pPAR); with PAR-1, PAR-2, LGL-1; (Hoege and Hyman, 2013). During zygotic polarisation, anterior PAR proteins (aPAR), PAR-3, PAR-6 and PKC-3, are dragged toward the anterior side because of the cortical flow. Posterior PAR proteins (pPAR), PAR-1 and PAR-2 are localised to the posterior side because of the antagonistic effect against the aPAR and their ability to enhance the downregulation of NMY-2 (Lang and Munro, 2017). Importantly, by the end of the cell cycle, the Anterior and the Posterior domains are defined and distributed asymmetrically, with a higher spatial distribution for the anterior pole, with molecular content such as NMY-2 and aPAR, for about 55% of the cellular volume (Figure 19.B) (Jankele et al., 2021; Ou et al., 2010; Pacquelet et al., 2015). The interface between these two asymmetric polarity domains will position the mitotic spindle and the associated cytokinetic ring, leading to an asymmetric division of the zygote (P0) into two daughter cells, AB from the anterior side and P1 from the posterior side(Figure 19.C). This first asymmetric division is the physical landmark of the AP axis establishment, thus sealing the fate of the future cell lineages with specific molecular segregation in each daughter cell.

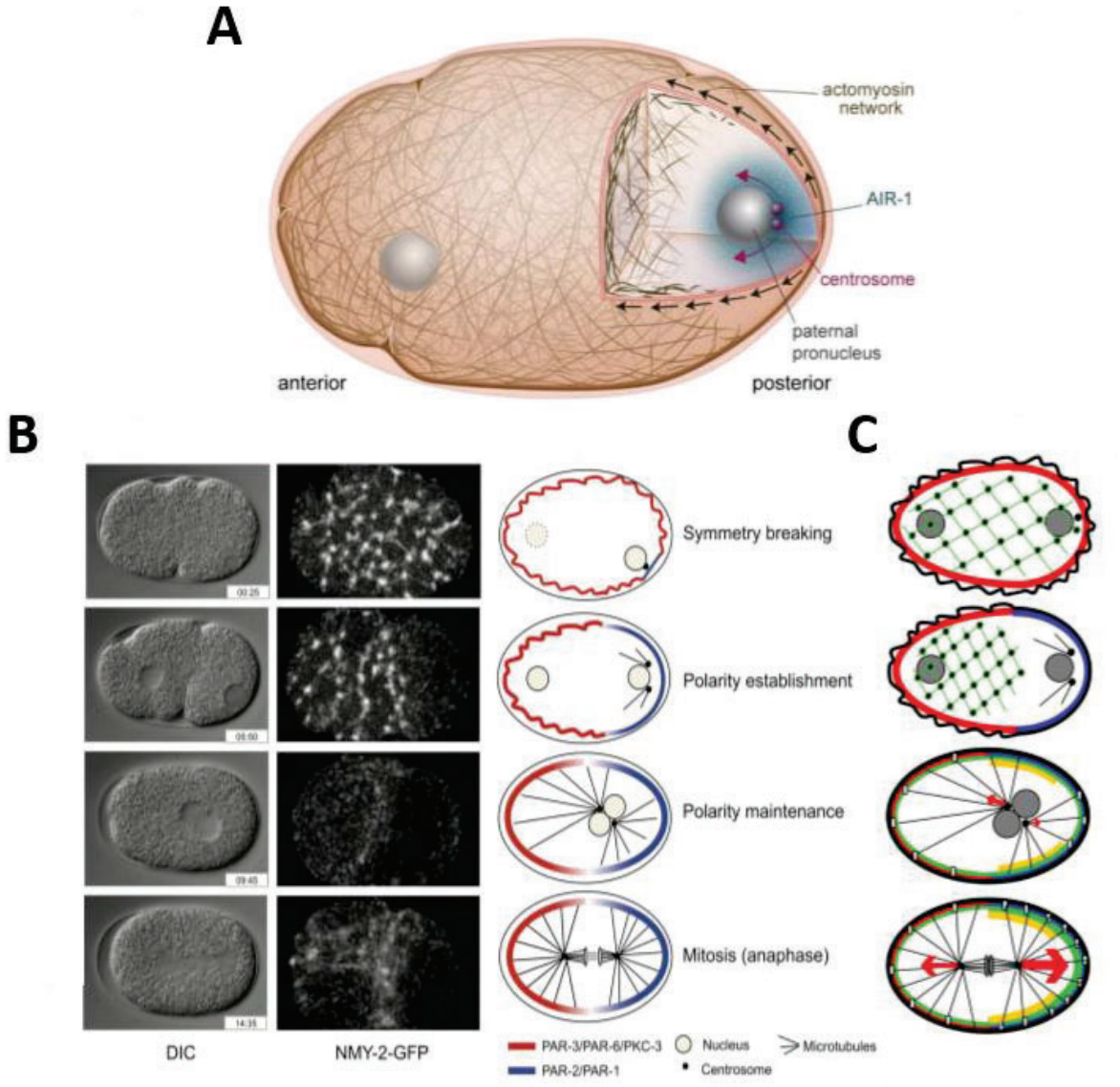

Figure 19: Zygotic polarisation and the establishment of the A-P axis

(**A**) Symmetry breaking in the one-cell embryo. AIR-1 (blue cloud) is the cue that initiates polarisation of the embryo. AIR-1 diffuses from the sperm centrosome (red spheres) and downregulates actomyosin at the adjacent cortex. This causes a local weakening, and produces cortical flows (black arrows) directed away from this point, which also serve to separate the centrosomes (red arrows). Figure and legends extracted from Samar et al. **(B)** Left: images from time-lapse differential interference contrast (DIC) microscopy, time is displayed in min:sec from the beginning of the recording. Middle: images from time-lapse fluorescence confocal microscopy at approximately corresponding stages.Right: corresponding schematics, illustrating the distribution of the anterior (red) and posterior (blue) PAR proteins. Embryo is approximately 50 µm long and is surrounded by an eggshell (visible in A and shown schematically. Figures and legends extracted from goncy rose. (**C**) Schematic representation of all the polarisation partners Centrosomes: black discs; microtubules: black lines; chromosomes, pronuclei and nuclei: gray ovals and discs; NMY-2: green network and foci; cortical PAR-3/PAR-6/PKC-3: red; cortical PAR-2 and PAR-1: blue; cortical GPR-1/2: green; cortical LET-99: gold; Cortical force generators are represented with empty rectangles, the net pulling force acting on each spindle pole with red arrows. Figures and legends extracted from (Rose and Gönczy, 2014).

b. The Dorsal-Ventral axis(D-V)

After this first division, molecular content is physically separated and specified according to their future cell fate. The developmental fates and division patterns of the first asymmetric division's daughters, AB and P1, differ. AB and P1 will divide asynchronously. The second cleavage is the division of the AB cell. Because of its anterior background, the AB cell has only aPAR (PAR-3) (Figure 20.A) (Bergmann et al., 2003; Cheng et al., 1995). The AB spindle is orientated according to the distribution of the PAR-3 protein. Indeed, spindle orientation on the AP axis is prevented by PAR-3, leading to a 90° orientation that position the mitotic spindle orthogonally along the AP axis, at the centre of mass of the AB cell and positioning the future cytokinetic ring at the cell equator (Bergmann et al., 2003; Cheng et al., 1995) (Figure 20.B). AB cell divides symmetrically into the two daughter cells, ABa and ABp. They are named according to their position along the Antero-Posterior axis and establish the founder cells for the lineage corresponding to the hypodermis, neurons, and pharynx. The third cleavage is the division of the P1 cell. As the AB cell, the P1 cell is de facto enriched in pPARs, PAR-1 and PAR-2. During the prophase of P1, an anterior PAR-3 domain arises and forms a gradient between aPAR (PAR-3) and pPAR (PAR-1, PAR-2). The two pPARs and P-granules are translocated further into the posterior side of P1 (Boyd et al., 1996; Goldstein and Hird, 1996; Guo and Kemphues, 1995). This second polarisation step establishes another asymmetric distribution of molecular content in the P1 cell. P1 divides asymmetrically, creating EMS and P2 (Figure 20.B).. Where EMS is localised more anteriorly and P2 more posteriorly, these two founder cells give rise to the Muscle and intestine for EMS and the Germline for P2. These two divisions, in combination with the confined ovoid environment of the eggshell, lead to the formation of a collection of cells with a stereotypical spatial arrangement with specific cell contacts with the so-called diamond shape of the 4-cell stage. This will favour signalling pathways that molecularly define the Dorso-Ventral (DV) body plan axis. Two major signalling pathways are implicated at the 4-cell stage: Notch signalling and Wnt signalling. Both of these pathways are triggered by the P2 cell and propagate toward the anterior cells of the embryo. P2 Notch signalling directly irradiates the ABp cell, which becomes the Dorsal cell (Crittenden et al., 1994; Evans et al., 1994), and P2 Wnt signalling targets the EMS cell, which becomes the Ventral cell (Rocheleau et al., 1997). After these two asynchronous divisions, specific cell arrangement and signalling pathway, the DV axis is established between ABp (Dorsal) and EMS

(Ventral), and lineages start to be determined with their proper cell fate determinants distribution in each cell.

c. The Left-Right axis (L-R)

The 4-cell stage set up a specific cell arrangement that allowed the proper induction of cell specification in dedicated lineage via signalling pathways. The subsequent division will be from the AB daughters. ABa and ABp divide simultaneously and symmetrically to form the future epithelial tissue (Sulston et al., 1983). The spindles of these two cells are arranged in an orthogonal manner regarding the AP and the DV axis. These spindles slope toward the anterior side during telophase, creating a left daughter cell which is more anterior with a different set of intercellular interactions (Figure 20.C.D). (Sulston et al., 1983; Wood, 1991). This last step physically establishes the LR body plan axis. After AB daughter division, EMS divide asymmetrically and creates the MS cell, the muscle precursor and the E cell, which is the precursor for intestinal tissue (Sulston et al., 1983). Taken together, the decision-making process governing the establishment of these body plan axes is ruled by two parameters, cellular interactions and the correct completion of asymmetric and symmetric divisions. This last parameter is determined by symmetry-breaking cues induced by specific protein segregation.

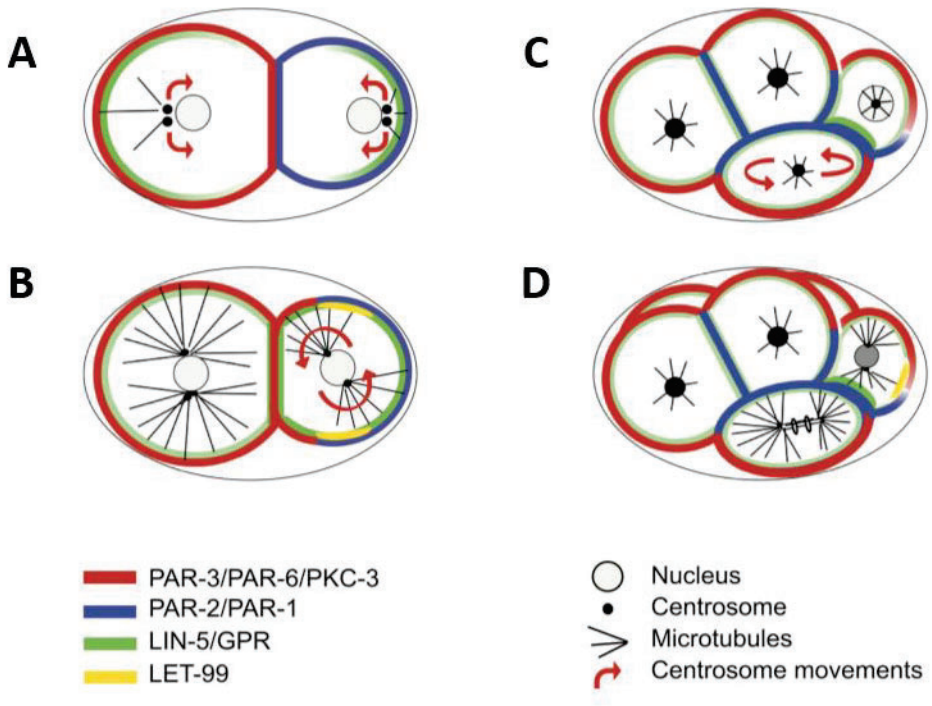

Figure 20: Polarity and spindle positioning from the 2 to 6-cell stage embryos.

(A) Early two-cell stage. As a result of asymmetric spindle elongation during anaphase, the first division is unequal and generates a larger anterior blastomere AB and a smaller posterior blastomere P1. (B) After the centrosomes migrate onto a transverse plane, the P1 nucleus rotates 90° during late prophase, aligning the centrosomes on the AP axis. By this time, asymmetric PAR domains have been reestablished .(C) At fourth cleavage, the spindles in the AB daughters initially set up along the left/right plane and the centrosomes in EMS are also on the left/right plane. PAR domains become established in the P2 cell, and GPR-1/2 become enriched at the P2/EMS cell contact. (D) In the AB daughters, the spindles shift slightly anteriorly during telophase, so the left daughters assume a more anterior position. In EMS, the nucleus rotates to align on the AP axis, and the P2 nucleus rotates so that one centrosome is adjacent to the P2/EMS cell contact. Figure Extracted from (Rose and Gönczy, 2014).

2- Cell identity acquisition

To establish a completely differentiated lineage, each differentiated cell needs to have a precise toolkit of molecular content. Some of these components are segregated specifically during lineage establishment with a mutualistic cooperative effect. During the first part, we already described the crucial impact of the polarity proteins, the PAR proteins and the different intercellular signalling pathways. Especially during the establishment of the A-P D-V body plan axis and their influence on the symmetrical properties of divisions, especially on the point that the cellular polarity influences the choice between symmetric or asymmetric division. This asymmetric division is the starting point of the creation of cellular diversity and, to an extent, cellular specificity.

Nevertheless, other molecular partners are specifically segregated and participate in the establishment of cellular identity. These other differentiation compounds are cell fate determinants and mRNA. Importantly, in parallel with the specific segregation of these molecular content, a targeted mechanism of protein and mRNA degradation occurs to ensure the proper molecular quantities of each of these components, thus reinforcing the effect of polarisation. These mechanisms, such as the ubiquitin pathways (DeRenzo and Seydoux, 2004; Pintard et al., 2004), are a completely different subject, not directly related to our questioning. This explains why I am not introducing these regulation machinery. Nevertheless, it is an essential feature that we consider when analysing our results.

a. Cell fate determinants

Downstream of the PAR proteins segregation, other segregated components are involved in the fate specification of cells; the polarity mediator: MEX-1, MEX-5, MEX-6, POS-1, and SPN-4. Downstream these polarity mediators some components are the cell fate regulators APX-1, GLP-1, PIE-1, and SKN-1. Here we presented a small portion of these protein categories that are precisely reviewed by Rose and Gönczy (Rose and Gönczy, 2014). All these components can bind and induce mRNA translation in a specific lineage. For instance, PIE-1 is related to the P lineage, and MEX-5,6 are related to the Anterior side ad the early AB lineage (Rose and Gönczy, 2014)(Figure 21). Another category of cell fate determinant is the P granules, also called “germ granules” because of their specificity to the P lineage. These, not membrane-

bound granules, contain mRNA and RNA-binding proteins specific to the differentiation of the P lineage (Smith et al., 2016). Cell fate determinants provided a complete genetic environment to allow genome expression. They are involved in translational control of the maternally loaded mRNA. As nicely suggested by the P granules distribution, a particular mRNA set is distributed in each cell. Nevertheless, P granules are only related to the P lineage; other lineages must have a specific mRNA abundance to differentiate in their appropriate lineage. To do so, mRNA outside of P granules must be precisely segregated in a particular manner among the different cells during early embryogenesis.

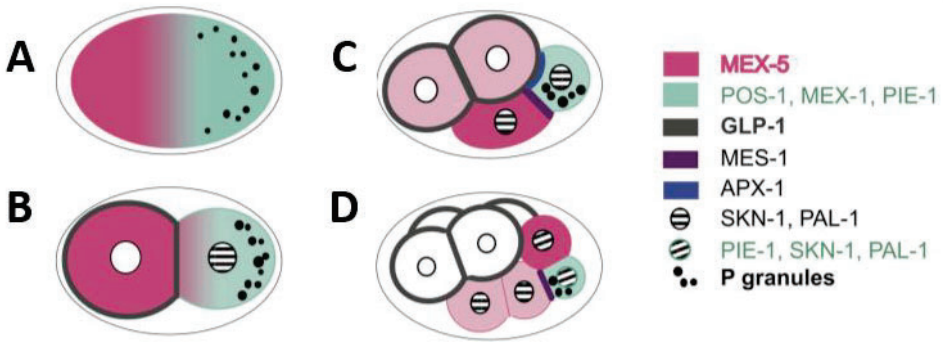

Figure 21: Asymmetric localisation of polarity mediators and cell fate regulators in the early embryo.

Mediators and cell fate regulators are localized to the cytoplasm (boxes and dots in legend), the membrane (thick lines) or nuclei (circles). In addition, all the polarity mediators and PIE-1 are localized on P granules during the early divisions. MEX-5, MEX-3, MEX-1, PIE-1, POS-1, and P granules are uniformly present in the cytoplasm just after fertilization, but become asymmetrically localized during the one-cell stage (A) and two-cell (B) stages. In addition to cytoplasmic localization, PIE-1 and SKN-1 enter the nucleus. As the cell cycle proceeds at the two-cell stage, MEX-5 becomes distributed in an anterior to posterior gradient in P1 and thus more MEX-5 is inherited by EMS. At the four-cell stage, MEX-5 begins to disappear (light pink) from the AB cells, but is still present in the EMS; MEX-5 is similarly lost from the other somatic daughters as divisions proceed. Figure and legends extracted from (Rose and Gönczy, 2014).

b. mRNA abundance among cells

C. elegans is the first multicellular organism completely sequenced, containing about 19 000 genes (*C. elegans* Sequencing Consortium, 1998). During embryogenesis, the first event of transcription and translation occurs during the Zygotic Genome Activation (ZGA), which is reported to happen at the four-cell stage in *C. elegans* (Evans and Hunter, 2005; Seydoux and Dunn, 1997; Tora and Vincent, 2021). This means that from fertilisation to the four-cell stage, cellular mRNA and protein distribution rely on specific segregation from the initial maternal loadings to bring the cell into a favourable genetical state for proper cell differentiation. In a recent study, these mRNA cell differences were quantified by using single-cell transcriptomics. They quantified the patterns of mRNA distribution between individual cells during early embryogenesis (Osborne Nishimura et al., 2015; Tintori et al., 2016). We extracted information regarding our proteins of interest using their online available data set. At the 2-cell stage, *cyk-1* and *cap-1* mRNA are slightly more enriched in AB compared to P1, and arx-2 mRNA is equivalently distributed between AB and P1. At the four-cell stage, they observed that c*yk-1* mRNA is more abundant in ABp, equivalent in ABa and P2 and almost absent in EMS; *arx-2* mRNA became significantly more distributed in P2 cells compared to the other; finally, *cap-1*, in the descending order, is more enrich ABp, ABa, P2 and then EMS (Tintori et al., 2016) (Figure 22). Although the meticulous and precise work realised by the Goldstein lab and the fabulous open-source information they provide, we need to consider that these single cells mRNA distributions were taken, as named, in a single-cell context. Without considering the cell cycle and inter-cellular interaction, which can affect cell fate markers distribution and mRNA degradation machinery. Nevertheless, my approach aims to verify some of their data at a protein scale and in an *in vivo* context.

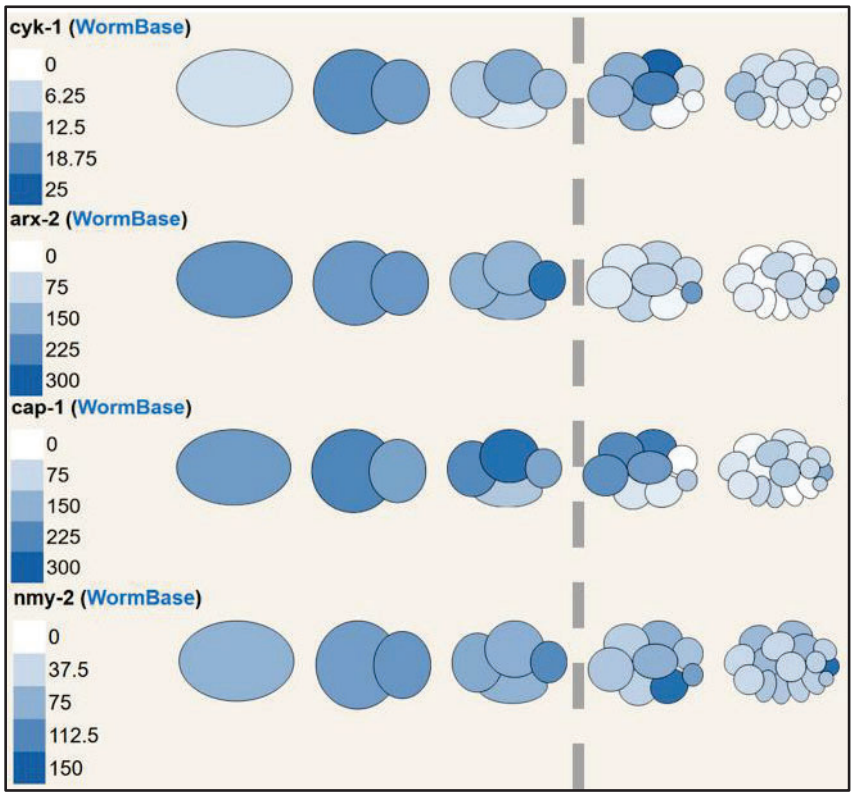

Figure 22: Relative transcript abundances of our targeted ABPs

Data extracted from the online freeware at: ***http://tintori.bio.unc.edu/***. The dashed line represent the Zygotic Genome Activation step. It represent the mRNA relative distribution from the 1 to the 16-cell stage, where we can already see a specific pattern of distribution.

3- Interplay between cell identity acquisition and actin cytoskeleton

All these molecular segregations, specifically the PAR proteins distribution, are influenced by the actomyosin cortex dynamics and Vice Versa; the actomyosin cortex dynamics is a crucial feature that impacts the PAR proteins distribution (Cowan and Hyman, 2007; Gan and Motegi, 2021; Munro et al., 2004; Ramanujam et al., 2018; Zonies, 2010).

a. Relationship between PAR and actomyosin cortex

To pursues the differentiation process in the early steps of embryogenesis, molecular content such as transcription factors, cell identity markers and mRNA are segregated in a specific manner (Gönczy and Rose, 2005; Rose and Gönczy, 2014; Tintori et al., 2016). On the one hand, many studies showed that perturbation of the actomyosin cortex impacts PAR proteins' distribution. In RNAi experiments, perturbation of the formin CYK-1 or the other actin nucleator, the Arp2/3 complex, during the zygotic stage affects the balance between the PAR-6 and the PAR-2 distribution. It influences the positioning of the future cytokinetic ring (Chan et al., 2019; Mangal et al., 2018; Pittman and Skop, 2012) (Figure 23.C).. The Arp2/3 complex is also implicated in the regulation of the RhoA signalling and especially the downstream Cdc42 foci present at the zygotic stage (Shivas and Skop, 2012) (Figure 23.D). At a later stage of development, the two subunits of the Arp2/3 complex, ARX-2 and ARX-3, are implicated in the cell epithelial cell fusion during the transition between the comma and the 2-fold stage, and a disruption of these two subunits leads to 100% of embryonic lethality (Zhang et al., 2017). At another scale, the entire actomyosin cortex, the cadherin HMR-1 is implicated in the link between the plasma membrane and the actomyosin cortex and the precise localisation of the PAR-2 and PAR -6 (Padmanabhan et al., 2017) as well as the global embryonic cohesion (Yamamoto and Kimura, 2017) (Figure 23.B).. On the other hand, other studies showed that a disruption in the PAR-2 distribution affects HMR-1 localisation (Yamamoto and Kimura, 2017). PAR protein distribution is finely regulated, and a perturbation drastically affects many cellular parameters at a different layer, such as embryonic inner cellular organisation cell shape and actin cytoskeleton organisation (Singh and Pohl, 2014) (Figure 23.A). Other studies have already linked mechanical properties of the actomyosin cortex, such as contractility, flow patterns or chirality, and early embryonic *C. elegans* lineage (Naganathan et al., 2018; Pimpale et al., 2020; Pohl and Bao, 2010). Still, up to now, it was

never explored if some single-cell differences exist in terms of actin nucleating capacities and how such differences impact cell identity acquisition.

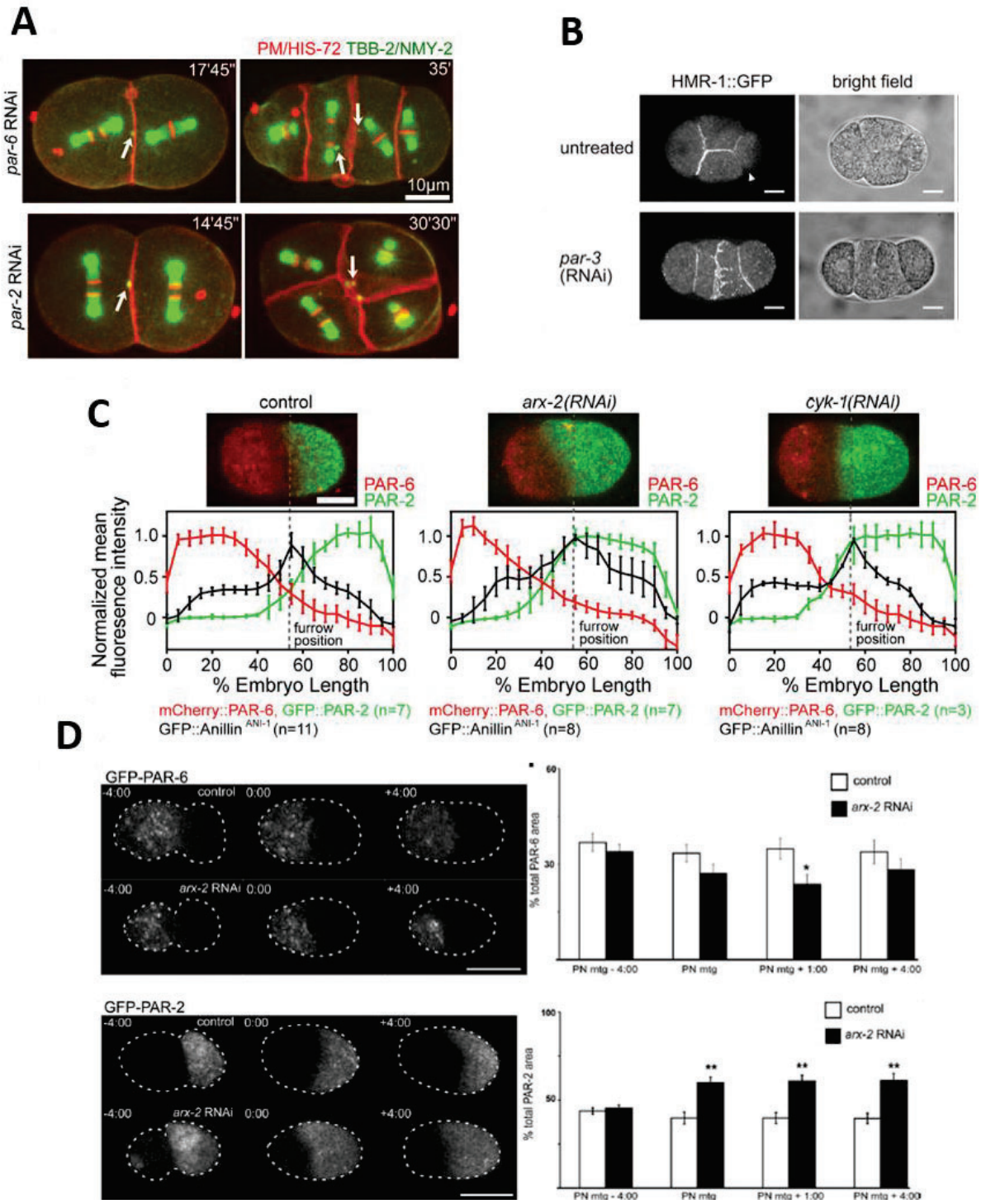

Figure 23: The close relationship between PAR proteins and ABPs

(**A**) Spindle rotation and MBR dynamics in par-2 and par-6 RNAi embryos. Maximum projection still images; arrows point to the AB-P1 Midbody. Figure extracted from (Singh and Pohl, 2014). (**B**) Micrographs of embryos expressing HMR-1 fused with GFP protein in untreated or par-3 RNAi condition. Figure extracted from (Yamamoto and Kimura, 2017). (**C**) Cortical plane images of control, ARX-2–depleted, or CYK-1 partially depleted embryos coexpressing GFP::PAR-2 and mCherry::PAR-6 at 50 s after anaphase onset. Mean fluorescence intensity (±95% CI) of cortical GFP::PAR-2 (green), mCherry::PAR-6 (red) and GFP::anillinANI-1 (black) along the length of control (left), ARX-2– depleted (middle), or CYK-1 partially depleted (right).Values from n number of embryos were normalized to the maximum mean signal in controls. Dashed line indicates the furrow position. Scale bars, 10 µm. Figure and legends adapted from (Chan et al., 2019). (**D**) ARX-2 affects actin dynamics and polarity establishment. i) (Left) Cortical Z-series projections of embryos expressing GFP–PAR-2 and treated with arx-2 RNAi. (Right)Percentage of total cortical area occupied by GFP–PAR-6 ii) (Left) Cortical Z-series projections of embryos expressing GFP–PAR-6 and treated with arx-2 RNAi. (Right) Percentage of total cortical area occupied by GFP–PAR-2 . Scale bars, 20 µm. Figure adapted from (Shivas and Skop, 2012).

b. ABPs specific segregation

In the previous section, we saw the relationship between actomyosin dynamics and the proper distribution of PAR proteins. In chapter 1, we saw how ABPs regulate the actin cortex dynamic and how this actin cortex can impact the differentiation process. Following this cortical organisation, especially during the zygotic stage, as the other molecular partners for the differentiation process, ABPs are segregated in a specific manner to tune the actin cytoskeleton of individual cells regarding their commitment to a particular lineage. Previous studies showed a distribution pattern for the different ABPs during one of the first cellular processes happening right after fertilisation, called polarisation. Cortical flow is initiated around the sperm pronucleus, dragging molecular components and actin proteome to the anterior side of the zygote. Here are a few examples of this process: actin filaments themselves are asymmetrically segregated, either by MOE-1 labelling (Shivas and Skop, 2012; Velarde et al., 2007) (Figure 24.A) or using the Lifeact probe (Reymann et al., 2016) (Figure 24.C). NMY-2, responsible for the contractility of the actin cortex, is segregated at the anterior side of the zygote after the polarisation step (Pacquelet, 2017; Reymann et al., 2016; Schonegg and Hyman, 2006). Other ABPs are non-equally distributed the scaffolding proteins, Septin (Jordan et al., 2016) (Figure 24.D); the E-cadherin HMR-1, implicated in adherent junctions (Padmanabhan et al., 2017) (Figure 25.B); DYN-1, a protein that regulates endocytosis and actin comet formation (Ai and Skop, 2009; Pittman and Skop, 2012). Regarding CYK-1, it has been reported that CYK-1 is equally distributed along the anterior-

posterior axis of the zygote and slightly enriched on the posterior side after the anaphase onset (Zaatri et al., 2021) (Figure 24.B). Other dissimilarities can be observed at later stages, such as the NMY-2 and the actin-F probe Lifeact::mKate2 at the 8-cell stage (Caroti et al., 2021) (Figure 25.A). Taken together, it shows the close interplay between these PAR proteins' distribution and the integrity of the actomyosin cortex and how a perturbation on one partner can affect the other and Vice Versa. ABPs are rulers of the actomyosin cortex dynamics. ABPs repartition among cells is a fundamental parameter that will directly influence the actomyosin cortex in individual cells and, by extent, participate in the proper polarisation of PAR proteins, cell fate determinants distribution and, in fine, cellular differentiation. (Fig 3. F). Nevertheless, these studies showed a specific ABPs distribution with precise measurements done during a particular snapshot of the embryogenesis. However, the dynamical establishment of these ABPs content differences still needs to be clarified and quantifying the mutual effect between ABPs amount and the cell fate determinants distribution still needs to be discovered.

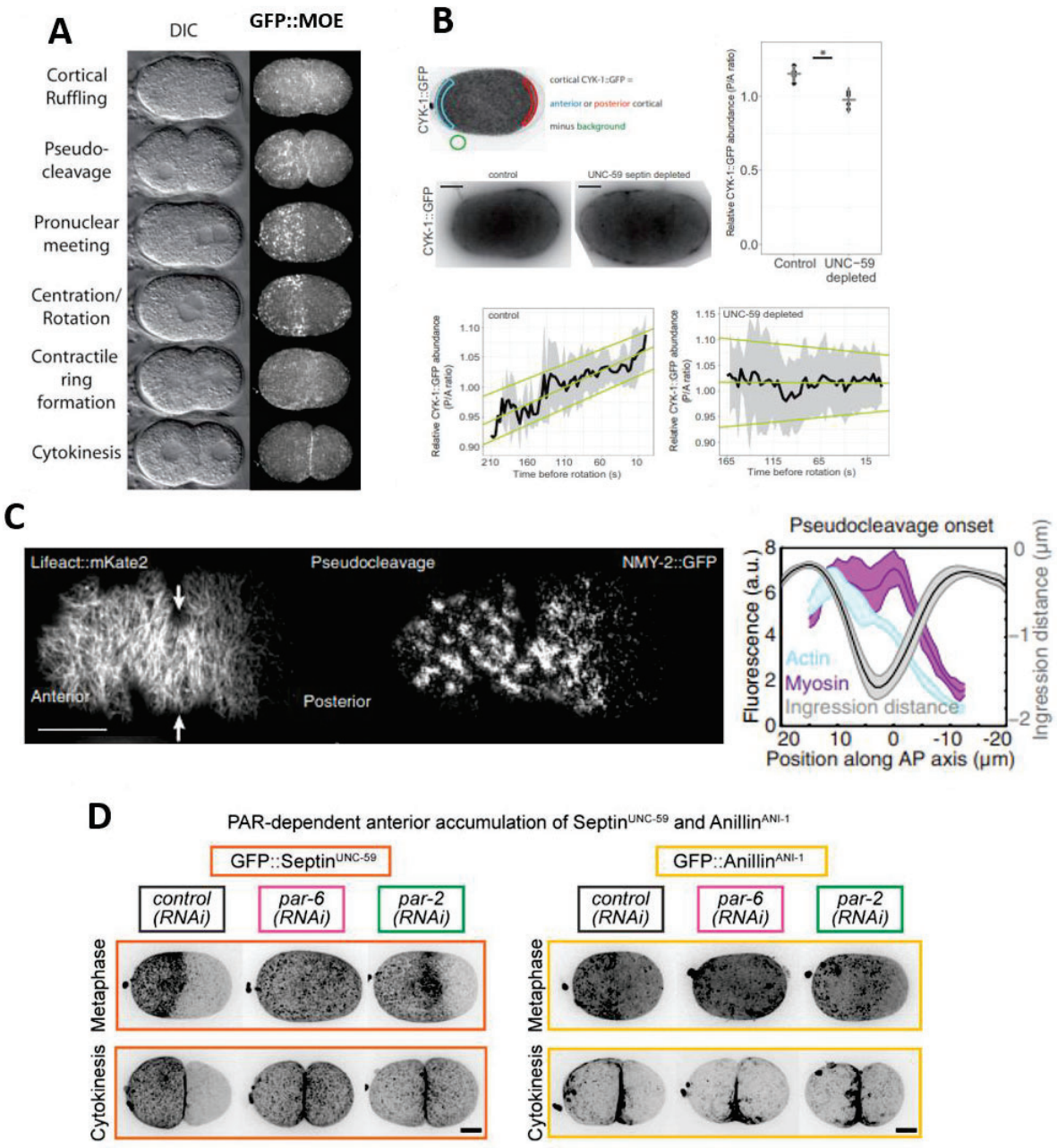

Figure 24: ABPs anteriorisation during polatisation

(**A**) DIC and Z projection of a Wild type embryo expressing GFP::MOE, tagging actin filaments. Figure extracted from velarde 2007. (**B**) CYK-1::GFP during the anaphasis with or without Unc-59 Septin RNAi treatment. Quantification of the relative CYK-1::GFP abundance in total (right plot) or seconds before rotation (bottom). Figure extracted from (Zaatri et al., 2021) (**C**) Cortical section embryos expressing Lifeact::mKate2 taging actin filaments and NMY-2::GFP during pseudocleavage. Figure extracted from (Reymann et al., 2016). (D) GFP::SEPTIN and GFP::ANILLIN during metaphase and cytokinesis with or without *par-6* and *par-2* RNAi treatment. Figure extracted from (Jordan et al., 2016)

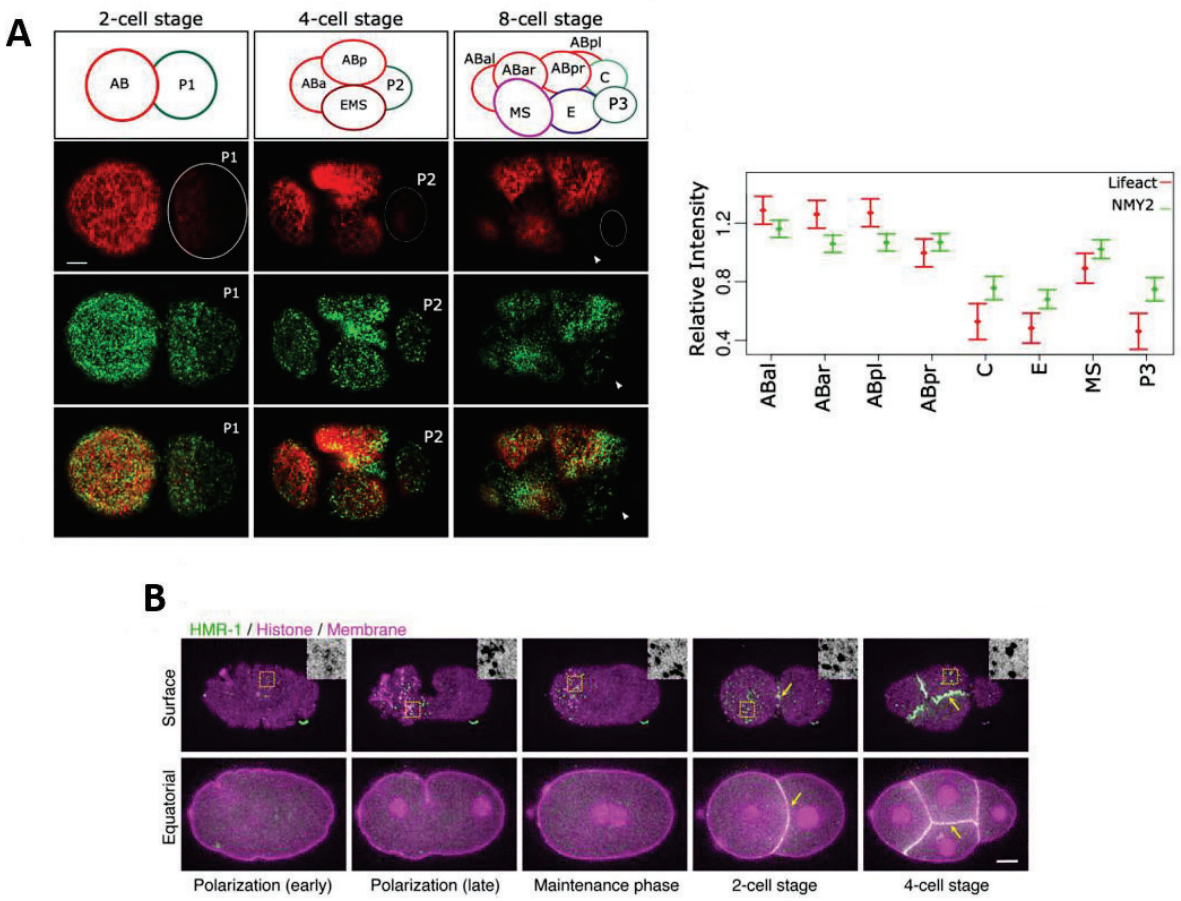

Figure 25: ABPs specific segregation at later cell stages

(**A**)Wild type embryos expressing Lifeact::mKate2 and NMY-2::GFP during the 2, the 4 and the 8-cell stages. Corresponding relative intensity on the right panel. Figure extracted from (Caroti et al., 2021). (**B**) Wild type embryos expressing HMR-1::GFP, Histone (Red) and membrane (Red) from the polarisation to the 4-cell stage. Figure extracted from (Padmanabhan et al., 2017).

Results

Reymann Lab "lens."

C. *elegans* embryogenesis follows a well-defined developmental pattern in which invariant cleavages lead in some divisions to a reproducible arrangement of cell interactions together with controlled distribution of cellular compounds required to define the first founder cells. These differentiated cells are set notably via cellular polarisation, asymmetric or symmetric divisions or intercellular signalling events. All these processes rely in part on the actin cytoskeleton, which is involved in cell shape and mechanical integrity, as well as the organisation of the intracellular space, while responding actively to the environment, such as cell positioning within the embryo. To do so, actin is organised in various functional structures that are tuned in a spatio-temporal manner, such as the thin actomyosin cortex attached to the plasma membrane, cytokinesis rings or filopodia. The regulation of these actin networks is orchestrated by a plethora of Actin Binding Proteins, such as nucleators, molecular motors or bundlers, that change the 3D organisation, dynamics and properties of these specific actin structures. The physical properties of these microscopic networks control the macroscopic cellular behaviours, can affect the process of cell commitment and gene expression profiles, and can therefore modulate and provide feedback into cell fate acquisition. In the early *C. elegans* embryo, correlations were already made between cortical properties like contractility, actin dynamics, flow patterns, chirality and lineage pattern or axis establishment.

One general objective of the Reymann lab is to understand how the nucleation of actin architectures is temporally and spatially controlled in the different founder cells of *C. elegans* embryos and how it can affect their fate. To decipher these mechanisms, we aim to answer the following questions: Are Actin Binding Proteins (ABP) equally distributed between sister cells? If not equally distributed, how do these protein imbalances impact actin architectures? How is the actin nucleation machinery spatiotemporally controlled? Are the cortical actin properties inheritable? My PhD project is part of this lab's big picture. My dedicated aim, duty, mission, and quest were thus to study the relationship between actin architectures, molecular content and cell identity throughout the early *C. elegans* embryogenesis. During this period, I pursued my objective and, following the path of discoveries, four aims emerged from this PhD work, which I will summarise here in a concise sentence; an exception is not the beginning of a habit, and I will detail it in the following pages.

Aims of the project

AIM 1: Spatio-temporal dynamics of the three major cortical actin regulators during the early embryogenesis of *C. elegans*.

Before gene regulation and intercellular signalling pathways occurred in the *C. elegans* embryo, as a result of every cell division pattern, each ABPs are segregated differently in each cell, defining a specific cortical identity and questioning the paradigm of symmetric division.

AIM 2: Molecular characterisation of membrane-rich microdomains appearing in the anterior cortex of the polarising *C. elegans* zygote and identified as filopodia.

During the polarisation phase, the anterior side of the zygote has tubular membrane microdomains that appear to be filopodia, once identified, these filopodia were also found at different cell-cell contact area.

AIM 3: Temporal characterisation of filopodia during the 2 and 4-cell stages.

In addition to the spatial localisation of these filopodia at the cell-cell contact area, their numbers at the cell-interface are dynamically correlating to the cell cycle progression.

AIM 4: Emergence of a lamellipodium-like structure during the 4 to 6-cell transition.

At the end of the 4-cell stage, filopodia that are present at the intercellular contact area between the AB daugthers completely disassemble and a fraction of second after, during the transition between the 4 to the 6-cell stage, the inner side of the EMS cell reorganise its cortical actin network into a lamellipodium-like structure.

AIM 1: Spatio-Temporal dynamics of the three major cortical actin dynamics regulators during the early embryogenesis of *C. elegans*.

In the introduction, I depict the close and mutualistic relationship between the actomyosin cortex and cell identity acquisition. Most of the studies on this crucial process are focused on the cell identity perspective and mechanical aspects of the cortex without a deep insight into the actin cortex composition. ABPs are the molecular regulators of this actin cortex, and some key players ABPs, responsible for the regulation of polymerisation dynamics (respectively growth and arrest), are the actin nucleation proteins and the capping protein. In *C. elegans*, these molecular players are the formin CYK-1, the Arp2/3 complex and the capping protein CAP-1. The first aim of my PhD project was to characterise the global dynamics of these three main actin cortex regulators during these early steps of embryogenesis, from the zygote to the 4-cell stage. As a first hint, single cells transcriptomics already informed us about the stereotypic segregation of their respective mRNA distribution. I aimed to verify these affirmations at the protein level and in a physiological manner, focusing on the dynamical endogenous protein expression in an *in ovo* context. To respect my approach, I used the CRISPR/Cas9 genome editing tool, spinning disk microscopy and bioinformatics image quantification. This allows me to map these three actin bindings proteins' relative abundance between each cell. I set up a pipeline of live imaging spinning disk microscopy and semi-automated quantitative image analysis giving as output a reference distribution of endogenous protein densities in each cell. This method allows to follow protein spatio-temporal abundance at the cortical and cytoplasmic planes and compare the differential segregation between cells. I found differences in proteins content between cells. At the 2-cell stage, CYK-1 is equilibrated between the AB and P1 cells. We can observe strong cortical recruitment during the cytokinesis ring building, and ARX-2 and CAP-1 are more concentrated in AB than in P1. Cellular differences arise particularly at the 4-cell stage. Surprisingly, it shows asymmetries between sister cells from a symmetric division such as ABa and ABp for all these 3 ABPs. There are also similarities between cells that came from different lineages, like ABp and EMS concerning CYK-1 and ABa and EMS for ARX-2 and CAP-1. Taken together, ABPs distribution is different between cells, and they are not following the lineage and the transcriptomics data. The cortical distribution of ABPs (actively recruited pool in the actin cortex) is more dynamic. It reflects the differences observed at the cytoplasmic pool (passive

pool) due to the spatio-temporal regulation at the cortex. A manuscript of this work is written and will be submitted for peer review in the short term. At the time of writing, January 2023, I present the manuscript as it is, with the understanding that is not submitted yet and additional figures and discussions will be added in the coming weeks.

Asymmetric distribution of actin-related proteins can precede known cell differentiation events in the early *C. elegans* embryo.

Grégoire Mathonnet[1,2,3,4], Roxane Benoit[1,2,3,4], Delphine Sunher[1,2,3,4], Nadine Arbogast[1,2,3,4], Christophe Reymann[5], Anne-Cécile Reymann[1,2,3,4]

1. Institut de Génétique et de Biologie Moléculaire et Cellulaire, IGBMC, Illkirch, F-67404, France.
2. Centre National de la Recherche Scientifique, CNRS, UMR7104, Illkirch, F-67404, France.
3. Institut National de la Santé et de la Recherche Médicale, INSERM, U1258, Illkirch, F-67404, France.
4. Université de Strasbourg, Strasbourg, F-67000, France.
5.

Abstract:

During the stereotypic embryogenesis of the nematode *Caenorhabditis elegans* and from the first division onwards, cell differentiation arises from a combination of cell polarisation, asymmetric or symmetric divisions and intercellular signalling processes. This pattern of embryonic cell differentiation is driven by the specific segregation of molecules occurring during each cell division, covering diverse categories of molecular content, such as polarity proteins or cell fate determinants, transcription factors, p-granules and mRNAs. These distribution patterns are coupled with the stereotypical dynamics of cortical actin, which also plays a crucial role in these processes. However, compared to other molecular contents, how the actin per se is segregated from the first asymmetric division onward remains poorly understood. This study presents quantification of the intracellular distribution of three essential actors of actin polymerisation: two nucleators, namely a formin CYK-1 and the Arp2/3 complex via ARX-2 as well as a capping protein CAP-1, from the zygote to the 4-cell stage. We found that asymmetric divisions correlate with asymmetries in actin-related content too. Surprisingly, differences in content are also revealed in the AB daughter cells before the onset of cell signalling events that lead to ABp differentiation. Thus, asymmetric

distribution of actin-related proteins can precede cell differentiation at these stages, opening a new scope for the role of actin in enabling cell identity acquisition in the early embryo.

Introduction:

The actin cytoskeleton is a significant actor controlling cell shape and cell mechanics. As such, it is required for different cell-cycle-specific events. To fulfil these fundamental purposes, the actin cytoskeleton is organised in various highly dynamic and sometimes temporary structures, notably at the cell periphery: the thin and contractile actomyosin cortex coupled to the plasma membrane, the cytokinesis ring assembled during cell division and physically separating the daughter cells, as well as cellular protrusions either filopodia or lamellipodia, actin filaments populating the cell cytoplasm or even assembled in the nucleus (Blanchoin et al., 2014; Etienne-Manneville, 2004). Actin can be found in a dynamic steady state: “filaments continuously assemble and disassemble while sometimes maintaining constant network structures” to full fill each of these functions (Plastino and Blanchoin, 2018). To control actin assembly dynamics, cells repress spontaneous polymerisation via G-actin sequestering proteins and actin nucleating agents to catalyse filament nucleation and elongation (Pollard, 2016). Two main actin nucleators are the formin family and the Arp2/3 complex. On the opposite side, some proteins block filament elongation, such as capping proteins, while others fragment filaments, such as the cofilin family. Suppose upstream signalling events are crucial in regulating the recruitment of specific Actin Binding Proteins (ABPs) in time and space. In that case, self-assembly properties about biochemical, mechanical and geometrical constraints are also at work because the different local combinations of these many proteins produce different types of actin networks. Local biochemical equilibrium, together with structural and mechanical feedback, thus maintains a diversity of co-existing

actin networks in a dynamic steady state (Manhart et al., 2019; Plastino and Blanchoin, 2018). To rapidly change actin networks, cells tune protein's availability and activity, thus modifying the mechanical properties of the emerging architectures (Naganathan et al., 2018) and controlling cells. In cascade, the actin cytoskeleton can therefore affect cells commitment during differentiation in different cell types as well as during critical morphogenetic events during embryogenesis, such as during epithelial sheet closure, to name just one (Fischer et al., 2019; Martín-Blanco and Knust, 2001; Williams-Masson et al., 1997).

C. elegans embryogenesis combines an invariant lineage and early cell specification from the zygotic stage onwards. A combination of symmetry-breaking events of different natures enables the "tour de force" of assigning each cell its identity and setting the fate of the respective lineages in the first few divisions. Cellular polarisation of membrane-associated proteins, segregation of cell fate determinants, mechanical, chemical or diffusion gradients, as well as phase-separated granules (De Henau et al., 2020; Hamill et al., 2002) or asymmetries in volume during division are but a few examples of the required symmetry breaking events driving these cell differentiation events (Gönczy and Rose, 2005; Rose and Gönczy, 2014; Samandar Eweis and Plastino, 2020). In addition, many studies have already revealed some of these events' interconnection and direct coupling. For example, mechano-chemical coupled mechanisms link the establishment of actomyosin-based cortical flow and membrane-associated polarity. Overall, this underlines the complexity of the scenario leading to the robust embryonic choreography at work in this nematode embryo.

The rapid segregation of cellular compounds has been intensively studied during the zygotic anterior-posterior polarisation stage: an actomyosin contractility gradient is established after fertilisation, inducing cortical flow towards the anterior pole. Cortical flow is thus dragging all actin-associated cortical and membrane-associated proteins to the anterior

side of the zygote. Mechanical forces via friction and chemical interactions via a change in protein turnover are coupling flows to establish anterior versus posterior protein domains (Delattre and Goehring, 2021; Goehring and Grill, 2013). In addition to PAR polarity proteins, studies have already revealed the anterior enrichment of actin filaments using the MOE-1 labelling system (Shivas and Skop, 2012; Velarde et al., 2007) or using the Lifeact probe (Reymann et al., 2016); NMY-2, responsible for the contractility of the actin cortex (Pacquelet, 2017; Reymann et al., 2016; Scholze et al., 2018; Schonegg and Hyman, 2006); the scaffolding proteins, Septin (Gilden and Krummel, 2010; Jordan et al., 2016; Nguyen et al., 2000); the E-cadherin HMR-1, implicated in adherent junctions (Padmanabhan et al., 2017); DYN-1, a protein that regulates endocytosis and actin comet formation (Ai and Skop, 2009; Shivas and Skop, 2012) as well as the Rho GTPase RHO-1 and CDC-42 and their Guanine nucleotide Exchange Factor (GEF) ECT-2 (Scholze et al., 2018). Regarding an essential formin in the early embryo, namely CYK-1, it has been reported that it is enriched in the outer anterior cortex and then progressively switching to an increase in the extreme posterior cortex just before the anaphase cortical rotation (Zaatri et al., 2021). These asymmetric distributions of cellular content define two non-identical cellular halves: giving rise to the larger AB daughter and smaller P1 daughter, which also differ in molecular content. This first cleavage is followed by the division of the AB cell, which is known to divide symmetrically, giving rise to the two AB daughters, ABa and ABp, which are named according to their position along the antero-posterior axis. A second PAR polarity gradient is established in the P1 cell, leading to its asymmetric division into the larger ventral EMS cell and the smaller posterior P2 cell (Delattre and Goehring, 2021; Gan and Motegi, 2021; Gönczy and Rose, 2005; Horvitz and Herskowitz, 1992; Rose and Gönczy, 2014; Sulston et al., 1983). Due to eggshell confinement and imposed cell-cell contacts of the diamond-shaped 4-cell stage, signalling from P2 leads to the

differentiation of EMS and ABp but not its sister cell ABa with whom P2 has no direct contact (Evans et al., 1994; Rocheleau et al., 1997). In conclusion, different studies have already linked mechanical properties of the actomyosin cortex, such as contractility, flow patterns or chirality and early embryonic *C. elegans* lineage (Naganathan et al., 2018; Pimpale et al., 2020; Pohl and Bao, 2010) but up to now, it was never explored if some single cell differences exist in terms of actin nucleating capacities and how much difference impact cell identity acquisition.

We aim to characterise the global dynamics of three main actin-binding proteins from the zygote to the four-cell stage known to impact actin polymerisation and cortical mechanics (Naganathan et al., 2018). We targeted three essential actors: two nucleators, a formin CYK-1 and the Arp2/3 complex via its subunit ARX-2, and a capping protein, CAP-1. CYK-1 belongs to the formin family and is known to be mandatory for the first cell cytokinesis completion (Jordan et al., 2016; Severson et al., 2002; Swan et al., 1998). Arp2/3 complex is required for cortical filament nucleation and stability in early embryogenesis (Severson et al., 2002; Yan et al., 2022) and is mandatory for cell migration during gastrulation (Knight and Wood, 1998; Yan et al., 2022). Interestingly, balanced nucleation via Arp2/3 and CYK-1 sets filaments homeostasis and is required for "timely assembly and constriction of the contractile ring" (Chan et al., 2018). CAP-1 also impacts actin organisation during the zygotic stage or in the adult germline (Ray and Zaidel bar, 2021). When each of these three proteins is partially depleted via RNAi, the physical properties of the cortex are affected: the hydrodynamic length is reduced in all three cases leading to a decrease in cortical chiral flows in the zygote (Naganathan et al., 2018) but an increase in the actomyosin based contractility in the gonad depleted of CAP-1 is observed (Ray and Zaidel bar, 2021). The balance between actin nucleation via formin or Arp2/3 sets the entanglement of actin networks, the amount of monomeric actin available for each of these polymerisation events, and the rate of filament

capping is critical to set filaments length, actin network organisation also determines contractile capacities and turnover. For all these reasons, CYK-1, ARX-2 and CAP-1 are thus crucial for determining the actin cytoskeletal steady state and contractility.

To sum up, some tight regulations of ABPs content impact cell specificities in terms of cytoskeletal architectures, scaling up to specificities in terms of mechanical properties and extending up to control of cell potency. Several recent findings are showing more and more direct causality links between actin dynamics and cell fate, one of the last being the study of Aloiso et al, which demonstrates how a slight imbalance of one actin nucleator can lead to a significant impact on cell state and cell fate (Aloisio and Barber, 2022). To better understand these particularities of the cellular specification process, there is a crucial need for a quantitative assessment of cellular content, especially of the actin regulation machinery. To fill this knowledge gap, we addressed the following questions using the model organism *C. elegans*: do these proteins have a specific spatio-temporal distribution in some early embryonic cells? Do all cells have equal actin nucleation capacities? These results will be fundamental to understanding how cortical actin properties are inherited over the first few divisions and how it could impact further lineage commitment. To answer these questions, we have set up a pipeline of live imaging spinning disk microscopy and semi-automated quantitative image analysis giving as output a reference map in space and time of endogenously expressed proteins densities in each cell. This method allowed us to follow protein spatio-temporal dynamics at the cortical and cytoplasmic planes and compare the differential segregation between cells during the early dynamical steps of *C. elegans* embryogenesis.

We found that at the 2-cell stage, CYK-1 is equilibrated between cells, whereas ARX-2 and CAP-1 are more concentrated in AB than in P1. Cellular differences arise particularly at

the 4-cell stage for all these 3 ABPs. We found that the larger EMS cell inherits more ABPs than its smaller P2 sister. Surprisingly, we also demonstrate the asymmetric distribution between sister cells that came from a symmetric division (ABa and ABp). Inversely, we found similarities at an inter-lineage level between ABp and EMS for CYK-1 distribution, and to a lesser extent, between ABa and EMS for ARX-2 and CAP-1 but only during the early step of the 4-Cell stage.

Results:

4D mapping of ABPs distribution during the early embryogenesis

To follow the localisation of some of the primary regulators of the actin polymerisation in the early *C. elegans* embryo, namely two actin nucleators, the formin CYK-1 and ARX-2, a subunit of the Arp2/3 complex, as well as the capping proteins, CAP-1, we make use of CRISPR/Cas9 engineered GFP Knock-In strains (Tables 1). The intensity of the observed fluorescence acquired using high resolution, and high sensitivity microscopy does thus reflect the endogenous protein content and should directly correlate with their respective local concentration. Acquisition in the equatorial section or mid-plane of the embryo reflects the cytosolic concentration, which can be considered a pool of proteins that transition between the activated and the inactivated states. Proteins mostly diffuse freely in the cytoplasm but can also encounter filaments there; indeed, if actin filaments are less densely populating the cytoplasm, they can also be associated with organelles(Velarde et al., 2007; Venkatesh et al., 2020) or freely floating in the cytosol and thus impact other cell functions such as via the regulation of cytoplasmic viscosity (Wagner et al., 1999). In contrast, acquisition in the cortical plane reflects protein density at the cell cortex. Thus, mainly the actively engaged proteins with cortical actin filaments or recruited proteins at the actin cortex-cell membrane interface

impact cell shape, cell-cell interfaces, and positioning. We obtained the precise timeline of ABPs distribution over 25 minutes time course ranging from zygote to the 6-cells stage (Figure 1). As cell cycle progression also affects actin organisation, we decomposed each cell stage in three phases, an “Early” and “Late” phase (Costache et al., 2022) as well as the cytokinesis phase, using as reference the onset of membrane ingression that correspond to the time “0” for each cell stage and represented by a red dashed line on our timeline (Figure 1.A).

As expected, in the equatorial plane, actin-binding proteins in the cytosol show fewer variations over time when rich actin dynamics are observed at the cell periphery. In addition to the cell steady-state actin cortex, different transient actin architectures are present notably at cell-cell interfaces. During the late 2-cell and the late 4-cell stages, membrane protrusions corresponding to actin structures, namely filopodia, are clearly distinguished by their characteristic tips labelled with CYK-1::GFP (Figure 1.B) (Hirani et al., 2019). These structures are enriched in ARX-2 at their base; CAP-1 in their core (Figure 1.C.D). Further characterisation was performed by the Reymann lab and will lead to a future dedicated publication. In addition to these actin structures at the cell periphery, we can also observe the precise dynamics of recruitment of these proteins during the cytokinesis ring assembly and compare each successive division.

CYK-1 is differentially recruited at the cortex during the cytokinesis of P0, AB and P1.

We first assessed quantitatively the overall spatio-temporal recruitment of our three proteins of interest at the cortex. Observation of the actin cortical plane shows some local actin-binding protein enrichment in correlation with the cell cycle, notably during cytokinesis

ring assembly in P0, AB, and P1 cells (Figure 2.A.B.C). We observe, as expected, significant recruitment of the CYK-1 formin (Reymann et al., 2016; Tim Davies et al., 2018) compared to the Arp2/3 complex and CAP-1 capping protein which show only minor or no overall cortical enrichment during this time cellular period.

In addition, our approach enables us to observe some previously not characterised cortical recruitments of ABPs. At the early 2-cell stage, between -400s and -200s, CAP-1 is specially recruited at the cortex of AB and not in the cortex of P1. ARX-2 is similarly cortically recruited in AB cellular cortex during this early 2-cell stage, between -400s and -250s (Figure 2.B.C). At the late 4-cell stage, cortical ABPs show smaller variation over time. Between 200s and 400s, CAP-1 is enriched differentially in function of the lineage. In the AB daughters, CAP-1 is cortically enriched for 11% between the early (200s) and the late 4 (400s)-cell stage (Figure 2.D.E). In contrast, in the P1 daughters, CAP-1 is not particularly recruited at the cortex in EMS, and it decreases by 10% in P2 (Figure 2.F.G). ARX-2 is also cortically enriched in AB daughter's cortex for 10% during the same time phase (Figure 2.D.E) and not particularly in P1 daughters (Figure 2.F.G).

Surprisingly, time alignment with respect to individual ingression onset shows an asynchrony in the initiation of CYK-1 recruitment between AB and P1, especially earlier for P1, both if we take the reference time of cytokinesis initiation of AB, light purple, or the reference time specific for P1, dark purple, as well as a non-equal rate of recruitment between P0, AB and P1 (Figure 2.H). Indeed, we observe that formin recruitment at the cortex starts at 300s before ingression onset for P1, at 200s before for AB and 150s for P0. (Figure 2.H). We also observed a non-systematic correlation between the maximum CYK-1 cortical recruitment and the ingression onset, especially for P0 and P1 (Figure 2.H). Alignment with respect to the peak

of recruitment shows that the recruitment rate is faster for cells showing a shorter assembly phase (Figure 2.I).

In conclusion, our quantification procedure enables us to compare the recruitment dynamics of actin-binding proteins, notably during cytokinesis ring assembly, which shows cell-to-cell variations in terms of timing and rate or amplitude of recruitment. Actin nucleators trigger the assembly of actin filaments with some local and temporal control in relation to the cell state, such as to trigger cytokinesis ring formation or the assembly of subcellular specific actin structures(Hirani et al., 2019; Reymann et al., 2016; Yan et al., 2022). On the one hand, such assemblies are regulated via upstream signalling cascades leading to the recruitment of active Rho (Li et al., 2022; Michaux et al., 2018; Scholze et al., 2018), which activates formin, or the recruitment of WASP family, or CDC42 activator of the Arp2/3 complex at the membrane. On the other hand, the concentration of the proteins required for actin assembly: the nucleator, the available monomeric actin molecule often in complex with profilin, and the filament's density for Arp2/3 side branching are also important factors to consider (Pollard, 2016; Svitkina and Borisy, 1999; Volkmann et al., 2001), especially if the availability of any of these proteins is a limited factor (Carlier, 1998; Suarez and Kovar, 2016; Ti and Pollard, 2011).

Cytosolic ABPs are differently segregated in each blastomere, even between sister cells.

To follow the partitioning of our actin-binding protein of interest at each division step, we focused first on the quantification of intensities in the cytoplasmic cross-section of the embryo, thus on the global pool of proteins available in each cell. Observation of the raw time evolution of the mean intensity in each cell in single embryos shows the inequality of

cytoplasmic mean intensities in these cells (Figure 3.A). We can observe that the mean cytoplasmic intensity in the larger AB cell is higher than in its smaller P1 sister cell (Figure 3.A). The ABp cytosolic fraction is enriched at the four-cell stage compared to ABa and EMS, and the smaller P2 is significantly lower (Figure 3.A). To better assess cell-to-cell variability and the comparison of different embryos altogether, we used two approaches to compare cells. On one side, the ratio of the mean intensity of two cells taken at each time point in the midplane section enables following the time evolution of the contents of cells present during the same time intervals (Figure 3.B.C.D.E.F). On another side, we used the probability distribution function of the intensities found in each cell type, and we compiled the convolution of the normalised distributions for each cell pair giving in a statistically significant manner the cell pair content differences covering all-time point in each sample (Figure 3.G).

The time evolution of the average mean intensity cell-to-cell ratio between AB and P1 confirms an imbalance in favour of AB (Figure 3.B). At the maximum, CAP-1 is 13% more concentrated in AB than P1, and ARX-2 is 7% more concentrated in AB than P1 (Figure 3.B). These differences could be the consequence of the zygotic asymmetric division. The formin CYK-1 is also observed enriched in the AB cell during the early 2-cell stage, for about 4% compared to P1 cytoplasm (Figure 3.B). This CYK-1 difference is equilibrated only between the two sister cells just before the cytokinesis onset of AB when P1 is also recruiting CYK-1 at its cortex. This observation gives a first hint about the close relation between cytosolic and cortical content (Figure 3.B).

At the 4-cell stage, ABp is slightly but stably enriched in all three ABPs compared to ABa, similarly for about 5% for all time points recorded (Figure 3.C). This observation confronts the paradigm about molecular content in sister cells that came from a symmetric division (Gan and Motegi, 2021; Priess and Thomson, 1987) and, in fact, show an asymmetric distribution

of actin-related content. All these three proteins show a clear enrichment in EMS compared to P2 at all steps of the cell stage, with maximum differences of 19% for CAP-1 and ARX-2 and 15% for CYK-1 (Figure 3.D).

We also found similarities between cells even though they came from different lineages. Indeed, ABa and EMS about their ARX-2 and CAP-1 cytosolic proteins pool, which is equally distributed transiently during the early 4-cell stage and tend to be more enriched in the ABa cytosol at the end of the 4-cell stage (Figure 3.E). Between ABp and EMS, their CYK-1 cytosolic pool, which starts to be 7% different in favour of EMS, becomes rapidly equal during the 4-cell stage (Figure 3.F). Despite these inter-lineage similarities, we also observed essential differences between cells from different lineages. EMS is more concentrated in CYK-1 than ABa, with a stable 7% difference (Figure 3.E). ABp is more enriched in ARX-2 and CAP-1 compared to EMS, and this progressive enrichment has a special dynamic because it increases by about 5% throughout the 4-cell stage (Figure 3.F).

Our second quantification method based on the difference in cell pairs probability distribution functions confirms that significant cell-to-cell differences exist (Figure 3.G). First, looking at the difference in raw intensity gives us additional information, as no normalisation procedure between cells is required in this method. We thus observe that for all cell pairs, CAP-1 shows a more significant difference, followed by ARX-2 and CYK-1 (Figure 3.G). The shift of differences observed here is coherent with the above-discussed cell pair ratio of intensities corresponding to the first quantification method.

In conclusion, cytoplasmic differences are observed along cell separation during the first three cell divisions. Our results show differences that are more pronounced in the case of asymmetric partitioning, but that can also surprisingly exist in the case of apparently equal partitioning of the AB cell. These results indicate that each cell between the 1 to the 4-cell

stages contains a different set of cytosolic concentrations of the formin CYK-1, the Apr2/3 complex, and CAP-1 capping protein.

ABPs differential segregation are enhanced at the cortex with a specific dynamic.

Following this first important finding, we aimed to verify whether differences at the cytoplasmic level correlate with differences in protein abundance at the cell periphery. To assess if the cytoplasmic concentration of proteins could affect the density of active proteins targeted to the actin cortical plane. Note first that the cortical plane includes the actin cortex per se and the embedded actin architectures described above, such as filopodia, endocytotic patches or lamellipodia. Second, in this part of the study, we refer to the cortex as the cell surface area facing the eggshell, i.e. the cell-free cortex. We excluded the cell-cell contact interfaces for technical reasons, notably due to the impossibility of attributing the proteins found at each of these interfaces to one or the neighbouring cell. We thus compared the quantification of the mean intensities at the cortical planes of each cell, following the same approaches used for the cytoplasmic plane.

We start by observing the raw time evolution of the mean intensity in each cell cortex in single embryos. We saw an inequality of cortical mean intensities in these cells (Figure 4.A). We can observe that the mean cortical intensity in the larger AB cell is higher than in its smaller P1 sister cell, especially regarding CAP-1 (Figure 4.A). The ABp, ABa and EMS cortical fractions are enriched at the four-cell stage compared to the total mean intensity of the embryo and the P2 cell (Figure 4.A).

At the 2-cell stage, we observed a clear enrichment of ARX-2 and CAP-1 in the AB cell compared to the P1 cell with a maximum of 14% and 22%, respectively (Figure 4.B). CYK-1 cortical distribution, however, is more balanced between these two sister cells and oscillates around equality (Figure 4.B). This fluctuation can be explained by the fact that the AB cortex is more enriched in CYK-1 compared to the P1 cortex, but CYK-1 recruitment starts much earlier in P1 than in AB, as described in the previous results (Figure 2.H). Nevertheless, when reaching the AB cytokinesis onset, the AB cortex gets rapidly enriched in CYK-1 compared to P1, for about 7% in favour of the AB cortex, before dropping back as P1 enters ingression onset too (Figure 4.B). As a result, overall AB and P1 cortex show comparable CYK-1 content.

At the 4-cell stage, the two daughter cells, ABa and ABp, are not equal in terms of ABPs density found at their cell periphery (Figure 4.C). All three ABPs are more enriched in ABp, with distinct dynamics (Figure 4.C). On the one hand, ARX-2 and CAP-1 are enriched in ABp compared to ABa, with a distribution in favour of ABp for about 8% and 12%, respectively, at the end of the 4-cell stage. On the other hand, CYK-1 is equilibrated between these two cells with a slight enrichment in the ABp cortex in the late as well as early 4-cell stage (Figure 4.C). During the 4-cell stage, the EMS cortical plane is enriched for all three proteins compared to the P2 cortex. These differences increase at the end of the 4-cell stage for CYK-1 and CAP-1 for about 16% and 30%, respectively (Figure 4.D). Notably, only ARX-2 distribution between these two cells tends to decrease, starting at 25% at the beginning of the 4-cell stage and equilibrating between these two cells at the end of the 4-cell stage with still a 14% increase in EMS (Figure 4.D).

Comparing the inter-lineage cortex, ABPs have a different dynamic between cells. Between ABa and EMS (Figure 4.E), CYK-1 oscillate between 11% differences in favour of EMS and equality as in the ABa/ABp ratio, whereas ARX-2 and CAP-1 differences increase at the

end of the 4-cell stage for about 9% and 7% respectively (Figure 4.E). Between ABp and EMS (Figure 4.F), as for cytosolic measurements, we observe a general shift up of the curves, thus oscillating around equality for CYK-1 and more clearly in favour of ABp for ARX-2 and CAP-1 for a maximum of about 18% at the end of this cell stage (Figure 4.F).

We found concordant results using the probability distribution function of the intensities covering each sample's time points (Figure 3.G). To sum up, the following 4-cell stage ranking in decreasing order can be drawn. For ARX-2 and CAP-1, the ABp cortex is the cell with the highest protein density, followed by ABa, EMS, and P2. For CYK-1, ABp and EMS cells are equivalent, then ABa and P2.

Additionally, comparing these data to those obtained in the cytoplasmic plane, we can observe a general correlation between cortical and cytoplasmic cell pair contents (Figure 5). These results confirm the hypothesis that the cytoplasm constitutes a buffered reservoir of available actin nucleator and capping proteins. Their cortical regional recruitment depends on the general availability of proteins in these stages with some spatio-temporal control via signalling pathways and cell cycle control.

From ABPs concentration gradients to differential pools of proteins.

(paragraph in preparation)

Up to now, we have compared the mean fluorescence intensity of endogenously labelled proteins in the cytoplasm or present at the cortical plane, thus correlating respectively with concentration throughout the volume of the cell and with cortical densities in the 2D surface of the cell periphery. Next, we questioned whether correlations between cell volume and cell content could be found. The embryo initially divides from a constant total

volume, and each successive division can be either asymmetric or symmetric, leading to major differences in volumes for these different cells (Cao et al., 2020). From our data, one can use the mid-plane section surface ratio as a proxy of cell-to-cell volume difference. The correlation between these surface and intensity ratios shows (Figure X). Going a step further, we can also use more precise published measurements of each cell volume and cell surface (Cao et al., 2020; Thiels et al., 2021) to relate mean concentration to global protein quantities in the cytoplasm and cortical cell region. Results from these calculations are given in table X.

Discussion

The early embryo relies initially on maternally provided proteins loaded in its large oocyte (Zacharias and Murray, 2016). In *C. elegans*, this initial pool of proteins is split through divisions into the different daughter cells, asymmetrically or symmetrically, along a fixed lineage and must be sufficient to ensure the success of these first initial divisions (Gönczy and Rose, 2005; Rose and Gönczy, 2014). Asymmetries have already been characterised for several proteins, including cell fate determinants and differences in cell contents were shown to be drivers in early cell identity acquisition. Regarding cytoskeleton proteins, only a few studies mentioned asymmetries between cells, as for actin (Reymann et al., 2016; Shivas and Skop, 2012) or myosin (Munro et al., 2004; Pacquelet, 2017; Reymann et al., 2016; Schonegg and Hyman, 2006) for which a gradient of free NMY-2 molecules in the cytoplasm was recently characterised (Najafabadi et al., 2022). Here we have shown that temporal and spatial variation of other master regulators of actin assembly, such as formin, the Arp2/3 complex or capping proteins, exist both in the cytoplasm and the cortical plane, leading to unequal distributions of these proteins between sister cells. These data suggest that concentration gradients of freely diffusing actin-binding proteins in the cytoplasm can exist, a gradient which

could impact the amount of actively recruited proteins regulating actin nucleation and dynamics at the cell cortical plane.

Moreover, we have seen that these spatio-temporally controlled distributions can be inherited in daughter cells. As a result, these asymmetries could amplify cell-to-cell differences in terms of actin assembly dynamics along the lineage of the early *C. elegans* embryo. Previous measurements using single particle tracking of CYK-1 to assess actin filament elongation rate suggested no significant differences in elongation rate, thus probably no differences in the availability of actin monomers existing between the one to four-cell stage embryo (Costache et al., 2022). Modulating the availability of actin nucleators, as we have observed, is an alternative mechanism to modify differentially actin dynamics between cells.

A key result from our work is the precocious asymmetry observed in the AB daughter cells, ABa and ABp. Concentrations of CYK-1, ARX-2 and CAP-1 are spatially enriched in the ABp cell from AB division onwards, thus indicating that a concentration gradient is probably set ahead or concomitant to AB division. This means earlier than known signalling pathways coming from P2 direct interaction and leading to the differentiation of the ABp cell. In other words, the asymmetric distribution of actin-related proteins can precede cell differentiation in this cellular context. Further perturbation experiments using partial RNAi depletion or mutants will have to be performed to decipher how these actin content asymmetries impact cell fate, as well as to test what is the mechanism at work accounting for these existing differences.

Waiting for these results, we can, however, discuss on potential hypothesis. In most cases, all actin-binding proteins follow the same trend with respect to cell-cell ratios, indicating that there might be a generic mechanism at work to regulate the symmetry or asymmetric distribution of actin-binding proteins. One hypothesis would be that cortices with

higher actin densities, such as the anterior half of the zygote while offering numerous binding sites for actin-binding proteins, could also induce a local gradient of cytoplasmic concentrations. Gradient could be amplified over time with some feedback mechanism (more nucleators leading to more filaments leading to more binding sites). The binding and unbinding rates to actin filaments and an overall turnover of actin networks would thus be key parameters controlling such a mechanism. Observation of the distribution of the two Lifeact probes in the early lineage could support this hypothesis. Lifeact is a peptide binding to actin filament with fast binding and unbinding kinetics; it was previously shown that when coupled to mKate2 fluorescent probe, its turnover was one order magnitude slower than when bound to GFP (Hirani et al., 2019), as a result, Lifeact:mKate2 turnover is comparable to the turnover of cortical F-actin in the *C. elegans* cortex (Robin et al., 2014). In the early embryo, we have been observing an enhanced asymmetry in the Lifeact:mKate2 compared to Lifeact:GFP: it is notably enriched in the anterior side of the zygote as well as in the AB cell at the two-cell stage and also more intense in AB daughter cells at the four-cell stage compared to EMS and P2 (Reymann et al., 2016). This was not observed with the previously used Lifeact::GFP probe, which is more homogenously distributed at the two and four-cell stages. Thus, an anterior enrichment of cortical density in the zygote is sufficient to maintain a cellular asymmetry of a binding partner with the same unbinding kinetics as that of the stably bound actin-binding protein, which would be released upon disassembly of actin only.

For this reason, we predict that the turnover rate of actin-binding proteins might be critical in the process of asymmetric inheritance along the lineage. In *C. elegans,* early embryo actin turnover was estimated in the same range as CYK-1 formin bulk cortical turnover rate (Costache et al., 2022). Thus this process could be applicable, as well as for the Arp2/3 or Capping Protein which are thought to be long-lived on actin filaments.

However, some singularities are also observed, and some proteins show increased asymmetries compared to other actin-binding proteins, indicating that specific mechanisms may also exist to maintain equality between the cells or enhance a spatial distribution pattern. For instance, the CYK-1 formin is surprisingly equally distributed between AB and P1, unlike actin filament density or Lifeact::mKate2 densities at this stage. One potential explanation could be that many CYK-1 proteins are relocalised at the cytokinesis ring during division, thus positioned equally apart from the cell-cell dividing interface. A lesser amount is generally bound in the rest of the cell cortical plane. This enhanced presence at the cytokinesis throughout division would ensure an equal partitioning in the daughter cells. This is not the case for the ARX-2 or CAP-1, which maintain more asymmetries in the cortical and cytoplasm before and after division. Additionally, we will have to invest in the future whether endocytosis, a process involving the Arp2/3 complex probably together with capping protein, which is abundant in the early embryo and also spatially enriched in the anterior side of the zygote, for instance (Shivas and Skop, 2012) could play a role in the concentration gradient observed for these two proteins.

In conclusion, we here question the potential of an embryonic control of differential cellular actin homeostasis and actin cytoskeletal steady states. Concentration gradients could be sufficient to drive and maintain cellular asymmetries at important actin-binding proteins' cytoplasmic and cortical levels. Some of the acquired cell-specific cytoskeleton properties might be key in future steps of cell differentiation events in the early *C. elegans* embryo. They could be extended to other processes of cell fate acquisition in other systems.

Materials and Methods

Strains maintenance

C. elegans strains were maintained on nematode growth medium (NGM) plates seeded with OP50 E. coli under standard conditions (Brenner, 1974) at 20°C. The strains used in this study are presented in the followingTable 1.

Name	Genotype	Source
SWG019	*cyk-1(ges1[cyk-1::GFP +* LoxP *unc-119*(+) LoxP) III; *unc-119(ed3)* III.	(Reymann et al., 2016)
SWG052	*cap-1 (ges3 [cap-1::GFP* + LoxP *unc-119(+)* LoxP]) IV; *unc-119 (ed3)* III	This work
GOU2047	*cas607 [arx-2*::gfp knock-in]	(Zhu et al., 2016)
OD70	*ltIs44[pie-1p::mCherry::PH*(PLC1delta1) *+ unc-119(+)]*V)	(Scholze et al., 2018)
LP539	*cpIs90[mex-5p::mNG::HaloTag::tbb-2* 3'UTR + LoxP] II	(Dickinson et al., 2017)
ACR004	*cyk-1(ges1[cyk-1::GFP* + LoxP *unc-119(+)* LoxP] III*; unc-119 (ed3)* III; *ltIs44pAA173; [pie-1p::mCherry::PH*(*PLC1delta1) + unc-119(+)]* V	This work
ACR011	*cap-1 (ges3 [cap-1::GFP +* LoxP *unc-119(+)* LoxP]) IV; *unc-119 (ed3)* III ; *ltIs44pAA173 ([pie-1p::mCherry::PH(PLC1delta1) + unc-119(+)])* V	This work
ACR013	cas607 [arx-2::gfp *knock-in]; ltIs44[pie-1p::mCherry::PH(PLC1delta1) + unc-119(+)]*V)	This work
ACR090	*cpIs90[mex-5p::mNG::HaloTag::tbb-2 3'UTR* + LoxP] II; *ltIs44[pie-1p::mCherry::PH(PLC1delta1) + unc-119(+)]*V)	This work

Table 1: Strain list

Slide preparation

For all samples, L4 adults were collected 24H before embryo imaging. The corresponding sexually mature hermaphrodites were dissected on a coverslip in M9 buffer (6 g Na,HPO, 3 g KH,PO, 5 g NaCl and 0.25 g MgSO4.7H,O per litre) and mounted under a 2% or agarose pad and sealed with VALAP (1:1:1, Vaseline, lanolin and paraffin wax).

Image acquisition

All Microscopy samples were collected using an Inverted Nikon Eclipse Ti equipped with a Yokogawa CSU-X1 scan head, a simultaneous dual camera with two Prime 95B cameras (Photometrics) and a 100×1.4 NA objective lens, configured by Gataca Systems (Massy, France). Image acquisition was controlled by MetaMorph software (Molecular Devices, Sunnyvale, CA) in a temperature-controlled room set to 20°C. Imaging conditions were developed to ensure minimal photobleaching and no photo-toxicity to allow for live observation in three optical sections over ten minutes of embryonic development but with sufficient sensitivity enabling the detection of low expressed levels of proteins (Figure Sup 2). Then for sample gathering, fluorophore excitation is done by 20% 491nm and 30% 568nm laser. Each stack is timely separated by 10sec for a total duration of 10min. A perfect focus system is set at the cortical plane to track the cortical variation precisely and will correspond to the first images acquired in each stack. Each Timepoint is composed of 3 different confocal planes spaced by 3µm, the cortical plane (Z=1), the intermediate plane (Z=2), and the equatorial plane (Z=3).

Segmentation

To access single-cell content and average them in space and time for different representative embryos, we developed a pipeline of analysis. Standardised samples were processed and separated by Time and spatial position using the free software Fiji (Schindelin et al., 2012). Next, we used an interactive segmentation toolkit based on machine learning algorithms named ILASTIK (Berg et al., 2019). The training was performed on the equatorial (Z3) and the intermediate plane (Z2). The segmentation of the complete timelapse was then obtained automatically. The output obtained was a binary for each time point for these two confocal planes. The binary of Z2 was then transferred in Matlab and eroded to segment the cortical plane (Z1).

Quantification

To reposition each embryo acquired for 10 minutes over the timeline of its development, we used a reference time point chosen as the onset of membrane ingression observed in the equatorial section (Z3) or shallow membrane deformation (Chan et al., 2018). (Figure 1.A). This time point is then used as our t=0 in each further quantification.

We quantified a mean GFP intensity for each cell at each time point in each optical section. To quantify the spatio-temporal dynamics of recruitment of our protein of interest at the cortex, we normalised the mean cortical intensity by the mean intensity in the cytoplasm for each time point (Figure 2), thus correcting for the bleaching effect and enabling comparison between embryos.

We used two approaches to quantify cellular differences. First, we performed cell-to-cell ratio for cytosolic or cortical mean fluorescence intensities for each time point. This mean

intensity ratio allowed us to estimate the relative proportion of ABPs between cells. Second, we used the probability distribution function of the intensities found in each cell. We compiled the convolution of the normalised distributions for each cell pair giving in a statistically significant manner the cell pair content differences for all time points (Figure 3.G 4.G). All these quantification approaches are realised with a homemade code developed in Matlab. The corresponding step-by-step annotated codes are available on our Lab's Github.

Correlations were made on Matlab, using the mean value of each cell-to-cell mean intensities ratio at the cortex and the cytoplasm, fitting a linear model (f(x) = p1*x+p2) (Figure 5).

Acknowledgements

The authors would like to thank members of the Goehring lab and Jarriault lab for their critical comments. Karine Crell, Stephan Grill, Pierre Gönczy and the Ou lab for providing worms lines. We would also like to thank the Imaging Center of IGBMC (ici.igbmc.fr) with the assistance of Elvire Guiot, Erwan Grandgirard Marine Sylvin, Yves Lutz and Bertrand Vernay.

Competing interests

The authors declare no competing or financial interests.

Author contributions

Conceptualisation:

Methodology:

Formal analysis:

Investigation:

Resources:

Writing – original draft preparation:

Writing – review and editing:

Supervision:

Project administration:

Funding acquisition:

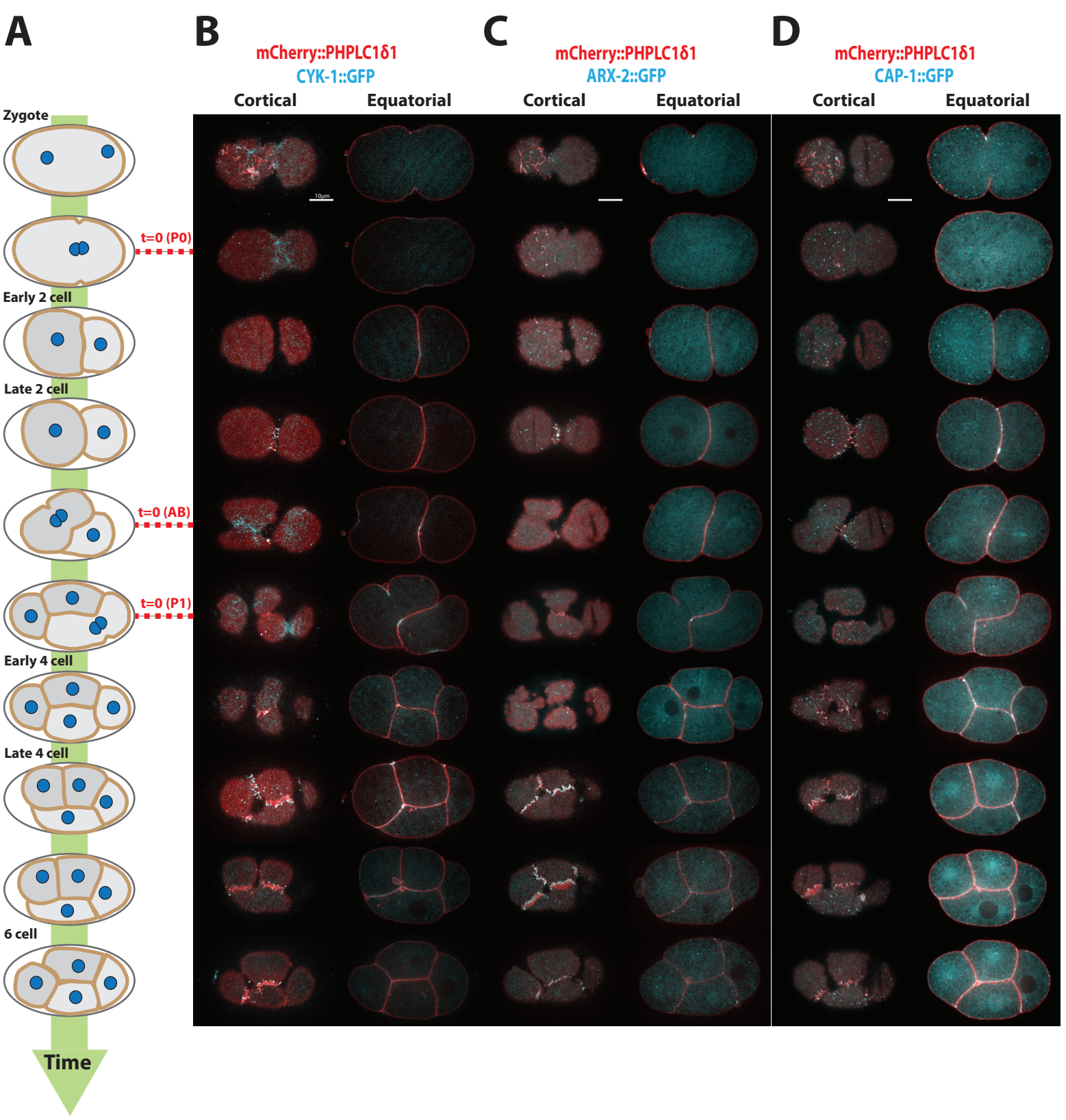

Figure 1: 4D mapping of ABPs distribution during the early embryogenesis

Schematic representation of the early steps of embryogenesis in chronologic order; from top to bottom, starting with the zygotic stage and ending at the 6-cell stage **(A)** The red dashed lines correspond to the cytokinesis onset corresponding to each cell stage, used as a time reference for sample time alignement. Spatio-Temporal distribution of 3 ABPs (Cyan) and the membrane marker with PHPLC1δ1 (Red), focused at the cellular cortex (right panel) and the equatorial plane (right panel); CYK-1::GFP (**B**), ARX-2::GFP (**C**), CAP-1::GFP(**D**).

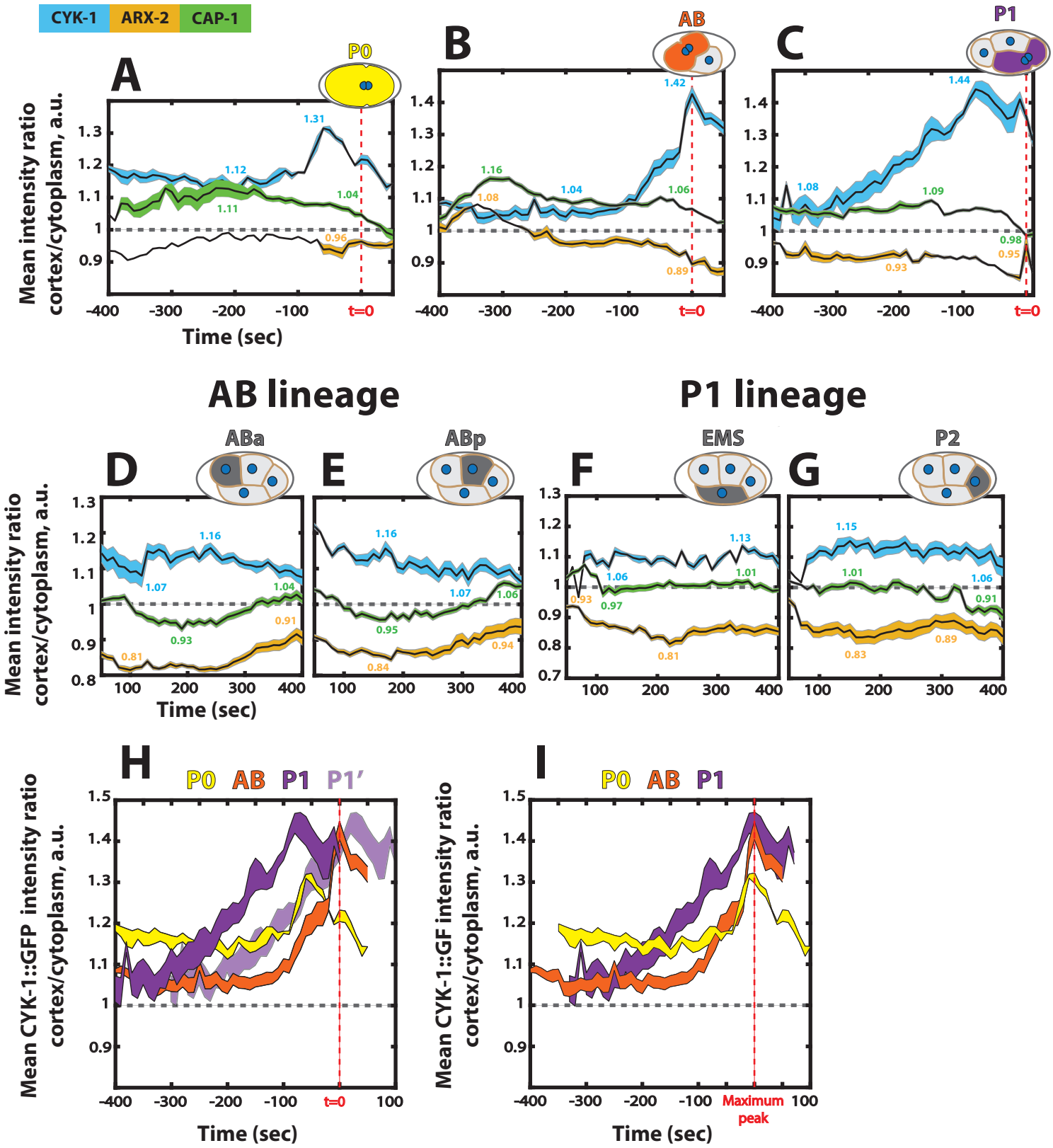

Figure 2: CYK-1 is differentially recruited at the cortex during the cytokinesis of P0, AB and P1.

Mean fluorescence intensities at the cortical plane normalised by the mean fluorescence intensities at the equatorial plane, for each time point. Samples are aligned according to their t=0 corresponding to the membrane ingression onset. Quantified proteins are CYK-1 (blue curve), ARX-2 (orange curve), CAP-1(green curve). Overall dynamics of cortical ABP::GFP in each cell of the early embryo; P0 (**A**), AB (**B**), P1 (**C**), ABa (**D**), ABp (**E**), EMS (**F**), P2 (**G**). Comparison of CYK-1::GFP cortical recruitment for cytokinesis ring assembly in P0 (Yellow), AB(Deep orange), P1(purple). time alignment is done with respects to individual ingression onset except for P1' (light purple) which is aligned regarding the AB cytokinesis initiation(**H**); Alignment with respect to the maximum peak of CYK-1::GFP cortical recruitment (**I**). Samples numbers; A : cyk-1(n=4), arx-2(n=4), cap-1(n=6); B,C : cyk-1(n=6), arx-2(n=6), cap-1(n=14); D,E,F,G : cyk-1(n=5), arx-2(n=7), cap-1(n=10).

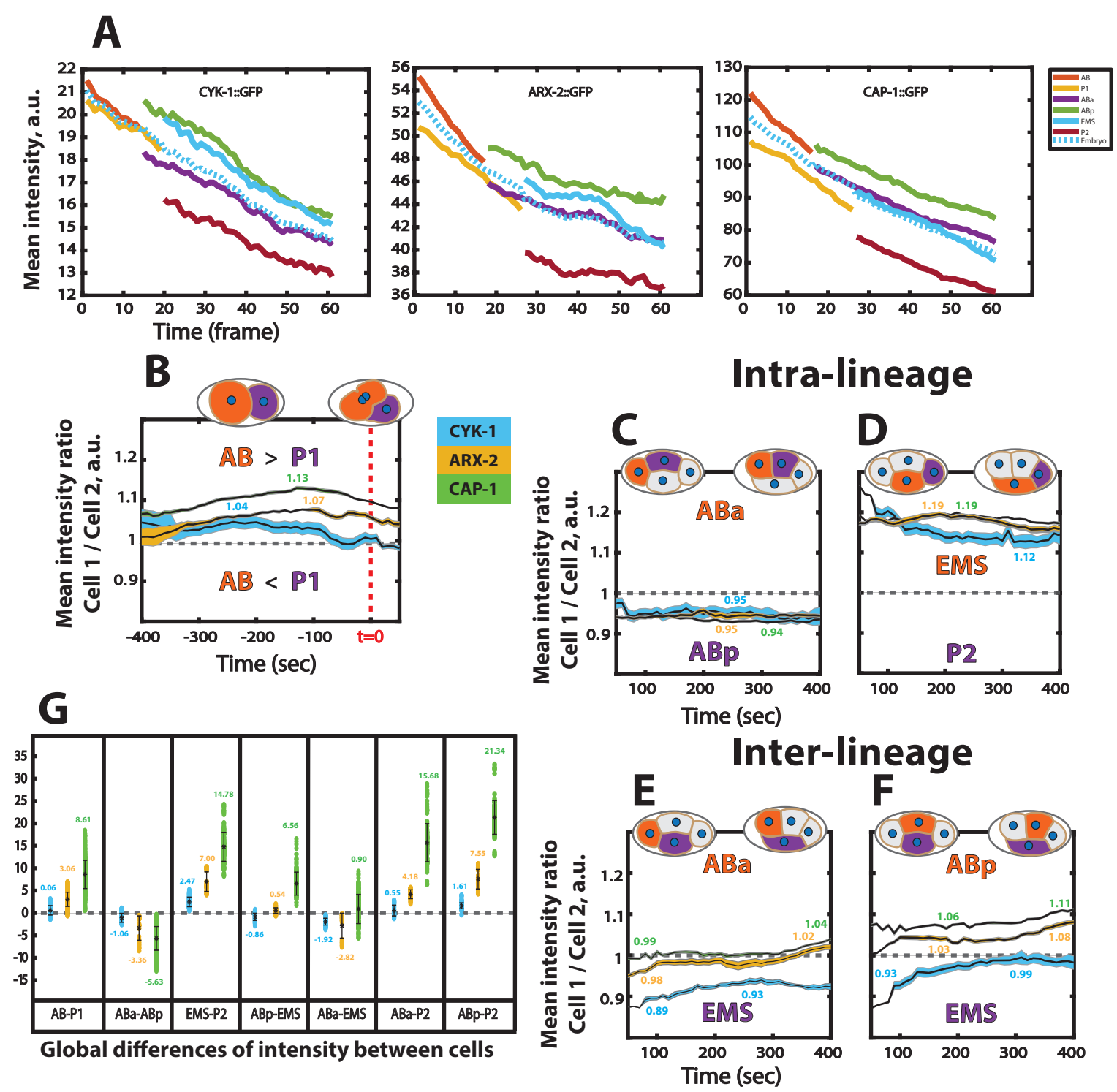

Figure 3: Cytosolic ABPs are differently segregated in each blastomeres, even between sister cells.
Time evolution of the mean intensity at the equatorial plane in each cell in single embryos (**A**), CYK-1::GFP (left panel), ARX-2 (middle panel), CAP-1(right panel). Relative cytosolic ABPs abundance; Ratio of the mean GFP intensities between the equatorial plane of each cell at each time point. AB/P1 (**B**), ABa/ABp (**C**), EMS/P2 (**D**), ABa/EMS (**E**), ABp/EMS (**F**); quantified proteins are CYK-1 (blue curve), ARX-2 (orange curve), CAP-1(green curve), maximum and minimum mean differences are directly annoted to the plot, in the color corresponding to their proteins. Total difference of intensity between cells using the convolution of two normalised density probability distributions (**G**); proteins color codes is still the same and the mean value of these differences are directly annotated in the plot. Samples numbers; B: cyk-1(n=6), arx-2(n=6), cap-1(n=14); C,D,E,F:cyk-1(n=5), arx-2(n=7), cap-1(n=10)

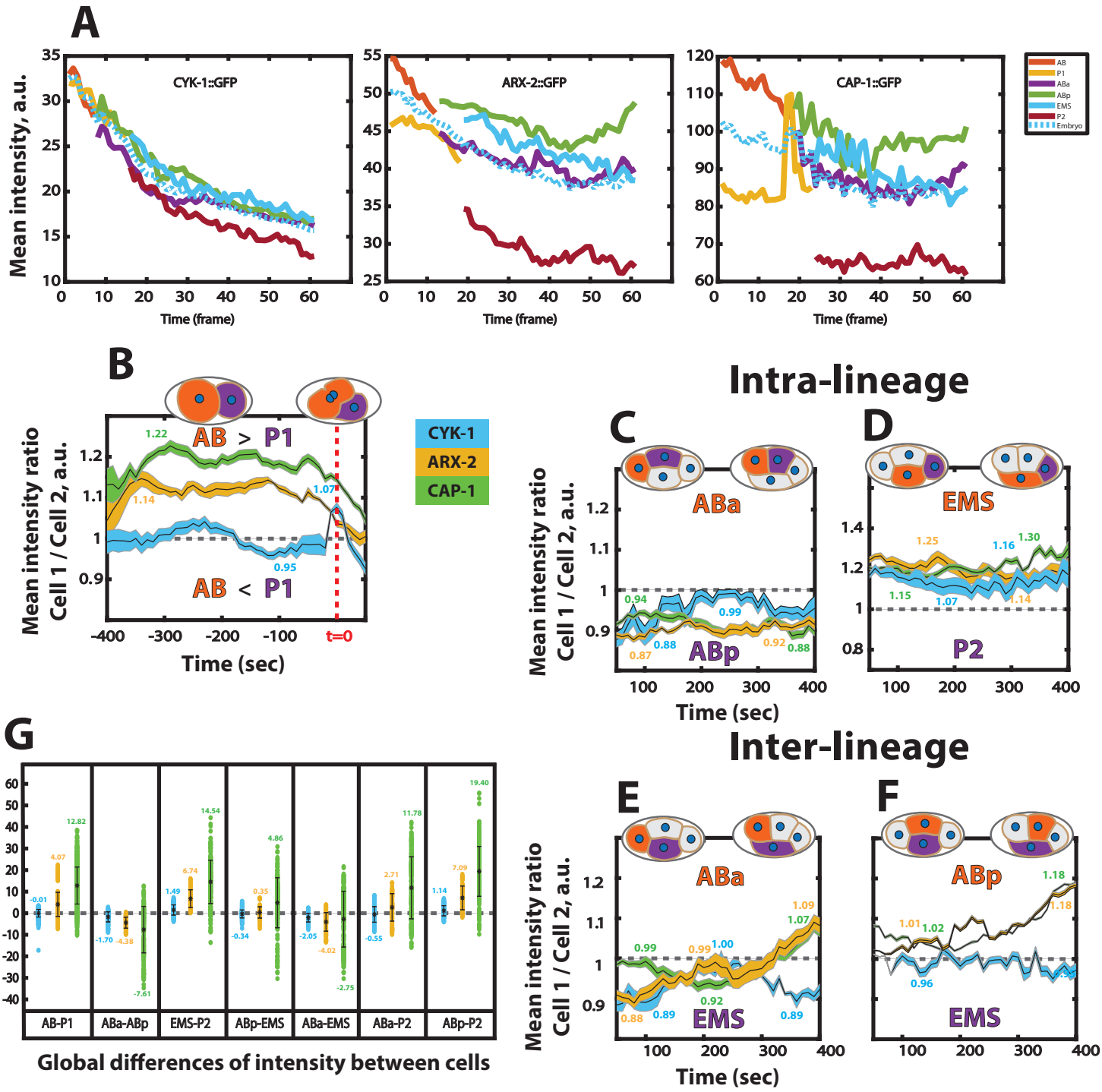

Figure 4: ABPs differential segregation are enhanced at the cortex, with a specific dynamic.
Time evolution of the mean intensity at the cortical plane in each cell in single embryos (**A**), CYK-1::GFP (left panel), ARX-2 (middle panel), CAP-1(right panel). Relative cortical ABPs abundance; Ratio of the mean GFP intensities between the cortical plane of each cell at each time point. AB/P1 (**B**), ABa/ABp (**C**), EMS/P2 (**D**), ABa/EMS (**E**), ABp/EMS (**F**); quantified proteins are CYK-1 (blue curve), ARX-2 (orange curve), CAP-1(green curve), maximum and minimum mean differences are directly annoted to the plot, in the color corresponding to their proteins. Total difference of intensity between cells using the convolution of two normalised density probability distributions (**G**); proteins color codes is still the same and the mean value of these differences are directly annotated in the plot.Samples numbers; B: cyk-1(n=6), arx-2(n=6), cap-1(n=14); C,D,E,F:cyk-1(n=5), arx-2(n=7), cap-1(n=10).

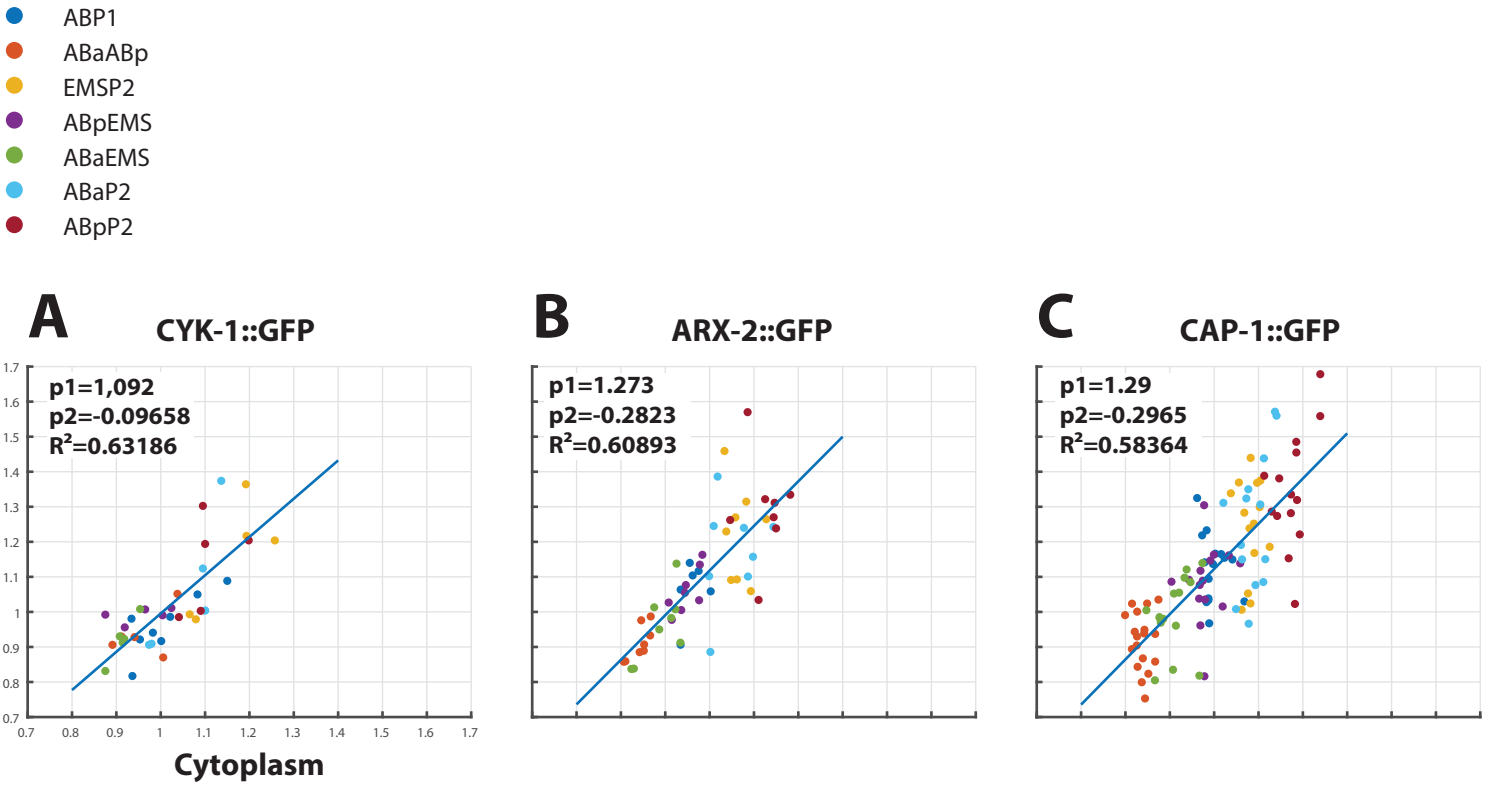

Figure 5: Correlation of the ratio between cells of the mean intensity at the cortex and the cytoplasm

Correlation were made using the mean value of each cell-cell mean intensities ratio at te cortex and at the cytoplasm, fitting a linear model: f(x) = p1*x+p2. CYK-1::GFP(**A**), ARX-2:: (**B**), CAP-1::GFP (**C**). Corresponding p1, p2 and R^2 are directly annotated in the graph.

References

Ai, E., Skop, A.R., 2009. Endosomal recycling regulation during cytokinesis. Commun Integr Biol 2, 444–447. https://doi.org/10.4161/cib.2.5.8931

Aloisio, F.M., Barber, D.L., 2022. Arp2/3 complex activity is necessary for mouse ESC differentiation, times formative pluripotency, and enables lineage specification. Stem Cell Reports 17, 1318–1333. https://doi.org/10.1016/j.stemcr.2022.05.002

Berg, S., Kutra, D., Kroeger, T., Straehle, C.N., Kausler, B.X., Haubold, C., Schiegg, M., Ales, J., Beier, T., Rudy, M., Eren, K., Cervantes, J.I., Xu, B., Beuttenmueller, F., Wolny, A., Zhang, C., Koethe, U., Hamprecht, F.A., Kreshuk, A., 2019. ilastik: interactive machine learning for (bio)image analysis. Nat Methods 16, 1226–1232. https://doi.org/10.1038/s41592-019-0582-9

Blanchoin, L., Boujemaa-Paterski, R., Sykes, C., Plastino, J., 2014. Actin Dynamics, Architecture, and Mechanics in Cell Motility. Physiological Reviews 94, 235–263. https://doi.org/10.1152/physrev.00018.2013

Cao, J., Guan, G., Ho, V.W.S., Wong, M.-K., Chan, L.-Y., Tang, C., Zhao, Z., Yan, H., 2020. Establishment of a morphological atlas of the Caenorhabditis *elegans* embryo using deep-learning-based 4D segmentation. Nat Commun 11, 6254. https://doi.org/10.1038/s41467-020-19863-x

Carlier, M.-F., 1998. Control of actin dynamics. Current Opinion in Cell Biology 10, 45–51. https://doi.org/10.1016/S0955-0674(98)80085-9

Chan, F.-Y., Silva, A.M., Saramago, J., Pereira-Sousa, J., Brighton, H.E., Pereira, M., Oegema, K., Gassmann, R., Carvalho, A.X., 2018. The ARP2/3 complex prevents excessive formin activity during cytokinesis. Mol Biol Cell 30, 96–107. https://doi.org/10.1091/mbc.E18-07-0471

Costache, V., Prigent Garcia, S., Plancke, C.N., Li, J., Begnaud, S., Suman, S.K., Reymann, A.-C., Kim, T., Robin, F.B., 2022. Rapid assembly of a polar network architecture drives efficient actomyosin contractility. Cell Reports 39, 110868. https://doi.org/10.1016/j.celrep.2022.110868

De Henau, S., Pagès-Gallego, M., Pannekoek, W.-J., Dansen, T.B., 2020. Mitochondria-Derived H2O2 Promotes Symmetry Breaking of the *C. elegans* Zygote. Developmental Cell 53, 263-271.e6. https://doi.org/10.1016/j.devcel.2020.03.008

Delattre, M., Goehring, N.W., 2021. Chapter Nine - The first steps in the life of a worm: Themes and variations in asymmetric division in *C. elegans* and other nematodes, in: Jarriault, S., Podbilewicz, B. (Eds.), Current Topics in Developmental Biology, Nematode Models of Development and Disease. Academic Press, pp. 269–308. https://doi.org/10.1016/bs.ctdb.2020.12.006

Dickinson, D.J., Schwager, F., Pintard, L., Gotta, M., Goldstein, B., 2017. A single-cell biochemistry approach reveals PAR complex dynamics during cell polarization. Dev Cell 42, 416-434.e11. https://doi.org/10.1016/j.devcel.2017.07.024

Etienne-Manneville, S., 2004. Actin and Microtubules in Cell Motility: Which One is in Control? Traffic 5, 470–477. https://doi.org/10.1111/j.1600-0854.2004.00196.x

Evans, T.C., Crittenden, S.L., Kodoyianni, V., Kimble, J., 1994. Translational control of maternal glp-1 mRNA establishes an asymmetry in the *C. elegans* embryo. Cell 77, 183–194. https://doi.org/10.1016/0092-8674(94)90311-5

Fischer, R.S., Lam, P.-Y., Huttenlocher, A., Waterman, C.M., 2019. Filopodia and focal adhesions: An integrated system driving branching morphogenesis in neuronal pathfinding and angiogenesis. Dev Biol 451, 86–95. https://doi.org/10.1016/j.ydbio.2018.08.015

Gan, W.J., Motegi, F., 2021. Mechanochemical Control of Symmetry Breaking in the Caenorhabditis *elegans* Zygote. Frontiers in Cell and Developmental Biology 8.

Gilden, J., Krummel, M.F., 2010. Control of cortical rigidity by the cytoskeleton: Emerging roles for septins. Cytoskeleton 67, 477–486. https://doi.org/10.1002/cm.20461

Goehring, N.W., Grill, S.W., 2013. Cell polarity: mechanochemical patterning. Trends in Cell Biology 23, 72–80. https://doi.org/10.1016/j.tcb.2012.10.009

Gönczy, P., Rose, L.S., 2005. Asymmetric cell division and axis formation in the embryo. WormBook 1–20. https://doi.org/10.1895/wormbook.1.30.1

Hamill, D.R., Severson, A.F., Carter, J.C., Bowerman, B., 2002. Centrosome Maturation and Mitotic Spindle Assembly in *C. elegans* Require SPD-5, a Protein with Multiple Coiled-Coil Domains. Developmental Cell 3, 673–684. https://doi.org/10.1016/S1534-5807(02)00327-1

Hirani, N., Illukkumbura, R., Bland, T., Mathonnet, G., Suhner, D., Reymann, A.-C., Goehring, N.W., 2019. Anterior-enriched filopodia create the appearance of asymmetric membrane microdomains in polarizing *C. elegans* zygotes. J Cell Sci 132, jcs230714. https://doi.org/10.1242/jcs.230714

Horvitz, H.R., Herskowitz, I., 1992. Mechanisms of asymmetric cell division: two Bs or not two Bs, that is the question. Cell 68, 237–255. https://doi.org/10.1016/0092-8674(92)90468-r

Jordan, S.N., Davies, T., Zhuravlev, Y., Dumont, J., Shirasu-Hiza, M., Canman, J.C., 2016. Cortical PAR polarity proteins promote robust cytokinesis during asymmetric cell division. J Cell Biol 212, 39–49. https://doi.org/10.1083/jcb.201510063

Knight, J.K., Wood, W.B., 1998. Gastrulation initiation in Caenorhabditis *elegans* requires the function of gad-1, which encodes a protein with WD repeats. Developmental Biology 198, 253–265. https://doi.org/10.1016/S0012-1606(98)80003-1

Li, W., Chung, W.-L., Kozlov, M.M., Medalia, O., Geiger, B., Bershadsky, A.D., 2022. Chiral growth of adherent filopodia (preprint). Cell Biology. https://doi.org/10.1101/2022.06.09.495577

Manhart, A., Icheva, T.A., Guerin, C., Klar, T., Boujemaa-Paterski, R., Thery, M., Blanchoin, L., Mogilner, A., 2019. Quantitative regulation of the dynamic steady state of actin networks. eLife 8, e42413. https://doi.org/10.7554/eLife.42413

Martín-Blanco, E., Knust, E., 2001. Epithelial morphogenesis: filopodia at work. Curr Biol 11, R28-31. https://doi.org/10.1016/s0960-9822(00)00039-7

Michaux, J.B., Robin, F.B., McFadden, W.M., Munro, E.M., 2018. Excitable RhoA dynamics drive pulsed contractions in the early *C. elegans* embryo. J Cell Biol 217, 4230–4252. https://doi.org/10.1083/jcb.201806161

Munro, E., Nance, J., Priess, J.R., 2004. Cortical Flows Powered by Asymmetrical Contraction Transport PAR Proteins to Establish and Maintain Anterior-Posterior Polarity in the Early *C. elegans* Embryo. Developmental Cell 7, 413–424. https://doi.org/10.1016/j.devcel.2004.08.001

Naganathan, S.R., Fürthauer, S., Rodriguez, J., Fievet, B.T., Jülicher, F., Ahringer, J., Cannistraci, C.V., Grill, S.W., 2018. Morphogenetic degeneracies in the actomyosin cortex. eLife 7, e37677. https://doi.org/10.7554/eLife.37677

Najafabadi, F.R., Leaver, M., Grill, S.W., 2022. Orchestrating nonmuscle myosin II filament assembly at the onset of cytokinesis. Mol Biol Cell 33, ar74. https://doi.org/10.1091/mbc.E21-12-0599

Nguyen, T.Q., Sawa, H., Okano, H., White, J.G., 2000. The *C. elegans* septin genes, unc-59 and unc-61, are required for normal postembryonic cytokineses and morphogenesis but have no essential function in embryogenesis. Journal of Cell Science 113, 3825–3837. https://doi.org/10.1242/jcs.113.21.3825

Pacquelet, A., 2017. Asymmetric Cell Division in the One-Cell *C. elegans* Embryo: Multiple Steps to Generate Cell Size Asymmetry. Results Probl Cell Differ 61, 115–140. https://doi.org/10.1007/978-3-319-53150-2_5

Padmanabhan, A., Ong, H.T., Zaidel-Bar, R., 2017. Non-junctional E-Cadherin Clusters Regulate the Actomyosin Cortex in the *C. elegans* Zygote. Current Biology 27, 103–112. https://doi.org/10.1016/j.cub.2016.10.032

Pimpale, L.G., Middelkoop, T.C., Mietke, A., Grill, S.W., 2020. Cell lineage-dependent chiral actomyosin flows drive cellular rearrangements in early Caenorhabditis *elegans* development. eLife 9, e54930. https://doi.org/10.7554/eLife.54930

Plastino, J., Blanchoin, L., 2018. Dynamic stability of the actin ecosystem. J Cell Sci 132, jcs219832. https://doi.org/10.1242/jcs.219832

Pohl, C., Bao, Z., 2010. Chiral forces organize left-right patterning in *C. elegans* by uncoupling midline and anteroposterior axis. Dev Cell 19, 402–412. https://doi.org/10.1016/j.devcel.2010.08.014

Pollard, T.D., 2016. Actin and Actin-Binding Proteins. Cold Spring Harb Perspect Biol 8, a018226. https://doi.org/10.1101/cshperspect.a018226

Priess, J.R., Thomson, J.N., 1987. Cellular interactions in early *C. elegans* embryos. Cell 48, 241–250. https://doi.org/10.1016/0092-8674(87)90427-2

Ray, S., Zaidel bar, 2021. Actin capping protein regulates actomyosin contractility to maintain germline architecture in *C. elegans* 19.

Reymann, A.-C., Staniscia, F., Erzberger, A., Salbreux, G., Grill, S.W., 2016. Cortical flow aligns actin filaments to form a furrow. eLife 5, e17807. https://doi.org/10.7554/eLife.17807

Robin, F.B., McFadden, W.M., Yao, B., Munro, E.M., 2014. Single-molecule analysis of cell surface dynamics in Caenorhabditis *elegans* embryos. Nat Methods 11, 677–682. https://doi.org/10.1038/nmeth.2928

Rocheleau, C.E., Downs, W.D., Lin, R., Wittmann, C., Bei, Y., Cha, Y.-H., Ali, M., Priess, J.R., Mello, C.C., 1997. Wnt Signaling and an APC-Related Gene Specify Endoderm in Early *C. elegans* Embryos. Cell 90, 707–716. https://doi.org/10.1016/S0092-8674(00)80531-0

Rose, L., Gönczy, P., 2014. Polarity establishment, asymmetric division and segregation of fate determinants in early *C. elegans* embryos. WormBook 1–43. https://doi.org/10.1895/wormbook.1.30.2

Samandar Eweis, D., Plastino, J., 2020. Roles of Actin in the Morphogenesis of the Early Caenorhabditis *elegans* Embryo. International Journal of Molecular Sciences 21, 3652. https://doi.org/10.3390/ijms21103652

Schindelin, J., Arganda-Carreras, I., Frise, E., Kaynig, V., Longair, M., Pietzsch, T., Preibisch, S., Rueden, C., Saalfeld, S., Schmid, B., Tinevez, J.-Y., White, D.J., Hartenstein, V., Eliceiri, K., Tomancak, P., Cardona, A., 2012. Fiji: an open-source platform for biological-image analysis. Nat Methods 9, 676–682. https://doi.org/10.1038/nmeth.2019

Scholze, M.J., Barbieux, K.S., De Simone, A., Boumasmoud, M., Süess, C.C.N., Wang, R., Gönczy, P., 2018. PI(4,5)P2 forms dynamic cortical structures and directs actin distribution as well as polarity in Caenorhabditis *elegans* embryos. Development 145, dev164988. https://doi.org/10.1242/dev.164988

Schonegg, S., Hyman, A.A., 2006. CDC-42 and RHO-1 coordinate acto-myosin contractility and PAR protein localization during polarity establishment in *C. elegans* embryos. Development 133, 3507–3516. https://doi.org/10.1242/dev.02527

Severson, A.F., Baillie, D.L., Bowerman, B., 2002. A Formin Homology Protein and a Profilin Are Required for Cytokinesis and Arp2/3-Independent Assembly of Cortical Microfilaments in *C. elegans*. Current Biology 12, 2066–2075. https://doi.org/10.1016/S0960-9822(02)01355-6

Shivas, J.M., Skop, A.R., 2012. Arp2/3 mediates early endosome dynamics necessary for the maintenance of PAR asymmetry in *Caenorhabditis elegans*. MBoC 23, 1917–1927. https://doi.org/10.1091/mbc.e12-01-0006

Suarez, C., Kovar, D.R., 2016. Internetwork competition for monomers governs actin cytoskeleton organization. Nat Rev Mol Cell Biol 17, 799–810. https://doi.org/10.1038/nrm.2016.106

Sulston, J.E., Schierenberg, E., White, J.G., Thomson, J.N., 1983. The embryonic cell lineage of the nematode Caenorhabditis *elegans*. Dev Biol 100, 64–119. https://doi.org/10.1016/0012-1606(83)90201-4

Svitkina, T.M., Borisy, G.G., 1999. Arp2/3 complex and actin depolymerizing factor/cofilin in dendritic organization and treadmilling of actin filament array in lamellipodia. J Cell Biol 145, 1009–1026. https://doi.org/10.1083/jcb.145.5.1009

Swan, K.A., Severson, A.F., Carter, J.C., Martin, P.R., Schnabel, H., Schnabel, R., Bowerman, B., 1998. cyk-1: a *C. elegans* FH gene required for a late step in embryonic cytokinesis. Journal of Cell Science 111, 2017–2027. https://doi.org/10.1242/jcs.111.14.2017

Thiels, W., Smeets, B., Cuvelier, M., Caroti, F., Jelier, R., 2021. spheresDT/Mpacts-PiCS: cell tracking and shape retrieval in membrane-labeled embryos. Bioinformatics 37, 4851–4856. https://doi.org/10.1093/bioinformatics/btab557

Ti, S.-C., Pollard, T.D., 2011. Purification of actin from fission yeast Schizosaccharomyces pombe and characterization of functional differences from muscle actin. J Biol Chem 286, 5784–5792. https://doi.org/10.1074/jbc.M110.199794

Tim Davies, , Han X Kim, Natalia Romano Spica, , Benjamin J Lesea-Pringle, Julien Dumont, , Julie C Canman, *, 2018. Cell-intrinsic and -extrinsic mechanisms promote cell-type-specific cytokinetic diversity. eLife 7, e36204. https://doi.org/10.7554/eLife.36204

Velarde, N., Gunsalus, K.C., Piano, F., 2007. Diverse roles of actin in *C. elegans* early embryogenesis. BMC Dev Biol 7, 142. https://doi.org/10.1186/1471-213X-7-142

Venkatesh, K., Mathew, A., Koushika, S.P., 2020. Role of actin in organelle trafficking in neurons. Cytoskeleton 77, 97–109. https://doi.org/10.1002/cm.21580

Volkmann, N., Amann, K.J., Stoilova-McPhie, S., Egile, C., Winter, D.C., Hazelwood, L., Heuser, J.E., Li, R., Pollard, T.D., Hanein, D., 2001. Structure of Arp2/3 complex in its activated state and in actin filament branch junctions. Science 293, 2456–2459. https://doi.org/10.1126/science.1063025

Wagner, O., Zinke, J., Dancker, P., Grill, W., Bereiter-Hahn, J., 1999. Viscoelastic Properties of f-actin, Microtubules, f-actin/α-actinin, and f-actin/Hexokinase Determined in Microliter Volumes with a Novel Nondestructive Method. Biophysical Journal 76, 2784–2796. https://doi.org/10.1016/S0006-3495(99)77432-1

Williams-Masson, E.M., Malik, A.N., Hardin, J., 1997. An actin-mediated two-step mechanism is required for ventral enclosure of the *C. elegans* hypodermis. Development 124, 2889–2901. https://doi.org/10.1242/dev.124.15.2889

Yan, V.T., Narayanan, A., Wiegand, T., Jülicher, F., Grill, S.W., 2022. A condensate dynamic instability orchestrates actomyosin cortex activation. Nature 609, 597–604. https://doi.org/10.1038/s41586-022-05084-3

Zaatri, A., Perry, J.A., Maddox, A.S., 2021. Septins and a formin have distinct functions in anaphase chiral cortical rotation in the Caenorhabditis *elegans* zygote. Mol Biol Cell 32, 1283–1292. https://doi.org/10.1091/mbc.E20-09-0576

Zacharias, A.L., Murray, J.I., 2016. Combinatorial decoding of the invariant *C. elegans* embryonic lineage in space and time. Genesis 54, 182–197. https://doi.org/10.1002/dvg.22928

Zhu, Z., Chai, Y., Jiang, Y., Li, Wenjing, Hu, H., Li, Wei, Wu, J.-W., Wang, Z.-X., Huang, S., Ou, G., 2016. Functional Coordination of WAVE and WASP in *C. elegans* Neuroblast Migration. Developmental Cell 39, 224–238. https://doi.org/10.1016/j.devcel.2016.09.029

AIM 2: Molecular characterisation of membrane-rich microdomains appearing in the anterior cortex of the polarising *C. elegans* zygote and identified as filopodia.

During the beginning of my microscopist journey, the lab and I observed specific membrane PIP2 microdomains that are localised in the anterior side of the zygote and especially during the polarisation phase. The second aim of my PhD project was to characterise actin organisation within these PIP2 microdomains. This work was realised in collaboration with the lab of Nate Goehring, as we realised early on that we had been working on a similar topic. We combined our approach with the Goehring lab, which focused more on the membrane dynamics, when we concentrated more on ABPs composition. Observations of elongated tubular structures projecting from the cell that resembled filopodia provided a hint about the morphological nature of these PIP2 microdomains. The formin protein, CYK-1, is observed at the tips of these microdomains and the core body of these PIP2 extended tubular structures appears to contain F-Actin and the plastin protein, PLST-1. These architectures appear right after fertilisation and specifically during the polarisation phase and the pseudocleavage step at the zygotic stage. where they are pressed against the eggshell. They are also present at the 2-cell and the 4-cell stages, with the same structures and molecular organisation are observed. Indeed, they are located in a specific area corresponding to the cellular interface and arranged in an interdigitated manner. At the 2-cell stage, they are located at the interface between the AB and P1 cells. At the 4-cell stage, they are located between the AB daughter cells (ABa and ABp) and between the EMS cells and the AB daughter cells. RNAi experiment revealed the combined requirement of formin CYK-1 and the Arp2/3 complex to build this finger-like structure. Taken together, these PIP2 microdomains have all the molecular characteristics to be called filopodia. This work has been published (Hirani et al., 2019).

© 2019. Published by The Company of Biologists Ltd | Journal of Cell Science (2019) 132, jcs230714. doi:10.1242/jcs.230714

SHORT REPORT

Anterior-enriched filopodia create the appearance of asymmetric membrane microdomains in polarizing *C. elegans* zygotes

Nisha Hirani[1], Rukshala Illukkumbura[1], Tom Bland[1,2], Grégoire Mathonnet[3], Delphine Suhner[3], Anne-Cecile Reymann[3] and Nathan W. Goehring[1,2,4,*]

ABSTRACT

The association of molecules within membrane microdomains is critical for the intracellular organization of cells. During polarization of the *C. elegans* zygote, both polarity proteins and actomyosin regulators associate within dynamic membrane-associated foci. Recently, a novel class of asymmetric membrane-associated structures was described that appeared to be enriched in phosphatidylinositol 4,5-bisphosphate (PIP_2), suggesting that PIP_2 domains could constitute signaling hubs to promote cell polarization and actin nucleation. Here, we probe the nature of these domains using a variety of membrane- and actin cortex-associated probes. These data demonstrate that these domains are filopodia, which are stimulated transiently during polarity establishment and accumulate in the zygote anterior. The resulting membrane protrusions create local membrane topology that quantitatively accounts for observed local increases in the fluorescence signal of membrane-associated molecules, suggesting molecules are not selectively enriched in these domains relative to bulk membrane and that the PIP_2 pool as revealed by $PH_{PLC\delta1}$ simply reflects plasma membrane localization. Given the ubiquity of 3D membrane structures in cells, including filopodia, microvilli and membrane folds, similar caveats are likely to apply to analysis of membrane-associated molecules in a broad range of systems.

KEY WORDS: *C. elegans*, PAR proteins, PIP_2, Cell cortex, Cell polarity, Filopodia

INTRODUCTION

Micro- to nano-scale heterogeneity in the distribution of proteins and lipids in the plasma membrane has emerged as a fundamental organizing principle of the cell (Simons and Ikonen, 1997; Balla, 2013; Schink et al., 2016; Stone et al., 2017). By partitioning molecules into distinct compartments, local clustering can also serve a potentially powerful mechanism for regulating molecular behavior.

During polarity establishment in the *C. elegans* zygote, clustering of a conserved set of PAR proteins (PAR-3, PAR-6 and PKC-3) on the membrane is critical for their ability to be segregated into the nascent anterior by actomyosin cortical flows (Rodriguez et al., 2017; Wang et al., 2017; Dickinson et al., 2017), eventually allowing them to be replaced by a second opposing set of PAR proteins (PAR-1, PAR-2, LGL-1 and CHIN-1) on the posterior membrane (Rose and Gonczy, 2014; Goehring, 2014). Cortical flows are in turn controlled by local foci of RHO-1 activation, which drive pulsatile actin nucleation and contraction of the cortical actomyosin network (Nishikawa et al., 2017; Michaux et al., 2018) (summarized in Fig. 1A).

Asymmetric enrichment of phosphatidylinositol 4,5-bisphosphate (PIP_2), has been observed within another class of membrane-associated domains in the anterior of the *C. elegans* zygote (Nakayama et al., 2009; Wang et al., 2017; Scholze et al., 2018). Similar enrichment is seen for the polarity-related Rho-family GTPases CDC-42 and RHO-1, the RHO-1 regulator ECT-2, a CDC-42-associated sub-population of PAR-6 and PKC-3, and casein kinase (CSNK-1) (Motegi and Sugimoto, 2006; Schonegg et al., 2007; Panbianco et al., 2008; Wang et al., 2017). PIP_2-enriched microdomains have been proposed to serve as organizing platforms to coordinate regulation of cortical actin organization, cell polarity and asymmetric division of the zygote (Scholze et al., 2018). Despite being noted over a decade ago, the nature of these domains remains poorly understood. Here, we show that these apparent microdomains are filopodia, which create the illusion of local enrichment of membrane-associated molecules due to induction of changes in local membrane topology. Our data argues against local enrichment of PIP_2 within the anterior of the embryo or within micron-scale domains.

RESULTS AND DISCUSSION

Diverse membrane-associated molecules appear to be co-enriched in membrane structures

To reveal the nature of these PIP_2-enriched domains, we confirmed previous results that polarity-related proteins RHO-1, CDC-42, and CSNK-1 colocalized to a similar class of membrane-associated domains labeled by the PIP_2 probe, $PH_{PLC\delta1}$ in *C. elegans* zygotes. All proteins labeled similar domains, which varied with the cell cycle, peaked during polarity establishment and colocalized with >90% of PIP_2-labeled domains (Nakayama et al., 2009; Motegi and Sugimoto, 2006; Schonegg et al., 2007; Panbianco et al., 2008; Scholze et al., 2018) (Fig. 1B; Figs S1 and S2). Given this coincidence, we determined whether the co-labeling was specific. We therefore co-expressed $PH_{PLC\delta1}$ with various plasma membrane markers, including the syntaxin SYX-4 (Jantsch-Plunger and Glotzer, 1999), a myristoylated form of mKate, $mKate_{myr}$, and the plasma membrane protein EGG-1 (Kadandale et al., 2005). Surprisingly, all proteins marked >90% of $PH_{PLC\delta1}$-labeled domains (Fig. 1B–E). To further control for non-specific labeling of bulk plasma membrane, we examined localization of the membrane dye FM4-64, which also labeled >90% of $PH_{PLC\delta1}$-

[1]The Francis Crick Institute, 1 Midland Road, London NW1 1AT, UK. [2]Institute for the Physics of Living Systems, University College London, London WC1E 6BT, UK. [3]Institut de Génétique et de Biologie Moléculaire et Cellulaire, Centre National de la Recherche Scientifique, UMR7104, Institut National de la Santé et de la Recherche Médicale, U1258, and Université de Strasbourg, 67404 Illkirch, France. [4]MRC Laboratory for Molecular Cell Biology, University College London, Gower Street, London WC1E 6BT, UK.

*Author for correspondence (nate.goehring@crick.ac.uk)

R.I., 0000-0002-2131-678X; A.-C.R., 0000-0002-0517-5083; N.W.G., 0000-0001-8710-4467

Received 6 February 2019; Accepted 17 June 2019

Journal of Cell Science (2019) 132, jcs230714. doi:10.1242/jcs.230714

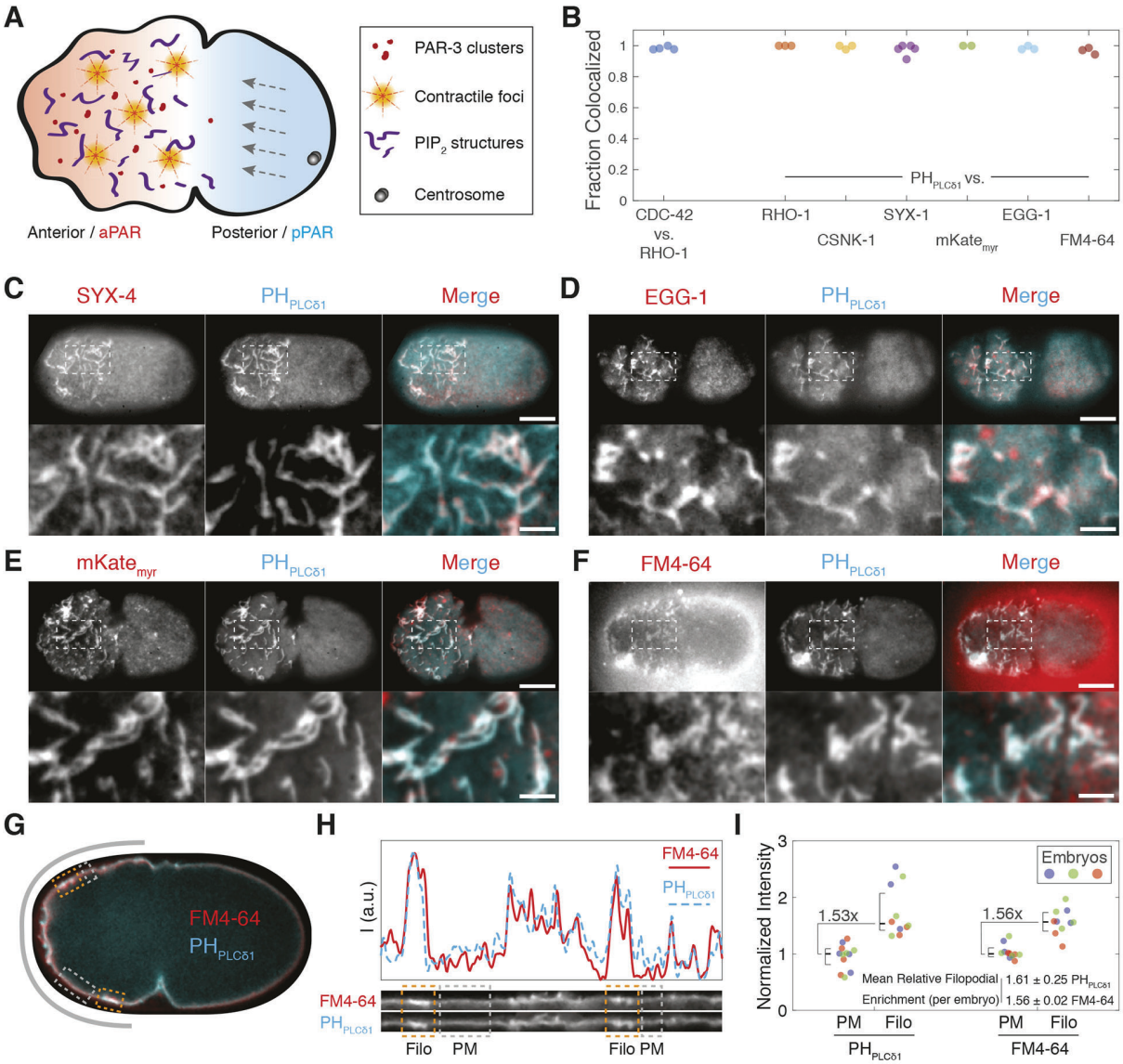

Fig. 1. Diverse membrane-associated molecules co-label common membrane structures. (A) Schematic of *C. elegans* zygote polarization, highlighting PAR-3 clusters, contractile foci and putative PIP_2-enriched membrane domains. Polarization of PAR proteins (red–blue) is induced by anterior-directed actomyosin cortical flows (gray arrows). (B) Fraction of membrane structures co-labeled by the indicated markers. Sample images are shown in C–F and Fig. S2. (C–F) Surface images of embryos expressing fluorescent protein (FP)-tagged $PH_{PLC\delta1}$ with transmembrane syntaxin, SYX-4 (GFP::SYX-4) (C), the oocyte-enriched membrane protein EGG-1 (GFP::EGG-1) (D), a myristoylated form of mKate, $mKate_{myr}$ (E) and the membrane dye FM4-64 (F). Individual channels and merged images are shown (whole embryo and a magnification of the indicated area). Scale bars: 10 µm (embryo), 2.5 µm (magnification). (G) Cross-section of embryo expressing GFP-tagged $PH_{PLC\delta1}$ with FM4-64 (n=3). Boxes highlight plasma membrane (gray, PM) and filopodia (orange, Filo). The gray band indicates the region straightened in H. (H) A 20-pixel-wide straightened region taken along the indicated path in G. $PH_{PLC\delta1}$ and FM4-64 intensity are shown individually with intensity plots (a.u., arbitrary units) above. Orange and gray boxes highlight regions marked in G. (I) Fluorescence intensity for PM and Filo regions from embryos co-labeled with $PH_{PLC\delta1}$ and FM4-64. Intensity normalized to embryo median (set as 1, color coded) with overall median±95% c.i. shown for all datapoints. Relative median filopodia enrichment between probes is indicated. The relative filopodia enrichment for individual embryo means is also provided (mean±s.d.).

positive domains (Fig. 1B,F; Movie 1). We observed quantitative agreement in the relative enrichment of the $PH_{PLC\delta1}$ and FM4-64 signal within the domains, indicating that there was no selective enrichment of molecules, including of PIP_2, within these domains relative to what is seen for bulk membrane (Fig. 1G–I).

Polarizing embryos exhibit asymmetric filopodia-like structures

What could be the origin of these $PH_{PLC\delta1}$-labeled domains that could explain their non-specific labeling by membrane-associated molecules? A clue came from observations of extended tubular structures protruding from the cell that were evocative of filopodia, which were particularly evident near the pseudocleavage furrow where the membrane pulls away from the eggshell (Fig. 2A).

Filopodia are thin, dynamic, actin-rich membrane protrusions. Their formation and extension is driven by actin polymerization downstream of Arp2/3 and formins, and is regulated by actin regulatory molecules including actin-bundling and -capping proteins (Mattila and Lappalainen, 2008), with Myosin-X and formins typically enriched at their tips (Jacquemet et al., 2019). Because

Journal of Cell Science (2019) 132, jcs230714. doi:10.1242/jcs.230714

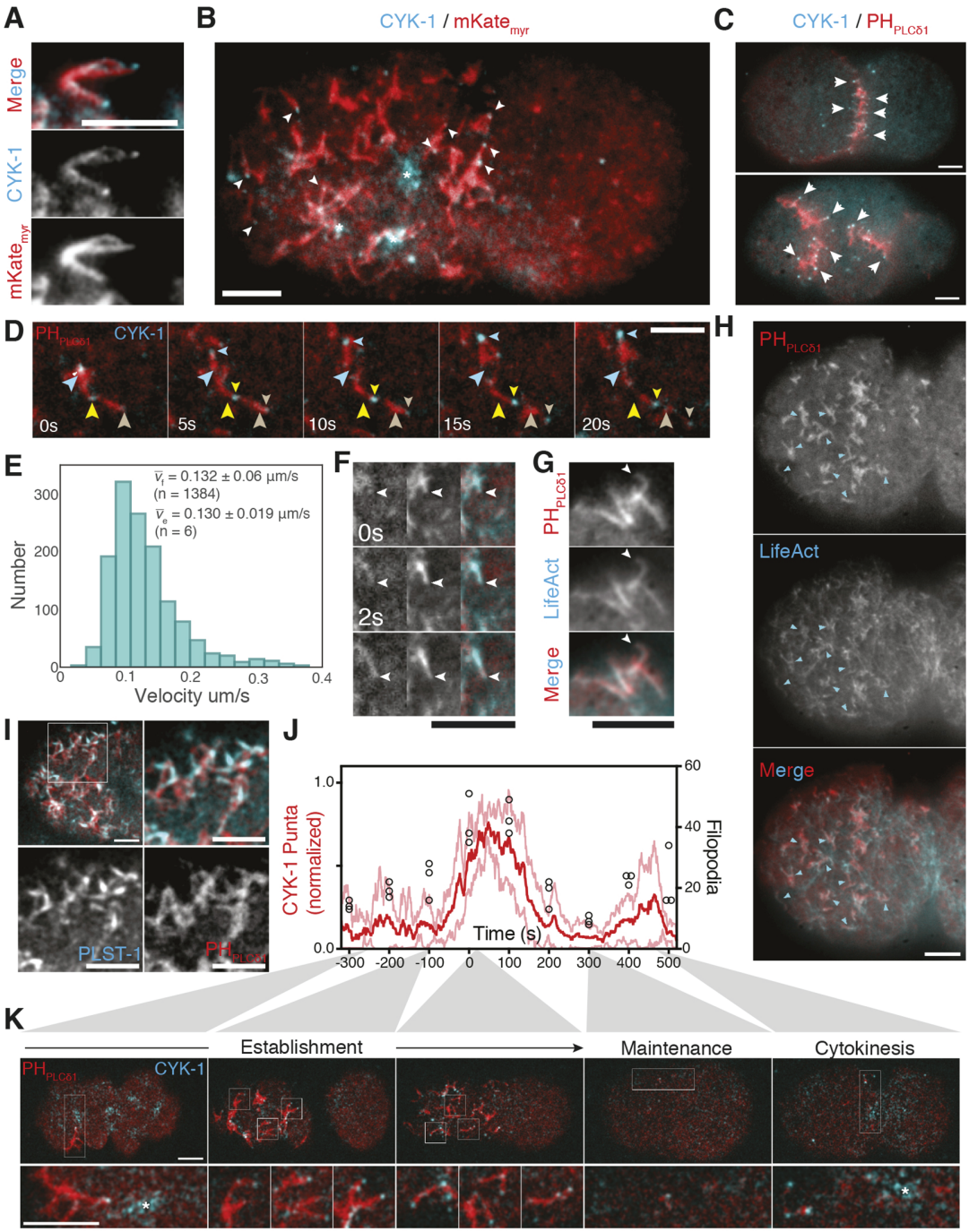

Fig. 2. Asymmetric cortical structures resemble filopodia. (A) Magnified region from the pseudocleavage furrow in embryo expressing mKate$_{myr}$ and CYK-1::GFP. See Movie 2. (B) CYK-1 localization to large contractile foci (*), and tips of filopodia-like structures revealed by mKate$_{myr}$ (arrowheads) in embryo anterior. (C) Surface images of two- and four-cell embryos expressing CYK-1::GFP and mCherry::PH$_{PLC\delta1}$. Arrowheads mark CYK-1-tipped membrane structures at cell contacts. (D) Time course of filopodia movement. Large arrowheads denote CYK-1::GFP puncta at time=0 s. Position in subsequent frames marked by small arrowheads of corresponding color. See Movie 3. (E) Histogram of CYK-1::GFP puncta velocities. v_f denotes mean±s.d. velocity for all CYK-1 puncta. v_e is the mean of embryo means. (F) Growth time course of a single filopodium (arrowhead) from embryo shown in H highlighting LifeAct localization throughout the extending structure (mCherry::PH$_{PLC\delta1}$, left; LifeAct::GFP, middle; merge, right). See Movie 4. (G) Example of LifeAct::GFP labeling throughout extended mCherry::PH$_{PLC\delta1}$-positive filopodia (arrowhead). Labeling observed in 13/13 extended filopodia (three embryos). (H) Extensive colocalization of LifeAct::GFP with mCherry::PH$_{PLC\delta1}$ within putative filopodia (arrowheads) (n=4). (I) Cortical image of embryo anterior showing mCherry::PH$_{PLC\delta1}$ and PLST-1::GFP (top left). The boxed area is magnified (top right) with individual channels shown below. Quantification and additional images are in Fig. S3A,B. (J) Number of CYK-1 puncta (normalized to peak number; mean in red with ±s.d. in pink) and PH$_{PLC\delta1}$-labeled structures (black circles) over time. Time 0 s is the transition between establishment and maintenance phase marked by relaxation of the pseudocleavage furrow. Cytokinesis occurs at between 400 and 500 s. (K) Confocal cortical images of embryo expressing CYK-1::GFP and mCherry::PH$_{PLC\delta1}$ at representative time points. Boxed areas are shown magnified 3× below. The asterisk indicates large pulsatile foci common at polarity establishment and cytokinesis. See Movie 5. Colocalization of CYK-1 puncta with mCherry::PH$_{PLC\delta1}$-labeled structures in Fig. S3A. Scale bars: 5 µm.

Journal of Cell Science

there is no homolog of Myosin-X in *C. elegans*, we examined localization of the embryonically expressed formin CYK-1 co-expressed with red fluorophore fusions to $PH_{PLC\delta1}$ or $mKate_{myr}$ (Swan et al., 1998). CYK-1 was enriched at the tips of extended tubular structures and comet-like structures at the cortex (Fig. 2A,B; Movies 2 and 3). We interpret the latter structures to be the same as extended tubular structures but pressed against the embryo surface by the eggshell. Intercalating CYK-1-tipped finger-like projections were also observed at regions of cell–cell contacts at both two- and four-cell stages (Fig. 2C). CYK-1 puncta were distinct from large pulsatile foci that are also present during the polarity establishment phase (Fig. 2B,K, asterisks) and which have been shown to coincide with pulsatile actomyosin (Michaux et al., 2018).

CYK-1-tipped structures were dynamic, exhibiting processive motion across the plasma membrane at velocities consistent with prior quantification of filopodia growth rates (Argiro et al., 1985) (Fig. 2D,E). To further establish the filopodia-like nature of these structures, we examined LifeAct::GFP, which extensively colocalized with the mCherry:: $PH_{PLC\delta1}$ signal in putative filopodia and appeared to extend throughout filopodia-like structures (Fig. 2F–H, Movie 4). We also found that >80% of filopodia-like structures were labeled by the *C. elegans* ortholog of the actin-bundling protein plastin (PLST-1 in *C. elegans*; Ding et al. 2017) (Fig. 2I, Fig. S3A,B), consistent with data from other systems (Jacquemet et al., 2019). Finally, the combined loss of both CYK-1 and ARP-2/3 function prevented their formation (Fig. S3C), consistent with prior work demonstrating the dependence of PIP_2 domains on actin (Scholze et al., 2018). By contrast, loss of either cortical contractility or PAR polarity did not affect the formation of filopodia, only their asymmetry along the anterior–posterior axis (Fig. S3D).

Numbers of CYK-1 puncta generally correlated with appearance of $PH_{PLC\delta1}$-labeled structures (Fig. 2J,K; Movie 5): Numbers of both were initially low, peaking after the transition to maintenance phase, which coincides with reorganization of the actin cortex (Fig. 2J,K, 0 s) (Munro et al., 2004; Velarde et al., 2007). Both then declined and remained largely absent until reappearing at the onset of cytokinesis (Fig. 2J,K, 400–500 s). This correlation suggests that filopodia account for the vast majority of $PH_{PLC\delta1}$-labeled structures in the zygote.

Preferential labeling of distinct F-actin populations by different LifeAct probes

The colocalization we observe between LifeAct::GFP and $PH_{PLC\delta1}$ differed from that described in previous work in which PIP_2 enrichment was reported to precede LifeAct::mKate enrichment by nearly 10 s (Scholze et al., 2018). We wondered whether the divergent results were due to employment of differently tagged versions of LifeAct. Co-expression of both GFP and mKate versions of LifeAct in embryos revealed distinct localization behaviors. Most noticeably, LifeAct::mKate appeared to segregate preferentially into the anterior (Fig. 3A,C) and was unequally inherited by the anterior daughter cell (AB) relative to its sister P1, and again by the P1 daughter EMS relative to its sister P2 (Fig. 3B). Neither behavior was observed for LifeAct::GFP. LifeAct::mKate also poorly labeled posterior structures that were labeled efficiently by LifeAct::GFP (Fig. 3A).

LifeAct::GFP and LifeAct::mKate also showed distinct labeling of filopodia. Whereas LifeAct::GFP efficiently labeled dynamic filopodia extending from the cell, LifeAct::mKate was depleted (Fig. 3D). LifeAct::mKate signal also lagged behind LifeAct::GFP signal in filopodia moving along the embryo surface and in cytoplasmic actin comets (Fig. 3E–H, Movies 6 and 7). Finally, we observed a spatial gap between CYK-1 puncta at filopodia tips and LifeAct::mKate signal, consistent with a time lag in labeling filopodia (Fig. 3I,J).

Lags in actin probe localization have been associated with slow turnover rates in the context of actin flow (e.g. for LifeAct versus utrophin; Bement et al., 2015; Maiuri et al., 2015). LifeAct is generally thought to turn over rapidly, but behavior can vary with fluorophore and expression level (Riedl et al., 2008; Spracklen et al., 2014; Courtemanche et al., 2016; van der Honing et al., 2011). We therefore performed fluorescence recovery after photobleaching (FRAP) assays to analyze the binding kinetics (Fig. 3K,L). LifeAct::mKate turnover rates were an order of magnitude slower than for LifeAct::GFP ($r_{1/2}$=21.6±8.9 versus 0.84±0.27 s; mean±s.d.), reaching time scales comparable to turnover of cortical F-actin in the *C. elegans* cortex (Robin et al., 2014). We conclude that slow turnover of LifeAct::mKate leads to its localization to a discrete, potentially more-stable or long-lived, sub-population of actin structures, which explains the previously observed lag in LifeAct::mKate localization to PIP_2-labeled structures (Scholze et al., 2018). The temporal lag we observe matches the reported delay between $PH_{PLC\delta1}$ and LifeAct::mKate (10 versus 9.3 s). Consistent with this interpretation, artificially stabilizing LifeAct::GFP at the membrane by co-expression with a membrane-tethered GFP-binding protein induced segregation of LifeAct::GFP, reproducing the segregation phenotype observed with LifeAct::mKate (Fig. 3M). Affinity differences in LifeAct probes could also potentially explain reported resistance of cortical actin to actin-disrupting agents in LifeAct::mKate-expressing lines relative to prior work (Goehring et al., 2011; Michaux et al., 2018; Scholze et al., 2018).

Membrane topology quantitatively accounts for local 'enrichment' of membrane-associated molecules

We next sought to determine how filopodia could result in apparent local enrichment of membrane-associated molecules. One possibility is that enrichment simply reflects the local accumulation of membrane within ruffles, tubes or folds within the imaging plane, increasing local fluorescence above that seen for the surrounding single membrane bilayer. This effect, described previously in mammalian cells, would occur even if protein concentration on the membrane was uniform (van Rheenen and Jalink, 2002).

To determine whether locally increased signal could be explained by membrane topology, we compared the distribution of fluorescence of mCherry::$PH_{PLC\delta1}$ obtained by confocal microscopy with what would be expected if membrane concentration were uniform, but a filopodia was immediately adjacent to the membrane. To this end, we obtained *z*-stacks of embryos expressing mCherry::$PH_{PLC\delta1}$ during the establishment phase. Bright spots were visible in individual planes which could be assigned to filopodia in 3-D renderings (Fig. 4A, arrowheads). These filopodia were brighter than regions containing a single membrane bilayer, but less bright than the double membrane bilayer of the pseudocleavage furrow (Fig. 4A, arrows). Quantification of experimental intensities were then compared to those obtained from a simulated image, which was constructed by assuming the presence of a single 5-nm-thick bilayer, flanked by a second bilayer in the region of the pseudocleavage furrow, and a 100-nm diameter filopodium, assuming uniform membrane concentration (Fig. 4C,D, see Materials and Methods). Intensity distributions were remarkably similar, with experimental measurements almost exactly matching predictions from simulated images (Fig. 4E,F).

Thus, for the molecules analyzed here, including PIP_2, RHO-1, CDC-42 and CSNK-1, local cortical signal in filopodia-like

Journal of Cell Science (2019) 132, jcs230714. doi:10.1242/jcs.230714

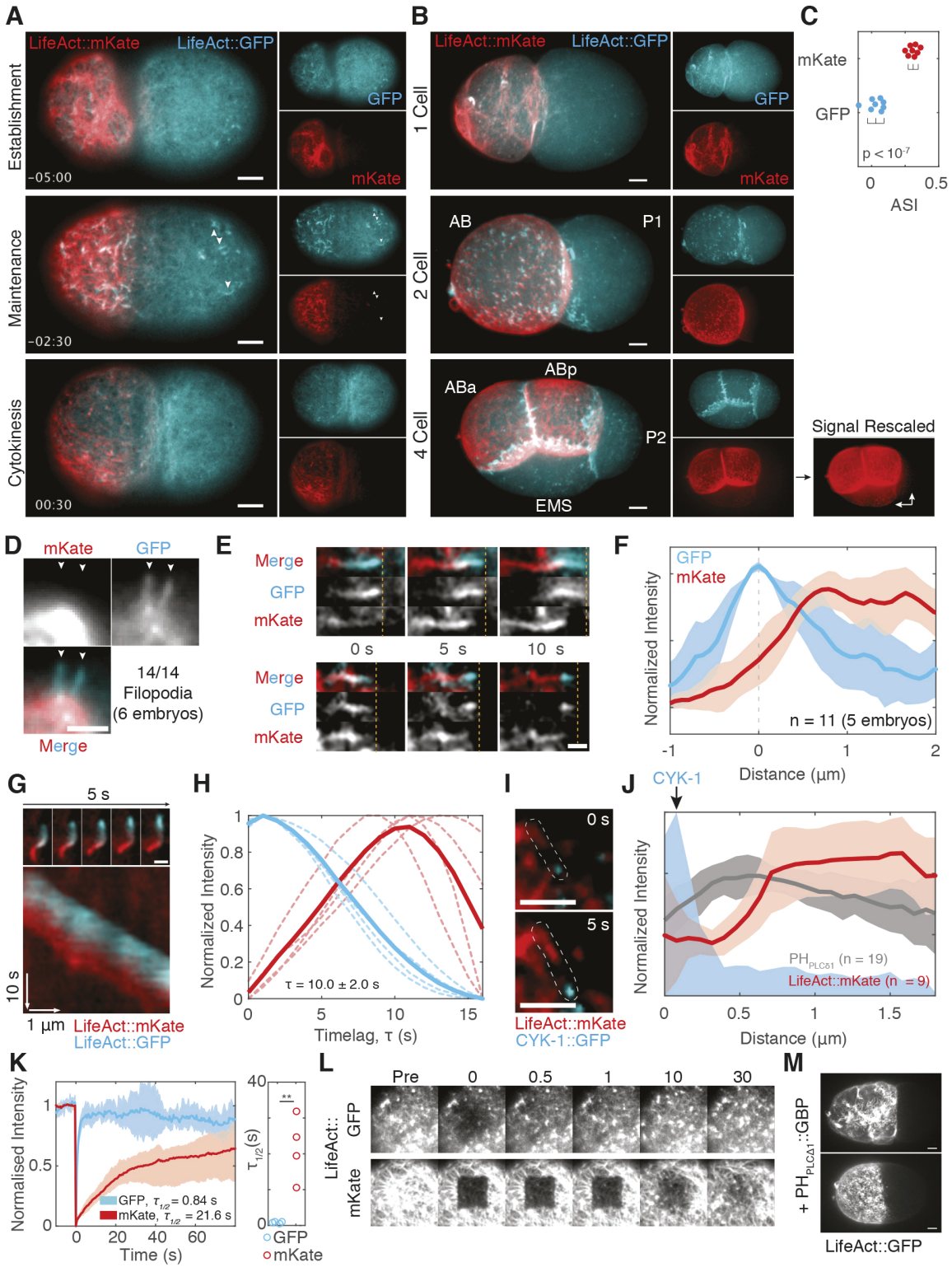

Fig. 3. See next page for legend.

structures can be fully explained by changes in local membrane topology, arguing against any concentration of these molecules within micron-scale domains in the plasma membrane or asymmetric enrichment of PIP_2 in the zygote anterior. While filopodia are the dominant features underlying this phenomenon in the zygote, any local changes in membrane topology would give a similar appearance of local enrichment of membrane-associated molecules, including membrane ruffles, folds or protrusions, making this a widespread problem for the quantification of local membrane concentration.

Fig. 3. LifeAct::GFP and LifeAct::mKate label distinct actin populations *in vivo*. (A) Cortical images of LifeAct::mKate vs LifeAct::GFP during the first cell cycle, quantified in (C). Arrowheads mark posterior filopodial structures that are only labeled by LifeAct::GFP. Time (min:sec) relative to cytokinesis. (B) Max 3D projections of 1-, 2- and 4-cell embryos. LifeAct::mKate signal in the 4-cell embryo is shown rescaled to highlight asymmetry between EMS and P2 (arrows). (C) Asymmetry (ASI) of LifeAct::GFP vs LifeAct::mKate signal in 1-cell establishment phase embryos (panel A). (D) LifeAct::GFP, but not LifeAct::mKate, labels filopodia extending from the cell surface. (E) LifeAct::mKate lags LifeAct::GFP labeling of two processive surface-associated filopodia. Computationally straightened images shown. Dashed lines mark leading edge of GFP signal for reference. See Movie 6. (F) Lag of LifeAct::mKate relative to peak LifeAct::GFP signal in fluorescence intensity traces along filopodia. (G) Time lapse images of a cytoplasmic actin comet labeled with LifeAct::mKate and LifeAct::GFP and an associated kymograph taken along a trace of the comet path. See Movie 7. (H) Quantification of LifeAct::mKate time lag measured from kymographs as in G. Average temporal change across a minimum of ten positions for each individual comet (dashed lines, n=4) shown along with mean of embryo means (solid lines). $\Delta\tau$ is the peak-to-peak time lag. (I) Time lapse of images of a filopodium (outlined) labeled by CYK-1::GFP and LifeAct::mKate. (J) Quantification of LifeAct::mKate or mCherry::$PH_{PLC\delta1}$ relative to GFP::CYK-1 puncta. Mean±s.d. shown. (K) FRAP analysis of cortical LifeAct::GFP versus LifeAct::mKate following bleaching of a 6.2×6.2 µm box. Mean FRAP trace (±max/min; shaded area) (left) shown along with $\tau_{1/2}$ for each replicate. **P<0.01 (two-tailed t-test). (L) Time series of FRAP experiments from K. (M) Stabilization of LifeAct::GFP by membrane-tethered GFP nanobody ($PH_{PLC\delta1}$::GBP)-induced segregation. Maximum z-projections at establishment (top) and maintenance phase (bottom) are shown (n=3). Scale bars: 5 µm (A,B,D,M), 2.5 µm (E,G,I).

It is noteworthy that despite similar asymmetry of anterior structures, only CDC-42, which is known to interact with anterior-enriched PAR proteins, exhibited pronounced polarity when quantified in cross-section and retained this asymmetric enrichment during the maintenance phase when filopodia largely disappeared. These data argue against overall asymmetry of either PIP_2 or RHO-1 or for filopodia being required for CDC-42 asymmetry (Fig. S4). One should also note that the localization of activity sensors for CDC-42 and RHO-1 tend not to match localization of the proteins overall (Nishikawa et al., 2017; Kumfer et al., 2010), consistent with local regulation of activity, rather than local accumulation alone, being critical for localized function of these GTPases. Anterior PIP_2 enrichment is also difficult to reconcile with observations that the PI4K kinase, PPK-1, is modestly enriched in the embryo posterior, which is opposite to what would be expected if high PIP_2 levels defined the anterior (Panbianco et al., 2008). LGL and PAR-2 are also both thought to rely on PIP_2 for membrane association, despite being enriched in the posterior (Motegi et al., 2011; Dong et al., 2015). We therefore favor a global, rather than local, role for PIP_2, which is consistent with the sensitivity of the zygote to bulk changes in PIP_2 levels (Scholze et al., 2018).

The existence of PIP_2 membrane domains remains controversial (van Rheenen and Jalink, 2002; Stone et al., 2017; van den Bogaart et al., 2011; Wang and Richards, 2012; Ji et al., 2015). While we cannot rule out the existence of PIP_2 membrane domains that are not revealed by the probes used to date, in light of our data, we feel there is currently no compelling experimental evidence to support the existence of PIP_2 microdomains or anterior PIP_2 enrichment in the *C. elegans* zygote.

MATERIALS AND METHODS

Strains, growth and media

C. elegans strains were maintained on nematode growth medium (NGM) under standard conditions (Brenner, 1974) at 16°C or 20°C unless otherwise indicated. Strains are listed in Table S1.

Strain construction

$mKate_{myr}$ consists of the first 11 amino acids of SRC-2, harboring the N-myristoylation site, followed by a 3×Myc tag, mKate and the coding sequence of iLID (Guntas et al., 2015). The coding sequence is expressed under the *mex-5* promoter and *nmy-2* 3′UTR in plasmid pNG17, which was introduced by biolistic bombardment into DP38 worms creating strain NWG0045 (Praitis et al., 2001). SWG19 was generated by backcrossing SWG4 (Reymann et al., 2016) to the N2 strain (four times). For membrane tethering of LifeAct::GFP, we crossed NWG0047 (PH::GBP::mKate) with TH220 (LifeAct::GFP).

RNAi

RNAi was performed according to previously described methods (Kamath et al., 2003). Briefly, HT115(DE3) bacterial feeding clones were inoculated from LB agar plates to LB liquid cultures and grown overnight at 37°C in the presence of 10 µg/ml carbenicillin. 100 µl of bacterial cultures was spotted onto 60 mm agar RNAi plates (10 µg/ml carbenicillin, 1 mM IPTG). L4 larva were added to RNAi feeding plates and incubated for 20–48 h depending on gene and temperature. RNAi clones targeting *arx-2*, *ect-2*, *par-2*, *perm-1*, *pkc-3* and *wve-1* were obtained from the Ahringer library, which is currently available via Source BioScience (Nottingham, UK).

Embryo dissection and mounting

For imaging, embryos were typically dissected in egg buffer (118 mM NaCl, 48 mM KCl, 2 mM $CaCl_2$, 2 mM $MgCl_2$, 25 mM HEPES pH 7.4) or M9 buffer, and mounted under a 2% or 3% agarose pad and sealed with VALAP (1:1:1, Vaseline, lanolin and paraffin wax). For FM4-64 experiments, *perm-1(RNAi)* embryos were dissected and mounted in 0.75% egg buffer, with 18–20 µm beads (Polysciences, Warrington, PA) under a coverslip, and two edges were sealed with VALAP to create a flow chamber (Carvalho et al., 2011; Goehring et al., 2011). FM4-64 (T13320, ThermoFisher UK, 5 µg/ml in 0.75% egg buffer) was then introduced by capillary action.

Microscopy and image acquisition

Confocal image acquisition

Midsection images were captured on a Nikon TiE with a 100×1.45 NA objective, further equipped with a custom X-Light V1 spinning disk system (CrestOptics, Rome, Italy) with 50 µm slits, Obis 488/561 fiber-coupled diode lasers (Coherent, Santa Clara, CA) and an Evolve Delta EMCCD camera (Photometrics, Tuscon, AZ). Imaging systems were run using Metamorph (Molecular Devices, San Jose, CA) and configured by Cairn Research (Kent, UK). Filter sets were from Chroma (Bellows Falls, VT): ZT488/561rpc, ZET405/488/561/640X, ET525/50m, ET630/75m and ET655LP.

Surface confocal images were acquired with spinning disk confocal microscope every 2 s [for CYK-1: Zeiss C-Apochromat with a Yokogawa CSU-X1 scan head, Orca-Flash4.0 camera (Hamamatsu Photonics, Japan) and a 100×/1.42 NA objective lens, run using Micro-Manager; for PLST-1: Inverted Nikon Eclipse Ti equipped with a Yokogawa CSU-X1 scan head, simultaneous dual camera with two Prime 95B cameras (Photometrics) and a 100×1.4 NA objective lens, configured by Gataca Systems (Massy, France) and run using Metamorph].

HiLo imaging

Unless otherwise specified, surface images were captured by HiLo microscopy (Konopka and Bednarek, 2008; Tokunaga et al., 2008) on a Nikon TiE with a 100× N.A. 1.49 objective, further equipped with a iLAS TIRF unit (Roper, Lisse, France), custom field stop, Obis 488/561 fiber-coupled diode lasers (Coherent) and an Evolve Delta camera. Imaging systems were run using Metamorph and configured by Cairn Research. Filter sets were from Chroma: ZT488/561rpc, ZET488/561x, ZET488/561m, ET525/50m, ET630/75m, ET655LP. FRAP was performed in a 6.2×6.2 µm box in the anterior of maintenance phase embryos with 20 prebleach frames and an imaging interval of 0.5 s.

Data analysis

Image processing and data analysis were performed in Python (www.python.org), Matlab (Mathworks, Natick, MA) and Fiji (Schindelin et al.,

Journal of Cell Science (2019) 132, jcs230714. doi:10.1242/jcs.230714

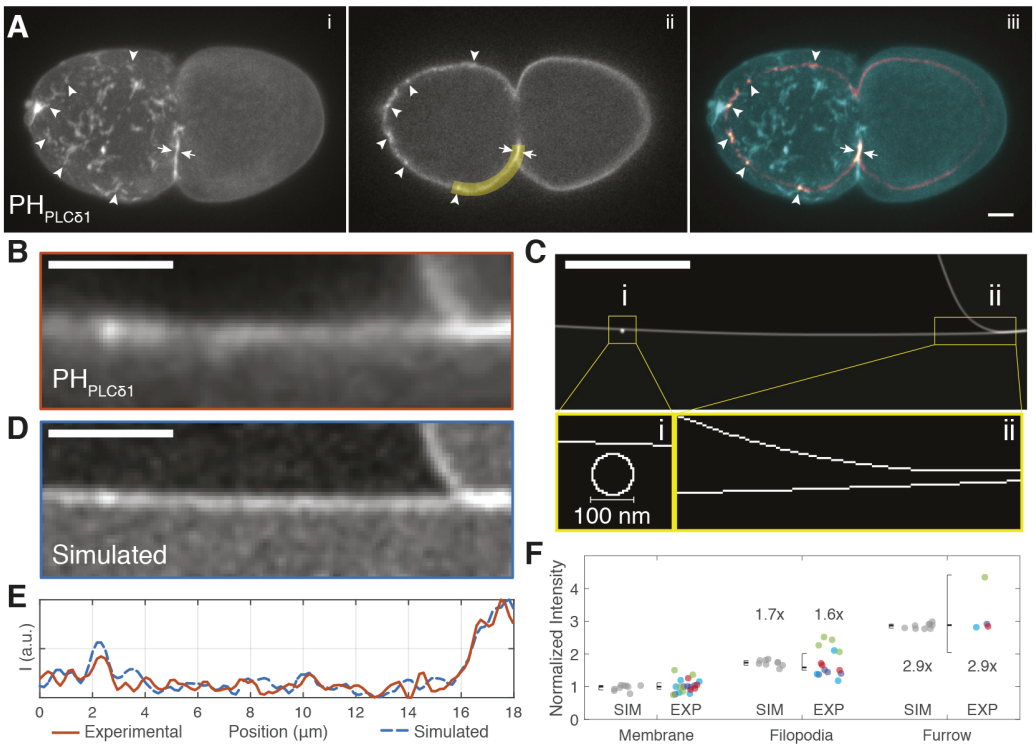

Fig. 4. Bulk membrane accumulation quantitatively accounts for observed cortical 'enrichment'. (A) Maximum *z*-projection (i), single plane (ii) and overlay (iii) of an establishment phase embryo expressing mCherry::$PH_{PLC\delta1}$. Arrowheads mark visible accumulations of signal in a single plane that can be identified as cross-sections of membrane structures based on the *z*-projection. White arrows mark double membrane generated at the pseudocleavage furrow. (B) Straightened cortical region of the experimental image taken along the yellow line in (Aii). (C) A 5 nm/pixel representation of our filopodia model of the image in B, including a 100-nm-diameter membrane tube (zoom, i) and a double membrane region at right (zoom, ii). (D) Simulated image following convolution of C. (E) Plot of mean-normalized intensity along the membrane in the experimental (B, red) and simulated image (D, dashed blue). (F) Quantification of fluorescence intensity of putative filopodia relative to single membranes and furrow regions in experimental and simulated images. Datapoints from individual embryos are color coded (n=4), normalized to median values and shown alongside median-normalized data from simulated image replicates (n=10). The median±95% c.i. is indicated by the whisker plot along with fold-change from median (set at 1). Scale bars: 5 µm.

2012). For statistical comparisons, all data points are shown and significance assessed using a Student's *t*-test, two-tailed.

FRAP

FRAP analysis was performed in Matlab using scripts provided in Goehring et al. (2010), but fit to a single exponential to extract $\tau_{1/2}$.

CYK-1 tracking

Filopodia tip velocity measurements were obtained by tracking CYK-1::GFP puncta, which was performed in Python using the 'trackpy' package (https://github.com/soft-matter/trackpy). Custom Python code developed for the analysis is available at https://github.com/lhcgeneva/SPT. Briefly, a Crocker–Grier algorithm detects local intensity peaks, which are then fit to a Gaussian point spread function with the detection threshold adjusted empirically for imaging conditions. An independently acquired dataset was quantified using the MOSAIC plugin in Fiji (http://mosaic.mpi-cbg.de/?q=downloads/imageJ) together with custom Matlab codes (available from corresponding author upon request) for data analysis to confirm results.

Spatial/temporal fluorescence profiles

In general, fluorescence profiles (both experimental and simulated) were obtained by tracking a 3-pixel-wide line along the membrane from images subjected to a Gaussian Blur (σ=1 px) to reduce noise. Mean normalized profiles after subtraction of chip background were extracted and plotted in Matlab.

For Fig. 3G, clear filopodia-like structures were identified that were isolated from other structures that would complicate analysis. After obtaining fluorescence profiles along filopodia in both channels, data from each filopodium was aligned based on the peak of GFP::LifeAct intensity.

For Fig. 3H, fluorescence profiles along the path of the actin comets were obtained over time, and the data plotted as a two-channel kymograph. Temporal change was calculated across a minimum of ten spatial positions for each individual comet, the resulting data aligned by the time of peak GFP fluorescence, before averaging to obtain the average temporal profile of GFP and mKate for each comet. $\Delta\tau$ was defined as the peak-to-peak time difference between maximal GFP and mKate accumulation calculated from average temporal profiles of each comet.

For Fig. 3K, profiles of LifeAct::mKate and $PH_{PLC\delta1}$ relative to CYK-1 puncta were obtained by first identifying clear filopodia with comet-like morphologies from a minimum of three embryos each. A 3-pixel line beginning at the center of the CYK-1 focus and running through the PH- or LifeAct-labeled region was then defined and straightened in Fiji. Fluorescence profiles were then extracted in Matlab, normalized to the mean intensity and plotted as a function of distance from CYK-1 puncta at the filopodia tip.

For quantification of relative peak intensities in Figs 1I and 4F, 3-pixel-wide profiles across membrane features were extracted; then, cytoplasmic background was subtracted, and the top three peak intensity pixels summed. Data was normalized to median intensities obtained in regions of the plasma membrane devoid of membrane structures, representing a single bilayer configuration, in the same embryo. Simulated images were treated identically except that they were normalized to the median value of all single membrane peaks.

Colocalization

Regions of interest (ROIs) were manually defined for a minimum of 30 well-defined and separated structures in the reference channel for each embryo,

usually using the channel showing fluorescent protein fusions to $PH_{PLC\delta1}$. ROIs were then queried in the test channel to score whether the structure was labeled by the other molecule, scoring either for the presence of a similar structure or a tip-localized punctum, in the case of CYK-1. The fraction of structures showing colocalization was calculated for each embryo.

Asymmetry index

For Fig. 3C, the asymmetry index (ASI) of cortical LifeAct was calculated by first obtaining mean fluorescence values from selected regions of the cell cortex in the anterior and posterior halves of the zygote in background subtracted images. We then calculated ASI according to the equation ASI=(A−P)/[2(A+P)], where A and P are the fluorescence values in the anterior and posterior, respectively. The resulting values for ASI range from −0.5 to 0.5, with 0 being symmetric, and −0.5 and 0.5 being maximally polarized towards posterior or anterior, respectively.

In Fig. S4, the ASI was calculated from membrane intensity profiles around the circumference of the embryo extracted from cross-sectional confocal images. Briefly, a 50-pixel-wide line following the membrane around the embryo was computationally straightened, and a normalized cytoplasmic GFP curve was subtracted to isolate membrane signal following the procedure described in Reich et al. (2019). Mean intensity values corresponding to the posterior and anterior regions of the embryo (each representing one-third of the total circumference) were then used to calculate ASI as above.

Image simulations

To simulate fluorescence microscopy images of hypothesized experimental membrane configurations, a starting image of resolution 5 nm/pixel was generated to match the dimensions of the experimental image in Fig. 4B. The membrane bilayer was simulated as a 1-pixel-wide line, which was used to trace the hypothesized membrane configuration from the experimental image. This included a region containing part of the pseudocleavage furrow, which generates a double membrane as well as a circle 100 nm in diameter to mimic the cross section of the filopodial membrane. A uniform background level of photons was added before subjecting the resulting image to a 200-nm-wide Guassian blur and resampling to the experimental resolution of 0.155 µm/pixel. Modulated Poisson noise and readout noise (five standard deviations) was then added before processing identically to the experimental image. All manipulations were performed in Fiji.

Acknowledgements

The authors would like to thank members of the Goehring lab for critical comments, and Stephan Grill and Julie Canman for providing worm lines. Some imaging was supported by the Imaging Center of IGBMC (ici.igbmc.fr) with assistance from Elvire Guiot, Erwan Grandgirard and Bertrand Vernay. Some strains were provided by the *C. elegans* Genome Center (CGC), which is funded by NIH Office of Research Infrastructure Programs (P40 OD010440).

Competing interests

The authors declare no competing or financial interests.

Author contributions

Conceptualization: A.-C.R., N.W.G.; Methodology, N.H., R.I., T.B.; Formal analysis: R.I., T.B., A.-C.R., N.W.G.; Investigation: N.H., R.I., T.B., G.M., D.S., A.-C.R., N.W.G.; Resources, N.H., G.M., D.S.; Writing – original draft preparation, N.W.G.; Writing – review and editing, N.H., R.I., T.B., G.M., D.S., A.-C.R., N.G.; Supervision: A.-C.R., N.W.G.; Project administration: A.-C.R., N.W.G.; Funding acquisition: A.-C.R., N.W.G.

Funding

This work was supported by the Francis Crick Institute (N.W.G.), which receives its core funding from Cancer Research UK (FC001086), the UK Medical Research Council (FC001086), and the Wellcome Trust (FC001086), the EU Horizon 2020 research and innovation programme under the H2020 Marie Skłodowska-Curie Actions (grant agreement 675407 to N.W.G.), the IGBMC (A.-C.R.) via grant ANR-10-LABX-0030-INRT, a French State fund managed by the Agence Nationale de la Recherche (ANR) under the frame program Investissements d'Avenir ANR-10-IDEX-0002-02, and support by the initiative of excellence IDEX-Unistra from the same frame program (A.-C.R.). G.M. is an IGBMC International PhD Programme fellow supported by LabEx INRT funds. N.W.G. and A.-C.R. are members of the GENiE network supported by European Cooperation in Science and Technology (COST) Action (BM1408) and European Molecular Biology Organization (EMBO). Deposited in PMC for immediate release.

Supplementary information

Supplementary information available online at
http://jcs.biologists.org/lookup/doi/10.1242/jcs.230714.supplemental

References

Argiro, V., Bunge, M. B. and Johnson, M. I. (1985). A quantitative study of growth cone filopodial extension. *J. Neurosci. Res.* **13**, 149-162. doi:10.1002/jnr.490130111

Balla, T. (2013). Phosphoinositides: tiny lipids with giant impact on cell regulation. *Physiol. Rev.* **93**, 1019-1137. doi:10.1152/physrev.00028.2012

Bement, W. M., Leda, M., Moe, A. M., Kita, A. M., Larson, M. E., Golding, A. E., Pfeuti, C., Su, K.-C., Miller, A. L., Goryachev, A. B. et al. (2015). Activator–inhibitor coupling between Rho signalling and actin assembly makes the cell cortex an excitable medium. *Nat. Cell Biol.* **17**, 1471-1483. doi:10.1038/ncb3251

Brenner, S. (1974). The genetics of *Caenorhabditis elegans*. *Genetics* **77**, 71-94.

Carvalho, A., Olson, S. K., Gutierrez, E., Zhang, K., Noble, L. B., Zanin, E., Desai, A., Groisman, A. and Oegema, K. (2011). Acute drug treatment in the early *C. elegans* embryo. *PLoS ONE* **6**, e24656. doi:10.1371/journal.pone.0024656

Courtemanche, N., Pollard, T. D. and Chen, Q. (2016). Avoiding artefacts when counting polymerized actin in live cells with LifeAct fused to fluorescent proteins. *Nat. Cell Biol.* **18**, 676-683. doi:10.1038/ncb3351

Dickinson, D. J., Schwager, F., Pintard, L., Gotta, M. and Goldstein, B. (2017). A single-cell biochemistry approach reveals PAR complex dynamics during cell polarization. *Dev. Cell* **42**, 416-434.e11. doi:10.1016/j.devcel.2017.07.024

Ding, W. Y., Ong, H. T., Hara, Y., Wongsantichon, J., Toyama, Y., Robinson, R. C., Nédélec, F. and Zaidel-Bar, R. (2017). Plastin increases cortical connectivity to facilitate robust polarization and timely cytokinesis. *J. Cell Biol.* **216**, 1371-1386. doi:10.1083/jcb.201603070

Dong, W., Zhang, X., Liu, W., Chen, Y.-J., Huang, J., Austin, E., Celotto, A. M., Jiang, W. Z., Palladino, M. J., Jiang, Y. et al. (2015). A conserved polybasic domain mediates plasma membrane targeting of Lgl and its regulation by hypoxia. *J. Cell Biol.* **211**, 273-286. doi:10.1083/jcb.201503067

Goehring, N. W. (2014). PAR polarity: from complexity to design principles. *Exp. Cell Res.* **328**, 258-266. doi:10.1016/j.yexcr.2014.08.009

Goehring, N. W., Chowdhury, D., Hyman, A. A. and Grill, S. W. (2010). FRAP analysis of membrane-associated proteins: lateral diffusion and membrane-cytoplasmic exchange. *Biophys. J.* **99**, 2443-2452. doi:10.1016/j.bpj.2010.08.033

Goehring, N. W., Hoege, C., Grill, S. W. and Hyman, A. A. (2011). PAR proteins diffuse freely across the anterior–posterior boundary in polarized *C. elegans* embryos. *J. Cell Biol.* **193**, 583-594. doi:10.1083/jcb.201011094

Guntas, G., Hallett, R. A., Zimmerman, S. P., Williams, T., Yumerefendi, H., Bear, J. E. and Kuhlman, B. (2015). Engineering an improved light-induced dimer (iLID) for controlling the localization and activity of signaling proteins. *Proc. Natl. Acad. Sci. USA* **112**, 112-117. doi:10.1073/pnas.1417910112

Jacquemet, G., Stubb, A., Saup, R., Miihkinen, M., Kremneva, E., Hamidi, H. and Ivaska, J. (2019). Filopodome mapping identifies p130Cas as a mechanosensitive regulator of filopodia stability. *Curr. Biol.* **29**, 202-216.e7. doi:10.1016/j.cub.2018.11.053

Jantsch-Plunger, V. and Glotzer, M. (1999). Depletion of syntaxins in the early *Caenorhabditis elegans* embryo reveals a role for membrane fusion events in cytokinesis. *Curr. Biol.* **9**, 738-745. doi:10.1016/S0960-9822(99)80333-9

Ji, C., Zhang, Y., Xu, P., Xu, T. and Lou, X. (2015). Nanoscale landscape of phosphoinositides revealed by specific pleckstrin homology (PH) domains using single-molecule superresolution imaging in the plasma membrane. *J. Biol. Chem.* **290**, 26978-26993. doi:10.1074/jbc.M115.663013

Kadandale, P., Stewart-Michaelis, A., Gordon, S., Rubin, J., Klancer, R., Schweinsberg, P., Grant, B. D. and Singson, A. (2005). The egg surface LDL receptor repeat-containing proteins EGG-1 and EGG-2 are required for fertilization in *Caenorhabditis elegans*. *Curr. Biol.* **15**, 2222-2229. doi:10.1016/j.cub.2005.10.043

Kamath, R. S., Fraser, A. G., Dong, Y., Poulin, G., Durbin, R., Gotta, M., Kanapin, A., Le Bot, N., Moreno, S., Sohrmann, M. et al. (2003). Systematic functional analysis of the *Caenorhabditis elegans* genome using RNAi. *Nature* **421**, 231-237. doi:10.1038/nature01278

Konopka, C. A. and Bednarek, S. Y. (2008). Variable-angle epifluorescence microscopy: a new way to look at protein dynamics in the plant cell cortex. *Plant J.* **53**, 186-196. doi:10.1111/j.1365-313X.2007.03306.x

Kumfer, K. T., Cook, S. J., Squirrell, J. M., Eliceiri, K. W., Peel, N., O'Connell, K. F. and White, J. G. (2010). CGEF-1 and CHIN-1 regulate CDC-42 activity during asymmetric division in the *Caenorhabditis elegans* embryo. *Mol. Biol. Cell* **21**, 266-277. doi:10.1091/mbc.e09-01-0060

Maiuri, P., Rupprecht, J.-F., Wieser, S., Ruprecht, V., Bénichou, O., Carpi, N., Coppey, M., De Beco, S., Gov, N., Heisenberg, C.-P. et al. (2015). Actin flows mediate a universal coupling between cell speed and cell persistence. *Cell* **161**, 374-386. doi:10.1016/j.cell.2015.01.056

Mattila, P. K. and Lappalainen, P. (2008). Filopodia: molecular architecture and cellular functions. *Nat. Rev. Mol. Cell Biol.* **9**, 446-454. doi:10.1038/nrm2406

Michaux, J. B., Robin, F. B., McFadden, W. M. and Munro, E. M. (2018). Excitable RhoA dynamics drive pulsed contractions in the early *C. elegans* embryo. *J. Cell Biol.* **217**, 4230-4252. doi:10.1083/jcb.201806161

Motegi, F. and Sugimoto, A. (2006). Sequential functioning of the ECT-2 RhoGEF, RHO-1 and CDC-42 establishes cell polarity in *Caenorhabditis elegans* embryos. *Nat. Cell Biol.* **8**, 978-985. doi:10.1038/ncb1459

Motegi, F., Zonies, S., Hao, Y., Cuenca, A. A., Griffin, E. E. and Seydoux, G. (2011). Microtubules induce self-organization of polarized PAR domains in *Caenorhabditis elegans* zygotes. *Nat. Cell Biol.* **13**, 1361-1367. doi:10.1038/ncb2354

Munro, E., Nance, J. and Priess, J. R. (2004). Cortical flows powered by asymmetrical contraction transport PAR proteins to establish and maintain anterior-posterior polarity in the early *C. elegans* embryo. *Dev. Cell* **7**, 413-424. doi:10.1016/j.devcel.2004.08.001

Nakayama, Y., Shivas, J. M., Poole, D. S., Squirrell, J. M., Kulkoski, J. M., Schleede, J. B. and Skop, A. R. (2009). Dynamin participates in the maintenance of anterior polarity in the *Caenorhabditis elegans* embryo. *Dev. Cell* **16**, 889-900. doi:10.1016/j.devcel.2009.04.009

Nishikawa, M., Naganathan, S. R., Jülicher, F. and Grill, S. W. (2017). Controlling contractile instabilities in the actomyosin cortex. *eLife* **6**, e19595. doi:10.7554/eLife.19595

Panbianco, C., Weinkove, D., Zanin, E., Jones, D., Divecha, N., Gotta, M. and Ahringer, J. (2008). A casein kinase 1 and PAR proteins regulate asymmetry of a PIP2 synthesis enzyme for asymmetric spindle positioning. *Dev. Cell* **15**, 198-208. doi:10.1016/j.devcel.2008.06.002

Praitis, V., Casey, E., Collar, D. and Austin, J. (2001). Creation of low-copy integrated transgenic lines in *Caenorhabditis elegans*. *Genetics* **157**, 1217-1226.

Reich, J. D., Hubatsch, L., Illukkumbura, R., Peglion, F., Bland, T., Hirani, N. and Goehring, N. W. (2019). Regulated activation of the PAR polarity network ensures a timely and specific response to spatial cues. *Curr. Biol.* **29**, 1911-1923.e5. doi:10.1016/j.cub.2019.04.058

Reymann, A.-C., Staniscia, F., Erzberger, A., Salbreux, G. and Grill, S. W. (2016). Cortical flow aligns actin filaments to form a furrow. *eLife* **5**, e17807. doi:10.7554/eLife.17807

Riedl, J., Crevenna, A. H., Kessenbrock, K., Yu, J. H., Neukirchen, D., Bista, M., Bradke, F., Jenne, D., Holak, T. A., Werb, Z. et al. (2008). Lifeact: a versatile marker to visualize F-actin. *Nat. Methods* **5**, 605-607. doi:10.1038/nmeth.1220

Robin, F. B., McFadden, W. M., Yao, B. and Munro, E. M. (2014). Single-molecule analysis of cell surface dynamics in *Caenorhabditis elegans* embryos. *Nat. Methods* **11**, 677-682. doi:10.1038/nmeth.2928

Rodriguez, J., Peglion, F., Martin, J., Hubatsch, L., Reich, J., Hirani, N., Gubieda, A. G., Roffey, J., Fernandes, A. R., St Johnston, D. et al. (2017). aPKC cycles between functionally distinct PAR protein assemblies to drive cell polarity. *Dev. Cell* **42**, 400-415.e9. doi:10.1016/j.devcel.2017.07.007

Rose, L. and Gonczy, P. (2014). Polarity establishment, asymmetric division and segregation of fate determinants in early *C. elegans* embryos. In *WormBook*, ed. The *C. elegans* Research Community, WormBook, http://www.wormbook.org. doi:10.1895/wormbook.1.7.1

Schindelin, J., Arganda-Carreras, I., Frise, E., Kaynig, V., Longair, M., Pietzsch, T., Preibisch, S., Rueden, C., Saalfeld, S., Schmid, B. et al. (2012). Fiji: an open-source platform for biological-image analysis. *Nat. Methods* **9**, 676-682. doi:10.1038/nmeth.2019

Schink, K. O., Tan, K.-W. and Stenmark, H. (2016). Phosphoinositides in Control of Membrane Dynamics. *Annu. Rev. Cell Dev. Biol.* **32**, 143-171. doi:10.1146/annurev-cellbio-111315-125349

Scholze, M. J., Barbieux, K. S., De Simone, A., Boumasmoud, M., Süess, C. C. N., Wang, R. and Gönczy, P. (2018). PI(4,5)P2 forms dynamic cortical structures and directs actin distribution as well as polarity in *Caenorhabditis elegans* embryos. *Development* **145**, dev164988. doi:10.1242/dev.164988

Schonegg, S., Constantinescu, A. T., Hoege, C. and Hyman, A. A. (2007). The Rho GTPase-activating proteins RGA-3 and RGA-4 are required to set the initial size of PAR domains in *Caenorhabditis elegans* one-cell embryos. *Proc. Natl. Acad. Sci. USA* **104**, 14976-14981. doi:10.1073/pnas.0706941104

Simons, K. and Ikonen, E. (1997). Functional rafts in cell membranes. *Nature* **387**, 569-572. doi:10.1038/42408

Spracklen, A. J., Fagan, T. N., Lovander, K. E. and Tootle, T. L. (2014). The pros and cons of common actin labeling tools for visualizing actin dynamics during *Drosophila* oogenesis. *Dev. Biol.* **393**, 209-226. doi:10.1016/j.ydbio.2014.06.022

Stone, M. B., Shelby, S. A. and Veatch, S. L. (2017). Super-resolution microscopy: shedding light on the cellular plasma membrane. *Chem. Rev.* **117**, 7457-7477. doi:10.1021/acs.chemrev.6b00716

Swan, K. A., Severson, A. F., Carter, J. C., Martin, P. R., Schnabel, H., Schnabel, R. and Bowerman, B. (1998). *cyk*-1: a *C. elegans* FH gene required for a late step in embryonic cytokinesis. *J. Cell Sci.* **11**, 2017-2027.

Tokunaga, M., Imamoto, N. and Sakata-Sogawa, K. (2008). Highly inclined thin illumination enables clear single-molecule imaging in cells. *Nat. Methods* **5**, 159-161. doi:10.1038/nmeth1171

van den Bogaart, G., Meyenberg, K., Risselada, H. J., Amin, H., Willig, K. I., Hubrich, B. E., Dier, M., Hell, S. W., Grubmüller, H., Diederichsen, U. et al. (2011). Membrane protein sequestering by ionic protein–lipid interactions. *Nature* **479**, 552. doi:10.1038/nature10545

van der Honing, H. S., van Bezouwen, L. S., Emons, A. M. C. and Ketelaar, T. (2011). High expression of Lifeact in *Arabidopsis thaliana* reduces dynamic reorganization of actin filaments but does not affect plant development. *Cytoskeleton* **68**, 578-587. doi:10.1002/cm.20534

van Rheenen, J. and Jalink, K. (2002). Agonist-induced PIP(2) hydrolysis inhibits cortical actin dynamics: regulation at a global but not at a micrometer scale. *Mol. Biol. Cell* **13**, 3257-3267. doi:10.1091/mbc.e02-04-0231

Velarde, N., Gunsalus, K. C. and Piano, F. (2007). Diverse roles of actin in *C. elegans* early embryogenesis. *BMC Dev. Biol.* **7**, 142. doi:10.1186/1471-213X-7-142

Wang, J. and Richards, D. A. (2012). Segregation of PIP2 and PIP3 into distinct nanoscale regions within the plasma membrane. *Biol. Open* **1**, 857-862. doi:10.1242/bio.20122071

Wang, S.-C., Low, T. Y. F., Nishimura, Y., Gole, L., Yu, W. and Motegi, F. (2017). Cortical forces and CDC-42 control clustering of PAR proteins for *Caenorhabditis elegans* embryonic polarization. *Nat. Cell Biol.* **19**, 988-995. doi:10.1038/ncb3577

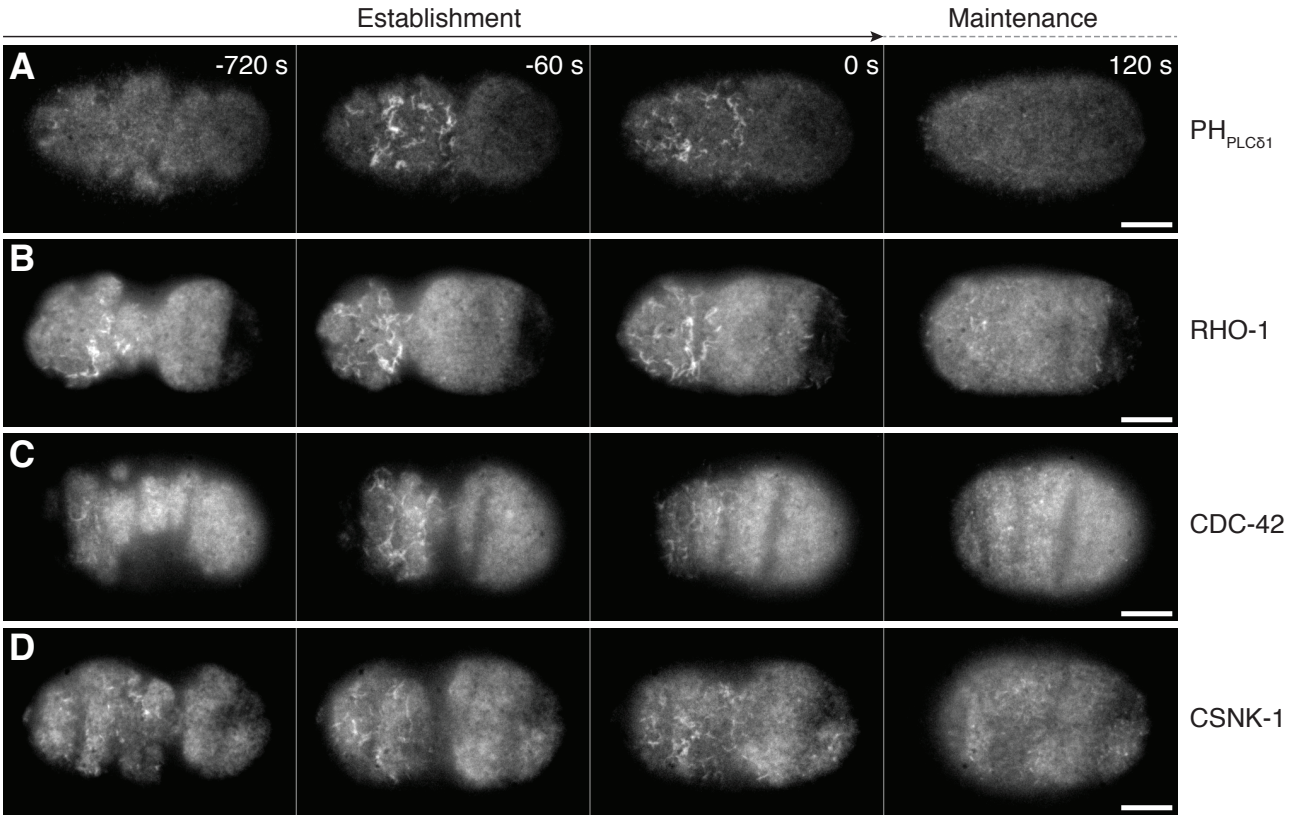

Figure S1. Diverse signaling molecules appear enriched in cortical structures. (A-D) HiLo microscopy images of mCherry::$PH_{PLC\delta1}$ (n>5) (A), GFP::RHO-1 (n = 2) (B), CDC-42::mCherry (n = 3) (C), and GFP::CSNK-1 (n = 2) (D) at the cell cortex are shown from early symmetry-breaking to maintenance phase. All show cortical structures with a distinct pattern of appearance, subsequent enrichment in the anterior and dissipation upon entry to maintenance phase. Time (s) relative to the end of establishment phase. Scale bar = 10 um.

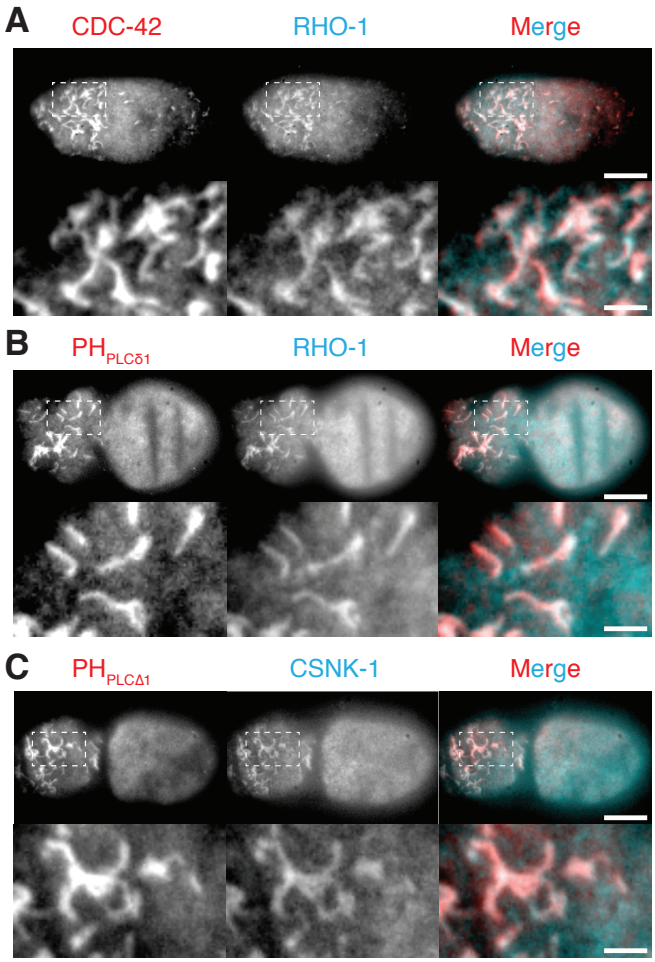

Figure S2. Colocalization of signaling molecules with the PIP_2 probe $PH_{PLC\delta1}$. (A) Sample image of surface of embryo co-expressing GFP::RHO-1 and mCherry CDC-42. Individual channels and merge shown with zoom of inset region to highlight structures. **(B)** As in (A), but GFP::RHO-1 with mCherry::$PH_{PLC\delta1}$. **(C)** As in (A), but GFP::CSNK-1 with mCherry::$PH_{PLC\delta1}$. Co-enrichment quantified in Figure 1B. Scale bars = 10 um.

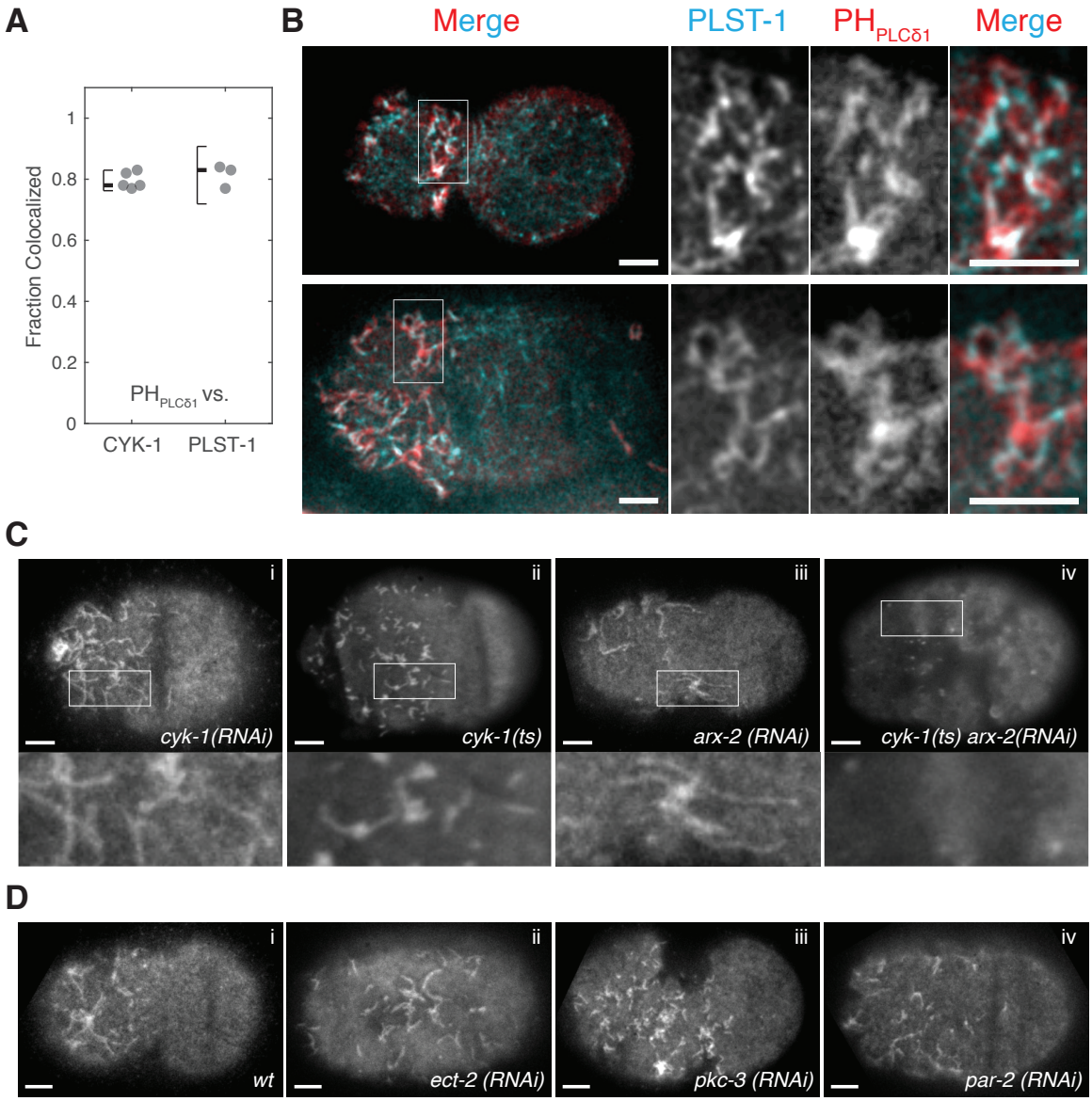

Figure S3. Filopodia are enriched in actin bundling proteins, require actin polymerization, and respond to polarity cues. **(A)** Fraction of selected $PH_{PLC\delta1}$-labeled structures that exhibit colocalized CYK-1 puncta at tips or enrichment in PLST-1. Datapoints from individual embryos shown. Median ± 95%CI indicated. **(B)** Cortical images of two embryos expressing PLST-1::GFP and mCherry::$PH_{PLC\delta1}$. Inset is marked and magnified on right showing merged and single channel images. **(C)** Disruption of both CYK-1 and ARX-2 lead to loss of filopodia like structures. mCherry (i,iii) or GFP (ii,iv) fusions to $PH_{PLC\delta1}$ persist when either ARX-2 or CYK-1 are disrupted on their own, but not when both are compromised. Insets magnified below to highlight filopodia structure. **(D)** Formation of filopodia is not affected when contractility is compromised by depletion of the RhoGEF, ECT-2, or when polarity is disrupted by depletion of PKC-3 or PAR-2 by RNAi. However, asymmetry of filopodia is reduced in all three cases consistent with their asymmetry requiring polarity. ECT-2 depletion compromises symmetry-breaking during the establishment phase (***Zonies et al., 2010***). Images shown reflect a timepoint of peak filopodial density just before relaxation of the cortex and filopodial disassembly. Scale bars = 5 μm.

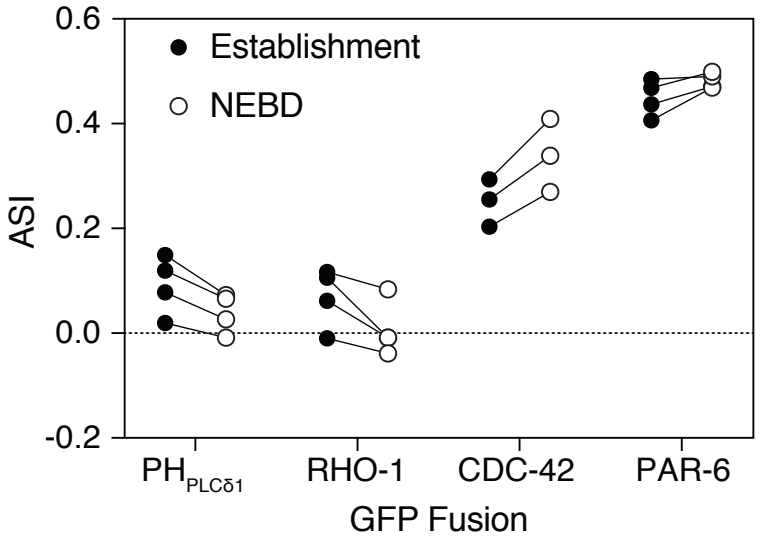

Figure S4. Asymmetry in membrane concentration from midplane images. Membrane fluorescence profiles were traced from midplane images of embryos expressing the indicated GFP fusions at mid-establishment (5 min pre-NEBD) or mid-maintenance phase (NEBD). For each embryo the asymmetry index (ASI) was calculated at each timepoint from the extracted profiles. Note asymmetry of both $PH_{PLC\delta1}$ and RHO-1 is low at establishment phase and is reduced further at maintenance phase when filopodia dissipate, consistent with filopodia contributing to weak apparent asymmetry during the establishment phase. By contrast, CDC-42 exhibits moderate asymmetry during establishment when anterior filopodia are high, but its asymmetry increases further by NEBD, when filopodia dissipate. For reference, the polarity protein PAR-6, which is not prominently enriched in these structures due to association with PAR-3 clusters, is highly polarized at both time points. Together these data suggest that filopodia-like structures, despite being highly asymmetric, do not contribute significantly to overall polarity in membrane concentrations.

Table S1. *C. elegans* strains used in this work.

Strain	Genotype	Source
ACR004	*cyk-1(ges1[cyk-1::eGFP + LoxP unc-119(+) LoxP] III; unc-119 (ed3) III; ltIs44pAA173; [pie-1p::mCherry::PH(PLC1delta1) + unc-119(+)] V*	This work
ACR010	*plst-1(ges2[plst-1::eGFP + LoxP unc-119(+) LoxP] IV; unc-119 (ed3) III; ltIs44pAA173; [pie-1p::mCherry::PH(PLCδ1) + unc-119(+)] V*	This work
AD189	*unc-119(ed3) III; asIs2[unc-119(+) + pie-1p::GFP::egg-1]*	CGC, ***Kadandale et al.*** (***2005***)
FT204	*unc-119(ed3) III; xnIs87[syn-4p::GFP::syn-4::syn-4 3'UTR + unc-119(+)]*	CGC
JA1354	*unc-119(e2498) III; weIs12[unc-119(+) + pie-1p::GFP::csnk-1]*	CGC, ***Panbianco et al.*** (***2008***)
JCC146	*cyk-1(or596ts); unc-119(ed3); ltIs38 [pAA1; pie-1p::GFP::PH(PLCδ1) + unc-119 (+)]; ltIs37 [pAA64; pie-1p::mCherry::his-58; unc-119 (+)]IV*	***Jordan et al.*** (***2016***)
KK1248	*par-6(it310[par-6::gfp]) I*	CGC, Ken Kemphues
NWG0045	*unc-119(ed3) III; crkIs16[mex-5p::mKate::iLiD::nmy-2 3'UTR + unc-119(+)]*	This work
NWG0047	*unc-119(ed3)III; crkEx1[pNG19: mex-5p::PH(PLCδ1)::GBP::mKate::nmy- 2 3'UTR + unc-119(+)]; him-5 (e1490) V*	***Rodriguez et al.*** (***2017***)
OD58	*unc-119(ed3) III; ltIs38[pAA1; pie-1p::GFP::PH(PLCδ1) + unc-119(+)]*	CGC, ***Audhya et al.*** (***2005***)
OD70	*unc-119(ed3) III; ltIs44pAA173; [pie-1p-mCherry::PH(PLCδ1) + unc-119(+)] V*	CGC, ***Kachur et al.*** (***2008***)
SA115	*tjIs1[pie-1::GFP::rho-1 + unc-119(+)]*	CGC, ***Motegi and Sugimoto*** (***2006***)
SWG1	*mex-5p::Lifeact::mKate2*	***Reymann et al.*** (***2016***)
SWG5	*plst-1(ges2[plst-1::eGFP + LoxP unc-119 (+) LoxP] IV; unc-119 (ed3) III)*	***Reymann et al.*** (***2016***)
SWG19	*cyk-1(ges1[cyk-1::eGFP + LoxP unc-119(+) LoxP) III; unc-119(ed3) III.*	***Reymann et al.*** (***2016***)
TH159	*ddIs46[WRM0625bA11 GLCherry::cdc-42; Cbr-unc-119(+)]*	***Rodriguez et al.*** (***2017***)
TH220	*unc-119(ed3) III; ddIs86[pie-1p::LifeAct::GFP; unc-119(+)]*	***Redemann et al.*** (***2010***)
WS5018	*cdc-42(gk388) opIs295[cdc-42p::GFP::cdc-42(genomic)::cdc-42 3'UTR + unc-119(+)] II.*	CGC, ***Neukomm et al.*** (***2014***)

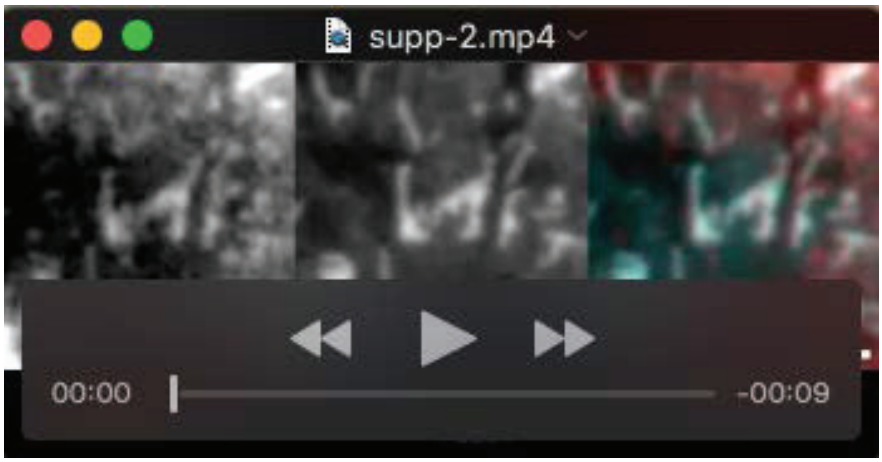

Movie 1. Timelapse video of the surface of a permeabilized embryo expressing $PH_{PLC\delta1}$::GFP (middle, cyan) and stained with FM4-64 (left, red). Scale bar, 2.5 µm. Elapsed time (sec). See related Figure 1F.

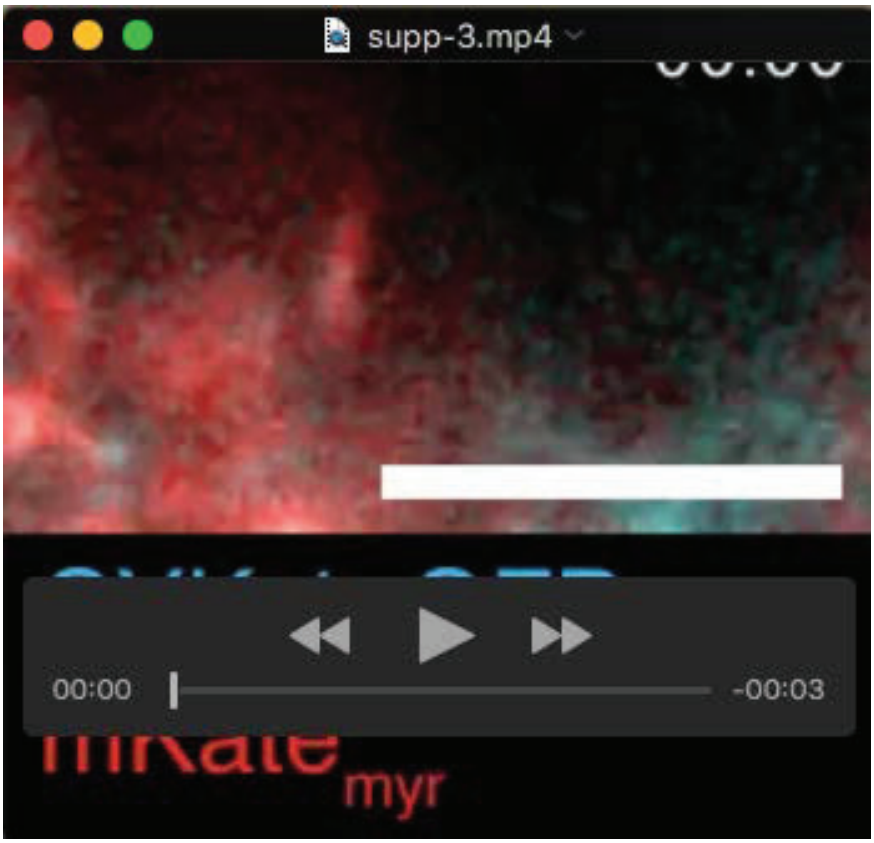

Movie 2. Timelapse video of filopodia extending into the pseudocleavage furrow in an embryo expressing CYK-1::GFP and mKate$_{myr}$. Scale bar, 5 µm. Elapsed time (mm:ss) shown. See related Figure 2A.

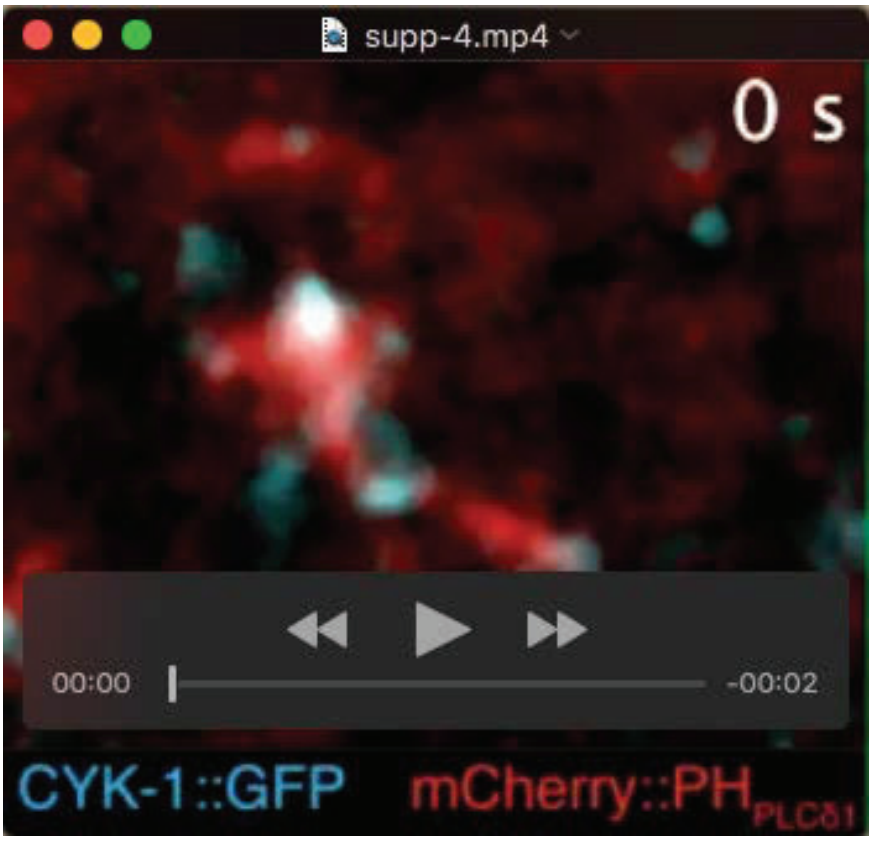

Movie 3. Timelapse video of dynamic filopodia on the surface of an embryo expressing CYK-1::GFP and $_{PLC\delta1}$::mCherry. Scale bar, 5 µm. Elapsed time (sec) shown. See related Figure 2D.

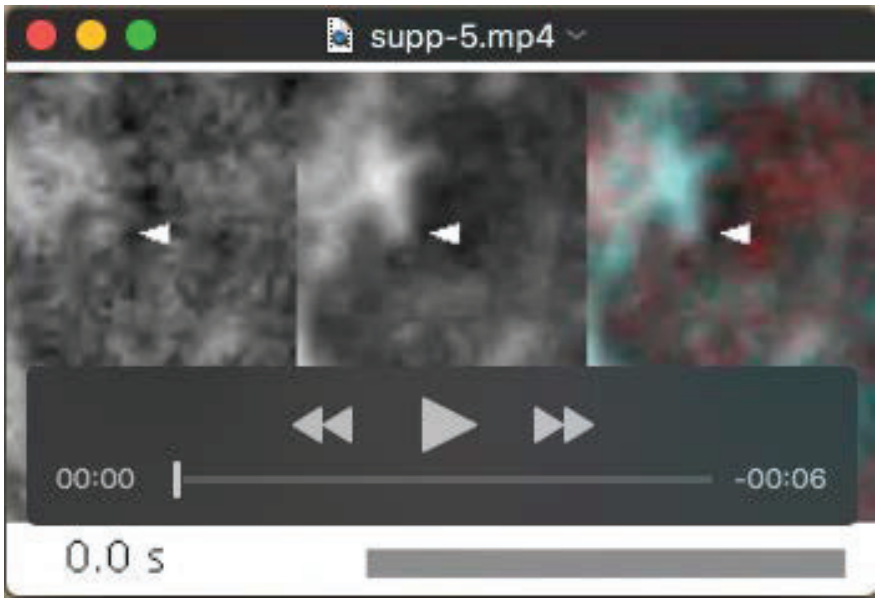

Movie 4. Timelapse video of an extending filopodium labeled with LifeAct::GFP and $_{PLC\delta1}$::mCherry on the surface of a one-cell embryo. Elapsed time (sec) shown. Scale bar, 5 µm. See related Figure 2F.

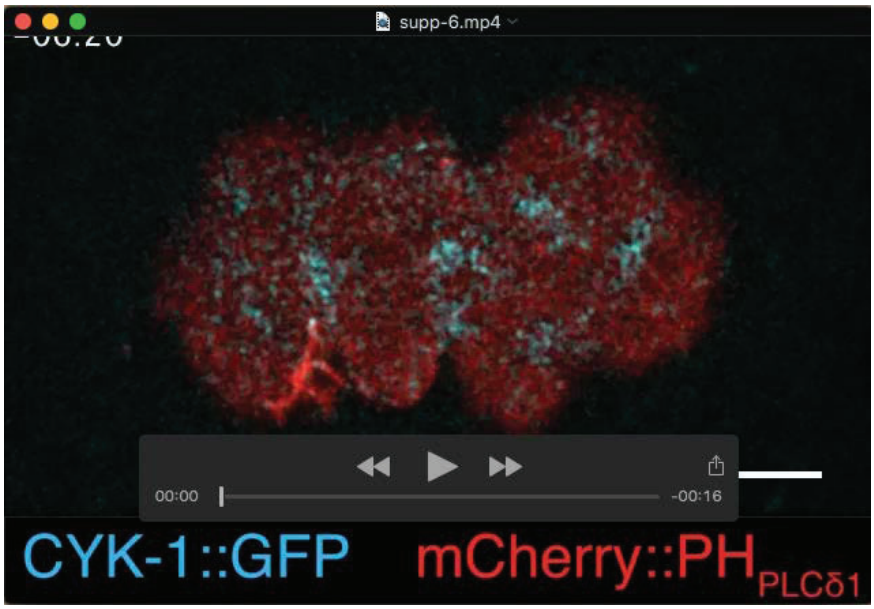

Movie 5. Timelapse video of the surface of an embryo expressing CYK-1::GFP and $PH_{PLC\delta1}$::mCherry by confocal microscopy showing the appearance, accumulation, segregation and dissipation of filopodia. Elapsed time shown (mm:ss). Scale bar, 5 µm. See related Figure 2K.

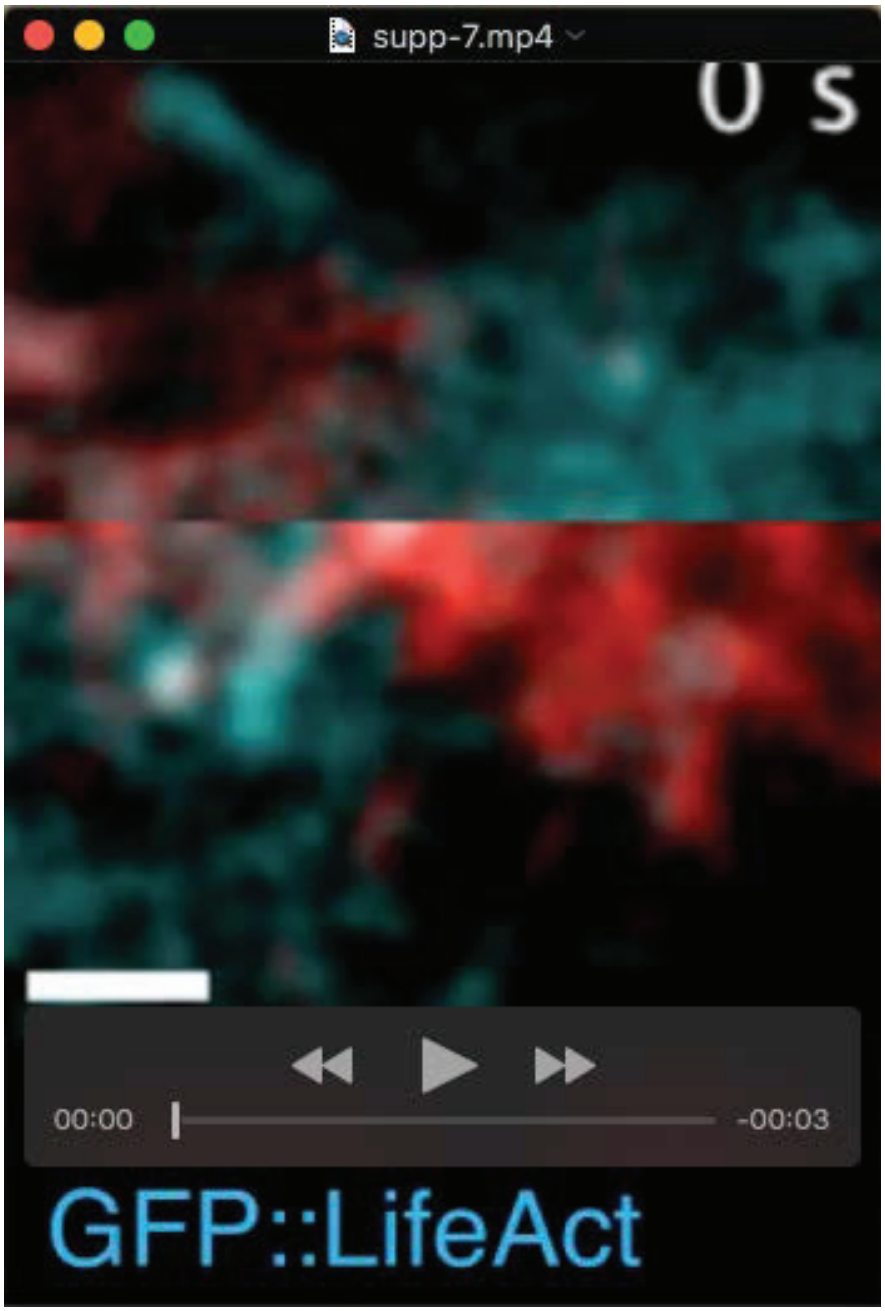

Movie 6. Timelapse video of two filopodia labeled with LifeAct::mKate (red) and LifeAct::GFP (cyan) corresponding to straightened filopodia shown in Figure 3E. Note lag of LifeAct::mKate signal relative to LifeAct::GFP yielding a cyan tip followed by a red tail. Elapsed time shown (sec). Scale bar, 2.5 µm. See related Figure 3F-G.

Movie 7. Timelapse video of cytoplasmic actin comet labeled with LifeAct::mKate (red) and LifeAct::GFP (cyan). Note lag of LifeAct::mKate signal relative to LifeAct::GFP yielding a cyan tip followed by a red tail. Elapsed time shown (sec). Scale bar, 2.5 μm. See related Figure 3G-H.

References

Audhya A., Hyndman F., McLeod I.X., Maddox A.S., Yates J.R., Desai A., Oegema K. (2005). A complex containing the Sm protein CAR-1 and the RNA helicase CGH-1 is required for embryonic cytokinesis in *Caenorhabditis elegans*. *J. Cell Biol.* 171, 267–279.

Cuenca A.A., Schetter A., Aceto D., Kemphues K., Seydoux G. (2003). Polarization of the *C. elegans* zygote proceeds via distinct establishment and maintenance phases. *Development* 130, 1255–1265.

Jordan S.N., Davies T., Zhuravlev Y., Dumont J., Shirasu-Hiza M., Canman J.C. (2016). Cortical PAR polarity proteins promote robust cytokinesis during asymmetric cell division. *J. Cell Biol.* 212, 39–49.

Kachur T.M., Audhya A., Pilgrim D.B. (2008). UNC-45 is required for NMY-2 contractile function in early embryonic polarity establishment and germline cellularization in *C. elegans*. *Dev. Biol.* 314, 287–299.

Neukomm L.J., Zeng S., Frei A.P., Huegli P.A., Hengartner M.O. (2014). Small GTPase CDC-42 promotes apoptotic cell corpse clearance in response to PAT-2 and CED-1 in *C. elegans*. *Cell Death Differ.* 21, 845–853.

Redemann S., Pecreaux J., Goehring N.W., Khairy K., Stelzer E.H.K., Hyman A.A., Howard J. (2010). Membrane Invaginations Reveal Cortical Sites that Pull on Mitotic Spindles in One-Cell *C. elegans* Embryos. *PLoS ONE.* 5, e12301.

Zonies S., Motegi F., Hao Y., Seydoux G. (2010). Symmetry breaking and polarization of the *C. elegans* zygote by the polarity protein PAR-2. *Development* 137, 1669–1677.

AIM 3: Temporal characterisation of filopodia during the 2 and 4-cell stages.

Careful observation of my data, in association with the findings in Aim 2, made me feel that filopodia have a proper time window for their appearance. The third aim of my PhD project was to answer the following question: do filopodia have a specific dynamic of appearance regarding the cell cycle? The conduction of preliminary data showed that they appear in a transient and regulated-temporal pattern during the early embryogenesis of *C. elegans,* and I decided to extend these investigations. This work was conducted by myself and a student name Rita Harik that joined the lab for a master 1 internship. To correlate filopodia appearance and cell cycle timing, we used a strain with histone fluorescently labelled to be informed about the condensation state of histones and their global organisation that correlates with the cell cycle, this strain is endogenously expressing CYK-1::GFP. We observe 2-cell and 4-cell stages embryos with 4D spinning disk microscopy at two focal planes: the cortical plane to observe filopodia appearance and the equatorial plane to observe the histone states. These preliminary data showed a temporal link between the histone state and the number of filopodia at the interface (Figure 26. A). Rita and I manually quantified the number of bright spot in the GFP channel, that correspond to CYK-1::GFP particles, in a Region Of Interest (ROI) corresponding to the cortical cellular interface (Figure 26. B) and correlated it with the histone state in a double-blind approach. Despite the guilty pleasure we had to look carefully and count manually, we wanted to confirm our quantification by an automated counting method. We used two different bioinformatical counting methods. The first one is a homemade Fiji macro using a threshold base approach for automatically counting maximum intensities particles. The second one used the automatic segmentation Fiji plugin named MOSAIC (Shivanandan et al., 2013) . Despite slight variations due to human eye detection or bioinformatic parameters, all these three counting methods revealed the same result, the maximum number of particles of CYK-1::GFP at the cellular interface was suddenly increasing between the asynchronous Nuclear Envelop Break Down (NEBD) events of the AB cell and the P1 cell (Figure 26. C). Nevertheless, questions remain about the cellular origin of these filopodia and their temporal link with the cell cycle. In addition, other preliminary results recorded during the 4-cell stage converge with the same conclusion (Figure 27). We are considering presenting these data in a short article such as micropublication (to be written).

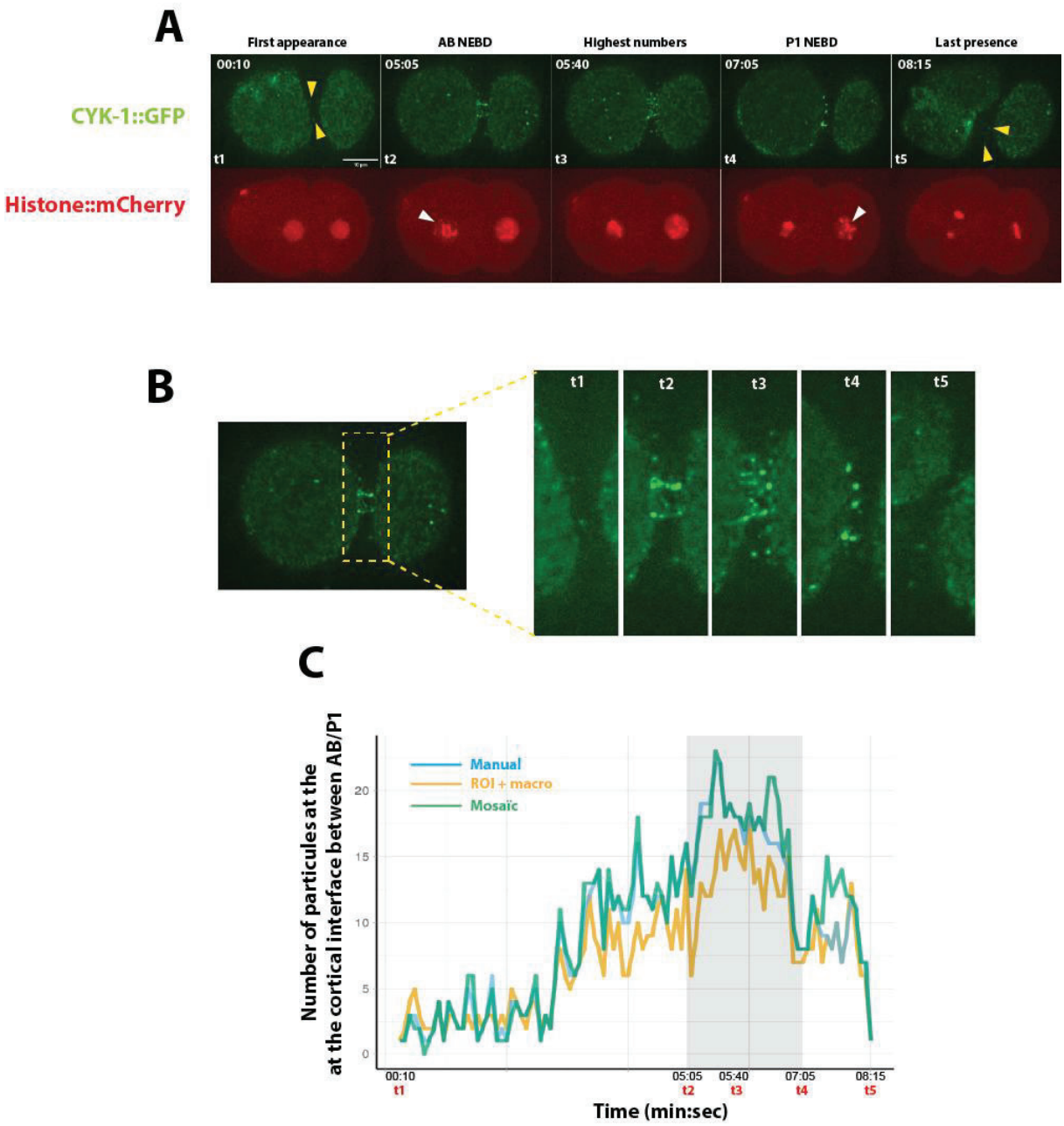

Figure 26: Temporal dynamics of CYK-1::GFP at the cell-cell cortical interface at the 2-cell stage embryo

Timeline of CYK-1::GFP enrichment at the cortical interface between AB-P1.(**A**) Double timeline of CYK-1::GFP (top panel) and Histone::mCherry (bottom panel). Yellow arrow target the first and the last appearance of a CYK-1::GFP particles at the cortical interface between AB-P1. White arrowheads indicate the first (AB) and the second (P1) NEBD event. Scale bar 10µm. (**B**) Zoomed timeline on the ROI corresponding only to the cellular interface (Yellow, dashed lines) for the fives timepoint used in (A). (**C**) Quantification of the number of CYK-1::GFP particles inside the ROI used in (B). 3 methods of quantification are used: Manual counting (Blue line), Thresholding and automatic counting (Yellow line), Mosaïc plugin (Green line). The time period between the two NEBD events is represented with the grey box, and the corresponding Timepoints in (A) are marked in red.

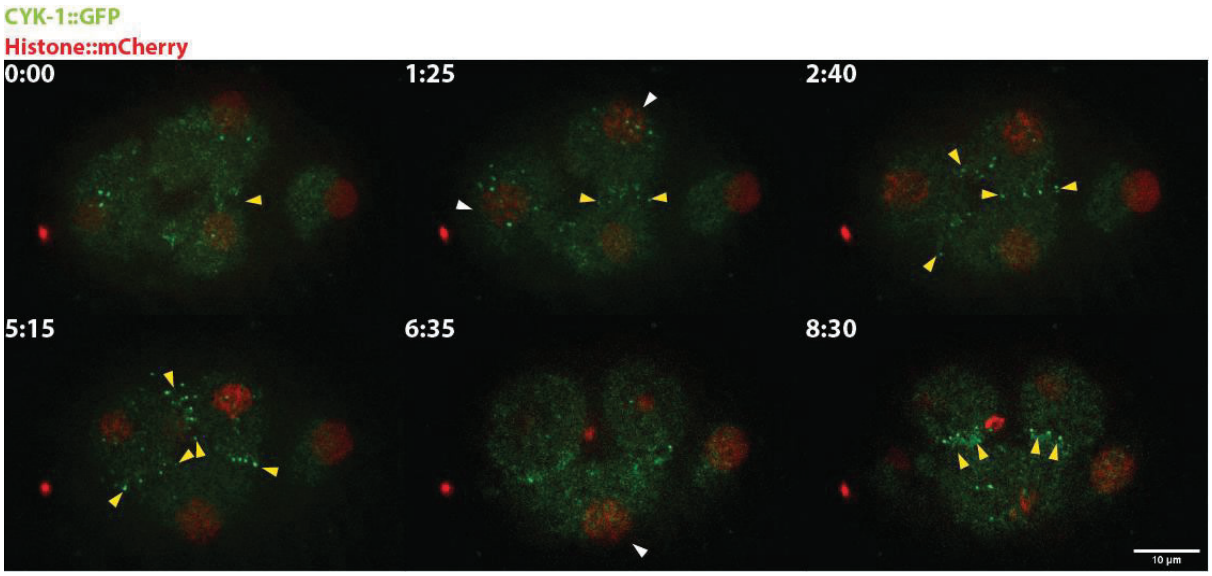

Figure 27: Temporal dynamics of CYK-1::GFP at the cell-cell cortical interface at the 4-cell stage embryo.

Preliminary data. Timelapse and Z projection of the equatorial plane with histone::mCherry onto the cortical plane with CYK-1::GFP. Yellow arrow target the filopodia's new appearance site at the cortical interface of AB daughters. Scale bar 10µm.

AIM 4: Identifying a lamellipodium-like structure during the 4 to 6-cell transition.

The 4-cell stage embryo revealed exciting actin architecture dynamics, notably due to the rich filopodia and specific sequence of actin network reorganisation at the cell-cell interfaces, especially during the transition between the 4-cell and 6-cell stages. We highlighted a particular structure at the cortical interface between the AB daughters (ABa and ABp) and EMS during the momentum of the AB daughter's division and the completion of their mitotic processes with the rise of the 6-cell stage. We used 4D imaging with a high spatial resolution to observe this cellular interface rearrangement. At the late 4-cell stage, the cellular interface between the ABa and ABp and between EMS and the AB daughters progressively enriches in interdigitated filopodia protrusions (Figure 28.A). Then filopodia between ABa and ABp are disassembled, and the EMS and the AB daughters morphologically change from filopodia into a sheet-like structure (Figure 28.B). All of these 3 ABPs are included in this flat sheet-like structure. CYK-1 is located at the tip of this membrane protrusion (Figure 28), whereas ARX-2 (Figure 29.B) and CAP-1 (Figure 29.A) are located at the front side of this structure. According to our observation of their spatial distribution and reported position in an actin sheet-like structure, we can conclude that this structure has a molecular organisation corresponding to a lamellipodium. This lamellipodia emanates from EMS and faces toward the AB daughters. Taken together and based on the morphology of this structure and her orientation, we decided to name it the EMS plate. Further investigations needed to be done to decipher the spatio-temporal characteristics of these embryonic cortical interface structures and their molecular organisation. In addition to Aim 3, we are considering starting a manuscript for this work.

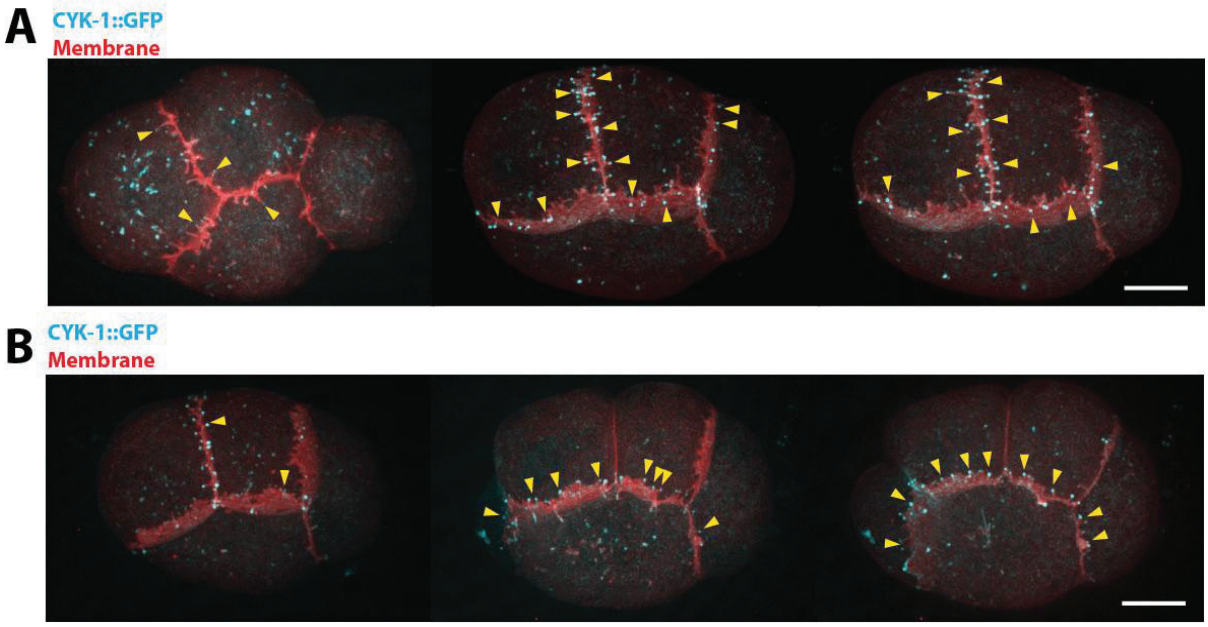

Figure 28:Lamellipodium-like structure during the 4 to 6-cell transition, decorated with CYK-1::GFP

Preliminary data. Z projection of Hight resolution timelapse on the whole embryonic volume. Embryos are expressing CYK-1::GFP (blue) and the membrane probe PLC1δ1 (red). Yellow arrowheads highlight the dynamic of CYK-1::GFP localisation. (A) Timelapse from the early 4-cell stage to the late 4-cell stage with the paroxysmal AB daughters interdigitated interactions. (B) Timelapse from the late 4-cell stage to the 4 to 6-cell transition with the establishment of the lamellipodial structure irradiating from EMS to its neighbourhood. Scale bar 10µm.

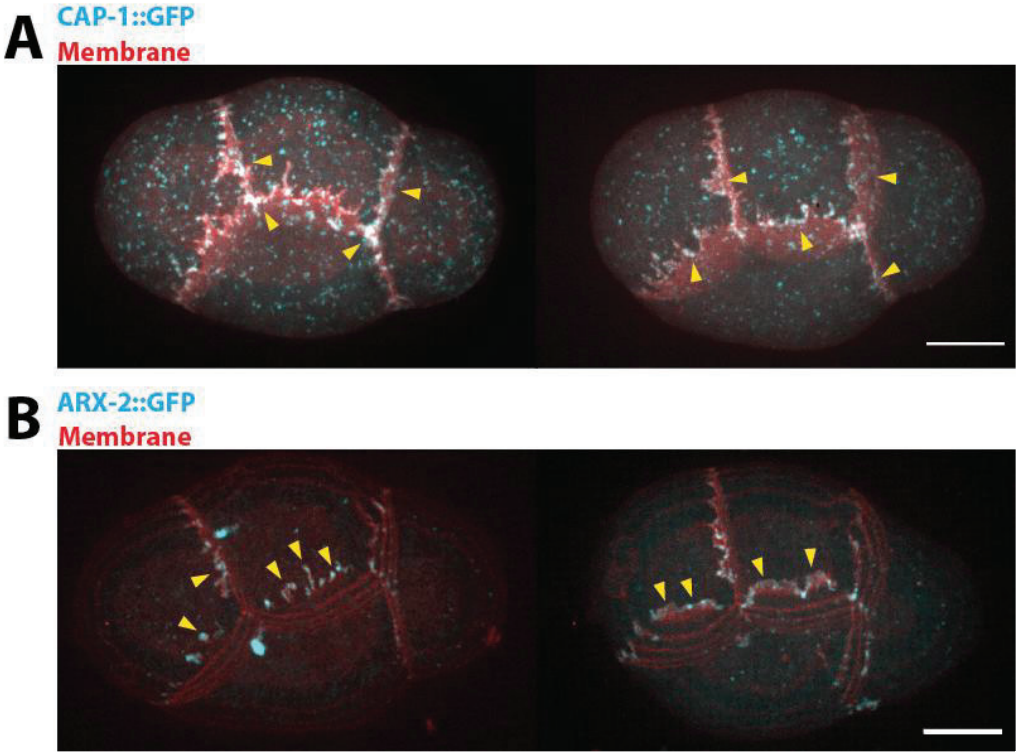

Figure 29: Localisation of ARX-2::GFP and CAP-1::GFP during the early and the late 4-cell stage.

Preliminary data. Z projection of Hight resolution timelapse on the whole embryonic volume. Embryos are expressing ABP::GFP (blue); CAP-1::GFP (**A**) or ARX-2::GFP (**B**); and the membrane probe PLC1δ1 (red). Timelapse from the early 4-cell stage to the late 4-cell, where CAP-1::GFP is located in the core of filopodia. (**B**) Timelapse from the early 4-cell stage to the late 4-cell, where ARX-2::GFP is located at the front side of these intercellular interaction sites. Yellow arrowheads point filopodia (left panel) and lamellipodia like structure (right panel). Images came from the same samples, scale bar 10µm.

Discussion

The privilege observations associated with completing these different aims create an exciting set of open questions which I will address in this section, divided into three parts. First, I will start by questioning the differences observed in terms of ABPs amount in each cell. Here, I propose hypothetical mechanism that could explain the regulation of these specific molecular segregations. Considering the different scales of regulation, either cortical actomyosin polarisation, genetic regulation and signalling pathways. Secondly, I will discuss the potential role(s) of filopodia found in early embryogenesis. With a particular focus on the difference between filopodia observed in a cell-free context during the zygotic phase and the filopodia encountered at the cellular interface regarding cell cycle progression. Last, this discussion section will also be the perfect occasion to depict the multiple perspectives that can follow my PhD work, with a plethora of questions that arise along this work and a multitude of additional experiments that can enhance my current work and also participate in deciphering the potential mechanism at work further discussed in part 1 and 2 of this section.

1- What are the mechanisms that can explain these ABPs segregation?

During the first steps of early embryogenesis, proteins rely on the segregation of a maternally loaded pool of molecular content. Our study shows that this particular segregation also applies to ABPs during all the early cell stages. This segregation leads to individual cellular ABPs differences. These differences are present since the polarisation steps up to the early 4-cell stage and, as seen in Aim1, becomes more contrasted, particularly during the second half of the 4-cell stage. These two different segregation dynamics highlight a minimum of two mechanisms for defining each ABPs enrichment in each cell, these will be detailed in the next paragraphs. First, the cortical enrichment is due to the actomyosin density. Second, the 4-cell stage begin to regulate mRNA translation and signalling pathways.These mechanisms organise the appropriate actin proteome content, leading to the acquisition of a specific cortical identity for each cell.

a. Actomyosin cortex drags their regulation partners

The first hypothetical mechanism takes place during the 1 and 2-cell stages. It is based on the mechanical segregation of ABPs that follow the needs of regulatory components of the

actomyosin cortex which is asymmetrically distributed during polarisation steps. At the 1-cell stage, these proteins, as PAR proteins, are initially homogenously distributed in the oocyte (Munro et al., 2004; Rose and Gönczy, 2014). Once fertilisation happens, it triggers the polarisation phase, reorganising the actomyosin cortex that is then preferentially enriched on the anterior side. This anteriorisation of the actomyosin cortex is associated with the anteriorisation of proteins that are directly linked to it, such as the aPAR proteins and ABPs that regulate the actomyosin cortex properties that, *in fine*, all these partners worked in a positive feedback loop mechanism that enhance their anteriorisation (Michaux et al., 2018; Munro et al., 2004; Reymann et al., 2016). After the zygotic asymmetric division, the Antero-Posterior polarity is establish, and molecular content are retained, it is also the case for cytosolic and cortical ABPs that are then asymmetrically distributed into two different lineages, the AB and P1.The AB cell derive from the previous anterior side of the zygote, its cortex is denser compare to P1 and it has, *de facto*, a higher proportion of ABPs. This mechanism is also happening at the 2-cell stage. On the posterior side of the embryo, the P1 cell will overcome a polarisation phase associated with an asymmetric division where the anterior side of P1 has its actomyosin cortex denser(Caroti et al., 2021) and will lead to the formation of the EMS cell. Following our hypothesis, the two pools of ABPs are segregated preferentially to the side where the actomyosin cortex is denser and contains more regulatory proteins, thus linked to the asymmetry of the division pattern. The work realised in Aim 1 found that ABPs are then preferential enrichment in the EMS cell, compared to the P2 cell. A good rule goes along with an exception. The surprise came from the anterior side of the embryo in the AB lineage. AB performs a symmetric division which gives birth to two supposedly twin cells: ABa and ABp (Priess and Thomson, 1987), which are, by extent, composed of two identical actomyosin cortexes and the same amount of ABPs. Following the symmetrical logic, we were expecting a straight similarity between them. Nevertheless, we observe slight but constant differences between ABa and ABp in terms of ABPs relative content in the cytosolic pool. Furthermore, we found a milder asymmetric distribution in the cortical pool. Despite the differences observed in the AB daughters, which will need further investigation, this actomyosin-based mechanism that drags ABPs that goes within it can explain the differences observed during the completion of the first steps of early embryogenesis, up to the 4-cell stage. However, the question of which components polarised first between the actomyosin cortex and the PAR proteins remains. But today, we can add

another layer of complexity: which ones are polarised first: PAR proteins, Actomyosin cortex or ABPs?

b. The awakening of the 4-cell stage

The second mechanism starts at a precise moment: as demonstrated in Aim 1, the second half of the 4-cell stage shows a sudden increase in ARX-2 and CAP-1 differences in the cytosolic and cortical fraction, specifically when comparing cells from a different lineage. Interestingly, compared to ARX-2 and CAP-1, this mechanism does not increase the differences between cells in terms of CYK-1, meaning that either CYK-1 initial content at the 4-cell stage stays relatively constant, maybe because it is not influenced by any mechanism, or it increases for the same proportion in all the cells. Furthermore, the asymmetric distribution of the cytosolic pool of ABPs in the AB daughters remains constant, indicating that the mechanism in question influences the two sister cells in an equivalent and synchronous manner. From these points, we can put forward two hypotheses to explain the appearance of these differences.

i. Zygotic Genome Activation

First, it can be the consequence of the beginning of the translation of preallocated mRNA and the transcription of new mRNA. This particular mechanism is called the Zygotic Genome Activation (ZGA), which is reported to happen at the four-cell stage in *C. elegans* (Evans and Hunter, 2005; Seydoux and Dunn, 1997; Tora and Vincent, 2021). If we assumed that the amount of newly translated proteins corresponds to the amount of available mRNA and using the data gathered in single cells transcriptomics (Osborne Nishimura et al., 2015; Tintori et al., 2016), we did not find a correlation with our protein's relative quantities in Aim 1. This can be explained by a direct degradation mechanism targeting mRNA or the proteins (DeRenzo and Seydoux, 2004) or a gene regulation induced by signalling pathways from the P2 cell (Evans et al., 1994; Rocheleau et al., 1997; Thorpe et al., 1997).

ii. Signalling pathways

Second, it is essential to note that the 4-cell stage can be separated into two different morphological shapes. The early 4-cell stage is called the diamond shape, and the late 4-cell stage is called the compacted shape. Cells during this compacted shape have a higher surface contact between them. This will favour the transmission of signalling pathways. Two major signalling pathways are implicated at the 4-cell stage: Notch signalling and Wnt signalling. Both of these pathways are triggered by the P2 cell and propagate toward the anterior cells of the embryo. P2 Notch signalling directly irradiates the ABp cell, which becomes the Dorsal cell (Crittenden et al., 1994), and P2 Wnt signalling targets the EMS cell, which becomes the Ventral cell (Rocheleau et al., 1997; Thorpe et al., 1997).

There are three potential mechanisms at work to explain these specific ABPs distributions during the early steps of embryogenesis : 1-The actomyosin density-based during each polarisation step; 2-the ZGA with and 3-Signalling pathways. These can be combined with mRNA and proteins degradation machinery. in Aim1, we observe a precise timing window where one, or some, of these mechanisms start at the 4-cell stage. Nevertheless, the questions about their relative impact remain complete.

2- What are the potential roles of Filopodia?

During Aim 2, 3, and 4, we characterised these actin structures throughout the early embryogenesis of *C. elegans*. Furthermore, filopodia are not a feature reserved for *C. elegans* embryogenesis; they are also present during the embryonic development of other model organisms. Nevertheless, for the moment, we do not find any myosin components in our filopodia, unlike in mice embryos, for instance (Fierro-González 2013). We demonstrate their different localisation in Aim 2 and Aim 4, the precise dynamical presence of this structure, and the close relation between cell cycle progression and the number of filopodia present at the cellular interface in Aim 3. We can consider that this structure is an investment of energy for this encapsulated embryo. For these reasons, this structure should have a precise purpose, and according to today's information, there is still a critical knowledge gap about their role.

Due to this lack of knowledge, I will mainly discuss my feelings about this structure, based on my expertise, which is the early *C. elegans* embryogenesis. Despite that, exciting parallels can indeed be drawn with other model organisms.

Filopodia are protrusions that face the extracellular environment, which can be Extra-Cellular Matrix (ECM) or neighbouring cells. In the case of the *C. elegans* embryo, there are two kinds of filopodia positioning. The first is where filopodia are in a cell-free context(Hirani et al., 2019). For instance, during the zygotic phase, these filopodia can only face the eggshell (Hirani et al., 2019). The second is where they are facing the neighbouring cells, for instance, between AB-P1 and the AB daughters (Hirani et al., 2019). Another important distinction between these two kinds of positioning is the stability of these structures. Indeed, their dynamics are pretty different. It appears that they are tiny and unstable structures in the case of the cell-free filopodia during the zygotic phase. In contrast, in inter-cellular contact, these filopodia come from one cell, stick to the neighbour, and are more stable. We can observe these two types easily by looking at the carrefour in a Y shape between two cellular interfaces (e.g. AB-P1 or AB daughters) (Figure 30.A.B), where we can observe filopodia with no matched neighbours that are floating towards the ECM and that are short-lived. These floating filopodia make me think about the “spinning” structures described by Andrew in Sea Urchin embryos (E.A Andrew, 1897), whereas, in the meantime, filopodia at the interface are stable and maintain coherence with their neighbour by surrounding all the intercellular (Figure 30.B). These observations give us an essential first hint about their potential roles.

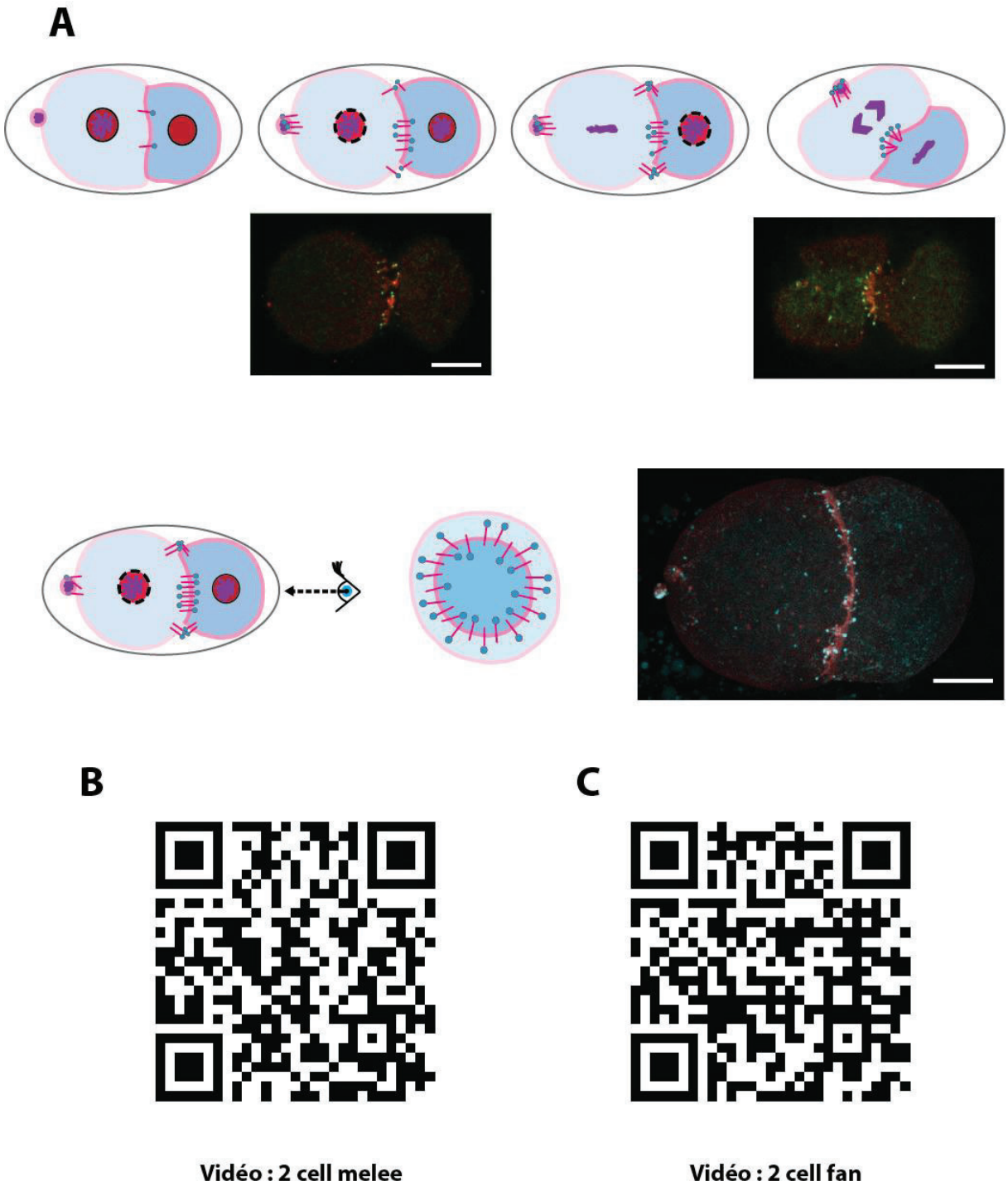

Figure 30 : 2 cell embryonic cohesion

(**A**) Hypothetic schematic representation of filopodia dynamics during the 2-cell stage. Highlights of the position at the cell interface, the polarbody and the fan shape. One image from one sample was added to the corresponding steps. 2 vidéos in high-resolution 4D were added : (**B**) Embryonic coherence of the 2 cell stage and the crown of the polarbody. (**C**) AB cytokinesis onset and the fan of filopodia. Scale bars, 10µm.

a. Actomyosin cortex anchoring to the plasma membrane

Looking at the behaviour of filopodia in a cell-free context, filopodia are a labile structure that is formed in the anterior side of the zygote during the polarisation phase. What can be the purposes of this small structure, known to be engaged in a multicellular environment or a migrating context? The anchorage of the actomyosin cortex is crucial for precisely localising the RhoA signalling and the forces distribution among the actomyosin cortex (Salbreux et al., 2012; Sens and Plastino, 2015). Proteins that compose filopodia in other model systems, such as cadherin, are involved in the cortical anchorage in *C. elegans* embryos, such as HMR-1 (Padmanabhan et al., 2017). My first hypothesis about their role is that filopodia participate in the anchorage between the actomyosin cortex and the plasma membrane. They are bringing a way to mechanically force the anchorage between these two layers to seal the link between anchoring proteins and the plasma membrane. Combining this mechanical anchor and the molecular one assures a good signal positioning and forces transmission to participate in the proper conduct of the polarisation phase of the actomyosin cortex in the zygote and the correct segregation of molecular content.

b. Embryonic cohesion and cell positioning

Interestingly, the following specific localisations still need to be studied and can be another excellent indication of another potential role. Filopodia are also nicely enriched around the polar body located at the anterior side of the zygote and the AB cell at the 2-cell stage. They decorate and surround the polar body in a crown shape (Figure 30.B). We can also note that this polar body will be further internalised during the AB division (Fazeli et al., 2018). In addition, they are organised in a particular way during the transition between the 2 and the 3-cell stages. They are arranged in a fan-like structure (Figure 30.C), originating from the P1 cell and facing the AB cell during mitosis. In more detail, they are located where the P1 anterior membrane is in contact with the posterior side of the AB cytokinesis ring and both the membrane of the future AB daughters. These specific positions during the 2 to 3-cell stages transition can be related to the chirality and the midbody position involved in this particular cell stage transition (Singh and Pohl, 2014). To illustrate this filopodia dynamics in a sporting register, we can compare this type of structure with the organisation and the behaviour during

a rugby melee where the filopodia are the players; they expand and pressure the other team, they torque to gather the balloon, which is the midbody.

After observing the differences between subgroups of filopodia and their different dynamics in ovo, as well as the specific positioning during cell stage transition, I hypothesise that filopodia are responsible for the general embryonic cohesion between cells as well as cell positioning by participating in the proper intercellular organisation during each cellular stage. For instance, between AB-P1 or AB daughters (Figure 30.A) and also during cell stages transition. The case of the 4-cell stage particularly supports this idea about their implication in embryonic cohesion. This stage is the momentum of the proper transduction of the different signalling pathways, Wnt and NOTCH (Crittenden et al., 1994; Rocheleau et al., 1997; Thorpe et al., 1997), which are crucial for cell differentiation and body axis formation. This phenomenon needs a strong embryonic cohesion to transmit the signal with less loss as possible. At the 4-cell stage, filopodia are here to increase the membrane contact area between cells and maintain this interaction during the propagation of this signal until it is no longer needed. To confirm this ON and OFF mechanism of embryonic cohesion, I want you to focus on the precise dynamics of the cellular interface between the transition of the 4 to the 6-cell stage (Figure 31.A). At the beginning of the 4-cell stage, few filopodia were present; when the embryo arrived at the late 4-cell stage, filopodia were strongly enriched all around the AB daughters interface; after the Wnt and NOTCH pathways occurred, the AB daughters entered into mitosis, and suddenly the strong cluster of filopodia between ABa and ABp completely disappears (Figure 31.B). In addition, during this event, another structure occurs between the EMS cell's cortex and the cortex of the two future AB daughters, ABar and ABpr (Figure 31.C), called the EMS plate in Aim 4. Indeed, as shown in Aim 4, the EMS cortical interface changed to a completely different shape. Starting with filopodia originating from EMS and irradiating its neighbourhood, the EMS interface totally changes its shape to a lamellipodium-like structure during the momentum of the AB daughters start their division. This EMS plate has a large surface of interaction with neighbouring cells, and I hypothesise that it also participates in embryonic cohesion during the transition 4 to 6 cell stages.

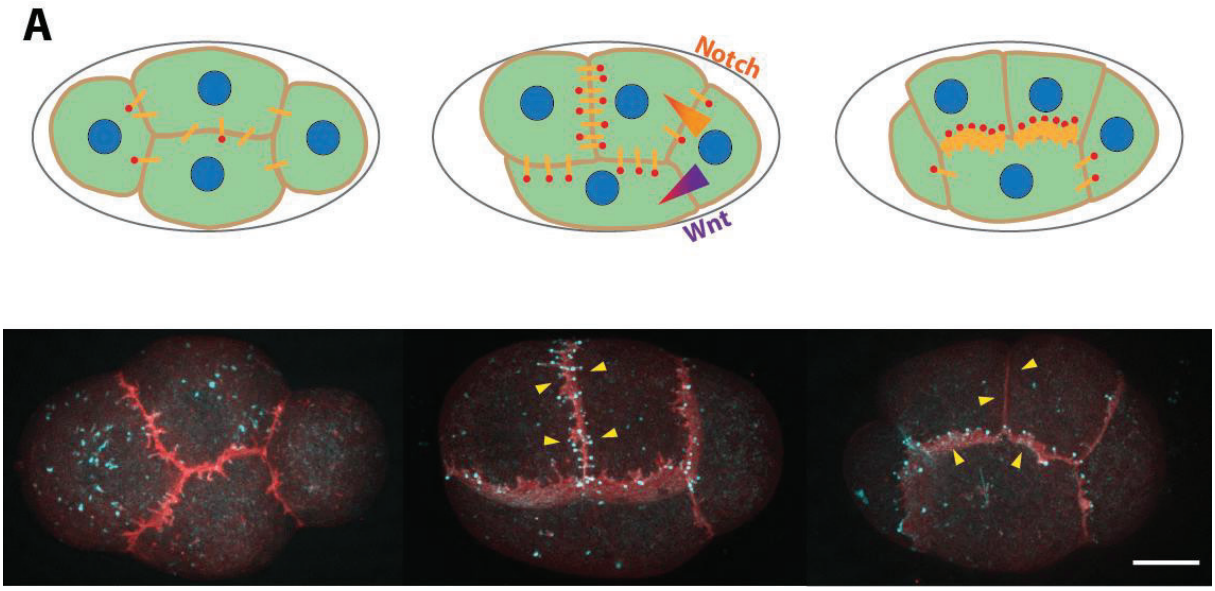

B

Vidéo : Late 4 cell

C

Vidéo : EMS plate

Figure 31 Embryonic coherence at the 4-cell stage.

(**A**) Hypothetic schematic representation of filopodia dynamics during the 4-cell stage. I am highlighting the position at the cell interface between the AD daughters and their sudden disappearance. One image from one sample was added to the corresponding steps and the structure are pointed with orange arrowheads. 2 vidéos in high-resolution 4D were added: (**B**) Embryonic coherence of the 4 cell stage and the brutal removed of AB daughters filopodia. (**C**) Dynamical locsalition of CYK-1::GFP at the EMS interface and the formation of the EMS plate. Scale bars, 10µm.

c. Tuning the cortical tension regarding cell cycle progression

Inter-cellular contact and embryonic coherence need to be directly linked to the individual cell cortex characteristic as well as the progression of the cell cycle to ensure the perfect synchronisation between cell division and cell differentiation. When the zygote divide, the actomyosin cortex is set and anchored. In addition, due to spatial reduction after the division and space limitation because of the eggshell, cells maintain the conformation between the cortex and the membrane. Nevertheless, cells still need to tune their cortical tension to prepare for the subsequent mitotic phases in a process called roundification, where cortical rigidity increases and cells get rounder upon a maximum reached during metaphasis (Kunda et al., 2008; Stewart et al., 2011). We demonstrated in Aim 3 that the maximum filopodia number appears at a precise timing window, between NEBD and before anaphase. During this particular period, cells get rounder and enter mitosis. I hypothesise that each filopodium protrudes and locally tenses the cortex and sticks it to the neighbouring cells. To illustrate, it is the same mechanical effect when we use the plastic barrier food wrap on our plates. We pull it and stick it to the plate's other side to locally tense the plastic barrier, and we repeat this step all around the container, which will result in a global increase in the plastic barrier tension. Interestingly, a study in drosophila embryos shows apical actin protrusion remodelling during cell cycle progression. These apical actin protrusions were long during interphase and shorter during metaphase (Sherlekar et al., 2020). This gives a hint about the relationship between filopodia extension and the progression of the cell cycle. Taken together, it leads to my third hypothesis about filopodia's role. Filopodia are involved in locally regulating cortical tension, or vice versa, and helping the roundification process just before cells enter mitosis. Importantly this third hypothesis can work in cooperation with the supposition about embryonic cohesion.

From my biased point of view, these embryonic filopodia could have multiple functions. At the 1-cell stage, they may anchor the actomyosin cortex to the plasma membrane. At the 2, 4 and 6 cell stages, they could be implicated in tuning the cortical tension during the roundification process regarding cell cycle progression. They could manage embryonic cohesion and cellular positioning during crucial differentiation steps. All these hypotheses will need further investigation to reveal if they are right or wrong. In anyways, it

will bring additional and exceptional output to understand more the complexity of their roles in this fascinating context, the early embryogenesis.

3- Remaining questions, future questions and perspectives

In this section, I will discuss the future experiments that can be realised to first directly continue my actual work and second to confirm or infirm my hypothesis; I also want to point out some semantic evolution needed to properly characterise the filopodia encountered during embryogenesis which are different from their fellow member in other experimental systems.

a. Improvement of the ABPs quantification

To follow directly the work done during my PhD, especially concerning Aim 1, it can be interesting to improve the quantification methods used to quantify ABPs variation during early embryogenesis. We compared the mean intensity between cells at each time point. The problem with this approach is that we are virtually diluting some crucial information about the number of proteins, especially when quantifying the endogenous expression of lowly expressed proteins such as CYK-1. In addition, due to a problem of cellular assignment, we voluntarily eroded the quantification surface by removing the area corresponding to the cell interface, which contains the brightest particles, reducing by extent the total mean intensities. In parallel, a recent paper developed an interesting approach using particle counting (Najafabadi 2022). Suppose we managed to implement a particle counting method with the addition of the interface area. In that case, we could improve our quantification and estimate the different ABPs segregations even more precisely. We also need to estimate the total concentration of our proteins. Before that, we need to evaluate the cell volume over time precisely. In the *C. elegans* community, interesting studies are already made on cell volume (Cao et al., 2019). I was particularly interested in the work realised by Rob Jellier's lab and, specifically, the work realised by Wim Thiels (Thiels et al., 2021). His image analysis and segmentation tool where he can track in 4D the volume, the shape and the contact area. He used the same in vivo data acquisition methods and membrane labelling. These additions to our approach can allow us to precisely and automatically map and calculate the quantity and

the concentration of any ABPs endogenous expression during the early *C. elegans* embryogenesis.

b. How do these asymmetries in the AB daughters arise?

In Aim 1, we observed an asymmetric distribution of ABPs between the AB daughters, especially in the cytosolic pool of proteins. These differences are slight but constant all along the cell stage. Roxane Benoit and I are trying to decipher the momentum and the mechanism that can explain the establishment of this asymmetric distribution. We are performing laser ablation of the membrane that separates the two daughters. We want to see if the sum of ABPs quantities in the daughter cells matches the ABPs amount in the mother cell. Inspired by the remarkable job of Carvalho et al (Carvalho et al., 2016) we are also making laser ablation of the cytokinesis ring during its constriction. By doing so, we will be able to understand when these asymmetries came, before or after cytokinesis completion.

c. Targeting other ABPs?

Observing other ABPs can provide interesting perspectives about the global regulation of the actin cortex during early embryogenesis, the more detailed cortical identity and all our hypotheses. Some strains are already available in the lab, fused with a GFP and crossed with the membrane probe tagged in mCherry. HMR-1 can be an exciting target to decipher the implication of the actin cortex on the ABPs segregation, referring to hypotheses 1. a, 2. a and 2. b of this section. HMR-1 is implicated in actomyosin cortex anchoring at the plasma membrane. It was shown that HMR-1 is also involved in tethering the cortex to the cell membrane, spatially regulating the upstream Rho Signalling that affects the actomyosin cortex stability, flows, and attachment to the cell membrane (Padmanabhan et al., 2017). Currently, a whole data set for HMR-1 is being quantified and will be added to the publication associated with Aim 1. Another ABPs that are already available in the lab is PLST-1. This actin bundler plays an essential role in regulating the interconnectivity of the actin network, tuning the anterior cortical tension (Ding et al., 2017), and being part of filopodia (Hirani et al., 2019).

We can also observe the actomyosin cortex's first primordial component, which is the actin itself. To observe these filaments in vivo, we are using the Lifeact probes (Reymann et

al., 2016). These probes are either tag with GFP or mCherry. They are both able to bind actin filaments with different kinetics giving a complete view of the diverse composition of actin filaments within the cortex (Hirani et al., 2019). Nevertheless, to use our quantification approach on Lifeact::mCherry, we will need another membrane labelling, such as PIP2 tagged with GFP for quantifying Lifeact::mCherry. The second major component of the actomyosin cortex is NMY-2. It is a widely studied protein in the C.elegans actin community. It can inform us on many cortical parameters such as in the following non-exhaustive list: RhoA signalling (Michaux et al., 2018), filament assembly during cytokinesis (Najafabadi et al., 2022), actomyosin cortex polarisation (Munro et al., 2004), cortical flow (Reymann et al., 2016) and chirality (Pimpale et al., 2020). Nevertheless, NMY-2 is not found in filopodia during these early embryogenesis steps. On this point, it can be interesting to focus our interest on other molecular motors, such as other members of the myosin family or Microtubules Associated Proteins such as Dynein or Kinesin.

d. Molecular composition of filopodia

During my PhD's first years, I created a CRISPR strain expressing CYK-1::HALOTAG. This strain was created for the purpose of observing, in live imaging, the localisation of CYK-1 and, in the meantime, other ABPs fused with a GFP marker such as ARX-2::GFP or CAP-1::GFP. After strain creation and validation by sequencing, Roxane Benoit and myself tried to observe this strain regarding an already published and concisely sparse protocol adapted for *C. elegans* embryos (Dickinson et al., 2017). Unfortunately, we faced different technical issues that prevented us from getting data out of this strain. Very recently, Dickinson published a detailed protocol for quantifying membrane proteins labelled with Halotag (Chang and Dickinson, 2022) with much more interesting details that were missing in the 2017 version. We will use this publication well and retry our Halotag experiment, informing us about filopodia molecular composition. In addition, we would also like to use an immune-fluorescence approach to asses filopodia molecular composition and their spatial distribution at one precise moment. We have already tried and faced other experimental limitations due to the complicated embryo accessibility for antibodies to pass through the eggshell barrier and the structure's size and stability. Nevertheless, we are working on optimising protocols with the help of Dr LUTZ Yves from the IGBMC imaging platform.

e. Filopodia appearance at the 4-cell stage?

This question was already addressed and partially answered by preliminary data in Aim 3 (Fig XX). More data are required to fully validate our hypothesis about cell timing and filopodia appearance at this particular cell stage. We could also take advantage of the perspectives described for ABPs quantification and consider only the particles that are "outside" of the detection area and can be considered filopodia. This approach can help us to quantify their number automatically.

We can also untangle the mechanism that influences the previously described hypothesis. We need to add another layer of quantification by looking at cortical tension and cell roundness and see if the number of particles at the cellular interface, corresponding to filopodia, correlates with these physical parameters. After this wild-type characterisation, we could asses the importance of filopodia in these processes by perturbing either the CYK-1 dynamics at the interface using a CYK-1 thermosensitive strain (Jordan et al., 2016) and applying global heating to disrupt any CYK-1 activities or making a local at the cellular interface to see how it affects other parameters. We can also use laser ablation to perturb cortical tension locally.

f. Targeting other cellular localisation?

Since my master 2 internships in the lab of Sandrine Etienne-Mannevile, on the subject: A role for Cdc42 in the nucleus, the seed about the subject of actin localisation in the nucleus has grown over time. During the beginning of my PhD, some of the data acquired on the ARX-2 strain showed some enrichment of ARX-2::GFP near the nucleus. In addition, using the same strain, I saw actin comet tails in the cytoplasm. This structure is highly mobile, and its directionality is inconsistent (Velarde et al., 2007). Unfortunately, I did not investigate further after these observations, but it can be an exciting path.

Another interesting subcellular localisation is the "scar" left by the cytokinesis ring called the midbody. The midbody is known to be stereotypically inherited during the early lineage, and its position impact cell positioning and cell fate (König et al., 2017; Singh and Pohl, 2014; Thieleke-Matos et al., 2017). Its position can be an excellent reporter to see the implication of filopodia in cell positioning and cohesion

4- The embryonic's first steps

Filopodia have different roles in their cellular context, such as sensing, anchoring, signal transduction, and pulling. The only paradigm is based on the linear protrusion shape and the fact that they are structures related to actin, with filaments that are elongated with formin and parallelly aligned with actin binding proteins. For the other components, all the studies agree that the precise molecular composition and the initiation mechanism of these structures are still unclear and specific to the experimental model. To tackle the differences and name this actin structure, Higgs and co-workers establish a generic name for this structure: linear extension or filopodia (Nicholson-Dykstra and Higgs, 2008). Despite this general name, we observe differences between the filopodia observed in embryonic cells and filopodia in other systems.

First, I want to focus on the fact that we are looking at non-differentiated embryonic stem cells with an indeterminate fate. Embryonic cells are the premiere with a wide range of future possibilities. In contrast, the other model systems look at the terminal ones, with a wholly differentiated and functionalised protein toolkit that allows them to execute their predetermined cellular behaviour. It is probably one of the reasons why the roles of filopodia in differentiated cells are reasonably identified, whereas the role of filopodia in embryonic stem cells is still unknown.

Second, the filopodia present during embryonic development have a specific localisation during morphogenetics events. This feature is shared in a wide variety of organisms that are phylogenetically distant from each other (2-cell stage, 4-cell stage, Epithelial epiboly). This specificity highlights something unique compared to their relatives in differentiated migrating cells, and it is a shared feature between different embryonic development.

Third, even the paradigm about the shape can be contested or more precisely defined. Indeed, the size is much shorter in embryonic stem cells. The general shape and their dynamic changes from floating and unstable structures that protrude toward the extracellular environment to a straight and stable linear protrusion when they find matches. This observation goes along with the "spinning" structures observed by Andrews (Andrews 1897).

My PhD work focuses on the early embryogenesis of *C. elegans* and the spatio-temporal distribution of Actin Binding Proteins. In this confined environment. I have observed this structure for four years. When trying to understand their roles and regulation, I found many differences between these embryonic filopodia and the “classical” filopodia. The reason appears quite simple: they are dedicated to embryonic development. They must have multiple roles to adapt to any situation during the developing embryo, specifically during the early stages.

Taking it together, the generic name of filopodia that groups all sorts of actin linear protrusion can be subdivided with another group specific to the filopodia encountered during embryonic development. I name this new family of embryonic-related actin linear architecture: **Protopodia**. From ancient Greek, I used the prefix proto-, meaning the first or at the beginning and the suffix -podia, meaning foot. Assembled, it means the first foot. I chose this primary name regarding the totipotent state of the zygote and the first apparition of this structure in an organism’s lifetime that can be used to walk virtually.

References

Agarwal, P., Zaidel-Bar, R., 2019. Principles of Actomyosin Regulation In Vivo. Trends in Cell Biology 29, 150–163. https://doi.org/10.1016/j.tcb.2018.09.006
Ai, E., Skop, A.R., 2009. Endosomal recycling regulation during cytokinesis. Commun Integr Biol 2, 444–447. https://doi.org/10.4161/cib.2.5.8931
Albertson, D.G., 1984. Formation of the first cleavage spindle in nematode embryos. Developmental Biology 101, 61–72. https://doi.org/10.1016/0012-1606(84)90117-9
Almo, S.C., Pollard, T.D., Way, M., Lattman, E.E., 1994. Purification, Characterization and Crystallization of Acanthamoeba Profilin Expressed in Escherichia coli. Journal of Molecular Biology 236, 950–952. https://doi.org/10.1006/jmbi.1994.1200
Bergmann, D.C., Lee, M., Robertson, B., Tsou, M.-F.B., Rose, L.S., Wood, W.B., 2003. Embryonic handedness choice in *C. elegans* involves the Gαprotein GPA-16. Development 130, 5731–5740. https://doi.org/10.1242/dev.00839
Bhanshali, F., 2016. Understanding the role of CAP proteins in the polarization process of *C. elegans*.
Biro, M., Romeo, Y., Kroschwald, S., Bovellan, M., Boden, A., Tcherkezian, J., Roux, P.P., Charras, G., Paluch, E.K., 2013. Cell cortex composition and homeostasis resolved by integrating proteomics and quantitative imaging. Cytoskeleton (Hoboken) 70, 741–754. https://doi.org/10.1002/cm.21142
Blanchoin, L., Amann, K.J., Higgs, H.N., Marchand, J.B., Kaiser, D.A., Pollard, T.D., 2000. Direct observation of dendritic actin filament networks nucleated by Arp2/3 complex and WASP/Scar proteins. Nature 404, 1007–1011. https://doi.org/10.1038/35010008
Blanchoin, L., Boujemaa-Paterski, R., Sykes, C., Plastino, J., 2014. Actin Dynamics, Architecture, and Mechanics in Cell Motility. Physiological Reviews 94, 235–263. https://doi.org/10.1152/physrev.00018.2013
Block, J., Stradal, T. e. b., Hänisch, J., Geffers, R., Köstler, S. a., Urban, E., Small, J. v., Rottner, K., Faix, J., 2008. Filopodia formation induced by active mDia2/Drf3. Journal of Microscopy 231, 506–517. https://doi.org/10.1111/j.1365-2818.2008.02063.x
Bornschlögl, T., 2013. How filopodia pull: What we know about the mechanics and dynamics of filopodia. Cytoskeleton 70, 590–603. https://doi.org/10.1002/cm.21130
Boyd, L., Guo, S., Levitan, D., Stinchcomb, D.T., Kemphues, K.J., 1996. PAR-2 is asymmetrically distributed and promotes association of P granules and PAR-1 with the cortex in *C. elegans* embryos. Development 122, 3075–3084. https://doi.org/10.1242/dev.122.10.3075
Bretscher, A., Edwards, K., Fehon, R.G., 2002. ERM proteins and merlin: integrators at the cell cortex. Nat Rev Mol Cell Biol 3, 586–599. https://doi.org/10.1038/nrm882
Brockes, J.P., Martin, P., Redd, M.J., Cooper, L., Wood, W., Stramer, B., Martin, Paul, 2004. Wound healing and inflammation: embryos reveal the way to perfect repair. Philosophical Transactions of the Royal Society of London. Series B: Biological Sciences 359, 777–784. https://doi.org/10.1098/rstb.2004.1466
Burke, T.A., Christensen, J.R., Barone, E., Suarez, C., Sirotkin, V., Kovar, D.R., 2014. Homeostatic Actin Cytoskeleton Networks Are Regulated by Assembly Factor Competition for Monomers. Current Biology 24, 579–585. https://doi.org/10.1016/j.cub.2014.01.072
C. elegans Sequencing Consortium, 1998. Genome sequence of the nematode *C. elegans*: a platform for investigating biology. Science 282, 2012–2018. https://doi.org/10.1126/science.282.5396.2012
Calarco, P.G., Epstein, C.J., 1973. Cell surface changes during preimplantation development in the mouse. Developmental Biology 32, 208–213. https://doi.org/10.1016/0012-1606(73)90233-9
Cao, J., Wong, M.-K., Zhao, Z., Yan, H., 2019. 3DMMS: robust 3D Membrane Morphological Segmentation of *C. elegans* embryo. BMC Bioinformatics 20, 176. https://doi.org/10.1186/s12859-019-2720-x
Caroti, F., Thiels, W., Vanslambrouck, M., Jelier, R., 2021. Wnt Signaling Induces Asymmetric Dynamics in the Actomyosin Cortex of the *C. elegans* Endomesodermal Precursor Cell. Frontiers in Cell and Developmental Biology 9.

Carvalho, A.X., Silva, A.M., Osório, D.S., Pereira, A.J., Maiato, H., Pinto, I.M., Rubinstein, B., Gassmann, R., Telley, I.A., 2016. Robust gap repair in the contractile ring ensures timely completion of cytokinesis. J Cell Biol 215, 789–799. https://doi.org/10.1083/jcb.201605080

Cavey, M., Lecuit, T., 2009. Molecular Bases of Cell–Cell Junctions Stability and Dynamics. Cold Spring Harb Perspect Biol 1, a002998. https://doi.org/10.1101/cshperspect.a002998

Chaigne, A., Campillo, C., Gov, N.S., Voituriez, R., Azoury, J., Umaña-Diaz, C., Almonacid, M., Queguiner, I., Nassoy, P., Sykes, C., Verlhac, M.-H., Terret, M.-E., 2013. A soft cortex is essential for asymmetric spindle positioning in mouse oocytes. Nat Cell Biol 15, 958–966. https://doi.org/10.1038/ncb2799

Chan, C.E., Odde, D.J., 2008. Traction dynamics of filopodia on compliant substrates. Science 322, 1687–1691. https://doi.org/10.1126/science.1163595

Chan, F.-Y., Silva, A.M., Saramago, J., Pereira-Sousa, J., Brighton, H.E., Pereira, M., Oegema, K., Gassmann, R., Carvalho, A.X., 2018. The ARP2/3 complex prevents excessive formin activity during cytokinesis. Mol Biol Cell 30, 96–107. https://doi.org/10.1091/mbc.E18-07-0471

Chang, Y., Dickinson, D.J., 2022. Non-invasive chimeric HaloTag labeling to study clustering and diffusion of membrane proteins. STAR Protocols 3, 101857. https://doi.org/10.1016/j.xpro.2022.101857

Charras, G., Paluch, E., 2008. Blebs lead the way: how to migrate without lamellipodia. Nat Rev Mol Cell Biol 9, 730–736. https://doi.org/10.1038/nrm2453

Chen, M., Zhu, W., Liang, Z., Yao, S., Zhang, X., Zheng, Y., 2021. Effect of F-Actin Organization in Lamellipodium on Viscoelasticity and Migration of Huh-7 Cells Under pH Microenvironments Using AM-FM Atomic Force Microscopy. Frontiers in Physics 9.

Chen, Z., Borek, D., Padrick, S.B., Gomez, T.S., Metlagel, Z., Ismail, A.M., Umetani, J., Billadeau, D.D., Otwinowski, Z., Rosen, M.K., 2010. Structure and control of the actin regulatory WAVE complex. Nature 468, 533–538. https://doi.org/10.1038/nature09623

Cheng, N.N., Kirby, C.M., Kemphues, K.J., 1995. Control of cleavage spindle orientation in Caenorhabditis elegans: the role of the genes par-2 and par-3. Genetics 139, 549–559. https://doi.org/10.1093/genetics/139.2.549

Chereau, D., Kerff, F., Graceffa, P., Grabarek, Z., Langsetmo, K., Dominguez, R., 2005. Actin-bound structures of Wiskott–Aldrich syndrome protein (WASP)-homology domain 2 and the implications for filament assembly. Proc Natl Acad Sci U S A 102, 16644–16649. https://doi.org/10.1073/pnas.0507021102

Chhabra, E.S., Higgs, H.N., 2007. The many faces of actin: matching assembly factors with cellular structures. Nat Cell Biol 9, 1110–1121. https://doi.org/10.1038/ncb1007-1110

Collins, J.H., Elzinga, M., 1975. The primary structure of actin from rabbit skeletal muscle. Completion and analysis of the amino acid sequence. J Biol Chem 250, 5915–5920.

Cooper, J.A., Sept, D., 2008. New insights into mechanism and regulation of actin capping protein. Int Rev Cell Mol Biol 267, 183–206. https://doi.org/10.1016/S1937-6448(08)00604-7

Courtemanche, N., 2018. Mechanisms of formin-mediated actin assembly and dynamics. Biophys Rev 10, 1553–1569. https://doi.org/10.1007/s12551-018-0468-6

Courtemanche, N., Pollard, T.D., 2012. Determinants of Formin Homology 1 (FH1) Domain Function in Actin Filament Elongation by Formins. J Biol Chem 287, 7812–7820. https://doi.org/10.1074/jbc.M111.322958

Cowan, C.R., Hyman, A.A., 2007. Acto-myosin reorganization and PAR polarity in *C. elegans*. Development 134, 1035–1043. https://doi.org/10.1242/dev.000513

Crittenden, S.L., Troemel, E.R., Evans, T.C., Kimble, J., 1994. GLP-1 is localized to the mitotic region of the *C. elegans* germ line. Development 120, 2901–2911. https://doi.org/10.1242/dev.120.10.2901

De Henau, S., Pagès-Gallego, M., Pannekoek, W.-J., Dansen, T.B., 2020. Mitochondria-Derived H2O2 Promotes Symmetry Breaking of the *C. elegans* Zygote. Developmental Cell 53, 263-271.e6. https://doi.org/10.1016/j.devcel.2020.03.008

Delattre, M., Goehring, N.W., 2021. Chapter Nine - The first steps in the life of a worm: Themes and variations in asymmetric division in *C. elegans* and other nematodes, in: Jarriault, S., Podbilewicz, B. (Eds.), Current Topics in Developmental Biology, Nematode Models of Development and Disease. Academic Press, pp. 269–308. https://doi.org/10.1016/bs.ctdb.2020.12.006

DeRenzo, C., Seydoux, G., 2004. A clean start: degradation of maternal proteins at the oocyte-to-embryo transition. Trends in Cell Biology 14, 420–426. https://doi.org/10.1016/j.tcb.2004.07.005

Dickinson, D.J., Schwager, F., Pintard, L., Gotta, M., Goldstein, B., 2017. A single-cell biochemistry approach reveals PAR complex dynamics during cell polarization. Dev Cell 42, 416-434.e11. https://doi.org/10.1016/j.devcel.2017.07.024

Ding, W.Y., Ong, H.T., Hara, Y., Wongsantichon, J., Toyama, Y., Robinson, R., Nedelec, F., Zaidel-Bar, R., 2017. Plastin increases cortical connectivity to facilitate robust polarization and timely cytokinesis. The Journal of cell biology 16. https://doi.org/10.1083/jcb.201603070

Ducibella, T., Ukena, T., Karnovsky, M., Anderson, E., 1977. Changes in cell surface and cortical cytoplasmic organization during early embryogenesis in the preimplantation mouse embryo. Journal of Cell Biology 74, 153–167. https://doi.org/10.1083/jcb.74.1.153

E.A Andrew, 1897. Embryology [WWW Document]. https://doi.org/10.1086/276721

Eads, J.C., Mahoney, N.M., Vorobiev, S., Bresnick, A.R., Wen, K.K., Rubenstein, P.A., Haarer, B.K., Almo, S.C., 1998. Structure determination and characterization of Saccharomyces cerevisiae profilin. Biochemistry 37, 11171–11181. https://doi.org/10.1021/bi9720033

Eckert, C., Goretzki, A., Faberova, M., Kollmar, M., 2012. Conservation and divergence between cytoplasmic and muscle-specific actin capping proteins: insights from the crystal structure of cytoplasmic Cap32/34 from Dictyostelium discoideum. BMC Struct Biol 12, 12. https://doi.org/10.1186/1472-6807-12-12

Edwards, M., Zwolak, A., Schafer, D.A., Sept, D., Dominguez, R., Cooper, J.A., 2014. Capping Protein Regulators Fine-Tune Actin Assembly Dynamics. Nat Rev Mol Cell Biol 15, 677–689. https://doi.org/10.1038/nrm3869

Ege, N., Dowbaj, A.M., Jiang, M., Howell, M., Hooper, S., Foster, C., Jenkins, R.P., Sahai, E., 2018. Quantitative Analysis Reveals that Actin and Src-Family Kinases Regulate Nuclear YAP1 and Its Export. Cell Syst 6, 692-708.e13. https://doi.org/10.1016/j.cels.2018.05.006

Engler, A.J., Sen, S., Sweeney, H.L., Discher, D.E., 2006. Matrix elasticity directs stem cell lineage specification. Cell 126, 677–689. https://doi.org/10.1016/j.cell.2006.06.044

Escuin, S., Vernay, B., Savery, D., Gurniak, C.B., Witke, W., Greene, N.D.E., Copp, A.J., 2015. Rho-kinase-dependent actin turnover and actomyosin disassembly are necessary for mouse spinal neural tube closure. J Cell Sci 128, 2468–2481. https://doi.org/10.1242/jcs.164574

Etienne-Manneville, S., Hall, A., 2002. Rho GTPases in cell biology. Nature 420, 629–635. https://doi.org/10.1038/nature01148

Evans, T.C., Crittenden, S.L., Kodoyianni, V., Kimble, J., 1994. Translational control of maternal glp-1 mRNA establishes an asymmetry in the *C. elegans* embryo. Cell 77, 183–194. https://doi.org/10.1016/0092-8674(94)90311-5

Evans, T.C., Hunter, C.P., 2005. Translational control of maternal RNAs. WormBook.

Falet, H., Hoffmeister, K.M., Neujahr, R., Hartwig, J.H., 2002. Normal Arp2/3 complex activation in platelets lacking WASp. Blood 100, 2113–2122. https://doi.org/10.1182/blood.V100.6.2113

Fazeli, G., Stetter, M., Lisack, J.N., Wehman, A.M., 2018. *C. elegans* Blastomeres Clear the Corpse of the Second Polar Body by LC3-Associated Phagocytosis. Cell Reports 23, 2070–2082. https://doi.org/10.1016/j.celrep.2018.04.043

Fierro-González, J.C., White, M.D., Silva, J.C., Plachta, N., 2013. Cadherin-dependent filopodia control preimplantation embryo compaction. Nat Cell Biol 15, 1424–1433. https://doi.org/10.1038/ncb2875

Fischer, R.S., Lam, P.-Y., Huttenlocher, A., Waterman, C.M., 2019. Filopodia and focal adhesions: An integrated system driving branching morphogenesis in neuronal pathfinding and angiogenesis. Dev Biol 451, 86–95. https://doi.org/10.1016/j.ydbio.2018.08.015

Földi, I., Szikora, S., Mihály, J., 2017. Formin' bridges between microtubules and actin filaments in axonal growth cones. Neural Regeneration Research 12, 1971. https://doi.org/10.4103/1673-5374.221148

Fritzsche, M., Lewalle, A., Duke, T., Kruse, K., Charras, G., 2013. Analysis of turnover dynamics of the submembranous actin cortex. Mol Biol Cell 24, 757–767. https://doi.org/10.1091/mbc.E12-06-0485

Fujii, T., Iwane, A.H., Yanagida, T., Namba, K., 2010. Direct visualization of secondary structures of F-actin by electron cryomicroscopy. Nature 467, 724–728. https://doi.org/10.1038/nature09372

Galbraith, C.G., Yamada, K.M., Galbraith, J.A., 2007. Polymerizing Actin Fibers Position Integrins Primed to Probe for Adhesion Sites. Science 315, 992–995. https://doi.org/10.1126/science.1137904

Gan, W.J., Motegi, F., 2021. Mechanochemical Control of Symmetry Breaking in the Caenorhabditis elegans Zygote. Front Cell Dev Biol 8, 619869. https://doi.org/10.3389/fcell.2020.619869

Gates, J., Mahaffey, J.P., Rogers, S.L., Emerson, M., Rogers, E.M., Sottile, S.L., Van Vactor, D., Gertler, F.B., Peifer, M., 2007. Enabled plays key roles in embryonic epithelial morphogenesis in Drosophila. Development 134, 2027–2039. https://doi.org/10.1242/dev.02849

Goldstein, B., Hird, S.N., 1996. Specification of the anteroposterior axis in Caenorhabditis elegans. Development 122, 1467–1474. https://doi.org/10.1242/dev.122.5.1467

Goldstein, B., Macara, I.G., 2007. The PAR Proteins: Fundamental Players in Animal Cell Polarization. Dev Cell 13, 609–622. https://doi.org/10.1016/j.devcel.2007.10.007

Goley, E.D., Rodenbusch, S.E., Martin, A.C., Welch, M.D., 2004. Critical conformational changes in the Arp2/3 complex are induced by nucleotide and nucleation promoting factor. Mol Cell 16, 269–279. https://doi.org/10.1016/j.molcel.2004.09.018

Gönczy, P., Rose, L.S., 2005. Asymmetric cell division and axis formation in the embryo. WormBook 1–20. https://doi.org/10.1895/wormbook.1.30.1

Gross, P., Kumar, K.V., Goehring, N.W., Bois, J.S., Hoege, C., Jülicher, F., Grill, S.W., 2019. Guiding self-organized pattern formation in cell polarity establishment. Nat. Phys. 15, 293–300. https://doi.org/10.1038/s41567-018-0358-7

Guo, S., Kemphues, K.J., 1995. par-1, a gene required for establishing polarity in *C. elegans* embryos, encodes a putative Ser/Thr kinase that is asymmetrically distributed. Cell 81, 611–620. https://doi.org/10.1016/0092-8674(95)90082-9

Hakanpaa, L., Kiss, E.A., Jacquemet, G., Miinalainen, I., Lerche, M., Guzmán, C., Mervaala, E., Eklund, L., Ivaska, J., Saharinen, P., 2018. Targeting β1-integrin inhibits vascular leakage in endotoxemia. Proceedings of the National Academy of Sciences 115, E6467–E6476. https://doi.org/10.1073/pnas.1722317115

Hamill, D.R., Severson, A.F., Carter, J.C., Bowerman, B., 2002. Centrosome Maturation and Mitotic Spindle Assembly in *C. elegans* Require SPD-5, a Protein with Multiple Coiled-Coil Domains. Developmental Cell 3, 673–684. https://doi.org/10.1016/S1534-5807(02)00327-1

He, K., Sakai, T., Tsukasaki, Y., Watanabe, T.M., Ikebe, M., 2017. Myosin X is recruited to nascent focal adhesions at the leading edge and induces multi-cycle filopodial elongation. Sci Rep 7, 13685. https://doi.org/10.1038/s41598-017-06147-6

Henson, J.H., Ditzler, C.E., Germain, A., Irwin, P.M., Vogt, E.T., Yang, S., Wu, X., Shuster, C.B., 2017. The ultrastructural organization of actin and myosin II filaments in the contractile ring: new support for an old model of cytokinesis. Mol Biol Cell 28, 613–623. https://doi.org/10.1091/mbc.E16-06-0466

Higgs, H.N., 2005. Formin proteins: a domain-based approach. Trends Biochem Sci 30, 342–353. https://doi.org/10.1016/j.tibs.2005.04.014

Hiraiwa, T., Salbreux, G., 2016. Role of Turnover in Active Stress Generation in a Filament Network. Phys. Rev. Lett. 116, 188101. https://doi.org/10.1103/PhysRevLett.116.188101
Hirani, N., Illukkumbura, R., Bland, T., Mathonnet, G., Suhner, D., Reymann, A.-C., Goehring, N.W., 2019. Anterior-enriched filopodia create the appearance of asymmetric membrane microdomains in polarizing *C. elegans* zygotes. J Cell Sci 132, jcs230714. https://doi.org/10.1242/jcs.230714
Hird, S.N., White, J.G., 1993. Cortical and cytoplasmic flow polarity in early embryonic cells of Caenorhabditis elegans. Journal of Cell Biology 121, 1343–1355. https://doi.org/10.1083/jcb.121.6.1343
Hoege, C., Hyman, A.A., 2013. Principles of PAR polarity in Caenorhabditis elegans embryos. Nat Rev Mol Cell Biol 14, 315–322. https://doi.org/10.1038/nrm3558
Hoffmann, A.-K., Naj, X., Linder, S., 2014. Daam1 is a regulator of filopodia formation and phagocytic uptake of Borrelia burgdorferi by primary human macrophages. The FASEB Journal 28, 3075–3089. https://doi.org/10.1096/fj.13-247049
Holmes, K.C., Popp, D., Gebhard, W., Kabsch, W., 1990. Atomic model of the actin filament. Nature 347, 44–49. https://doi.org/10.1038/347044a0
Hyman, A.A., White, J.G., 1987. Determination of cell division axes in the early embryogenesis of Caenorhabditis elegans. Journal of Cell Biology 105, 2123–2135. https://doi.org/10.1083/jcb.105.5.2123
Jacinto, A., Woolner, S., Martin, P., 2002. Dynamic Analysis of Dorsal Closure in Drosophila: From Genetics to Cell Biology. Developmental Cell 3, 9–19. https://doi.org/10.1016/S1534-5807(02)00208-3
Jacquemet, G., Stubb, A., Saup, R., Miihkinen, M., Kremneva, E., Hamidi, H., Ivaska, J., 2019. Filopodome Mapping Identifies p130Cas as a Mechanosensitive Regulator of Filopodia Stability. Current Biology 29, 202-216.e7. https://doi.org/10.1016/j.cub.2018.11.053
Jaiswal, R., Breitsprecher, D., Collins, A., Corrêa, I.R., Xu, M.-Q., Goode, B.L., 2013. The Formin Daam1 and Fascin Directly Collaborate to Promote Filopodia Formation. Current Biology 23, 1373–1379. https://doi.org/10.1016/j.cub.2013.06.013
Jankele, R., Jelier, R., Gönczy, P., 2021. Physically asymmetric division of the *C. elegans* zygote ensures invariably successful embryogenesis. eLife 10, e61714. https://doi.org/10.7554/eLife.61714
Johnson, M.H., Maro, B., Takeichi, M., 1986. The role of cell adhesion in the synchronization and orientation of polarization in 8-cell mouse blastomeres. Development 93, 239–255. https://doi.org/10.1242/dev.93.1.239
Johnson, M.H., Pratt, H.P.M., Handyside, A.H., 1981. The Generation and Recognition of Positional Information in the Preimplantation Mouse Embryo, in: Glasser, S.R., Bullock, D.W. (Eds.), Cellular and Molecular Aspects of Implantation. Springer US, Boston, MA, pp. 55–74. https://doi.org/10.1007/978-1-4613-3180-3_5
Jordan, S.N., Davies, T., Zhuravlev, Y., Dumont, J., Shirasu-Hiza, M., Canman, J.C., 2016. Cortical PAR polarity proteins promote robust cytokinesis during asymmetric cell division. J Cell Biol 212, 39–49. https://doi.org/10.1083/jcb.201510063
Kabsch, W., Mannherz, H.G., Suck, D., Pai, E.F., Holmes, K.C., 1990. Atomic structure of the actin:DNase I complex. Nature 347, 37–44. https://doi.org/10.1038/347037a0
Kage, F., Winterhoff, M., Dimchev, V., Mueller, J., Thalheim, T., Freise, A., Brühmann, S., Kollasser, J., Block, J., Dimchev, G., Geyer, M., Schnittler, H.-J., Brakebusch, C., Stradal, T.E.B., Carlier, M.-F., Sixt, M., Käs, J., Faix, J., Rottner, K., 2017. FMNL formins boost lamellipodial force generation. Nat Commun 8, 14832. https://doi.org/10.1038/ncomms14832
Kang, F., Purich, D.L., Southwick, F.S., 1999. Profilin Promotes Barbed-end Actin Filament Assembly without Lowering the Critical Concentration*. Journal of Biological Chemistry 274, 36963–36972. https://doi.org/10.1074/jbc.274.52.36963
Kemphues, K., 2000. PARsing embryonic polarity. Cell 101, 345–348. https://doi.org/10.1016/s0092-8674(00)80844-2

Kemphues, K.J., Priess, J.R., Morton, D.G., Cheng, N.S., 1988. Identification of genes required for cytoplasmic localization in early *C. elegans* embryos. Cell 52, 311–320. https://doi.org/10.1016/s0092-8674(88)80024-2

Kim, J., Lee, J.E., Heynen-Genel, S., Suyama, E., Ono, K., Lee, K., Ideker, T., Aza-Blanc, P., Gleeson, J.G., 2010. Functional genomic screen for modulators of ciliogenesis and cilium length. Nature 464, 1048–1051. https://doi.org/10.1038/nature08895

Kim, M.-C., Silberberg, Y.R., Abeyaratne, R., Kamm, R.D., Asada, H.H., 2018. Computational modeling of three-dimensional ECM-rigidity sensing to guide directed cell migration. Proceedings of the National Academy of Sciences 115, E390–E399. https://doi.org/10.1073/pnas.1717230115

Kimble, J., Hirsh, D., 1979. The postembryonic cell lineages of the hermaphrodite and male gonads in Caenorhabditis elegans. Developmental Biology 70, 396–417. https://doi.org/10.1016/0012-1606(79)90035-6

Knöll, B., Beck, H., 2011. The cytoskeleton and nucleus: the role of actin as a modulator of neuronal gene expression. e-Neuroforum 17, 1–5. https://doi.org/10.1007/s13295-010-0013-y

König, J., Frankel, E.B., Audhya, A., Müller-Reichert, T., 2017. Membrane remodeling during embryonic abscission in Caenorhabditis elegans. J Cell Biol 216, 1277–1286. https://doi.org/10.1083/jcb.201607030

Korobova, F., Svitkina, T., 2008. Arp2/3 complex is important for filopodia formation, growth cone motility, and neuritogenesis in neuronal cells. Mol Biol Cell 19, 1561–1574. https://doi.org/10.1091/mbc.e07-09-0964

Kovar, D.R., Pollard, T.D., 2004. Progressing actin: Formin as a processive elongation machine. Nat Cell Biol 6, 1158–1159. https://doi.org/10.1038/ncb1204-1158

Kunda, P., Pelling, A.E., Liu, T., Baum, B., 2008. Moesin Controls Cortical Rigidity, Cell Rounding, and Spindle Morphogenesis during Mitosis. Current Biology 18, 91–101. https://doi.org/10.1016/j.cub.2007.12.051

Kyheröinen, S., Vartiainen, M.K., 2020. Nuclear actin dynamics in gene expression and genome organization. Semin Cell Dev Biol 102, 105–112. https://doi.org/10.1016/j.semcdb.2019.10.012

Lagarrigue, F., Vikas Anekal, P., Lee, H.-S., Bachir, A.I., Ablack, J.N., Horwitz, A.F., Ginsberg, M.H., 2015. A RIAM/lamellipodin–talin–integrin complex forms the tip of sticky fingers that guide cell migration. Nat Commun 6, 8492. https://doi.org/10.1038/ncomms9492

Landry, E.S., Rouillard, C., Levesque, D., Guertin, P.A., 2006. Profile of immediate early gene expression in the lumbar spinal cord of low-thoracic paraplegic mice. Behavioral Neuroscience 120, 1384–1388. https://doi.org/10.1037/0735-7044.120.6.1384

Lang, C.F., Munro, E., 2017. The PAR proteins: from molecular circuits to dynamic self-stabilizing cell polarity. Development 144, 3405–3416. https://doi.org/10.1242/dev.139063

Larue, L., Ohsugi, M., Hirchenhain, J., Kemler, R., 1994. E-cadherin null mutant embryos fail to form a trophectoderm epithelium. Proceedings of the National Academy of Sciences 91, 8263–8267. https://doi.org/10.1073/pnas.91.17.8263

Lebensohn, A.M., Kirschner, M.W., 2009. Activation of the WAVE Complex by Coincident Signals Controls Actin Assembly. Molecular Cell 36, 512–524. https://doi.org/10.1016/j.molcel.2009.10.024

Lecuit, T., Lenne, P.-F., Munro, E., 2011. Force generation, transmission, and integration during cell and tissue morphogenesis. Annu Rev Cell Dev Biol 27, 157–184. https://doi.org/10.1146/annurev-cellbio-100109-104027

Leite, J., Osorio, D.S., Sobral, A.F., Silva, A.M., Carvalho, A.X., 2018. Network Contractility During Cytokinesis-from Molecular to Global Views. Biomolecules 9, E194. https://doi.org/10.3390/biom9050194

Levayer, R., Lecuit, T., 2012. Biomechanical regulation of contractility: spatial control and dynamics. Trends Cell Biol 22, 61–81. https://doi.org/10.1016/j.tcb.2011.10.001

Li, Y., Munro, E., 2021. Filament-guided filament assembly provides structural memory of filament alignment during cytokinesis. Dev Cell 56, 2486-2500.e6. https://doi.org/10.1016/j.devcel.2021.08.009
Loisel, T.P., Boujemaa, R., Pantaloni, D., Carlier, M.F., 1999. Reconstitution of actin-based motility of Listeria and Shigella using pure proteins. Nature 401, 613–616. https://doi.org/10.1038/44183
Ma, L., Rohatgi, R., Kirschner, M.W., 1998. The Arp2/3 complex mediates actin polymerization induced by the small GTP-binding protein Cdc42. Proc Natl Acad Sci U S A 95, 15362–15367. https://doi.org/10.1073/pnas.95.26.15362
Machesky, L.M., Gould, K.L., 1999. The Arp2/3 complex: a multifunctional actin organizer. Curr Opin Cell Biol 11, 117–121. https://doi.org/10.1016/s0955-0674(99)80014-3
Machesky, L.M., Insall, R.H., 1998. Scar1 and the related Wiskott–Aldrich syndrome protein, WASP, regulate the actin cytoskeleton through the Arp2/3 complex. Current Biology 8, 1347–1356. https://doi.org/10.1016/S0960-9822(98)00015-3
Machesky, L.M., Mullins, R.D., Higgs, H.N., Kaiser, D.A., Blanchoin, L., May, R.C., Hall, M.E., Pollard, T.D., 1999. Scar, a WASp-related protein, activates nucleation of actin filaments by the Arp2/3 complex. Proceedings of the National Academy of Sciences 96, 3739–3744. https://doi.org/10.1073/pnas.96.7.3739
Machesky, Simon J. Atkinson, Christophe Ampe, Joel Vandekercldaove, Thomas D. Pollard, 1994. Purification of a cortical complex containing two unconventional actins from Acanthamoeba by affinity chromatography on profilin-agarose. J Cell Biol 127, 107–115.
Maddox, A.S., Burridge, K., 2003. RhoA is required for cortical retraction and rigidity during mitotic cell rounding. J Cell Biol 160, 255–265. https://doi.org/10.1083/jcb.200207130
Maître, J.-L., Turlier, H., Illukkumbura, R., Eismann, B., Niwayama, R., Nédélec, F., Hiiragi, T., 2016. Asymmetric division of contractile domains couples cell positioning and fate specification. Nature 536, 344–348. https://doi.org/10.1038/nature18958
Mangal, S., Sacher, J., Kim, T., Osório, D.S., Motegi, F., Carvalho, A.X., Oegema, K., Zanin, E., 2018. TPXL-1 activates Aurora A to clear contractile ring components from the polar cortex during cytokinesis. J Cell Biol 217, 837–848. https://doi.org/10.1083/jcb.201706021
Marchand, J.B., Kaiser, D.A., Pollard, T.D., Higgs, H.N., 2001. Interaction of WASP/Scar proteins with actin and vertebrate Arp2/3 complex. Nat Cell Biol 3, 76–82. https://doi.org/10.1038/35050590
Martin, P., Parkhurst, S.M., 2004. Parallels between tissue repair and embryo morphogenesis. Development 131, 3021–3034. https://doi.org/10.1242/dev.01253
Mattila, P.K., Lappalainen, P., 2008. Filopodia: molecular architecture and cellular functions. Nat Rev Mol Cell Biol 9, 446–454. https://doi.org/10.1038/nrm2406
Matzke, R., Jacobson, K., Radmacher, M., 2001. Direct, high-resolution measurement of furrow stiffening during division of adherent cells. Nat Cell Biol 3, 607–610. https://doi.org/10.1038/35078583
McBeath, R., Pirone, D.M., Nelson, C.M., Bhadriraju, K., Chen, C.S., 2004. Cell shape, cytoskeletal tension, and RhoA regulate stem cell lineage commitment. Dev Cell 6, 483–495. https://doi.org/10.1016/s1534-5807(04)00075-9
Mejillano, M.R., Kojima, S., Applewhite, D.A., Gertler, F.B., Svitkina, T.M., Borisy, G.G., 2004. Lamellipodial versus filopodial mode of the actin nanomachinery: pivotal role of the filament barbed end. Cell 118, 363–373. https://doi.org/10.1016/j.cell.2004.07.019
Michaux, J.B., Robin, F.B., McFadden, W.M., Munro, E.M., 2018. Excitable RhoA dynamics drive pulsed contractions in the early *C. elegans* embryo. J Cell Biol 217, 4230–4252. https://doi.org/10.1083/jcb.201806161
Millard, T.H., Martin, P., 2008. Dynamic analysis of filopodial interactions during the zippering phase of Drosophila dorsal closure. Development 135, 621–626. https://doi.org/10.1242/dev.014001

Mi-Mi, L., Votra, S., Kemphues, K., Bretscher, A., Pruyne, D., 2012. Z-line formins promote contractile lattice growth and maintenance in striated muscles of *C. elegans*. J Cell Biol 198, 87–102. https://doi.org/10.1083/jcb.201202053

Morone, N., Fujiwara, T., Murase, K., Kasai, R.S., Ike, H., Yuasa, S., Usukura, J., Kusumi, A., 2006. Three-dimensional reconstruction of the membrane skeleton at the plasma membrane interface by electron tomography. Journal of Cell Biology 174, 851–862. https://doi.org/10.1083/jcb.200606007

Motegi, F., Sugimoto, A., 2006. Sequential functioning of the ECT-2 RhoGEF, RHO-1 and CDC-42 establishes cell polarity in Caenorhabditis elegans embryos. Nat Cell Biol 8, 978–985. https://doi.org/10.1038/ncb1459

Moulding, D.A., Record, J., Malinova, D., Thrasher, A.J., 2013. Actin cytoskeletal defects in immunodeficiency. Immunological Reviews 256, 282–299. https://doi.org/10.1111/imr.12114

Mukhina, S., Wang, Y., Murata-Hori, M., 2007. α-Actinin Is Required for Tightly Regulated Remodeling of the Actin Cortical Network during Cytokinesis. Developmental Cell 13, 554–565. https://doi.org/10.1016/j.devcel.2007.08.003

Mullins, R.D., Heuser, J.A., Pollard, T.D., 1998. The interaction of Arp2/3 complex with actin: nucleation, high affinity pointed end capping, and formation of branching networks of filaments. Proc Natl Acad Sci U S A 95, 6181–6186. https://doi.org/10.1073/pnas.95.11.6181

Munjal, A., Lecuit, T., 2014. Actomyosin networks and tissue morphogenesis. Development 141, 1789–1793. https://doi.org/10.1242/dev.091645

Munro, E., Nance, J., Priess, J.R., 2004. Cortical Flows Powered by Asymmetrical Contraction Transport PAR Proteins to Establish and Maintain Anterior-Posterior Polarity in the Early *C. elegans* Embryo. Developmental Cell 7, 413–424. https://doi.org/10.1016/j.devcel.2004.08.001

Naganathan, S.R., Fürthauer, S., Rodriguez, J., Fievet, B.T., Jülicher, F., Ahringer, J., Cannistraci, C.V., Grill, S.W., 2018. Morphogenetic degeneracies in the actomyosin cortex. eLife 7, e37677. https://doi.org/10.7554/eLife.37677

Najafabadi, F.R., Leaver, M., Grill, S.W., 2022. Orchestrating nonmuscle myosin II filament assembly at the onset of cytokinesis. Mol Biol Cell 33, ar74. https://doi.org/10.1091/mbc.E21-12-0599

Nakayama, Y., Shivas, J.M., Poole, D.S., Squirrell, J.M., Kulkoski, J.M., Schleede, J.B., Skop, A.R., 2009. Dynamin Participates in the Maintenance of Anterior Polarity in the Caenorhabditis elegans Embryo. Developmental Cell 16, 889–900. https://doi.org/10.1016/j.devcel.2009.04.009

Nicholson-Dykstra, S.M., Higgs, H.N., 2008. Arp2 depletion inhibits sheet-like protrusions but not linear protrusions of fibroblasts and lymphocytes. Cell Motility 65, 904–922. https://doi.org/10.1002/cm.20312

Nobes, C.D., Hall, A., 1995. Rho, Rac, and Cdc42 GTPases regulate the assembly of multimolecular focal complexes associated with actin stress fibers, lamellipodia, and filopodia. Cell 81, 53–62. https://doi.org/10.1016/0092-8674(95)90370-4

Oda, T., Iwasa, M., Aihara, T., Maéda, Y., Narita, A., 2009. The nature of the globular- to fibrous-actin transition. Nature 457, 441–445. https://doi.org/10.1038/nature07685

Osborne Nishimura, E., Zhang, J.C., Werts, A.D., Goldstein, B., Lieb, J.D., 2015. Asymmetric Transcript Discovery by RNA-seq in *C. elegans* Blastomeres Identifies neg-1, a Gene Important for Anterior Morphogenesis. PLoS Genet 11, e1005117. https://doi.org/10.1371/journal.pgen.1005117

Osório, D.S., Chan, F.-Y., Saramago, J., Leite, J., Silva, A.M., Sobral, A.F., Gassmann, R., Carvalho, A.X., 2019. Crosslinking activity of non-muscle myosin II is not sufficient for embryonic cytokinesis in *C. elegans*. Development 146, dev179150. https://doi.org/10.1242/dev.179150

Otomo, T., Tomchick, D.R., Otomo, C., Panchal, S.C., Machius, M., Rosen, M.K., 2005. Structural basis of actin filament nucleation and processive capping by a formin homology 2 domain. Nature 433, 488–494. https://doi.org/10.1038/nature03251

Ou, G., Stuurman, N., D'Ambrosio, M., Vale, R.D., 2010. Polarized Myosin Produces Unequal-Size Daughters During Asymmetric Cell Division. Science 330, 677–680. https://doi.org/10.1126/science.1196112

Pacquelet, A., 2017. Asymmetric Cell Division in the One-Cell *C. elegans* Embryo: Multiple Steps to Generate Cell Size Asymmetry. Results Probl Cell Differ 61, 115–140. https://doi.org/10.1007/978-3-319-53150-2_5

Pacquelet, A., Uhart, P., Tassan, J.-P., Michaux, G., 2015. PAR-4 and anillin regulate myosin to coordinate spindle and furrow position during asymmetric division. Journal of Cell Biology 210, 1085–1099. https://doi.org/10.1083/jcb.201503006

Padmanabhan, A., Ong, H.T., Zaidel-Bar, R., 2017. Non-junctional E-Cadherin Clusters Regulate the Actomyosin Cortex in the *C. elegans* Zygote. Current Biology 27, 103–112. https://doi.org/10.1016/j.cub.2016.10.032

Paluch, E.K., Aspalter, I.M., Sixt, M., 2016. Focal Adhesion-Independent Cell Migration. Annu Rev Cell Dev Biol 32, 469–490. https://doi.org/10.1146/annurev-cellbio-111315-125341

Panbianco, C., Weinkove, D., Zanin, E., Jones, D., Divecha, N., Gotta, M., Ahringer, J., 2008. A Casein Kinase 1 and PAR Proteins Regulate Asymmetry of a PIP2 Synthesis Enzyme for Asymmetric Spindle Positioning. Developmental Cell 15, 198–208. https://doi.org/10.1016/j.devcel.2008.06.002

Parker, F., Baboolal, T.G., Peckham, M., 2020. Actin Mutations and Their Role in Disease. Int J Mol Sci 21, 3371. https://doi.org/10.3390/ijms21093371

Paul, A.S., Paul, A., Pollard, T.D., Pollard, T., 2008. The role of the FH1 domain and profilin in formin-mediated actin-filament elongation and nucleation. Curr Biol 18, 9–19. https://doi.org/10.1016/j.cub.2007.11.062

Pellegrin, S., Mellor, H., 2005. The Rho Family GTPase Rif Induces Filopodia through mDia2. Current Biology 15, 129–133. https://doi.org/10.1016/j.cub.2005.01.011

Pimpale, L.G., Middelkoop, T.C., Mietke, A., Grill, S.W., 2020. Cell lineage-dependent chiral actomyosin flows drive cellular rearrangements in early Caenorhabditis elegans development. eLife 9, e54930. https://doi.org/10.7554/eLife.54930

Pintard, L., Willems, A., Peter, M., 2004. Cullin-based ubiquitin ligases: Cul3–BTB complexes join the family. The EMBO Journal 23, 1681–1687. https://doi.org/10.1038/sj.emboj.7600186

Pittman, K.J., Skop, A.R., 2012. Anterior PAR proteins function during cytokinesis and maintain DYN-1 at the cleavage furrow in *Caenorhabditis elegans*. Cytoskeleton 69, 826–839. https://doi.org/10.1002/cm.21053

Pohl, C., Bao, Z., 2010. Chiral forces organize left-right patterning in *C. elegans* by uncoupling midline and anteroposterior axis. Dev Cell 19, 402–412. https://doi.org/10.1016/j.devcel.2010.08.014

Polet, D., Lambrechts, A., Ono, K., Mah, A., Peelman, F., Vandekerckhove, J., Baillie, D.L., Ampe, C., Ono, S., 2006. Caenorhabditis elegans Expresses Three Functional Profilins in a Tissue-Specific Manner. Cell Motil Cytoskeleton 63, 14–28. https://doi.org/10.1002/cm.20102

Pollard, T.D., 2016. Actin and Actin-Binding Proteins. Cold Spring Harb Perspect Biol 8, a018226. https://doi.org/10.1101/cshperspect.a018226

Pollard, T.D., 2007. Regulation of actin filament assembly by Arp2/3 complex and formins. Annu Rev Biophys Biomol Struct 36, 451–477. https://doi.org/10.1146/annurev.biophys.35.040405.101936

Pollard, T.D., Blanchoin, L., Mullins, R.D., 2000. Molecular Mechanisms Controlling Actin Filament Dynamics in Nonmuscle Cells. Annu. Rev. Biophys. Biomol. Struct. 29, 545–576. https://doi.org/10.1146/annurev.biophys.29.1.545

Pollard, T.D., Borisy, G.G., 2003. Cellular Motility Driven by Assembly and Disassembly of Actin Filaments. Cell 112, 453–465. https://doi.org/10.1016/S0092-8674(03)00120-X

Priess, J.R., Thomson, J.N., 1987. Cellular interactions in early *C. elegans* embryos. Cell 48, 241–250. https://doi.org/10.1016/0092-8674(87)90427-2

Pring, M., Weber, A., Bubb, M.R., 1992. Profilin-actin complexes directly elongate actin filaments at the barbed end. Biochemistry 31, 1827–1836. https://doi.org/10.1021/bi00121a035
Raich, W.B., Agbunag, C., Hardin, J., 1999. Rapid epithelial-sheet sealing in the Caenorhabditis elegans embryo requires cadherin-dependent filopodial priming. Current Biology 9, 1139-S1. https://doi.org/10.1016/S0960-9822(00)80015-9
Ramanujam, R., Han, Z., Zhang, Z., Kanchanawong, P., Motegi, F., 2018. Establishment of the PAR-1 cortical gradient by the aPKC-PRBH circuit. Nat Chem Biol 14, 917–927. https://doi.org/10.1038/s41589-018-0117-1
Remmerbach, T.W., Wottawah, F., Dietrich, J., Lincoln, B., Wittekind, C., Guck, J., 2009. Oral Cancer Diagnosis by Mechanical Phenotyping. Cancer Research 69, 1728–1732. https://doi.org/10.1158/0008-5472.CAN-08-4073
Reymann, A.-C., Staniscia, F., Erzberger, A., Salbreux, G., Grill, S.W., 2016. Cortical flow aligns actin filaments to form a furrow. eLife 5, e17807. https://doi.org/10.7554/eLife.17807
Ridley, A.J., 2006. Rho GTPases and actin dynamics in membrane protrusions and vesicle trafficking. Trends in Cell Biology, Membrane Dynamics 16, 522–529. https://doi.org/10.1016/j.tcb.2006.08.006
Ridley, A.J., Hall, A., 1992. The small GTP-binding protein rho regulates the assembly of focal adhesions and actin stress fibers in response to growth factors. Cell 70, 389–399. https://doi.org/10.1016/0092-8674(92)90163-7
Robinson, R.C., Turbedsky, K., Kaiser, D.A., Marchand, J.B., Higgs, H.N., Choe, S., Pollard, T.D., 2001. Crystal structure of Arp2/3 complex. Science 294, 1679–1684. https://doi.org/10.1126/science.1066333
Rocheleau, C.E., Downs, W.D., Lin, R., Wittmann, C., Bei, Y., Cha, Y.-H., Ali, M., Priess, J.R., Mello, C.C., 1997. Wnt Signaling and an APC-Related Gene Specify Endoderm in Early *C. elegans* Embryos. Cell 90, 707–716. https://doi.org/10.1016/S0092-8674(00)80531-0
Rodal, A.A., Sokolova, O., Robins, D.B., Daugherty, K.M., Hippenmeyer, S., Riezman, H., Grigorieff, N., Goode, B.L., 2005. Conformational changes in the Arp2/3 complex leading to actin nucleation. Nat Struct Mol Biol 12, 26–31. https://doi.org/10.1038/nsmb870
Rohatgi, R., Ma, L., Miki, H., Lopez, M., Kirchhausen, T., Takenawa, T., Kirschner, M.W., 1999. The interaction between N-WASP and the Arp2/3 complex links Cdc42-dependent signals to actin assembly. Cell 97, 221–231. https://doi.org/10.1016/s0092-8674(00)80732-1
Rose, L., Gönczy, P., 2014. Polarity establishment, asymmetric division and segregation of fate determinants in early *C. elegans* embryos. WormBook 1–43. https://doi.org/10.1895/wormbook.1.30.2
Rossant, J., Tam, P.P.L., 2009. Blastocyst lineage formation, early embryonic asymmetries and axis patterning in the mouse. Development 136, 701–713. https://doi.org/10.1242/dev.017178
Rottner, K., Faix, J., Bogdan, S., Linder, S., Kerkhoff, E., 2017. Actin assembly mechanisms at a glance. Journal of Cell Science 130, 3427–3435. https://doi.org/10.1242/jcs.206433
Rouiller, I., Xu, X.-P., Amann, K.J., Egile, C., Nickell, S., Nicastro, D., Li, R., Pollard, T.D., Volkmann, N., Hanein, D., 2008. The structural basis of actin filament branching by the Arp2/3 complex. J Cell Biol 180, 887–895. https://doi.org/10.1083/jcb.200709092
Salbreux, G., Charras, G., Paluch, E., 2012. Actin cortex mechanics and cellular morphogenesis. Trends in Cell Biology 22, 536–545. https://doi.org/10.1016/j.tcb.2012.07.001
Samandar Eweis, D., Plastino, J., 2020. Roles of Actin in the Morphogenesis of the Early Caenorhabditis elegans Embryo. International Journal of Molecular Sciences 21, 3652. https://doi.org/10.3390/ijms21103652
Sawa, M., Suetsugu, S., Sugimoto, A., Miki, H., Yamamoto, M., Takenawa, T., 2003. Essential role of the *C. elegans* Arp2/3 complex in cell migration during ventral enclosure. Journal of Cell Science 116, 1505–1518. https://doi.org/10.1242/jcs.00362
Schafer, D.A., Hug, C., Cooper, J.A., 1995. Inhibition of CapZ during myofibrillogenesis alters assembly of actin filaments. J Cell Biol 128, 61–70. https://doi.org/10.1083/jcb.128.1.61

Schirenbeck, A., Bretschneider, T., Arasada, R., Schleicher, M., Faix, J., 2005. The Diaphanous-related formin dDia2 is required for the formation and maintenance of filopodia. Nat Cell Biol 7, 619–625. https://doi.org/10.1038/ncb1266

Scholze, M.J., Barbieux, K.S., De Simone, A., Boumasmoud, M., Süess, C.C.N., Wang, R., Gönczy, P., 2018. PI(4,5)P2 forms dynamic cortical structures and directs actin distribution as well as polarity in Caenorhabditis elegans embryos. Development 145, dev164988. https://doi.org/10.1242/dev.164988

Schonegg, S., Constantinescu, A.T., Hoege, C., Hyman, A.A., 2007. The Rho GTPase-activating proteins RGA-3 and RGA-4 are required to set the initial size of PAR domains in Caenorhabditis elegans one-cell embryos. Proceedings of the National Academy of Sciences 104, 14976–14981. https://doi.org/10.1073/pnas.0706941104

Schonegg, S., Hyman, A.A., 2006. CDC-42 and RHO-1 coordinate acto-myosin contractility and PAR protein localization during polarity establishment in *C. elegans* embryos. Development 133, 3507–3516. https://doi.org/10.1242/dev.02527

Schönichen, A., Geyer, M., 2010. Fifteen formins for an actin filament: a molecular view on the regulation of human formins. Biochim Biophys Acta 1803, 152–163. https://doi.org/10.1016/j.bbamcr.2010.01.014

Schutt, C.E., Myslik, J.C., Rozycki, M.D., Goonesekere, N.C.W., Lindberg, U., 1993. The structure of crystalline profilin–β-actin. Nature 365, 810–816. https://doi.org/10.1038/365810a0

Sebé-Pedrós, A., Burkhardt, P., Sánchez-Pons, N., Fairclough, S.R., Lang, B.F., King, N., Ruiz-Trillo, I., 2013. Insights into the Origin of Metazoan Filopodia and Microvilli. Mol Biol Evol 30, 2013–2023. https://doi.org/10.1093/molbev/mst110

Sedzinski, J., Biro, M., Oswald, A., Tinevez, J.-Y., Salbreux, G., Paluch, E., 2011. Polar actomyosin contractility destabilizes the position of the cytokinetic furrow. Nature 476, 462–466. https://doi.org/10.1038/nature10286

Sellers, J.R., 2000. Myosins: a diverse superfamily. Biochimica et Biophysica Acta (BBA) - Molecular Cell Research 1496, 3–22. https://doi.org/10.1016/S0167-4889(00)00005-7

Sens, P., Plastino, J., 2015. Membrane tension and cytoskeleton organization in cell motility. J. Phys.: Condens. Matter 27, 273103. https://doi.org/10.1088/0953-8984/27/27/273103

Seydoux, G., Dunn, M.A., 1997. Transcriptionally repressed germ cells lack a subpopulation of phosphorylated RNA polymerase II in early embryos of Caenorhabditis elegans and Drosophila melanogaster. Development 124, 2191–2201. https://doi.org/10.1242/dev.124.11.2191

Sherlekar, A., Mundhe, G., Richa, P., Dey, B., Sharma, S., Rikhy, R., 2020. F-BAR domain protein Syndapin regulates actomyosin dynamics during apical cap remodeling in syncytial Drosophila embryos. J Cell Sci 133, jcs235846. https://doi.org/10.1242/jcs.235846

Shivanandan, A., Radenovic, A., Sbalzarini, I.F., 2013. MosaicIA: an ImageJ/Fiji plugin for spatial pattern and interaction analysis. BMC Bioinformatics 14, 349. https://doi.org/10.1186/1471-2105-14-349

Singh, D., Pohl, C., 2014. Coupling of Rotational Cortical Flow, Asymmetric Midbody Positioning, and Spindle Rotation Mediates Dorsoventral Axis Formation in *C. elegans*. Developmental Cell 28, 253–267. https://doi.org/10.1016/j.devcel.2014.01.002

Smith, J., Calidas, D., Schmidt, H., Lu, T., Rasoloson, D., Seydoux, G., 2016. Spatial patterning of P granules by RNA-induced phase separation of the intrinsically-disordered protein MEG-3. eLife 5, e21337. https://doi.org/10.7554/eLife.21337

Steffen, A., Faix, J., Resch, G., Wehland, J., Small, J., Rottner, K., Stradal, T., 2006. Filopodia Formation in the Absence of Functional WAVE- and Arp2/3-Complexes. Molecular biology of the cell 17, 2581–91. https://doi.org/10.1091/mbc.E05-11-1088

Steffen, A., Koestler, S.A., Rottner, K., 2014. Requirements for and consequences of Rac-dependent protrusion. European Journal of Cell Biology, Special Issue: SPP 1464: Actin Dynamics - Part II 93, 184–193. https://doi.org/10.1016/j.ejcb.2014.01.008

Steffen, A., Ladwein, M., Dimchev, G.A., Hein, A., Schwenkmezger, L., Arens, S., Ladwein, K.I., Margit Holleboom, J., Schur, F., Victor Small, J., Schwarz, J., Gerhard, R., Faix, J., Stradal, T.E.B., Brakebusch, C., Rottner, K., 2013. Rac function is crucial for cell migration but is not required for spreading and focal adhesion formation. J Cell Sci 126, 4572–4588. https://doi.org/10.1242/jcs.118232

Stephenson, R.O., Yamanaka, Y., Rossant, J., 2010. Disorganized epithelial polarity and excess trophectoderm cell fate in preimplantation embryos lacking E-cadherin. Development 137, 3383–3391. https://doi.org/10.1242/dev.050195

Stewart, M.P., Helenius, J., Toyoda, Y., Ramanathan, S.P., Muller, D.J., Hyman, A.A., 2011. Hydrostatic pressure and the actomyosin cortex drive mitotic cell rounding. Nature 469, 226–230. https://doi.org/10.1038/nature09642

Stradal, T.E., Scita, G., 2006. Protein complexes regulating Arp2/3-mediated actin assembly. Current Opinion in Cell Biology, Cell structure and dynamics 18, 4–10. https://doi.org/10.1016/j.ceb.2005.12.003

Strome, S., Wood, W.B., 1983. Generation of asymmetry and segregation of germ-line granules in early *C. elegans* embryos. Cell 35, 15–25. https://doi.org/10.1016/0092-8674(83)90203-9

Sulston, J.E., Horvitz, H.R., 1977. Post-embryonic cell lineages of the nematode, Caenorhabditis elegans. Developmental Biology 56, 110–156. https://doi.org/10.1016/0012-1606(77)90158-0

Sulston, J.E., Schierenberg, E., White, J.G., Thomson, J.N., 1983. The embryonic cell lineage of the nematode Caenorhabditis elegans. Dev Biol 100, 64–119. https://doi.org/10.1016/0012-1606(83)90201-4

Svitkina, T.M., Borisy, G.G., 1999. Arp2/3 complex and actin depolymerizing factor/cofilin in dendritic organization and treadmilling of actin filament array in lamellipodia. J Cell Biol 145, 1009–1026. https://doi.org/10.1083/jcb.145.5.1009

Thieleke-Matos, C., Osório, D.S., Carvalho, A.X., Morais-de-Sá, E., 2017. Emerging Mechanisms and Roles for Asymmetric Cytokinesis. Int Rev Cell Mol Biol 332, 297–345. https://doi.org/10.1016/bs.ircmb.2017.01.004

Thiels, W., Smeets, B., Cuvelier, M., Caroti, F., Jelier, R., 2021. spheresDT/Mpacts-PiCS: cell tracking and shape retrieval in membrane-labeled embryos. Bioinformatics 37, 4851–4856. https://doi.org/10.1093/bioinformatics/btab557

Thorn, K.S., Christensen, H.E., Shigeta, R., Huddler, D., Shalaby, L., Lindberg, U., Chua, N.H., Schutt, C.E., 1997. The crystal structure of a major allergen from plants. Structure 5, 19–32. https://doi.org/10.1016/s0969-2126(97)00163-9

Thorpe, C.J., Schlesinger, A., Carter, J.C., Bowerman, B., 1997. Wnt Signaling Polarizes an Early *C. elegans* Blastomere to Distinguish Endoderm from Mesoderm. Cell 90, 695–705. https://doi.org/10.1016/S0092-8674(00)80530-9

Tintori, S.C., Nishimura, E.O., Golden, P., Lieb, J.D., Goldstein, B., 2016. A Transcriptional Lineage of the Early *C. elegans* Embryo. Dev Cell 38, 430–444. https://doi.org/10.1016/j.devcel.2016.07.025

Tora, L., Vincent, S.D., 2021. What defines the maternal transcriptome? Biochem Soc Trans 49, 2051–2062. https://doi.org/10.1042/BST20201125

Turlier, H., Audoly, B., Prost, J., Joanny, J.-F., 2014. Furrow Constriction in Animal Cell Cytokinesis. Biophysical Journal 106, 114–123. https://doi.org/10.1016/j.bpj.2013.11.014

Vacquier, V.D., 1968. The connection of blastomeres of sea urchin embryos by filopodia. Experimental Cell Research 52, 571–581. https://doi.org/10.1016/0014-4827(68)90497-7

Vasioukhin, V., Bauer, C., Yin, M., Fuchs, E., 2000. Directed Actin Polymerization Is the Driving Force for Epithelial Cell–Cell Adhesion. Cell 100, 209–219. https://doi.org/10.1016/S0092-8674(00)81559-7

Velarde, N., Gunsalus, K.C., Piano, F., 2007. Diverse roles of actin in *C. elegans*early embryogenesis. BMC Developmental Biology 7, 142. https://doi.org/10.1186/1471-213X-7-142

Vignjevic, D., Kojima, S., Aratyn, Y., Danciu, O., Svitkina, T., Borisy, G.G., 2006. Role of fascin in filopodial protrusion. Journal of Cell Biology 174, 863–875. https://doi.org/10.1083/jcb.200603013

Vignjevic, D., Schoumacher, M., Gavert, N., Janssen, K.-P., Jih, G., Laé, M., Louvard, D., Ben-Ze'ev, A., Robine, S., 2007. Fascin, a Novel Target of β-Catenin-TCF Signaling, Is Expressed at the Invasive Front of Human Colon Cancer. Cancer Research 67, 6844–6853. https://doi.org/10.1158/0008-5472.CAN-07-0929

Volkmann, N., Amann, K.J., Stoilova-McPhie, S., Egile, C., Winter, D.C., Hazelwood, L., Heuser, J.E., Li, R., Pollard, T.D., Hanein, D., 2001. Structure of Arp2/3 complex in its activated state and in actin filament branch junctions. Science 293, 2456–2459. https://doi.org/10.1126/science.1063025

Wallenfang, M.R., Seydoux, G., 2000. Polarization of the anterior–posterior axis of *C. elegans* is a microtubule-directed process. Nature 408, 89–92. https://doi.org/10.1038/35040562

Wang, S.-C., Low, T.Y.F., Nishimura, Y., Gole, L., Yu, W., Motegi, F., 2017. Cortical forces and CDC-42 control clustering of PAR proteins for Caenorhabditis elegans embryonic polarization. Nat Cell Biol 19, 988–995. https://doi.org/10.1038/ncb3577

Wear, M.A., Yamashita, A., Kim, K., Maéda, Y., Cooper, J.A., 2003. How capping protein binds the barbed end of the actin filament. Curr Biol 13, 1531–1537. https://doi.org/10.1016/s0960-9822(03)00559-1

Welch, M.D., DePace, A.H., Verma, S., Iwamatsu, A., Mitchison, T.J., 1997. The Human Arp2/3 Complex Is Composed of Evolutionarily Conserved Subunits and Is Localized to Cellular Regions of Dynamic Actin Filament Assembly. J Cell Biol 138, 375–384.

Welch, M.D., Rosenblatt, J., Skoble, J., Portnoy, D.A., Mitchison, T.J., 1998. Interaction of human Arp2/3 complex and the Listeria monocytogenes ActA protein in actin filament nucleation. Science 281, 105–108. https://doi.org/10.1126/science.281.5373.105

Williams-Masson, E.M., Malik, A.N., Hardin, J., 1997. An actin-mediated two-step mechanism is required for ventral enclosure of the *C. elegans* hypodermis. Development 124, 2889–2901. https://doi.org/10.1242/dev.124.15.2889

Winter, D., Podtelejnikov, A.V., Mann, M., Li, R., 1997. The complex containing actin-related proteins Arp2 and Arp3 is required for the motility and integrity of yeast actin patches. Curr Biol 7, 519–529. https://doi.org/10.1016/s0960-9822(06)00223-5

Wood, W., Martin, P., 2002. Structures in focus—filopodia. The International Journal of Biochemistry & Cell Biology, Cell motility 34, 726–730. https://doi.org/10.1016/S1357-2725(01)00172-8

Wood, W.B., 1991. Evidence from reversal of handedness in *C. elegans* embryos for early cell interactions determining cell fates. Nature 349, 536–538. https://doi.org/10.1038/349536a0

Woychik, R.P., Maas, R.L., Zeller, R., Vogt, T.F., Leder, P., 1990. "Formins": proteins deduced from the alternative transcripts of the limb deformity gene. Nature 346, 850–853. https://doi.org/10.1038/346850a0

Xu, Y., Moseley, J.B., Sagot, I., Poy, F., Pellman, D., Goode, B.L., Eck, M.J., 2004. Crystal structures of a Formin Homology-2 domain reveal a tethered dimer architecture. Cell 116, 711–723. https://doi.org/10.1016/s0092-8674(04)00210-7

Yamada, K.M., Sixt, M., 2019. Mechanisms of 3D cell migration. Nat Rev Mol Cell Biol 20, 738–752. https://doi.org/10.1038/s41580-019-0172-9

Yamamoto, K., Kimura, A., 2017. An asymmetric attraction model for the diversity and robustness of cell arrangement in nematodes. Development 144, 4437–4449. https://doi.org/10.1242/dev.154609

Yan, V.T., Narayanan, A., Wiegand, T., Jülicher, F., Grill, S.W., 2022. A condensate dynamic instability orchestrates actomyosin cortex activation. Nature 609, 597–604. https://doi.org/10.1038/s41586-022-05084-3

Yang, C., Czech, L., Gerboth, S., Kojima, S., Scita, G., Svitkina, T., 2007. Novel Roles of Formin mDia2 in Lamellipodia and Filopodia Formation in Motile Cells. PLOS Biology 5, e317. https://doi.org/10.1371/journal.pbio.0050317

Yang, C., Svitkina, T., 2011. Filopodia initiation: focus on the Arp2/3 complex and formins. Cell Adh Migr 5, 402–408. https://doi.org/10.4161/cam.5.5.16971

Young, P.E., Richman, A.M., Ketchum, A.S., Kiehart, D.P., 1993. Morphogenesis in Drosophila requires nonmuscle myosin heavy chain function. Genes Dev. 7, 29–41. https://doi.org/10.1101/gad.7.1.29

Zaatri, A., Perry, J.A., Maddox, A.S., 2021. Septins and a formin have distinct functions in anaphase chiral cortical rotation in the Caenorhabditis elegans zygote. Mol Biol Cell 32, 1283–1292. https://doi.org/10.1091/mbc.E20-09-0576

Zhang, Y., Yang, Y., Zhu, Z., Ou, G., 2017. WASP-Arp2/3-dependent actin polymerization influences fusogen localization during cell-cell fusion in Caenorhabditis elegans embryos. Biology Open 6, 1324–1328. https://doi.org/10.1242/bio.026807

Zhao, P., Teng, X., Tantirimudalige, S.N., Nishikawa, M., Wohland, T., Toyama, Y., Motegi, F., 2019. Aurora-A Breaks Symmetry in Contractile Actomyosin Networks Independently of Its Role in Centrosome Maturation. Developmental Cell 48, 631-645.e6. https://doi.org/10.1016/j.devcel.2019.02.012

Zonies, 2010. Symmetry breaking and polarization of the *C. elegans* zygote by the polarity protein PAR-2 - PubMed [WWW Document]. URL https://pubmed.ncbi.nlm.nih.gov/20392744/ (accessed 11.24.22).

Résumé en français :

Etude des relations entre architecture d'actine, contenu moléculaire et identité cellulaire

Au cours l'embryogénèse précoce de *C.elegans.*

L'objectif principal de mon projet est de caractériser le contenu et l'organisation de l'actine propre à chaque cellule de l'embryon précoce de C. elegans. D'après, les données publiées de transcriptomique en cellule unique dans l'embryon et la mise en évidence récente, par une collaboration entre notre équipe et celle de Nathan Goehring, de l'existence de filopodes à des stades très précoces du développement embryonnaire de C. elegans, il existe des singularités entres les cellules aussi bien au niveau des Actin Binding Proteins (ABPs) qu'au niveau des structures d'actine spécifiques, en particulier les filopodes.

Mon but est d'une part, de vérifier au niveau protéique les variations des concentrations en ABP relevées par la transcriptomique, et d'autre part de caractériser la régulation spatio-temporelle des filopodes. Cela nous permettra de répondre aux questions suivantes : Les ABP sont-elles également réparties entre les cellules sœurs ? Comment ces déséquilibres protéiques affectent-ils les architectures d'actine ? Les propriétés corticales de l'actine sont-elles héréditaires ? Comment la machinerie de nucléation de l'actine est-elle contrôlée spatio-temporellement ? Les objectifs à long terme sont d'une part, de montrer comment ces différences liées à l'actine impactent la différenciation cellulaire dans l'embryon précoce et d'autre part de déterminer le rôle de ces filopodes au cours de ce développement. Mon projet de thèse peut être divisé en deux études principales :

1. **L'identification de la variation du contenu cytosquelettique de l'actine tout au long de la lignée précoce de l'embryon de C. elegans.** Ce premier objectif est de cartographier l'abondance relative des protéines de liaison à l'actine dans chaque cellule.

2. **Caractérisation des filopodes apparaissant dans des schémas transitoires dans l'embryon précoce.** Dans cette deuxième partie, l'accent est mis sur une structure spécifique que nous avons observée être régulée spatio-temporellement au sein des différentes cellules.

Pour répondre à ces questions, j'ai utiliser une approche interdisciplinaire de biologie quantitative dans l'embryon de C. elegans. Via l'édition génique par CRISPR/Cas9 permettant l'introduction de sondes fluorescentes, de la microscopie haute résolution in vivo et le développement d'outils d'analyse d'images personnalisés.

Résultats d'ores et déjà acquis

1. L'identification de la variation du contenu en protéine de régulation de l'actine tout au long de la lignée précoce de l'embryon de C. elegans.

1.1 Observation de l'expression endogène des ABP fusionnés avec la GFP

Ma première tâche a été de croiser des souches ABP::GFP avec d'autres souches marquées pour suivre en plus de notre protéine d'intérêt marquée de manière endogène, les filaments d'actine, la membrane ou le cycle cellulaire. Cela m'a permis de définir des références spatiales et temporelles entre les embryons. Ma deuxième tâche a été de développer un protocole d'imagerie 4D. Les paramètres d'imagerie sont désormais définis en fonction des différentes conditions expérimentales et des souches. Cette méthode, facilement transférable, m'a permis d'acquérir une banque de donnée standardisée pour la quantification au cours du temps de l'expression endogène de chacune de ces trois protéines de liaison à l'actine, CYK-1, ARX-2 et CAP-1 du stade 1 à 6 cellules.

1.2 Analyse et quantification d'images

Avec l'aide de ma directrice de thèse, Anne-Cécile Reymann, nous avons développé des méthodes de quantification par fluorescence des niveaux corticaux et cytoplasmiques des ABPs dans chaque cellule et au cours du temps. J'ai donc commencé à apprendre le codage Matlab, à partir de zéro, pour développer une méthode de segmentation cellulaire automatisée et personnalisée en utilisant des marqueurs membranaires. Pour améliorer la robustesse et la rapidité, nous sommes passés sur une méthode de Deeplearning avec ILASTIK. Après entraînement du logiciel, le résultat de segmentation de la membrane est très précis. L'analyse de l'intensité de fluorescence dans chaque cellule, cortical ou cytoplasmique est ensuite réalisée à l'aide de Matlab. L'analyse des résultats obtenues nous a montré que, au cours de l'embryogénèse précoce, chacune de ces trois protéines ont des variations inter- et intra-cellulaires avec une distribution et une dynamique qui leurs sont propre. Par ailleurs, il s'avère que ces résultats ne corrèlent pas systématiquement avec les données de transcriptomique en cellule unique obtenues par d'autre laboratoire. De plus, La répartition de ces ABP semble suivre un schéma qui corrèle avec l'établissement des premiers axes de symétrie de l'organisme, Antéro-Postérieur puis Dorso-Ventral. De manière surprenante, nos résultats ont montré l'existence d'une asymétrie, au niveau du contenu en ABP, entre deux cellules filles alors qu'elles sont issues d'une division reconnue comme symétrique.

Cette étude possède un manuscrit actuellement en préparation en vue d'une future publication.

2. Caractérisation des filopodes apparaissant de manières transitoires dans l'embryon précoce

2.1 Caractérisation des filopodes chez le zygote

A mon arrivé au laboratoire, ma directrice de thèse avait lancé un projet pour caractériser les protubérances en forme de doigts qui apparaissent dans le zygote et dans lesquelles la formine a été vue enrichie à leur extrémité. Le premier objectif était de prouver qu'il s'agissait d'extensions de filopodes : des faisceaux d'actine nucléés via la formine et Arp2/3, entourés d'une membrane créant l'apparence d'un enrichissement local en PiP2 (membrane). Ces travaux ont donné lieu à une publication en collaboration avec le laboratoire Goehring. J'ai participé à cette étude en fournissant des souches avec GFP::ABP croisées avec un marqueur membranaire, en acquérant des données et en analysant la colocalisation entre le marqueur membranaire et CYK-1, ARX-2 et PLST-1.

2.2 Organisation moléculaire et dynamique de nucléation au sein des filopodes

La composition moléculaire des filopodes de l'embryon précoce et leur mécanisme de nucléation et de leur extension ne sont pas encore élucidés chez C. elegans. Une observation plus détaillée est nécessaire, notamment la colocalisation de la formine et de l'Arp2 / 3 est manquante. Ma première tâche a été d'introduire un halotag en utilisant l'édition génique CRISPR au locus cyk-1. L'avantage d'utiliser halotag est qu'il peut être conjugué avec des colorants fluorescents existant dans différentes couleurs. La souche a été validée par séquençage. J'ai également effectué une approche d'immunofluorescence en embryon fixé pour pouvoir observer précisément la composition de ces structures. Malheureusement, j'ai été confronté à des difficultés de réalisation expérimentales et d'observation qui m'ont empêchés d'acquérir des données suffisantes pour conclure sur la composition moléculaire de ces architectures d'actine.

2.3 Distribution spatio-temporelle des filopodes dans l'embryon précoce

Mon prochain objectif était de caractériser la distribution spatiale et temporelle des filopodes à différents stades embryonaire. Au stade 4 cellules, j'ai remarqué qu'ils apparaissent de manière transitoire à différents interfaces cellule-cellule et en corrélation avec la forme embryonnaire et le cycle cellulaire. En effet, ces filopodes sont entremêlés au niveau des surfaces entre les cellules soeurs ABa et ABp ainsi qu'entre elles et EMS. De plus, pendant la transition 4 à 6 cellules, les structures actiniques entre EMS et les cellules Aba et ABp changent de conformation et passent d'une configuration de type filopode à une configuration de type lamellipode. Une étude sur la temporalité d'apparition de ces filopodes

entre AB et P1, a montré que leur nombre s'augmentait à mesure que le cycle cellulaire progressait et que le pique du nombre d'apparition s'effectuait entre les deux épisodes de rupture d'enveloppe nucléaire de ces deux cellules qui est, de facto, asynchrone. Par ailleurs des résultats préliminaires au stade 4 cellules montrent la même corrélation temporelle entre la rupture de l'enveloppe nucléaire et le pique d'apparition de ces filopodes à l'interface entre deux cellules.

Cette étude possède suffisamment de résultats pour envisager la préparation d'un manuscrit en vue d'une future publication.

Nos données récoltées sur les deux principaux nucléateurs d'actine (le complexe Arp2/3 et la formine CYK-1) ainsi que la protéine d'inhibition de l'élongation des filaments (CAP-1) nous ont amené les résultats suivants : Premièrement, ces ABPs ont une répartition inter-cellulaires différente le long du lignage et les deux cellules sœurs (Aba et ABp) issues d'une division connue pour être symétrique (AB), possèdent un contenu en ABP qui s'avère, quant à lui, asymétrique. Deuxièmement, nous avons révélé que les structures subcellulaires correspondantes aux filopodes, apparaissent de manière transitoire à différents interfaces cellule-cellule et en corrélation avec la forme embryonnaire et les stades cellulaire. Troisièmement, la cellule étant située sur la partie ventrale de l'embryon (EMS) possède une structure actinique correspondant à un lamellipode et ceci uniquement pendant une étape très précise du développement embryonnaire, la transition du stade 4-6 cellules et qui aboutit à la formation de l'axe du plan corporel Gauche-Droite. Ces résultats mettent en lumière la spécificité de répartition des ABPs au cours de l'embryogénèse précoce. Ils ont également révélé l'important dynamisme et la diversité des structures actiniques situés à l'interface intercellulaire ; ouvrant ainsi un nouveau domaine de recherche en Biologie de Développement précoce.

Liste des publications :

-Hirani, N., Illukkumbura, R., Bland, T., **Mathonnet, G**., Suhner, D., Reymann, A. C., & Goehring, N. W. (2019). Anterior-enriched filopodia create the appearance of asymmetric membrane microdomains in polarizing C. elegans zygotes. Journal of cell science, 132(14), jcs230714.

- Manuscrit en préparation pour la partie sur l'identification de la variation du contenu en protéine de régulation de l'actine tout au long de la lignée précoce de l'embryon de C. elegans.

Grégoire MATHONNET

Étude des relations entre architectures d'actine, contenu moléculaire et identité cellulaire au cours de l'embryogénèse précoce de *C. elegans*

Résumé

L'objectif principal de mon projet est de caractériser le contenu et l'organisation de l'actine propre à chaque cellule de l'embryon précoce de *C. elegans*. D'après, les données publiées de transcriptomique en cellule unique dans l'embryon et la mise en évidence récente, par une collaboration avec d'autres équipes internationale, de l'existence de filopodes à des stades très précoces du développement embryonnaire de *C. elegans*, il existe des singularités entres les cellules aussi bien au niveau des Actin Binding Proteins (ABPs) qu'au niveau des structures d'actine spécifiques, en particulier les filopodes.
Mon but est d'une part, de vérifier au niveau protéique les variations des concentrations en ABPs relevées par la transcriptomique, et d'autre part de caractériser la régulation spatio-temporelle des filopodes. Cela nous permettra de répondre aux questions suivantes : Les ABPs sont-elles également réparties entre les cellules sœurs ? Comment ces déséquilibres protéiques affectent-ils les architectures d'actine ? Les propriétés corticales de l'actine sont-elles héréditaires ? Comment la machinerie de nucléation de l'actine est-elle contrôlée spatio-temporellement ? Les objectifs à long terme sont d'une part, de montrer comment ces différences liées à l'actine impactent la différenciation cellulaire dans l'embryon précoce et d'autre part de déterminer le rôle de ces filopodes au cours de ce développement.

Mots clés : Biologie, Actine, Filopodes, Embryon

Summary

The main objective of my project is to characterise the content and organisation of the actin proteome in each cell of the early embryo of *C. elegans*. Based on published single-cell transcriptomic data in the embryo and recent evidence, through collaboration with other international teams, we discovered filopodia at a very early stages of embryonic development of *C. elegans*, There are cell-to-cell singularities in both the Actin Binding Proteins (ABPs) and specific actin structures, especially filopodia. My aim is to verify the variations of ABPs concentrations detected by transcriptomics at the protein level, and to characterise the spatio-temporal regulation of filopodia. This will allow us to answer the following questions: Are ABPs equally distributed among sister cells? How do these protein imbalances affect actin architectures? Are the cortical properties of actin hereditary? How is the mechanism of actin nucleation spatiotemporal controlled? The long-term objectives are to show how these differences related to actin affect cell differentiation in the early embryo and to determine the role of these filopodia during this development.

Keywords : Biologie, Actine, Filopodes, Embryon